THE PRECLINICAL AND CLINICAL PHARMACOLOGY OF BENZALDEHYDE DIMETHANE SULFONATE (BEN) FOR THE TREATMENT OF RENAL CELL CARCINOMA

by

Robert A Parise

Bachelor of Science (B.S) Northern Illinois University, DeKalb IL, 1992

Submitted to the Graduate Faculty of

The School of Pharmacy in partial fulfillment

of the requirements for the degree of

Doctor of Philosophy

University of Pittsburgh 2014

UNIVERSITY OF PITTSBUGH

SCHOOL OF PHARMACY

This dissertation was presented

by

Robert A. Parise

It was defended on

April 2nd 2014

and approved by

Pamela A. Hershberger, PhD., Dept. of Pharmacology and Therapeutics, Roswell Park Cancer Institute

Michael A. Zemaitis, PhD., Dept. of Pharmaceutical Sciences, School of Pharmacy

Samuel M. Poloyac, Pharm D, PhD., Dept. of Pharmaceutical Sciences, School of Pharmacy

Jan Hendrik Beumer, Pharm D, PhD., Dept. of Pharmaceutical Sciences, School of Pharmacy

Raman Venkataraman, PhD., Dept. of Pharmaceutical Sciences, School of Pharmacy

Pre-Clinical and Clinical Pharmacology of

Benzaldehyde Dimethane Sulfonate (BEN)

for the Treatment of Renal Cell Carcinoma

Robert A. Parise

University of Pittsburgh, 2014

Over 65,000 people acquired renal cell carcinoma (RCC) and over 13,500 people died from the disease in the United States in 2012. The median survival for individuals with metastatic disease is 13 months. Limited therapeutic strategies exist for the treatment of RCC. Recent research has identified new targets for this disease and new targeted therapies have been developed. Despite this, the overall survival remains poor, and there remains a need for additional new therapies for RCC. Benzaldehyde dimethane sulfonate (BEN, DMS612) is a bifunctional alkylating agent with activity against renal cell carcinoma cell lines. The goal of the research conducted was to evaluate the preclinical and clinical pharmacology of BEN.

Benzaldehyde dimethane sulfonate is stable in plasma but is metabolized in blood by aldehyde dehydrogenase into an acid that decomposes in aqueous and biological matrices. Furthermore, the acid product decomposes into 6 different species of which none are as active as BEN in the renal carcinoma cells that we have tested. We also found that BEN had greater activity in renal carcinoma cell lines that expressed higher levels of aldehyde dehydrogenase. This led us to believe that BEN acts as a pro-drug with its main carboxylic acid metabolite exerting the activity against renal carcinoma cell lines.

Pre-Clinical and Clinical Pharmacology of

Benzaldehyde Dimethane Sulfonate (BEN)

for the Treatment of Renal Cell Carcinoma

Robert A. Parise

University of Pittsburgh, 2014

We determined that BEN is rapidly metabolized in mice and that the pretreatment of mice with the aldehyde dehydrogenase inhibitor disulfiram greatly increases the exposure to BEN. Furthermore the carboxylic decomposition products that were detected *in vitro* were also found in the mice along with corresponding glucuronides. Also, we found that BEN when administered to patients is very rapidly metabolized and the same glucuronides generated in mice were also detected in humans. The maximum tolerated dose in a phase I clinical trial in humans was 9.0 mg/m^2. The dose limiting toxicity was thrombocytopenia and neutropenia.

TABLE OF CONTENTS

PREFACE

I would like to express my greatest appreciation to Dr. Jan Beumer, my dissertation advisor, for his help and support during my graduate training. Without his guidance this dissertation would not have been possible. I would like to give thanks to the late Dr. Merrill Egorin for the support and encouragement he gave me during my studies. He is gone but not forgotten.

I would like to thank Dr. Julie Eiseman and Dana Liggett for the animal studies. They were a joy to work with and they taught me a lot about animal pharmacology. I would like to thank my co-advisor Dr.Venkataraman and committee members Dr. Poloyac, Dr. Zemaitis and Dr. Hershberger for taking the time to help me complete this dissertation.

Thanks are also due to my colleagues, Julianne Holleran, Susan Christner, and Brian Kiesel for their endless support. I would like to give a special thanks to Susan Price and Lori Schmotzer for excellent administrative assistance and advice they gave during my years as a graduate student.

I would like to thank my mother and father for providing me a loving and caring childhood. I would like to thank my wife Joni and kids Robert, Angelina and Alexandra for the patience they showed during the countless hours that I missed with them while I was conducting my graduate work.

1.0 INTRODUCTION

Renal cell carcinomas (RCC) originate within the renal cortex and comprise 80 to 85% of all renal neoplasms.[1] Patients with localized disease can be cured with surgery, however, in most cases the disease is not identified until it has metastasized. At this point surgery is not curative. In addition, many patients that have had surgery to remove a local lesion have recurrence of the disease. The median survival for persons with metastatic disease is 13 months.[1] Recent research has identified new targets for this disease and new targeted therapies have been developed. Despite this fact, the overall survival remains poor, and there remains a need for new therapies for RCC.

1.1 EPIDEMIOLOGY

In 2011, 65,000 people acquired RCC in the United States and in the same year nearly 13,500 died from the disease.[2] In 2008, there were 270,000 cases and 116,000 deaths worldwide.[3] The incidences of RCC vary widely worldwide. The highest incidences are seen in Europe and North America, while the lowest incidences are seen in Africa (Figure 1).[3]

In the United States, the incidence of RCC has increased over time (Figure 2).[4] Between 1975 and 1995 incidence rates per 100,000 person-years increased by 2.3, 3.1,

3.9, and 4.3 annually for white men, white women, black males and black females respectively. More recent data obtained from 1997 to 2007 shows a similar trend of a 2.6 percent yearly increase in the overall incidence of RCC (5).[3]

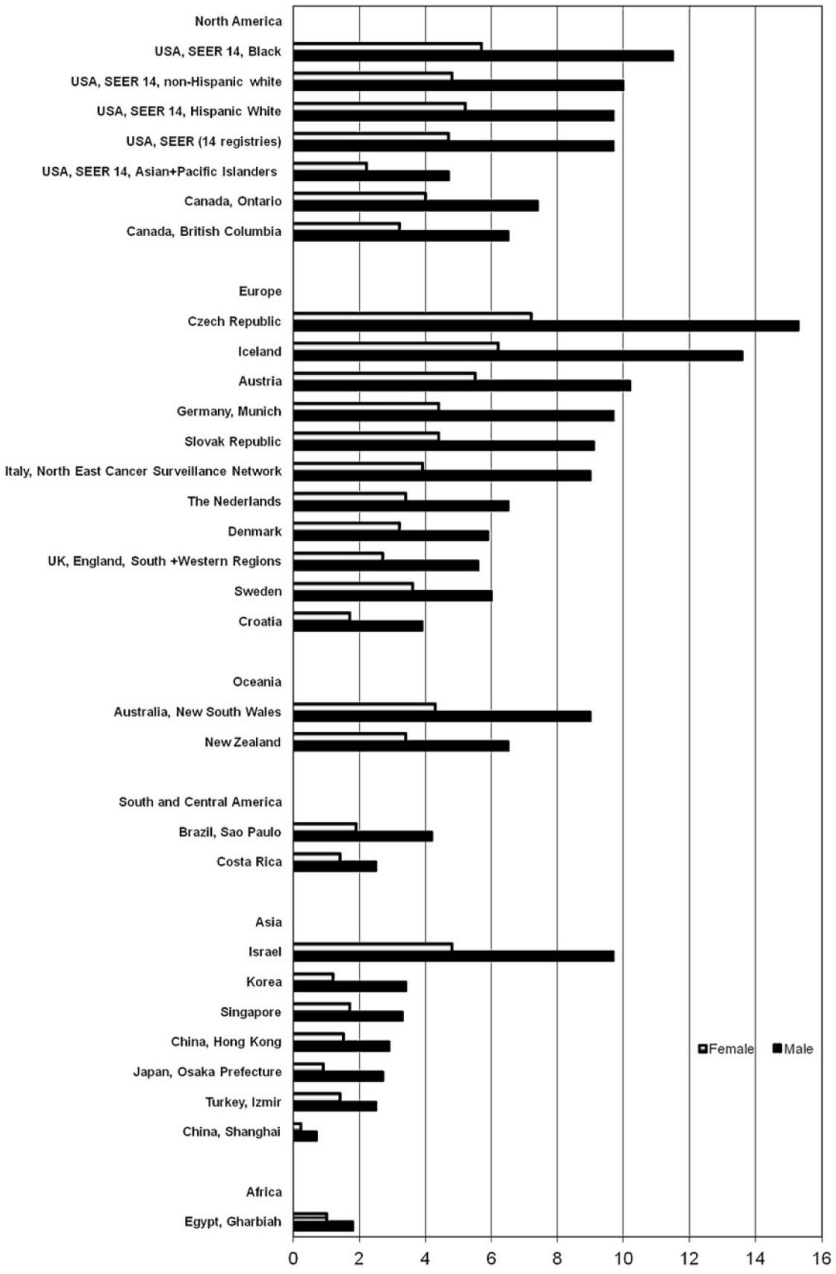

Figure 1. International variation in age-adjusted incidence rates (world) per 100,000, for histologic verified renal cell cancer in selected countries. (Reprinted from Hematology/Oncology Clinics of North America with permission from Elsevier©)[3]

Between 1970 and 1998, the incidental discovery of asymptomatic RCC increased from 10 to 60 percent, respectively.[5] The Surveillance, Epidemiology and End Results (SEER) database shows that while the incidence of RCC has increased in recent years this increase has been associated with a decrease in the average size of the tumor at first presentation (6.7 cm vs. 5.9 cm in 1988 and 2002, respectively). It may be that the widespread use of modern imaging techniques account for part of the increase in the observed incidence. [6,7]

Older studies show that RCC was at least twice as frequent in men than women, however newer data show that the gender gap is narrowing.[8] Data analyzed from the National Cancer Database from 1993 to 2004 show that the ratio of RCC in men compared to women is 1.65. The median age at diagnosis is 64 years. The disease is rare in people younger than 40 years old. The most recent study shows those patients younger than 40 make up less than 5 percent of the new cases.[9-11]

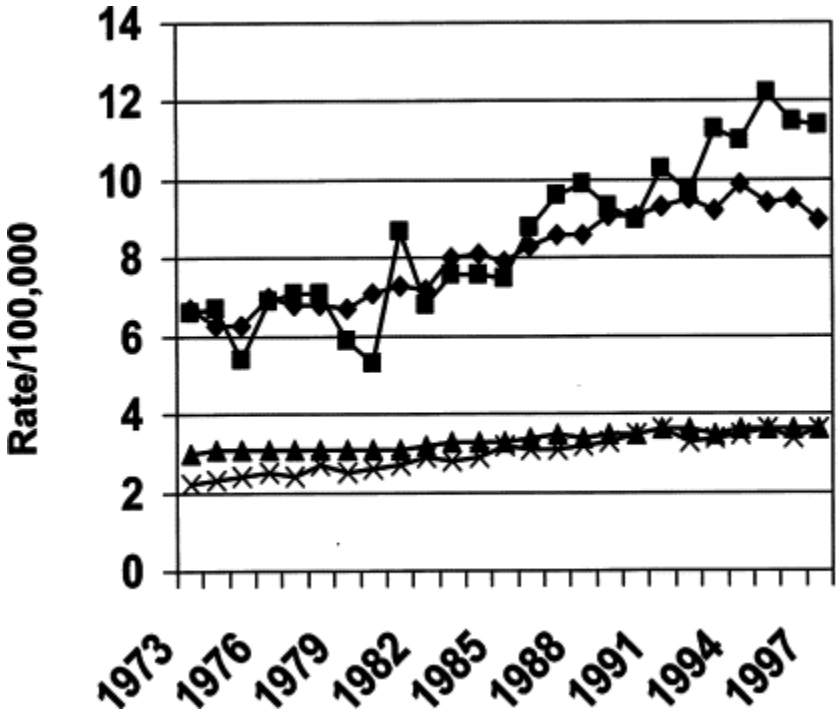

Figure 2. Incidence of renal cell carcinoma in the United States between the years 1973 and 1998. Whites incidence (♦), black incidence (■), whites mortality (▲), and black mortality (×). (reprinted from The Journal of Urology with permission from Elsevier©)[4]

1.2 ETIOLOGY

There are a number of environmental, genetic and clinical risk factors that are associated with the development of renal cell carcinoma. Environmental risk factors include cigarette smoking, analgesic abuse and occupational exposure.[12-14]

There is a statistically significant dose response for cigarette smoking and RCC for both males and females.[12] Cigarette smoking can be attributed to cause nearly one

third of all cases of RCC. Furthermore, the use of cigarettes by individuals with RCC is associated with more advanced disease at first presentation.[15]

Analgesic abuse and analgesic abuse nephropathy has been linked to the increased risk of RCC.[13,16,17] Data from a study from approximately 128,000 individuals found that the risk for RCC was increased among subjects that used non-aspirin non-steroidal anti-inflammatory agents (NSAIDs) on a regular basis.[16] The authors in this study defined regular use as more than 2 doses per week for 16 years.

There are a number of studies that have found an association between occupational exposure to chemicals and RCC. High levels of the industrial solvent trichloroethylene correlated with RCC.[18] In addition, exposure to cadmium, asbestos, gasoline and petroleum products have been shown to increase the risk of RCC.[14,19,20]

There are a number of clinical factors that are associated with RCC. These include hypertension, diabetes mellitus, obesity, and acquired cystic disease of the kidney.[21-25] A number of studies have found an association between hypertension and increased risk of developing RCC. A Korean study composed of 576,562 men found that hypertension (systolic > 160 mm) lead to an increased risk of mortality from RCC (RR 2.43) compared to individuals with normal blood pressure (systolic < 120 mm).[26] Another study composed of 296,638 European men and women found a relative risk of 2.48 when comparing persons with a systolic pressure of >160 mm with those having a pressure of <120 mm.[24] This study did not find a significant difference of risk estimate between sexes, and individuals taking anti-hypertensives were not at increased risk unless blood pressure was poorly controlled.

It has been shown that a history of diabetes mellitus has been associated with an increased risk of RCC. Studies conducted in the United States and Europe found a significant increase in the incidence of RCC in both men and women with a history of diabetes.[25,27,28] However, this increase in incidence may be due in part to obesity and hypertension.

Obesity is a risk factor in both men and women.[21,29,30] One study that divided body mass index (BMI) into 8 cohorts, showed that men with a BMI in the middle three cohorts had a 30 to 60% greater risk than men in the lower three cohorts to develop RCC. In addition, men in the highest two cohorts had nearly double the risk, when compared to the men in the lowest three cohorts.[21] There is also an increased risk of RCC in obese women. In a large European study, it was found that woman in the top 20% of weight had a significant increase in risk (2.13 RR) when compared to women in the lowest 20%.[29]

Another clinical condition that is associated with an increased risk of RCC is acquired cystic disease of the kidney. It is estimated that between 35 and 50% of patients who require chronic dialysis will develop cystic disease of the kidney and that 6% of these patients will develop RCC.[31] Malignant RCC usually develops after 8 to 10 years of dialysis. It has been found that among chronic dialysis patients males are at an increased risk for RCC with a male to female ratio of 7 to 1.[32]

Renal cell carcinoma can occur sporadically and through hereditary means.[3] There are genetic contributions that predispose individuals to RCC.[33,34] Although most cases of RCC are sporadic, there are several syndromes that can cause RCC such as: Von Hippel-Lindau (VHL) disease, hereditary papillary renal carcinoma (HPRC), hereditary

leiomyomatosis and renal cell cancer (HLRCC) syndrome, and Birt-Hogg-Dube (BHD) syndrome. These conditions will be explained in more detail in the pathology section.

There are other factors which have not been previously described above that predispose individuals to RCC. There is an increased risk of RCC in those individuals that have a first degree relative with the onset of disease before the age of 40.[35]. In addition, those that have been infected with hepatitis C have a significantly increased risk of developing RCC.[36]

1.3 PATHOLOGY

Renal cell carcinoma (RCC) is not a single disease. It consists of five different diseases which occur in the kidney. The five types of RCC and their prevalence are: clear cell (75%), type 1 and type 2 papillary (15%), chromophobe (5%), and oncocytoma (<5%).[37] In addition, less than 5% of RCC are considered unclassified. These diseases have different histology and are caused by different genetic abnormalities and/or genetic mutations.

Clear cell renal carcinoma originates in the proximal tubule and typically has a deletion in chromosome 3p.[38] These tumors are usually solid but may also be cystic in structure. Most cases of clear cell carcinoma are sporadic; however, this carcinoma is associated with von Hippel-Lindau disease.

Papillary carcinomas, which also originate in the proximal tubule, are divided into two groups based on histology and gene expression profiles.[39] The tumors of papillary

type 1 are well differentiated (low-grade) whereas tumors classified as type 2 tend to be less differentiated (high-grade).[39] There are molecular differences associated with type 1 and type 2 papillary carcinomas. Type 1 tumors tend to overexpress c-Met and have cell cycle G1-S checkpoint dysregulation, whereas type 2 carcinomas tend to have G2-M dysregulation.[40] The prognosis for patients with papillary type 1 carcinomas is much better than that of those with type 2 carcinomas.[40-43] A study that analyzed 130 patients showed that after 48 months the overall survival was 89% for type 1 carcinoma compared to 44% for type 2 carcinoma.[41]

Chromophobe carcinomas originate from the intercalated cells of the collecting system. Histologically, these tumors are very different from clear cell and papillary carcinoma. These cells are comprised of sheets of cells, are darker in color, and lack the lipids and glycogen found in other types of RCCs.[44-46] Also, chromophobe carcinomas have a hypodiploid number of chromosomes.[47,48] Most chromophobe cell carcinomas lack a variety of chromosomes. One study found that 17 of 19 tumors tested had a combination of chromosomes absent. In this study a combination of chromosome 1, 2, 6, 10, 13, 17 and 21 were found to be absent.[48] The median survival of patients suffering from chromophobe cell carcinoma is currently 29 months which is better than the average for RCC (13 months).[49]

Oncocytomas are very rare and originate from the collecting duct cells.[50] These cells tend to be large and well-differentiated with an overabundant number of mitochondria.[51] Renal oncocytoma is usually benign. However, in 10 to 30% of patients that have renal oncocytoma it is associated with other types of RCC.[52]

1.3.1 Hereditary forms of renal cell carcinoma

Although 96% - 98% of cases of RCC are sporadic there are four main hereditary syndromes which may lead to the development of RCC.[3] These are von Hippel-Lindau (VHL) syndrome, hereditary papillary renal carcinoma (HPRC), hereditary leiomyomatosis and renal cell cancer (HLRCC) syndrome, and Birt-Hogg-Dube (BHD) syndrome. There is a keen interest in these syndromes, and especially VHL, because the pathways involved in these familial diseases may be similar to the ones responsible for sporadic cases of RCC.[53,54]

1.3.1.1 Von Hippel-Lindau Syndrome

Von Hippel-Lindau (VHL) syndrome is an inherited syndrome.[34] Individuals with this syndrome inherit a defective allele of the VHL gene from a parent. The condition arises when the remaining wild type allele becomes inactivated through mutation or deletion.[37] Inactivation of the VHL gene has also been found in a high percentage of patients that have sporadic clear cell renal carcinoma. Mutations of the VHL gene have not been detected in individuals with other types of hereditary cancer syndromes. The gene abnormality that is the cause of VHL is present in 1 in 36,000 newborns.[55] The von Hippel-Lindau gene is located on chromosome 3p25.[56] This gene codes a protein, pVHL, which functions as a tumor suppressor protein.[57] pVHL regulates the transcription factor hypoxia-inducible factor (HIF). HIF is a heterodimer consisting of an α and β subunit. During normoxia, pVHL will bind to HIF1-α which will result in the subsequent polyubiquitination and proteasomal degradation of HIF1-α. When pVHL is absent or abnormally functioning, HIF1-α will accumulate and bind to HIF1-β. The

heterodimer will then bind to the DNA sequences which will result in the overexpression of angiogenic factors. The most notable of these factors are the vascular endothelial growth factor A (VEGF-A), platelet derived growth factor β, and transforming growth factor alpha (TGF-α) (Figure 3).[58] This series of events can lead to tumorigenesis.

Affected individuals are predisposed to develop tumors in various organs including the brain, spine, eyes, adrenal glands, pancreas, inner ear, epididymis, and kidney. Forty percent of those affected by von Hippel-Lindau syndrome develop bilateral tumors or cysts in their kidneys.[59] These tumors consist of clear cell renal carcinoma.

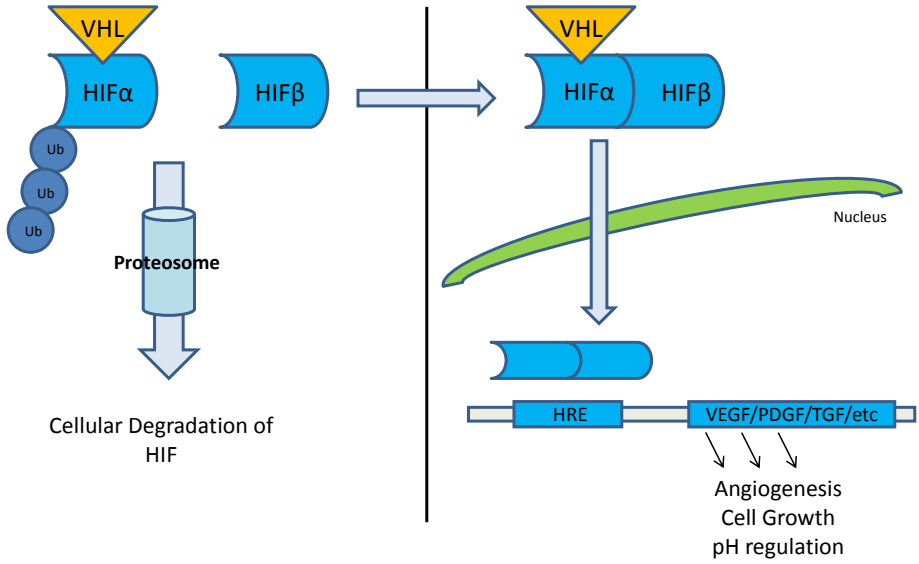

Figure 3. VHL pathways: normal VHL function (left) and loss of VHL (right). (Adapted from Tang PA, et al.)[60]

1.3.2 Hereditary Papillary Renal Carcinoma

Hereditary papillary renal cell carcinoma (HPRC) increases the risk of development of type 1 papillary RCC in affected individuals.[33]

The gene responsible for HPRC is the MET proto-oncogene which is located on chromosome 7.[61] The gene produces an intracellular tyrosine kinase that is bound to a membrane bound receptor for hepatocyte growth factor (HGF). Certain mutations in the MET gene cause the tyrosine kinase domain to be constantly active and predispose individuals to HPRC.[62]

1.3.3 Hereditary Leiomyomatosis and Renal Cell Cancer Syndrome

Hereditary Leiomyomatosis and Renal Cell Cancer Syndrome (HLRCC) is an inherited autosomal dominant syndrome that predisposes affected individuals to develop leiomyomas and/or papillary type 2 RCC. Studies have indicated that HLRCC is linked to the bi-allelic inactivation of the fumarate hydratase (FH) gene.[63] However, how these abnormalities lead to the disease is not understood. FH is an enzyme involved in the citric acid cycle and it is thought that inactive FH can lead to pseudohypoxia which is the aberrant activation of hypoxia response pathways under normal condition. This condition leads to an increase in expression of HIF-1α which can lead to tumor formation.[64,65]

1.3.4 Birt-Hogg-Dube Syndrome

Birt-Hogg-Dube (BHD) syndrome is inherited in an autosomal dominant fashion. Persons affected with this disease may develop dermatologic and pulmonary lesions as well as renal cell carcinoma.[66] This condition is caused by mutations in the folliculin (FLCN) gene.[67] Although the exact mechanism is not understood, FLCN may be involved in the mammalian target of rapamycin (mTOR) pathway.[68] Inhibition of mTOR decreased kidney pathology and increased survival in a mouse model.[69] The tumors of people with BHD consist mainly of chromophobe and oncocytic renal cancers.

1.4 PAST AND CURRENT TREAMENTS FOR METASTATIC RENAL CELL CARCINOMA

1.4.1 Classical cytotoxic agent

Renal cell carcinoma is curable if the disease is localized and surgically resected before metastasis. However, more than a third of the patients that undergo surgery for localized disease will have a reoccurrence and will have to be treated with chemotherapy.[1] A small number of patients, however, can be cured with high dose interleukin-2 therapy. The following is a short review of the past and current options for the treatment of metastatic renal cell carcinoma (mRCC).

Since the 1960's, a number of cytotoxic compounds have been used in an attempt to treat metastatic renal cell carcinoma. In 1988, Josef Kuhbock wrote a review of the literature which was a compilation of three surveys of the cytotoxic chemotherapy of metastatic renal cell carcinoma (mRCC).[70] The review covers a number of trials and includes the data from different classes of anti-neoplastic agents used. The agents are representative of the alkylating agents, anti-metabolites, vinca alkaloids, cytotoxic antibiotics and platinum analogues. The data includes the use of these compounds as both single agents and in combination therapy. The conclusion of the review was that although the use of a few substances such as vinblastine, lomustine, hydroxyurea, and ifosfamide is associated with some success (10-20% response rate) there was no specific agent available for the successful treatment of mRCC. A more extensive review of the literature was conducted by Yagoda.[71] This review analyzed the results from clinical trials conducted from 1983 to 1993 using both hormonal and cytotoxic agents. The author lists the response rate as a percent of patients that have either a complete response or a partial response. It should be noted that a complete response does not mean a cure because the tumor can recur. These trials consisted of single agent, two agent and multiple agent combinations. Also, some of the trials included the use of modulating agents along with chemotherapy in an attempt to modulate or enhance intracellular drug activity. Some examples of the enhancing agents used were cyclosporine-A, quinidine and verapamil. Also, in other trials, biological modulating agents such as interferon and leucovorin were used along with cytotoxic chemotherapy. The clinical trials used the agents that were available at the time of the studies. The classes of agents used were antimitotics and spindle inhibitors, hormones, alkylating agents, metals, antifolates, pyrimidines, purines,

anthracyclines, immunological agents and miscellaneous agents whose, mechanism of actions had yet to be determined. In all, the review covered 83 clinical trials in which 4,542 patients were enrolled and 4,093 patients completed the trails. Of the 4,093 evaluable patients 3,329 had no prior chemotherapy. The overall results of the study showed a response rate of 6% (95% CI of 5.3-6.8%) and the duration of the responses were short, generally only lasting a few months. Alkylating agents, antifolates, purines and intercalating agents had an overall response rate of 4%. Hormones, vinca alkaloids and antimitotic spindle inhibitors had response rates of 6.9%, 5.9%, and 5.0%, respectively. Also, drugs used to reverse multidrug resistance were found to be ineffective when administered with the cytotoxic agents. Immunologic agents showed a response rate of 11.3%. The drugs with the highest response rate of 14.6% and 10% were floxuridine and 5-fluorouracil, respectively. The authors suggest that these drugs should be the first cytotoxic chemotherapeutic choice for treating mRCC. Also, they believed that the high level of expression of Pgp, glutathione-S transferase, down regulation of topoisomerase 2 and lack of intracellular tumor drug concentration were likely reasons for the poor responses. [72]

1.4.2 Immunotherapy – Interleukin-2

Interleukin-2 (IL-2) was first used to treat mRCC in the mid-1980's. The results from 21 institutions showed that the use of high dose IL-2 (HD) could produce an objective response rate of up to 20%. Of the 20%, complete remission was seen in 7 to 10% of patients with very durable results, disease free up to 20 years.[73] This led the U.S.

Food and Drug Administration (FDA) to approve the use of HD IL-2 to treat mRCC in 1992. HD IL-2 is defined as a dose of 720,000 IU/kg administered intravenously over 15 minutes every 8 h as tolerated up to a maximum of 12 doses. Although HD IL-2 has cured a small percentage of patients, the treatment is limited based on health status. Since high dose IL-2 produces high grade toxicities, it is reserved for those individuals with healthy organ function.[74] Since IL-2 administered alone has displayed a high response rate, there have been several attempts to increase the efficacy of IL-2 by either adjusting the dosages or by combining IL-2 with other agents, most notably interferon alpha (INF-α). Because of the increased toxicities associated with the combination, without survival benefit, these studies proved not to be more advantageous than HD IL-2 administered alone[74]

1.4.3 Targeted Therapy

1.4.3.1 VEGF Inhibitors

Increased understanding of the molecular biology and pathogenesis of RCC has led to several targeted therapeutic approaches. The most notable of these is the discovery of the VHL tumor suppressor gene role in the plausible causation of RCC through the HIF pathway. During normoxia in the blood, the VHL protein complex regulates proteasome mediated degradation of HIF-α. Loss of function of the VHL protein causes accumulation of HIF-α and the resultant overexpression of a number angiogenic growth factors such as vascular endothelial growth factor (VEGF) and platelet derived growth factor (PDGF).[58] VEGF is a growth factor that binds to a family of VEGF receptors

(VGFR). The VEGFR consists of a membrane receptor and an intracellular tyrosine kinase domain. Binding to the receptor causes growth and migration of endothelial cells. Overexpression of VEGF and subsequent binding to the VEGFR can lead to over-proliferation of endothelial cells. This discovery has led to the development of VEGF ligand and receptor binding antibodies and tyrosine kinase inhibitors that block the action of VEGFR in RCC.

Bevacizumab is a humanized recombinant monoclonal antibody developed from murine anti-VEGF.[75] Bevacizumab acts by preventing the binding of VEGF to VEGFR. There were two large phase III clinical trials that compared the safety and efficacy of bevacizumab. In the first trial (the AVOREN trial), 649 patients from 18 countries were randomized 1:1 to either interferon plus 10 mg/kg bevacizumab every two weeks or interferon plus placebo. The results of the trial showed that the progression free survival (PFS) was increased in the bevacizumab arm compared to the interferon/placebo arm (10.2 months compared to 5.4 months, P = 0.0001).In addition, the partial responses were greater in the bevacizumab arm (31% vs 13%) although the overall survival was not different between the two arms (23.3 vs 21.3 months, P = 0.1291). The Cancer and Leukemia Group B (CALGB) 90206 trial was the second randomized trial. This trial enrolled 732 persons with mRCC that were administered interferon plus bevacizumab or interferon alone. The results of this trial were similar to the first trial. The PFS of the interferon plus bevacizumab arm was longer than the interferon alone arm.[76] The results of these data led to the FDA approval of bevacizumab for the treatment of RCC in 2009. Bevacizumab is the first VEGFR monoclonal antibody approved for the use in RCC. In

addition, there are three VEGFR tyrosine kinase inhibits that have been recently approved by the FDA for the use in RCC.[77] These are sunitinib, sorafenib and pazopanib.

Sunitinib is an inhibitor of VEGFR tyrosine kinase as well as other tyrosine kinases.[75,78] In a phase III clinical trial, 759 patients were administered either 50 mg/day sunitinib only for six weeks or interferon alpha (IFN-α) three times a week for three weeks. An increase in objective response rate (47 vs 12%), PFS (11 vs 5 months, HR= 0.54) and overall survival (26.4 vs 21.8 months, HR= 0.82, 95% CI 0.67 – 1.00, p=0.051) was seen in the sunitinib arm.[79] Sorafenib is an orally administered small molecule inhibitor of VEGFR and other tyrosine kinases.[75] Sorafenib has shown clinical activity in a phase III, randomized double-blind trial in which 903 patients who failed previous chemotherapy were randomized to receive either sorafenib or placebo.[80-82] The results of this trial showed that the PFS was significantly longer in those receiving sorafenib (5.5 vs 2.8 months, HR 0.44, 95% CI 0.35 – 0.55) while the overall survival was not significantly prolonged (17.8 vs 15.2 months, HR 0.88, 95% CI 0.74 – 1.04).[81] Pazopanib is another oral VEGFR tyrosine kinase inhibitor that also inhibits other tyrosine kinases. A phase III trial of pazopanib vs placebo in 435 patients demonstrated a significant increase in progression free survival with the patients that received pazopanib (9.2 vs 4.2 months, HR 0.46, 95% CI 0.34 - 0.62). Although an increase in survival was not seen (22.9 vs 20.5 months, HR 0.91, 95% CI 0.71 – 1.16).[83]

1.4.3.2 mTOR Inhibitors

Another pathway recently discovered pathway involved in RCC tumorigenesis is the serine/threonine kinase mammalian target of rapamycin (mTOR) pathway. mTOR is ubiquitously expressed in mammalian cells and is involved in cell metabolism and

protein synthesis, and frequent hyperactivation of the mTOR pathway has been found in human malignancies.[84,85] mTOR is involved in two separate protein complexes, mTORC1 and mTORC2. These protein complexes differ on their protein constituents except for the mTOR tyrosine kinase itself. Activation of the mTORC1 pathway leads to the production of many proteins such as cyclin D1, c-MYC and HIF-α that are responsible for cell cycle progression.[84] The function of mTORC2 is less understood, however, it too activates HIF-α. The overexpression of HIF-α is known to occur in RCC.

The drug rapamycin (sirolimus) is an antifungal antibiotic that was isolated from bacteria in the 1970s.[77] In addition, rapamycin proved to inhibit T cell function. This led to its use as an immunosuppressant drug for organ transplantation. Rapamycin has also displayed antitumor activity. Analogs of rapamycin have been developed to increase bioavailability. These analogs are termed "rapalogs". Two rapalogs, temsirolimus and everolimus were approved by the FDA for the treatment of mRCC in 2007 and 2009, respectively.[84] Rapamycin and its analogs do not bind nor inhibit mTOR directly. They exhibit their activity by binding to FK-binding protein 12 (FKBP-12). The binding to FKBP-12 causes an inhibition in the kinase activity of mTORC1. It is also known that these compounds do not affect the mTORC2 complex nor its pathway.[77]

There have been many cancer clinical trials conducted using temsirolimus and everolimus.[85] The Global Advanced Renal Cell Carcinoma trial was a three armed phase III trial that compared the efficacy of either temsirolimus iv alone, temsirolimus iv plus IFN-α iv or IFN-α alone in 626 patients. The PFS was significantly longer in the arms that received temsirolimus (1.9 months for IFN-α, 3.7 months for temsirolimus alone and 3.8 months for the combination, $P<0.001$). However, the overall survival was not

significantly different (7.3 months for IFN-α, 8.4 months for temsirolimus alone, and 10.9 months for the combination). The Renal Cell Cancer Treatment with Oral Rad001 given daily (RECORD-1) trial was a phase III trial that enrolled 410 patients with mRCC. The aim of this trial was to test the efficacy of everolimus (RAD001) against placebo. Patients were randomized 2:1 to receive either 10 mg po daily everolimus or placebo. The median PFS for the everolimus group was 4.0 months compared to 1.9 months for the placebo group. The results from these trials led the FDA to approve these drugs for the treatment of mRCC. There have been efforts to combine the VEGFR inhibitors with the mTOR inhibitors. However, these trials were stopped due to toxicities even at low doses.[77]

In summary, there was a lot of optimism about treating mRCC with targeted agents. The discovery of pathways that led to the development of mRCC led to the tyrosine kinase inhibitors and the mTOR inhibitors described above. Although these agents often produce fewer side effects than conventional cytotoxic agents, the response from these agents are relatively short lived. Despite the efforts of clinicians and researchers, the five year survival rate remains poor. mRCC is one of the most resistant forms of cancer.

1.5 DRUG RESISTANCE IN RCC

Although most cancers become resistant to chemotherapy, mRCC is one of the most resistant of all cancers.[86] Traditional chemotherapeutic agents such as the alkylating agents, plant alkaloids and taxanes show very little activity against mRCC as

response rates with these agents are less than 4%. Drugs that are not affected by multidrug resistance proteins such as 5-fluorouracil have a response rate of 6%.[71] mRCC also develops resistance to the newer targeted therapeutics (i.e. VEGF and mTOR inhibitors). There are a number of factors that are thought to be involved in the drug resistance of mRCC, however, the reasons for drug resistance is not clear cut or fully understood.[87] The contributing factors that have been uncovered thus far that are thought to make mRCC resistant to therapy are multidrug resistance (MDR) proteins, including the major vault protein, and glutathione-s-transferase (GST).[88-94]

1.5.1 Multidrug Resistance Proteins

mRCC tumors arise from the proximal tubule cells. The proximal tubule is involved in the active transport of endogenous and xenobiotic substrates from the kidney into the urine. Not surprisingly, these cells are known to contain every class of drug transporters. Furthermore, these transporters are expressed at high levels.[95] The classes of transporters that are located in the renal epithelial cells are; the organic anion transporters (OATs), the ATP-binding cassette (ABC) family which include multidrug resistance proteins (MRPs) and the P-glycoprotein (Pgp), organic cation transporters (OCTs), the peptide transporters, and the nucleoside transporters.[95] Many of the chemotherapeutic agents that are used today are known substrates for these transporters. Of these transporters, the most widely studied in cancer pharmacology is the ABC family of transporters. The ABC transporter family consists of 48 genes and is subdivided into seven subfamilies. The subfamilies are named ABC-A to ABC-G. The Pgp (ABCB1) and the multidrug resistant protein 1 (MRP-1, ABCC1) are two of the most studied in this

family of transporters and probably play the largest role in the clearing of chemotherapeutic agents from renal cells.[89,90,95]

These ATP dependent efflux pumps have demonstrated the ability to remove a large number of different anti-neoplastic agents out of tumor cells. There is a correlation between high levels of these transporters and drug resistance in lung, pancreatic and breast cancer,[89] although the correlation of Pgp and MRP-1 levels and drug resistance in mRCC remains a little more uncertain. A study conduct by Gamelin et al. measured the mRNA expression and efflux capabilities of Pgp and MRP-1 in primary tumors and metastatic tumors from 19 patients. It was determined that the primary site had high levels of Pgp expression while the more differentiated tumors of the metastases had lower levels of Pgp. The study suggested that the Pgp levels and efflux in the metastatic samples analyzed were not sufficient to contribute to drug resistance in the tumors. In addition, they found that MRP-1 did not contribute to drug resistance in these tumors.[87] A more recent and larger study conducted by Walsh et al. assessed the levels of Pgp and MRP-1 in the primary RCC tumors of 95 patients. The method employed was a semi-quantitative immunohistochemical technique that was able to determine low, medium and high levels of protein expression. The study determined that all tumors had detectable levels of Pgp and MRP-1. Furthermore, a majority of tumors had moderate to high levels of both transporter presents.[89] A search of the literature backs the findings of the previous two studies. Primary RCC tumors have high levels of Pgp and MRP-1 levels while more differentiated tumors have lower levels of these transporters.[96-99] It may be that the primary tumors are resistant to chemotherapy in large part due to the high levels

of transporters in the tumor cells while more differentiated distant metastasis have other mechanisms of resistance that make them unresponsive to conventional chemotherapy.

Another possible mechanism of resistance in RCC may be in part due to the presence of the major vault protein (MVP) also known as the lung resistance related protein (LRP). LRP, which is located in the cytoplasma and nuclear membrane, has shown the ability for membrane trafficking, bidirectional nucleocytoplasmic exchange and transport of compounds.[88,93] It is thought that LRP acts to carry compounds out of the nucleus. LRP is known to transport a wider range of compounds than either Pgp or MRP-1, including platinum compounds. A positive correlation has been shown between the expression of LPR and resistance to a number of antineoplastic agents. Many studies have been conducted in various tumors to show the correlation of LPR and drug resistance, but very few have been conducted using RCC. One such study conducted by Hodorova et al. compared the expression of LPR in 47 RCC tumor samples. The study used immunohistochemistry to measure Pgp, MRP-1 and LPR protein expression in samples from patients who had not previously received any chemotherapy. The study determined that the protein expression of LPR was greater than that of both Pgp and MRP-1 in the tumor samples. In addition, it was determined that the more differentiated tumors had less Pgp expression, but had higher levels of LPR expression.[93] This study demonstrated that LPR may play a part in the resistance of RCC to drugs. It also implies that the drug resistance of more differentiated tumors may be due in part to LPR, although more studies have to be completed to lend credence to this theory.

1.5.2 Glutathione-s-Transferase

Another possible reason for the resistance of RCC to drugs is the presence of glutathione s-transferases (GSTs). The GSTs are a family of phase II enzymes that are involved in detoxifying environmental chemicals and endogenous compounds.[100] The GSTs are divided into seven different classes, Alpha, Mu, Pi, Omega, Theta, Zeta and microsomal, however, the human kidney is known to contain three isoforms, Alpha, Mu and Pi. GST Alpha is the predominant isoform in the proximal tubule where RCC is thought to be derived from.[101,102] GSTs have several functions. They detoxify potentially damaging electrophilic endogenous and exogenous compounds by catalyzing the conjugation of glutathione to electrophiles. The resulting conjugates are more polar and increase the excretion of the compound. In addition to being a detoxifying mechanism, the GSTs are involved in cellular signaling. The GSTs are involved in the c-Jun-N-terminal kinase (JNK), mitogen activated protein kinase (MAPK) and apoptosis signal-regulating kinase pathways. Cysteine residues on GSTs bind to kinases in these pathways and regulate apoptosis. Overexpression of GSTs, which happens frequently with chemotherapy, can cause suppression in these pathways which can lead to increased cell survival.[100,101]

In normal cells, GSTs prevents carcinogenesis by detoxifying exogenous chemicals. In tumor cells, however, the GSTs are thought to render chemotherapeutic agents inactive.[103] A wide variety of anti-neoplastic agents are substrates for the GSTs and have been shown to be detoxified by the GSTs.[101] Furthermore, overexpression of GSTs and high levels of glutathione in various tumor types such as lung and breast are linked to multidrug resistance.[101] In the past 20 plus years there have been a number of

studies that have tried to determine the mRNA and protein expression levels and/or the enzyme activity of GST in RCC tumors. These studies have used northern blots, enzyme assays, immunoblots and immunohistochemical assays. Most of the studies conducted in the 1990s found decreased levels of expression and/or enzyme activity of GST in RCC compared to adjacent normal kidney tissue.[104-109] A more recent study, however, that used cDNA microarray chips to measure mRNA and antibody to measure protein expression in 70 RCC tumors (clear cell n = 43, papillary n = 6, oncocytoma n = 8, other n = 9) found GST Alpha to be over expressed in a majority of RCC samples that were clear cell tumors, while the other types of tumor cells did not have high levels of GST Alpha.[102] The more recent study differentiated tumor types where earlier studies did not differentiate between different tumor types. In summary it appears that there are conflicting results regarding the contribution of GSTs to the drug resistance displayed in RCC. It may be that RCC tumors that are of the clear cell type are partly resistant to drug therapy due to high levels of GSTs.

1.5.3 Topoisomerase

Another possible mechanism of multidrug resistance in RCC may be due to decreased levels of Topoisomerase-II alpha (TOPO-IIα).[110] However, it appears again that the results of the studies that have analyzed the correlation of these enzymes in RCC with regards to drug resistance are conflicting at least with TOPO-IIα.

TOPO-IIα is an enzyme that catalyzes the breaking and rejoining of DNA in order to straighten the DNA for many different cellular functions such as replication and

transcription.[111] It has been shown that expression of TOPO-IIα is increased in cells that are in a growth and replicating phase.[112] There are a number of antineoplastic agents such as doxorubicin and etoposide that target TOPO-IIα. There is evidence that suggests that cell lines that over express TOPO-IIα are hypersensitive to TOPO-IIα inhibitors.[113,114] Also, there is evidence that renal carcinoma cell lines that express low levels of TOPO-IIα are more resistant to TOPO-IIα inhibitors.[115] It also has been determined that the level of protein expression of TOPO-IIα in primary breast carcinoma tissue and bladder cancer tissue increase with increasing tumor grade.[116] However, there are conflicting reports in regards to TOPO-IIα expression in RCC tumors. A study conducted by Dekel et al. examined the TOPO-IIα protein expression in 27 RCC clear cell tumors from patients. They classified the tumors into different grades. They found that the TOPO-IIα protein levels increased greatly with increasing tumor grade.[111] Conversely, another study conducted by Oudard *et al*. examined the TOPO-IIα gene expression of 30 RCC tumors along with the adjacent normal tissue from 16 of the tumor biopsies. They found no significant difference in the expression levels of TOPO-IIα between the tumor samples and the normal adjacent tissues.[110] It should be noted that the authors of both studies claim that their sample sizes were small, and larger studies are required to confirm their findings. It may be that the level of TOPO-IIα plays a part in the drug resistance of RCC especially with regards to TOPO-IIα inhibitors. The TOPO-IIα inhibitors have had very little success against RCC with response rates between 4 and 6%.[71]

1.5.4 Resistance to Molecular Targeted Drugs

Drugs that target the VEGF and mTOR pathways have become the first choice when treating patients with mRCC that do not respond to IL-2 therapy. These targeted agents have shown activity especially in those who have clear cell renal carcinoma. Although these agents do show activity, the response is generally not durable and short-lived. The reason for the short-lived activity of these targeted therapies is thought to be due to the tumor's ability to develop resistance. It has been shown that treatment with the VEGF inhibitor sorafenib causes a decrease in tumor vascularization shortly after the start of treatment.[117] The tumor vascularization however, does return suggesting that alternative pathways less dependent on VEGF are activated in response to VEGF inhibition. Proteins have been identified that are modulated due to VEGF inhibition. Some of the proteins that have been identified are fibroblast growth factor, angiopoietin family proteins, interleukin-8 and placental growth factor.[118]

Temsirolimus and everolimus are the two mTOR inhibitors that have been approved for the use for mRCC. The response to these agents however, is also short-lived. These compounds inhibit the mTORC1 protein complex which acts to inhibit HIF-α and reduce tumor angiogenesis. The resistance developed to these agents is thought to be due to the lack of activity against the mTORC2 protein complex. The mTOR 2 protein complex can also cause over expression of HIF-α which can lead to tumor growth.[84]

In summary, there has been a lot of excitement recently in regards to the treatment of mRCC with the advent of the VEGFR and mTOR inhibitors and these agents have become the first line of treatment in individuals who are not able to tolerate or do not show activity with the use of IL-2. The therapeutic response generated by these agents,

however, is short-lived and are generally not durable. There is a need for new therapeutic agents for the treatment of mRCC.

1.6 ALTERNATIVE TREATMENTS FOR RCC

1.6.1 Bone Marrow Transplantation

Allogeneic bone marrow transplantation has been performed on patients with mRCC that did not respond to conventional treatment. The results of these trials proved that the toxicities involved and the limited applicability of this approach reduced its usefulness as only a small percentage of patients achieved a response to treatment.[119,120]

1.6.2 Tumor Vaccine

The development of a vaccine for the treatment of mRCC is currently being explored.[74] The early tumor vaccine trials used tumor lysates or irradiated tumors in order to induce an immunologic antitumor response. The results from these trials so far have been mixed. The first clinical trial using this type of tumor vaccine proved to be ineffective as there was not an increase in overall survival.[121] A recent review by Brokman-May et al. examined the results from the vaccine clinical trials in RCC conducted from 2002 to 2010, and reported a low response rate. [122]

1.6.3 Alkylating agents for the treatment of renal cell carcinoma

Alkylating agents act by attaching an alky group to DNA. This causes an interruption of DNA replication and leads to cell death. There are a number of alkylating agents used in the treatment of cancer. However, as previously explained in section 1.4.1, alkylating agents such chlorambucil, melphalan and busulfan have been used in the treatment of RCC but the response rate was less than 6 percent.

1.7 IDENTIFICATION OF BENZALDEHYDE DIMETHANE SULFONATE FOR THE TREATMENT IN RENAL CELL CARCINOMA

Benzaldehyde dimethane sulfonate (BEN, DMS612, NSC281612) (Figure 4) was selected by the National Cancer Institute (NCI) from the NCI drug screen data base which consists of over 80,000 cytotoxic agents. The selection was because BEN exhibited *in vitro* activity against renal lung cancer cell lines in the NCI 60 cell line panel.[123] The NCI 60 cell line consists of leukemia, melanoma, lung, colon, renal, breast, and prostate cancer cell lines. BEN is from a family of dimethane sulfonates (Figure 5) that showed activity against lung and renal cancer cell lines.

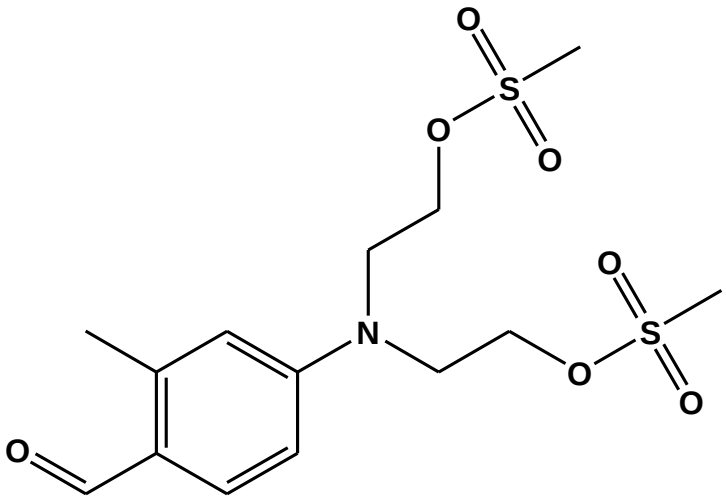

Figure 4. Benzaldehyde dimethane sulfonate

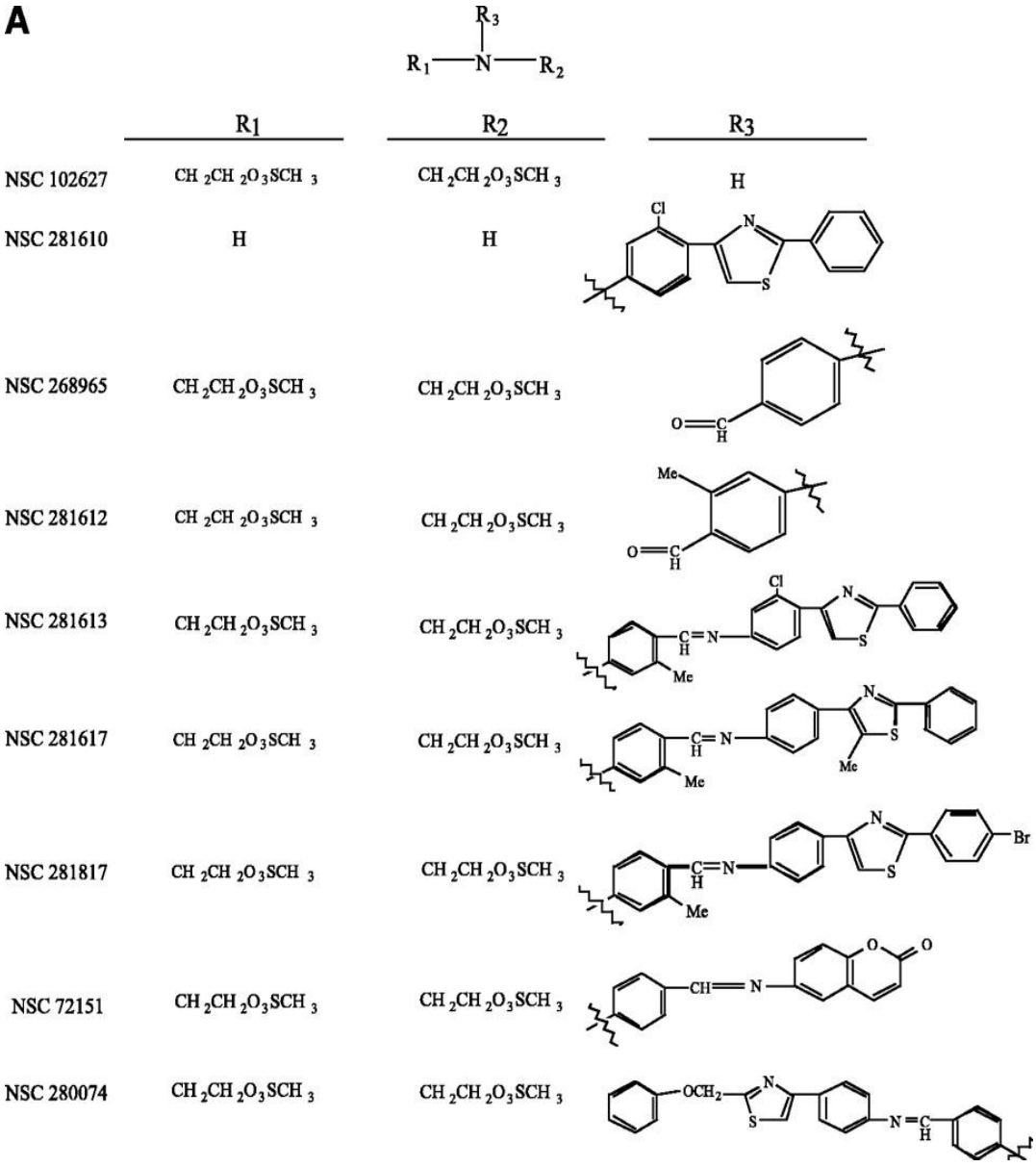

Figure 5. Structures of BEN (NSC281612) and related compounds. The dimethane sulfonate alone is NSC 102627. R_1 and R_2 are predicted alkylating groups while R_3 is a hydrophobic moiety. (Reprinted from Molecular Cancer Therapeutics with permission from American Association for Cancer Research©).[124]

Two dimethane sulfonates that displayed activity against RCC were NSC281617 and 281817. It was discovered however, that these compounds quickly dissociated in aqueous solution into an inactive aniline compound (NSC 281610) and an active aldehyde compound (BEN, NSC281612) which displayed activity against the NCI 60 cell line screen (Figure 6).

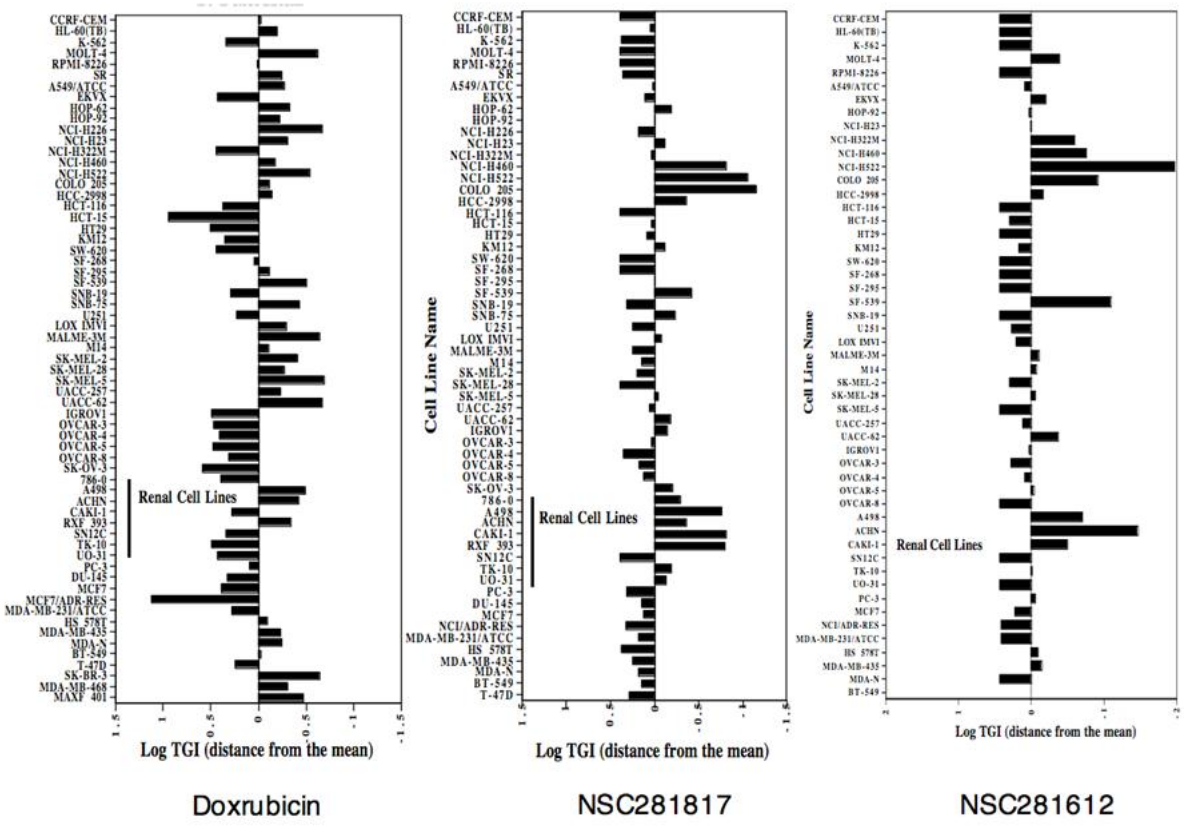

Figure 6. The fingerprint of BEN (NSC281612), NSC281817 and doxorubicin obtained from the 60 cell line NCI panel, with the mean IC_{50} for all cell lines tested plotted as the center of each bar graph and the deviation from the mean provided as a bar for each cell line, with bars to the left and to the right indicating resistance and sensitivity, respectively. (Reprinted with permission from Dr. Susan D. Mertins PhD)

1.7.1 The mechanism of action of BEN

A number of studies were conducted in order to determine the mechanism of action of BEN and related dimethane sulfonates. These studies include COMPARE analysis, DNA-protein crosslinking, P53 induction experiments, sperm DNA denaturing assay and cell cycle arresting assay. In addition, BEN was analyzed and compared to other compounds using Self-Organizing Maps (SOM).

The dimethane sulfonates have a hydrophobic moiety attached to a predicted alkylating group (Figure 4). It has been previously shown that the cytotoxicity pattern in the NCI 60 cell line screen can be used to compare the mechanism of action of various compounds by using the COMPARE algorithm.[125] A COMPARE analysis was conducted that calculates the Pearson Correlation Coefficient between the IC_{50} of dimethane sulfonates with IC_{50}s of chosen compounds in the NCI database. Similarities were found amongst the dimethane sulfonates along with the alkylating agents Yoshi 864 (NSC 102627), busulfan (NSC750), chlorambucil (NSC3088), and melphalan (NSC8806) however, there was little similarity to the alkylating agent carmustine (NSC409962) (Figure 7). In order to obtain a unique fingerprint to the non-alkylating portion of the dimethane sulfonates, a COMPARE analysis was made after subtracting the component of the correlation attributed to the alkylating agent moiety. The same COMPARE analysis was made with Yoshi 864 (NSC 102627), busulfan (NSC 750), chlorambucil (NSC 3088), melphalan (NSC 8806) and carmustine (NSC 409962) (Figure 8). The analysis showed that when the alkylating moiety was removed, BEN had very little correlation with the other alkylating agents. In addition, BEN had very little similarity with the other dimethane sulfonates.

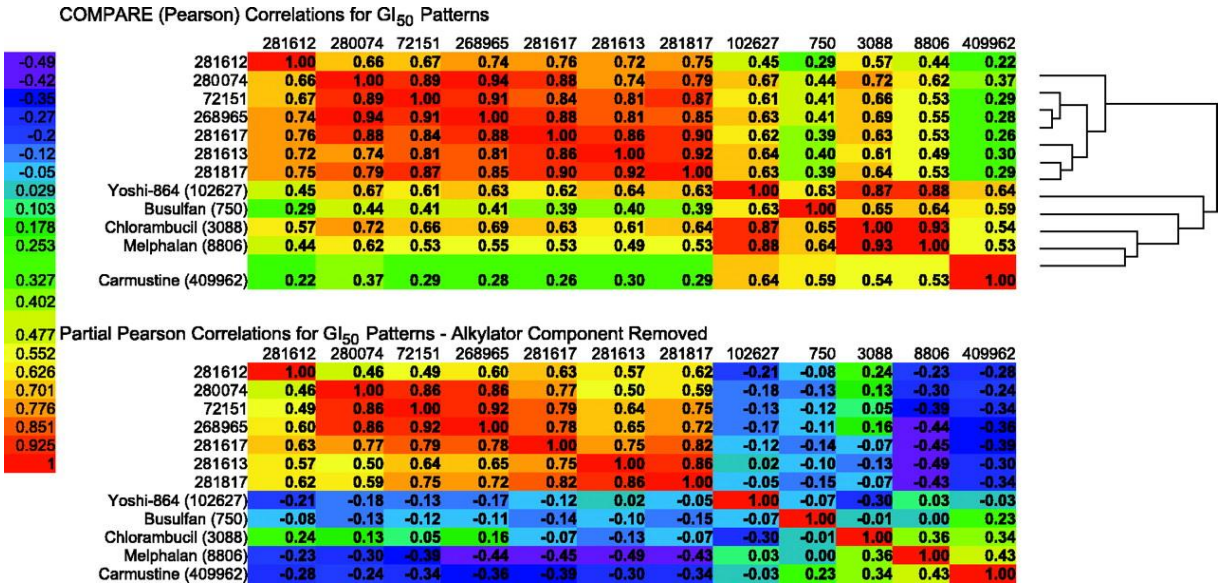

Figure 7. COMPARE analysis of Dimethane Sulfonates with various alkylating agents. Top: GI_{50} (IC_{50}) patterns of whole compound. Bottom: GI_{50} (IC_{50}) pattern without alkylator. (Reprinted from Molecular Cancer Therapeutics with permission from American Association for Cancer Research©).[124]

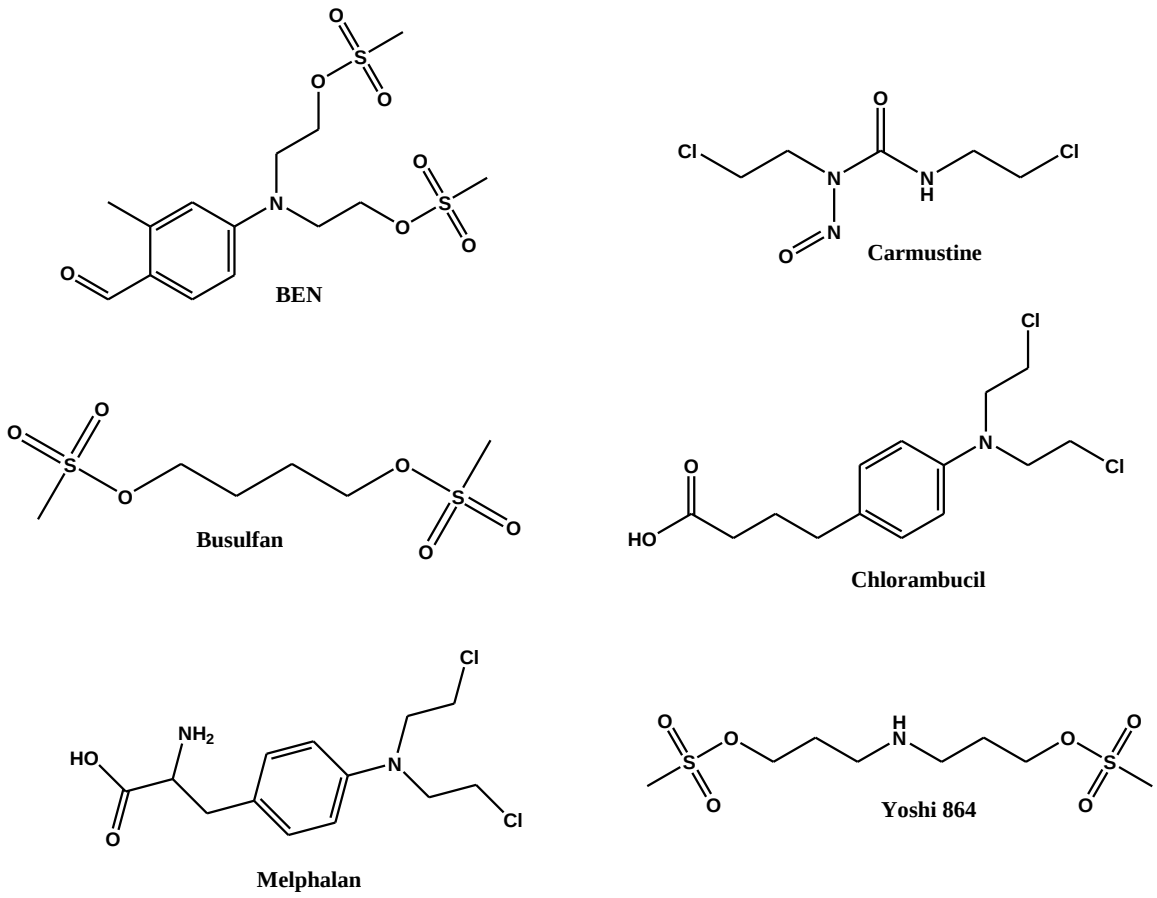

Figure 8. The structures of BEN compared to other alkylating agents.

In summary, the COMPARE analysis determined that BEN had a similar cytotoxic fingerprint to alkylating agents, with greatest similarity to the nitrogen mustards and the least to carmustine.

A number of experiments were conducted by Mertins et al. to determine the possible mechanism of action of BEN and the dimethane sulfonates.[124] The authors found that the dimethane sulfonates induced DNA-protein crosslinks, induced P53, and caused cell cycle arrest. These experiments showed that BEN possessed a similar mechanism of action as alkylating agents except for the fact that BEN has displayed

activity against renal cell carcinoma where as other alkylating agents do not have activity against these cells.

Self-Organizing Maps (SOM) are used to create clustering patterned data.[126] SOM are used to analyze IC_{50} data obtained from the NCI 60 cell line screen. Compounds are arranged in three dimensional space based on IC_{50} data. This type of data allows for the comparison of similar agents that might not be apparent from a linear comparison and it allows the mechanism of action to become regionalized. Classes of anti-cancer drugs are regionalized based on mechanism. The regions consist of: the M region (mitosis), P region (phosphatase and kinase inhibitors), S region (nucleic acid targeting), and N region (membrane active compounds; ion channel inhibitors). The dimethane sulfonates cluster in a region near to, but separate from, the classical alkylating agents (Figure 9). This suggests that the dimethane sulfonates may have a different mechanism than the classical alkylators.

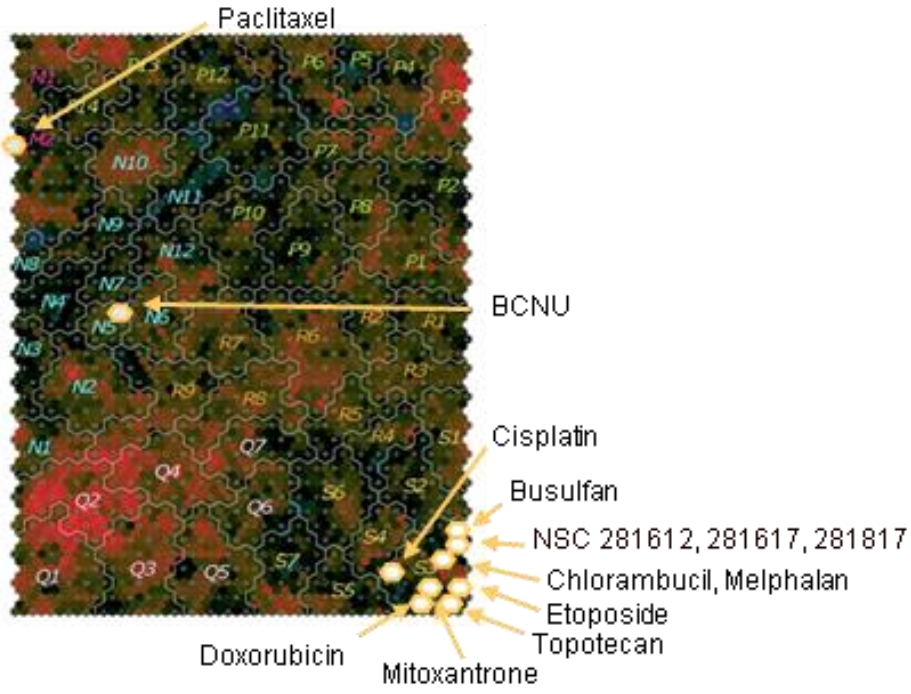

Figure 9. Self organizing map grouping GI50 fingerprints in the NCI Drug Screen data base (Reprinted with permission from Dr Susan D. Mertins PhD)

1.8 SUMMARY AND INTRODUCTION TO DISSERTATION

In 2011, 65,000 people acquired RCC in the United States and in the same year nearly 13,500 died from the disease.[2] In 2008, there were 270,000 cases and 116,000 deaths worldwide.[3] Despite recent advancements in the treatment of renal cell carcinoma (RCC) the 5 year survival remains poor. There is a need for new treatments of RCC.

Benzaldehyde dimethane sulfonate (BEN) has shown both *in vitro* and *in vivo* activity against RCC. This has led to the clinical development of BEN for the treatment

of RCC. BEN is a bifunctional alkylating agent. It was shown that the dimethane sulfonate groups are replaced by hydroxyl groups in aqueous medium.[127] It has not been determined if a similar occurrence takes place in biological media. If the degradation occurs, the activity of the resulting analytes against renal carcinoma cells is not known. In addition, the rate of the degradation of BEN in biological medium is currently not known. Also, the pharmacokinetics and metabolism of BEN is not known.

We hypothesized that BEN will undergo hydrolysis in blood to form less active products. We tested this hypothesis by characterizing the stability of BEN in both blood and plasma and determined the activity of degradation products in renal carcinoma cell lines (Chapter 2). During the stability testing we determined that BEN was metabolized in blood by aldehyde dehydrogenase (ALDH) to a carboxylic acid and that the acid was chemically converted into six different analogs which were less active than BEN . We determined the activity of BEN in renal cell carcinoma cell lines and characterized the metabolism of BEN in red blood cells (Chapter 3). We administered BEN to mice with and without the aldehyde dehydrogenase inhibitor disulfiram in order to characterize the pharmacokinetics of BEN and to determine if the exposure to BEN was increased after inhibition of ALDH (Chapter 4). Lastly, we determined the pharmacokinetics and metabolism of BEN administered to humans as part of a first in human phase I trial (Chapter 5).

2.0 *IN VITRO* AND *EX VIVO* CHARACTERIZATION OF BENZALDEHYDE DIMETHANE SULFONATE

Robert A. Parise, Bean N. Anyang, Julie L. Eiseman, Merrill J. Egorin, Joseph M. Covey, Jan H. Beumer, **Formation of active products of benzaldehyde dimethane sulfonate (NSC 281612, DMS612) in human blood and plasma and their activity against renal cell carcinoma lines.** Cancer Chemother Pharmacol. 2013 Jan;71(1):73-83.

2.1 ABSTRACT

Benzaldehyde dimethane sulfonate (BEN, DMS612, NSC281612) is a bifunctional alkylating agent with activity against renal cell carcinoma, and is being evaluated clinically. It was previously shown that BEN hydrolyzes in aqueous solution. We hypothesize that BEN will hydrolyze in human plasma to form potentially active compound. We developed an LC-MS/MS assay to detect and quantitate BEN and its metabolites/decomposition products in biological fluids. We tested the stability and degradation of BEN and benzoic acid dimethane sulfonate (BA) in plasma and blood. The assay was accurate, precise and reproducible. BEN and its metabolite BA were incubated in human blood and plasma at 37 °C or 4 °C. The generation and degradation of up to 12 analytes were monitored, and structures confirmed with available authentic standards. BEN was stable at both 4 °C and 37 °C, while BA was only stable at 4 °C. Lowering the pH of plasma greatly slowed the degradation of BA. The half-lives of BEN and BA in plasma were 220 and 4.8 min, respectively. Further, we determined the IC_{50} of BEN and BA, and revealed degradation products in five renal carcinoma cell lines. The IC_{50} for BEN was 5 to 500-fold lower than any of its products, while the cellular metabolic activity towards BEN correlated with ALDH activity and IC_{50}s. We detected six of the *in vitro* products and 6 glucuronides in murine plasma after iv dosing BEN. Most of the products have structures allowing continued ability to alkylate. The assay and knowledge of the stability and activity of BEN, BA and their products will be instrumental in the evaluation of the pharmacology of BEN in ongoing human trials.

2.2 INTRODUCTION

Approximately 13,000 people die from metastatic renal cell carcinoma (mRCC) in the United States every year.[2] Only 10-12% of patients achieve durable complete remission with high dose interleukin-2 therapy.[128] Agents targeting vascular endothelial growth factor and its receptor along with mTOR inhibitors have shown clinical activity.[94,129] However, responses to these agents are generally transient,[130] and there is a need for new treatment options for patients with mRCC.

Benzaldehyde dimethane sulfonate (BEN, DMS612, NSC281612) is one of a family of dimethane sulfonates that have demonstrated activity in the NCI 60 cell line screen. BEN is proposed to be a bifunctional alkylator with structural similarities to chlorambucil, busulfan and melphalan (Figure 10). However, unlike these compounds, BEN has specific activity against renal carcinoma cells in the NCI 60 cell line screen.[124] BEN causes cell cycle arrest in the G2-M phases,[124] and increases P53 levels, indicating DNA damage, in the renal carcinoma cell line 109, and in the breast cell line MCF-7. In addition, BEN has demonstrated antitumor activity in mice with orthotopic renal carcinoma xenografts, specifically, against human A498 and RXF-393 implanted subcutaneously or orthotopically under the renal capsule [Personal communication, Dr. M. Hollingshead, unpublished data].[131,132] The significant *in vitro* and *in vivo* activity against renal carcinoma has led to the ongoing evaluation of BEN in NCI-sponsored phase I clinical trials.

BEN, based on its structure, likely forms an aziridinium intermediate that is attacked by nucleophilic molecules such as DNA, proteins or water. Jumaa et al. reported hydrolysis of BEN in aqueous solution whereby the dimethane sulfonate groups are

replaced by hydroxy groups.[127] The hydrolysis of BEN, *in vivo* and *in vitro*, may lead to the formation of compounds that are less active as alkylating agents than BEN. In addition to BEN related analogues, we found benzoic acid (BA) analogues of BEN with their own reactivity.

In order to elucidate the pathways for decomposition and metabolism of BEN and to support ongoing clinical trials of BEN, we developed an LC-MS/MS assay for the detection and quantitation of BEN and its metabolites in plasma. Using this assay, we characterized the *in vitro* decomposition of BEN in plasma and blood, and compared the *in vitro* BEN products to products that were identified in the plasma from mice that were administered BEN. We suspect that aldehyde dehydrogenase (ALDH) in red blood cells is the enzyme responsible for the metabolism of BEN to BA and that BA may be the cytotoxic metabolite. Because BEN displays selective activity against renal cell carcinomas, we determined the IC_{50} of BEN and its metabolites in five different human renal carcinoma cell lines which were used in the NCI 60 cell line screen, and we correlated the metabolism of BEN to its carboxylic acid metabolite BA in renal carcinoma cells with the IC_{50} in these cells. The results of these studies will help to understand the activity of BEN and will aid in elucidating the pharmacology of BEN in the ongoing clinical trial.

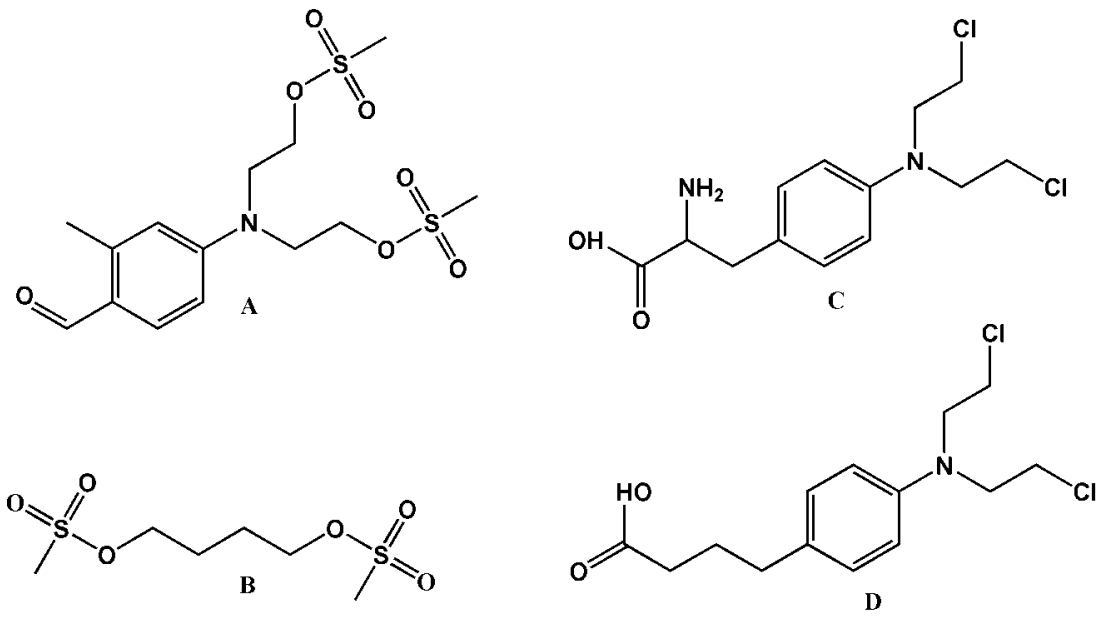

Figure 10. Chemical structures of BEN (A), busulfan (B), melphalan (C) and chlorambucil (D).

2.3 METHODS

2.3.1 Chemical and reagents

4-[bis[2-[(methylsulfonyl)-oxy]ethyl]amino]-2-methyl-benzaldehyde (BEN, NSC 281612), 4-[bis[2-[(methylsulfonyl)-oxy]ethyl]amino]-2-methyl-benzoic acid (BA, NSC 733609), 4-[bis[2-chloro-ethyl]amino]-2-methyl-benzaldehyde (BEN-Cl_2), 4-[bis[2-chloro-ethyl]amino]-2-methyl-benzoic acid (BA-Cl_2), 4-[bis[2-[(methylsulfonyl)-oxy]ethyl]amino]-benzaldehyde (desmethyl-BEN), and 4-[bis[2-chloro-ethyl]amino]-benzaldehyde (desmethyl-BEN-Cl_2) were obtained from the National Cancer Institute (NCI, Bethesda, MD). All solvents used for LC-MS/MS were high purity Burdick & Jackson and purchased from Fisher Scientific Co. (Fair Lawn, NJ). Formic acid was purchased from Sigma-Aldrich Chemical Co. (St. Louis, MO). Control human blood was obtained from the Central Blood Bank, Pittsburgh, PA and plasma was prepared by centrifugation of whole blood at 2000 x *g* at room temperature for 20 min. Nitrogen gas for the mass spectrometer was purified with a Parker Balston Nitrogen Generator (Haverhill, MA), and nitrogen gas for the sample evaporation was purchased from Valley National Gasses, Inc. (Pittsburgh, PA).

2.3.2 Generation of reference compounds

4-[bis[2-hydroxy-ethyl]amino]-2-methyl-benzaldehyde (BEN-$(OH)_2$ was generated by heating approximately 13.6 mg BEN in approximately 4 mL of 0.05 N aqueous NaOH for 48 h at 50 °C. The progression of the reaction was monitored by mass spectrometry. 4-[bis[2-hydroxy-ethyl]amino]-2-methyl-benzoic acid (BA-$(OH)_2$ was generated by heating approximately 13.2 mg BA in a solution of 0.03 N NaOH in 7 mL of acetonitrile/water (1:1, v/v) for 48 h at 50 ºC. The progression of the reaction was assessed by mass spectrometry and the conversion was 100% in both cases. The final solutions were neutralized with hydrochloric acid and acidified with formic acid for a final concentration of 1 mg/mL of the respective product.

2.3.3 Qualitative determination of metabolites

In order to determine the structures of the products generated by the *in vitro* decomposition experiments and by mice administered BEN, we established an LC-MS/MS system using both MS scan mode and enhanced product ion scan mode (EPI). The LC-MS/MS system consisted of an Agilent (Wilmington, DE, USA) 1200 SL thermostated autosampler, binary pump, DAD, thermal column compartment, and an ABI SCIEX (San Jose, CA, USA) 4000Q hybrid linear ion trap tandem mass spectrometer. The liquid chromatography was performed with a gradient mobile phase consisting of A: acetonitrile/0.1% formic acid (v/v) and B: water/0.1% formic acid (v/v). The mobile phase was pumped at a flow rate of 0.2 mL per minute and separation was achieved using

a Phenomenex (Torrance, CA) Hydro Synergi-RP 4 micron 100 x 2mm column. The gradient mobile phase was as follows: at time zero, solvent A was 15% and was increased linearly to 40% in twenty minutes. The percentage of solvent A was increased linearly to 80% at 21 minutes and the flow rate was increased to 0.4 mL. This was maintained for two minutes at which time solvent A was decreased linearly to 15% at 24 minutes. This was maintained for six minutes. The total run time was 30 minutes. During the first two minutes and the last six minutes of the LC run the flow leaving the column was diverted to waste. The parameters of the mass spectrometer were as follows; curtain gas 20, IS voltage 5500V, probe temperature 400 ºC, GS1 40, GS2 30, declustering potential 50V, collision energy 40V, collision energy spread of 10V, and scan rate of 1000 amu/sec.

2.3.4 Qualitative Analytical Method

This LC-MS/MS assay was modified to quantitate or monitor the metabolites generated in the decomposition study and in the mouse metabolism experiments. The instrumentation, mobile phase and column were the same as the qualitative method described above. First, BEN and BA were diluted to a concentration of 1 µg/mL in acetonitrile and each was continuously infused at a rate of 10 µL/min into the HPLC flow, which was an isocratic mobile phase of acetonitrile:water:formic acid (50:50:0.1, v/v/v) pumped at 0.2 mL/min. The tuning parameters of the mass spectrometer were adjusted to maximize the intensity of the $[M + H]^+$ ion of the analyte. After the largest $[M +H]^+$ ion was obtained, the mass spectrometer was operated in MRM mode and the

collision voltage was adjusted so that the largest product ion was determined. This procedure was repeated for BEN-Cl_2, BA, BA-Cl_2, BEN-$(OH)_2$, BA-$(OH)_2$ desmethyl-BEN, and desmethyl-BEN-Cl_2. For MRM transitions, see Table 1.

Table 1. MRM transitions and retention times of analytes.

Analyte	MRM transition	Internal Standard	Retention Time (min)
BEN[a]	380.0 → 160.0	Demethyl-BEN	15.5
BEN-OH-OSO_3	302.0 → 162.0	Demethyl-BEN	12.1
BEN-Cl_2[a]	260.0 → 120.0	Demethyl-BEN-Cl_2	22.4
BEN-Cl-OH	224.0 → 120.0	Demethyl-BEN	15.3
BEN-Cl-OSO_3	336.0 → 132.4	Demethyl-BEN	16.9
BEN-$(OH)_2$[a]	224.0 → 134.0	Demethyl-BEN	9.0
BA[a]	396.0 → 300.0	Demethyl-BEN	14.1
BA-OH-OSO_3	318.0 → 160.0	Demethyl-BEN	7.9
BA-Cl_2[a]	276.0 → 213.0	Demethyl-BEN-Cl_2	21.1
BA-Cl-OH	258.0 → 164.0	Demethyl-BEN	8.3
BA-Cl-OSO_3	336.0 → 132.4	Demethyl-BEN	16.9
BA-$(OH)_2$[a]	240.0 → 178.0	Demethyl-BEN	7.9
Demethyl-BEN (IS)	366.1 → 270.4	-	14.0
Demethyl-BEN-Cl_2 (IS)	246.1 → 106.4	-	20.9
BA-Gluc	572.0 → 300.0	Demethyl-BEN	10.9
BA-Cl_2-Gluc	452.0 → 276.0	Demethyl-BEN	15.4
BA-Cl-OH-Gluc	434.0 → 240.0	Demethyl-BEN	10.5
BA-OH-OSO_3	494.0 → 300.0	Demethyl-BEN	8.3
BA-$(OH)_2$-Gluc	416.0 → 300.0	Demethyl-BEN	5.6

2.3.4.1 Standard Curve

Stock solutions of BEN, BEN-Cl_2, BA, BA-Cl_2, BEN-$(OH)_2$ and BA-$(OH)_2$ were prepared separately at concentrations of 1.0 mg/ml in acetonitrile containing 0.1% formic acid. A mixture was made containing all six analytes at a concentration of 0.1 mg/ml by adding 100 µl of each analyte to 400 µl of acetonitrile with 0.1% formic acid. All stock solutions were stored at -80 °C in the dark. On assay days, this solution was diluted with acetonitrile to obtain the lower calibration working solutions of 0.01, and 0.001 mg/ml. These calibration working solutions were diluted in plasma with 2 M H_2SO_4 (5%, v/v) to produce 200-µl aliquots of the following concentrations: 10, 30, 100, 300, 500, 750, and 1000 ng/ml. Ten µL of a mixture of desmethyl-BEN and desmethyl-BEN-Cl_2 (1 µg/mL of both in acetonitrile) were added as internal standards. The analyte-to-internal standard ratio (response) was calculated for each standard by dividing the area of the compound peak area by the area of the compound's respective internal standard peak. Standard curves of each compound were constructed by plotting the analyte-to-internal standard ratio versus the nominal concentration of each analyte in each sample. Standard curves were fit by linear regression with weighting by $1/y^2$, without forcing the line through the origin, followed by the back-calculation of the concentrations. The deviations of these back-calculated concentrations from the nominal concentrations, expressed as percentage of the nominal concentration, reflected the assay performance over the concentration range studied.

2.3.4.2 Auto-sampler stability

In order to determine the stability of the compounds in the auto-sampler, we injected samples that contained 500 ng/ml of all six reference standards extracted from human plasma. The samples were reconstituted with acetonitrile:water (20:80), with either 5% 2M H_2SO_4 or 0.1% formic acid. The temperature of the autosampler was maintained at 4 °C, and 48 sequential injections were performed. The extent of decomposition at various times was assessed by comparing the peak area with the area observed at time zero.

2.3.5 Stability of BEN and products in human blood

We evaluated the stability of BEN, BEN-Cl_2, and BEN-$(OH)_2$ in blood (n=3). Each of the compounds was added separately to 10 mL of human blood (Central Blood Bank, Pittsburgh, PA, sodium citrate anti-coagulated) to achieve a concentration of 10 μg/mL. This was performed in triplicate. The samples were incubated in a shaking water bath at 37 ºC for 0, 5, 10, 15, 30, 45, 60, 120, 180, 240, 360 minutes, and 24, and 48 hours. At the specified time points, a 500 μL aliquot of blood was removed, and centrifuged at 12,000 x *g* for 2 minutes at 4 °C. Two hundred μL of the resultant plasma was removed and added to 10 μL 2M H_2SO4. The sample was briefly vortexed and 10 μL of internal standard solution and 1 mL of acetonitrile were added. The samples were then vortexed on a vortex genie on a setting of high for one minute, and then were centrifuged at 12,000 x g for 5 minutes. The resultant supernatant was blown to dryness at room temperature under a stream of nitrogen. The samples were reconstituted with 100 μL of

20:80 acetonitrile/H_2O with 5% 2 M H_2SO4 (v/v/v) and 10 µL was injected into the LC-MS/MS system. The extent of decomposition at various times was assessed by comparing the peak area with the area observed at time zero.

2.3.6 Stability of BEN, BA, and products in human plasma

BEN or BA was added to plasma to achieve a concentration of 10 µg/mL. Triple 200 µL aliquots were removed at the following time points: 0, 5, 15, 30, 60, 120, 180, and 240 minutes. The samples were immediately frozen at -80 ºC until they were analyzed by LC-MS/MS. The stability was assessed for each compound under the following conditions: room temperature, 4 ºC, with the addition of 5% (v/v) of either formic acid (95%) or 2 M H_2SO_4 to the plasma. Stability at each time point was evaluated relative to time zero.

2.3.7 BA degradation in phosphate buffered saline

To confirm that the observed degradation of BA in plasma was chemical, and did not require endogenous components in plasma, we compared the rate of decomposition of 10 µg/mL BA in plasma to the rate of degradation of BA in PBS with and without 50 mg/mL human albumin. Triplicate aliquots of 200 µL were taken at 5, 10, 15, 20, 25, and 30 minutes. The aliquots were added to a microcentrifuge tube that contained 10 µL of 2M H_2SO_4. The samples were then frozen at -80 °C until processed as described above.

2.3.8 Half-life of analytes

To determine the half-lives of the analytes in blood and plasma, we analyzed the data from the experiments with the software PK Solutions 2.0, using the log trapezoidal method (Summit Research Services, Montrose, CO; www.summitPK.com). In order to determine statistical parameters, half-lives and relative rates in PBS were determined by analysis of all the data with ADAPT5 based on a 1 compartmental model.[133]

2.3.9 Protein binding

In order to determine the protein binding of BA, a method used by Ehrsson et al. was modified and employed with the data generated in section 2.3.7.[134] They used their method to calculate the protein binding of chlorambucil to albumin using the equation $k_{obs} = k_1 f_{bound} + k_2 f_{free}$. Where k_1 is the rate constant of the degradation of compound that is bound to protein and k_2 is the rate of degradation of free compound. They found that free compound degrades approximately 100 times faster than bound compound. Our assumption is that only free compound is able to react with other material present in the matrices. The data generated was analyzed with Adapt 5.0 assuming first order elimination.

2.3.10 Cell Lines

Human renal carcinoma cell lines, ACHN, 786-0, A498, SN12K1 and CAKI-1 were obtained from the Developmental Therapeutics Program, Division of Cancer Treatment and Diagnosis, National Cancer Institute, National Institutes of Health (Bethesda, MD). Human non-small cell lung adenocarcinoma A549 cells for ALDH positive control were obtained from Dr. Pam Hershberger, University of Pittsburgh Cancer Institute (UPCI). Human colorectal carcinoma HCT116 cells used for ALDH negative control were obtained from Dr. Su-Shu Pan UPCI.

2.3.11 MTT assay

Human renal carcinoma cells (NCI, Bethesda, MD) were grown in RPMI 1640 complete medium containing 10% fetal bovine serum (FBS), containing penicillin and streptomycin at 37 ºC with 5% CO_2 at 95% humidity. On day 1, 100 µL of appropriate cell seeding density of each cell line was added to 96 well plates. SN12K1, CAKI-1 and A498 cells were plated at 2500 cells/well and, ACHN and 786-0 cells were plated at 1500 cells/well. Plates were incubated at 37 ºC at 5% CO_2 at 95% humidity. After 24 hours, BEN, BEN-Cl_2, BEN-$(OH)_2$ BA, BA-Cl_2 or BA-$(OH)_2$ was added to wells separately such that the final concentrations ranged between 1 and 30,000 ng/mL in medium containing 0.1% acetonitrile. The MTT assay was performed following the manufacturer's instructions using a TAC3 MTT cell proliferation assay (Trevigen, Gaithersburg, MD). As a control, acetonitrile 0.1% in medium was used. The absorbance

at 570 nm of each well was read on a Dynex NRX Revelation microplate reader (Dynex Technologies, Chantilly, VA). Readings from the quadruplicate wells for each treatment concentration were averaged and were compared with the average readings from wells containing vehicle-treated cells. The results were expressed as percentage of inhibition. The IC_{50}s of BEN and other products for each cell line were calculated from triplicate experiments using the Hill equation and the computer program ADAPT 5.

2.3.12 BEN metabolism in renal carcinoma cells

SNI2K1, ACHN, CAKI-1, 786-0 or A498 cells (3×10^5 cells) in logarithmic growth were plated separately into each well of 6-well culture plates in a total volume of 2 mL RPMI 1640 complete medium containing 10% FBS, penicillin and streptomycin. The cells were allowed to acclimate for 24 h and BEN was added to obtain a concentration of 1,000 ng/mL. 100 µL aliquot of cell medium was taken at 0, 2, 4, 6 and 24 hours. The aliquot was placed into a microcentrifuge tube that contained 5 µL 2M H_2SO_4. The sample was stored at -80 ºC until analysis.

2.3.13 Aldehyde dehydrogenase (ALDH) activity in renal carcinoma cells

SN12K1, A498, human colorectal HCT116, and human non-small cell lung cancer A549 cells were grown as described. Cells were harvested by scraping, washed with PBS and spun at 900 x g. Cells (1×10^8) were homogenized in 100 mM Tris HCl

buffer (pH 8.0) with a dounce homogenizer on ice. The resulting homogenate was centrifuged at 9,000 x g for 15 min at 4 ºC. The 9000 x g supernatant (300 µL) was added to 1.5 mL of 100 mM Tris HCl buffer pH 8.0, with 3 mM β-nicotinamide adenine dinucleotide (NAD), 4 mM acetaldehyde, 100 mM potassium chloride and 10 mM 2-mercaptoethanol. As a control, 9000 x g supernatants were added to the sample without the addition of acetaldehyde which served as the blank in the reaction. Absorbance at 340 nm was recorded for 5 min in a Beckman Coulter DU 640 spectrophotometer (Indianapolis, IN, USA) maintained at 37 ˚C. The rate of absorbance increase at 340 nm per minute was used to quantitate the reduction of NAD to NADH, which stochiometrically corresponds to the conversion of acetaldehyde to acetic acid. The activity is reported as the number of units per 1 x 10^7 cells. The experiment was performed thrice for each cell line.

2.3.14 *In vivo* products of BEN

In order to determine whether the products observed *in vitro* would be generated *in vivo*, we administered vehicle or BEN to mice. Mice were obtained and handled in accordance with the guide for the Care and Use of Laboratory Animals as previously described (Beumer et al., 2011).[135] Briefly described, mice were allowed to acclimate to the University of Pittsburgh Cancer Institute Animal Facility for ≥1 week before being used. To minimize infection, mice were maintained in micro-isolator cages in a separate room and handled in accordance with the Guide for the Care and Use of Laboratory

Animals (National Research Council, 1996) and on a protocol approved by the Institutional Animal Care and Use Committee of the University of Pittsburgh. Ventilation and air-flow were set to 12 changes per h. Room temperatures were regulated at 22 ± 1°C, and the rooms were kept on automatic 12-h light/dark cycles. Mice received Prolab ISOPRO RMH 3000 Irradiated Lab Diet (PMI Nutrition International, St. Louis, MO) and water ad libitum, except on the evening before dosing, when all food was removed. Adult female CD2F1 mice were administered 20 mg/kg i.v. bolus of BEN (2 mg/ml BEN in 50% hydroxyl-propyl-β-cyclodextrin in saline) or the 50% hydroxyl-propyl-β-cyclodextrin vehicle at 0.01 ml/g body weight. The mice were euthanized 30 minutes post dose. Blood was removed by cardiac puncture and the blood removed was immediately placed on ice. Plasma was obtained by centrifuging blood for 2 min at 14,000 x g at 4 ºC. A 200 µL aliquot of the resulting plasma was added to 10 µL 2M H_2SO_4 and frozen at -80 °C until analysis. Plasma obtained from the BEN-treated mouse was compared with plasma obtained from the vehicle-treated mouse.

2.4 RESULTS

2.4.1 Method development and performance

2.4.1.1 Chromatographic method

Our goal was to provide adequate separation for all 6 of the analytes and all the other possible products while minimizing the run-time. In order to achieve this, we

assessed three different columns; a Phenomenex Luna C18(2) 150 x 2 mm, Phenomenex Synergi 4µ Polar-RP 100 x 2 mm and a Phenomenex Synergi 4µ Hydro-RP 100 x 2 mm. In addition, the percentage of acetonitrile and water was varied over time. We found that the Synergi Hydro-RP and the gradient described above resulted in adequate separation with the shortest run time at 30 min. As expected, the BA analogs eluted before their respective BEN analogs, and modifications of the side chains resulted in the OH – OSO2CH3 – Cl elution order. We found that using two internal standards, desmethyl-BEN for the early eluting compounds and desmethyl-BEN-Cl_2 for later eluting peaks, resulted in a more precise and reproducible assay. A representative chromatogram is shown in Figure 11.

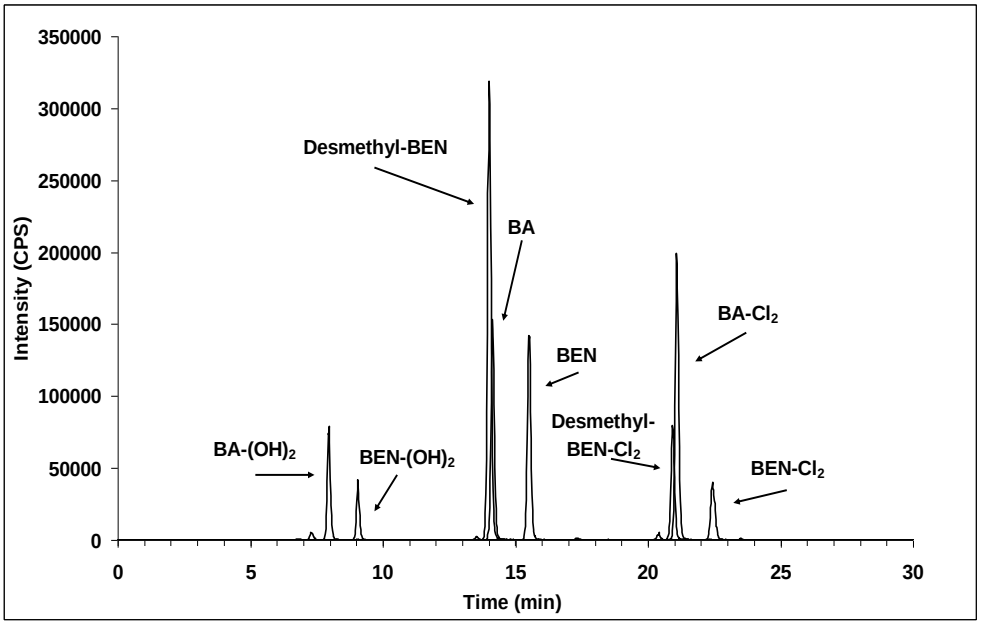

Figure 11. Representative LC-MS/MS chromatogram of BEN, BA, BEN-Cl_2, BA-Cl_2, BEN-$(OH)_2$, BA-Cl_2 and internal standards (Desmethyl-BEN and Desmethyl-BEN-Cl_2).

2.4.2 Plasma calibration curve and lower limit of quantitation (LLOQ)

The assay proved to be linear and had regression coefficients >0.989 for each of the three standard curves for each analyte. The lower limit of quantitation (LLOQ) was 1 ng/mL for BEN, BEN-Cl_2, BA, BA-Cl_2 and BA-OH_2 and 10 ng/mL for BEN-OH_2, at a signal-to-noise>10. The assay was accurate and precise with CV%< 15% at all concentrations. The mean and standard deviations of the back-calculated values in the standard curves of each analyte are displayed in Table 2.

Table 2. Accuracy and precision of BEN, BEN-Cl_2, BA, BA-Cl_2 and BA-OH_2 from 1 to 1000 ng/mL and 10 to 1000 ng/mL for BEN-OH_2.

Analyte	Accuracy (%)	Intra-assay precision (%)	Inter-assay precision (%)
BEN	92.3-111.8	3.1-14.4	4.0-12.9
BA	98.4-107.0	1.8-8.6	2.4-12.6
BEN-Cl_2	93.6-109.9	1.5-9.0	2.7-11.3
BA-Cl_2	91.9-116.1	2.8-11.0	3.0-14.1
BEN-$(OH)_2$	98.4-105.8	1.8-7.0	2.4-9.4
BA-$(OH)_2$	92.7-110.3	2.4-6.8	4.6-9.3

2.4.3 Autosampler stability

Analytes, neat or extracted from plasma, decomposed in the autosampler after reconstitution in acetonitrile or water. We found that 5% (v/v) of 2 M H_2SO_4 slowed down decomposition sufficiently to allow quantitation. The % loss after 48 sequential injections over 24 h in the presence of acid was: BEN 4.6%; BEN-Cl_2 6.3%; BEN-$(OH)_2$ 9.3%; BA 5.2%; BA-Cl_2 2.2%; and BA-$(OH)_2$ 4.0%.

2.4.4 Plasma stability

After 4 h at 4 °C in plasma, BEN and BA had not degraded (100% and 102% remaining), respectively, relative to time 0 h. At 37 ºC, while 92% of BEN was intact, only < 1% for BA remained intact. At 37 ºC with 2 M H_2SO_4 (5% v/v) the degradation of BEN and BA in plasma was slowed and the amounts of BEN and BA remaining after 4 h were 105% and 91%, respectively, see Figure 12.

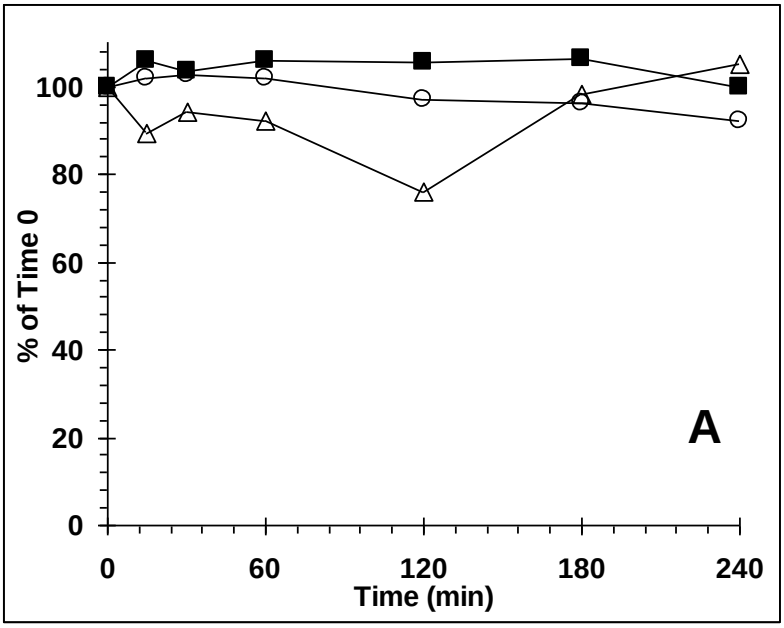

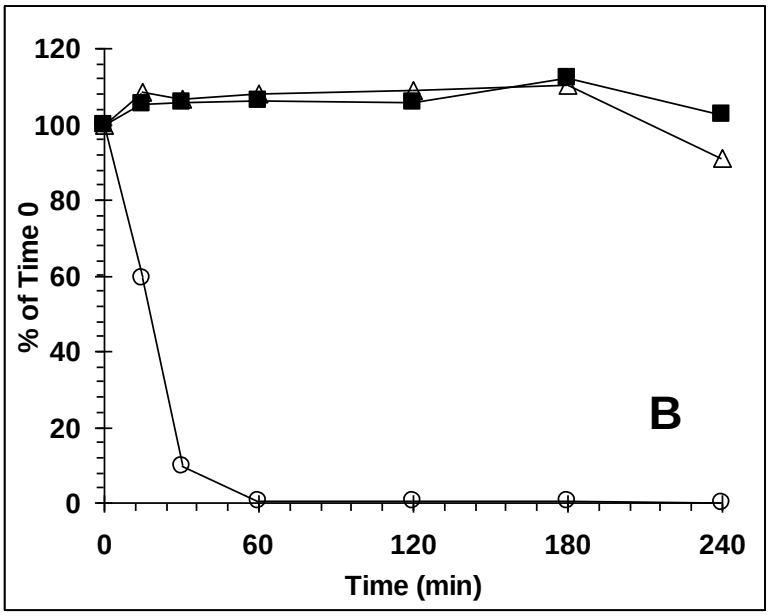

Figure 12. Stability of BEN (A) and BA (B) in plasma at room temperature (○), 4 °C (■), and at room temperature with 5% (v/v) 2 M sulphuric acid (Δ).

2.4.5 Incubation of BEN and products in human blood

In whole blood at 37° C, BEN had an overall apparent half-life of 18 min. BEN decomposed into at least eleven different products that were structural analogs of either BEN or BA. In addition, the BA analogs had peak areas much larger than the BEN analogs. These compounds were identified by LC-MS/MS and their structures are depicted in Figure 13.

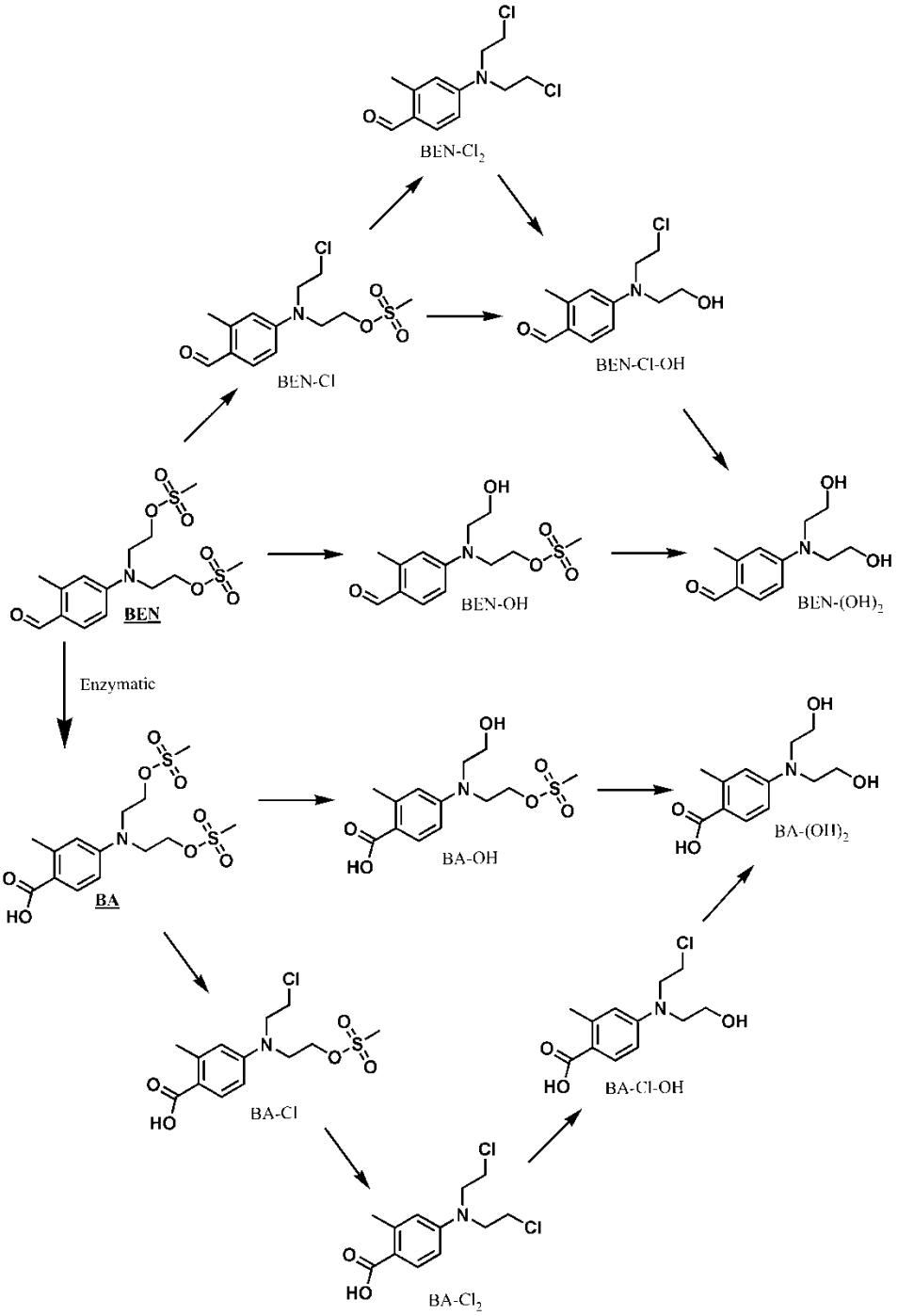

Figure 13. Proposed metabolic scheme for BEN in blood. BEN analogs can also be converted to their corresponding BA analogue. In plasma there is no conversion of BEN to BA. BEN is converted only to BEN analogs and BA is converted to BA analogs, respectively.

For both BEN and BA, we observed and structurally elucidated products in which one or both of the methane sulfonate leaving groups was replaced by either a chlorine (from plasma chloride ions) or hydroxyl (from plasma water) moiety, resulting in a total of 12 analytes, including parent compounds. We quantitated the absolute amount for compounds where standards were available or we used the peak area/IS area ratio for compounds in which standards were not available (Figure 14 and Figure 15).

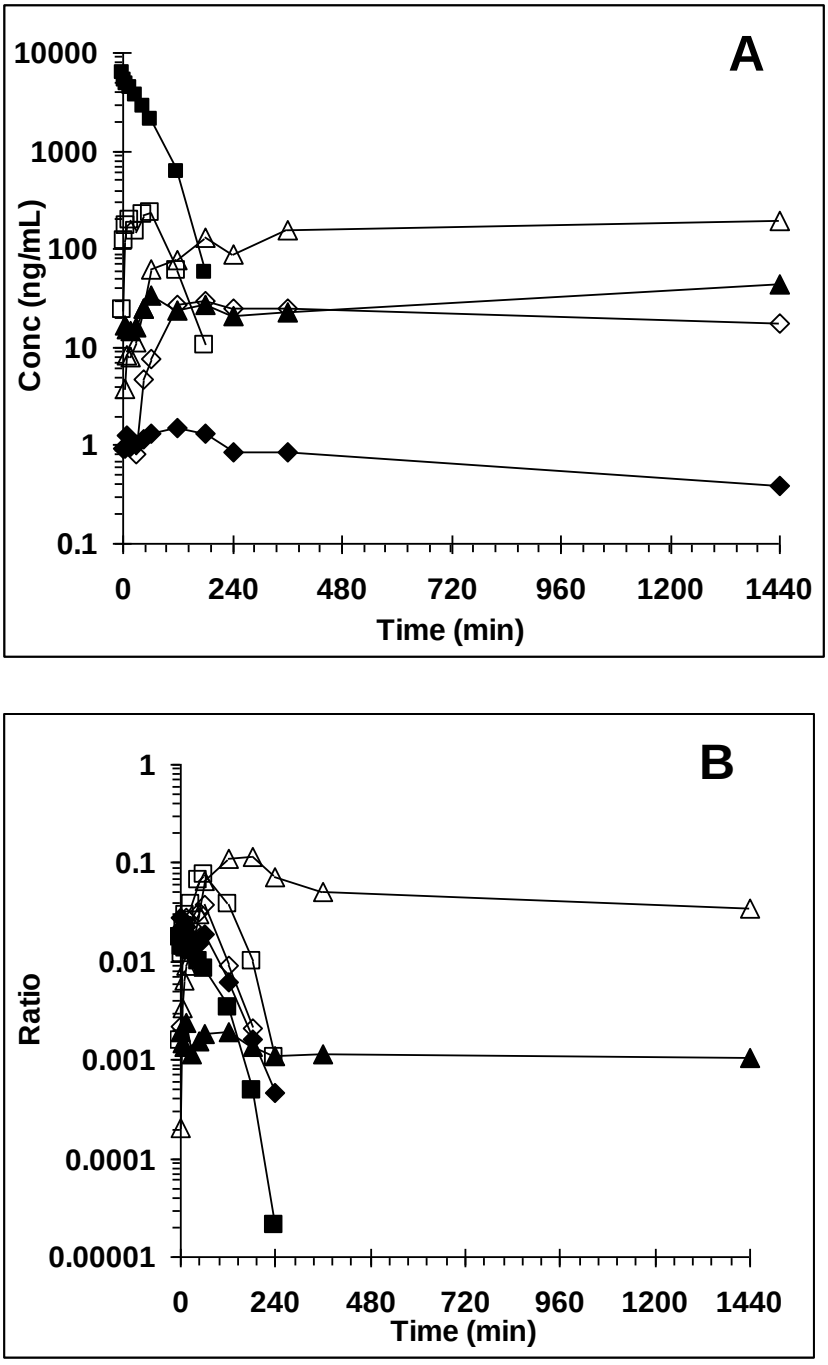

Figure 14. The disappearance of BEN in whole blood at 37° C from 0 to 1440 minutes. A: BEN (■), BEN-Cl_2 (♦), BEN-$(OH)_2$ (▲), BA (□), BA-Cl_2 (◊) and BA-$(OH)_2$ (Δ). B: BEN-Cl (■), BEN-OH (♦), BEN-Cl-OH (▲), BA-Cl (□), BA-OH (◊) and BA-Cl-OH (Δ)

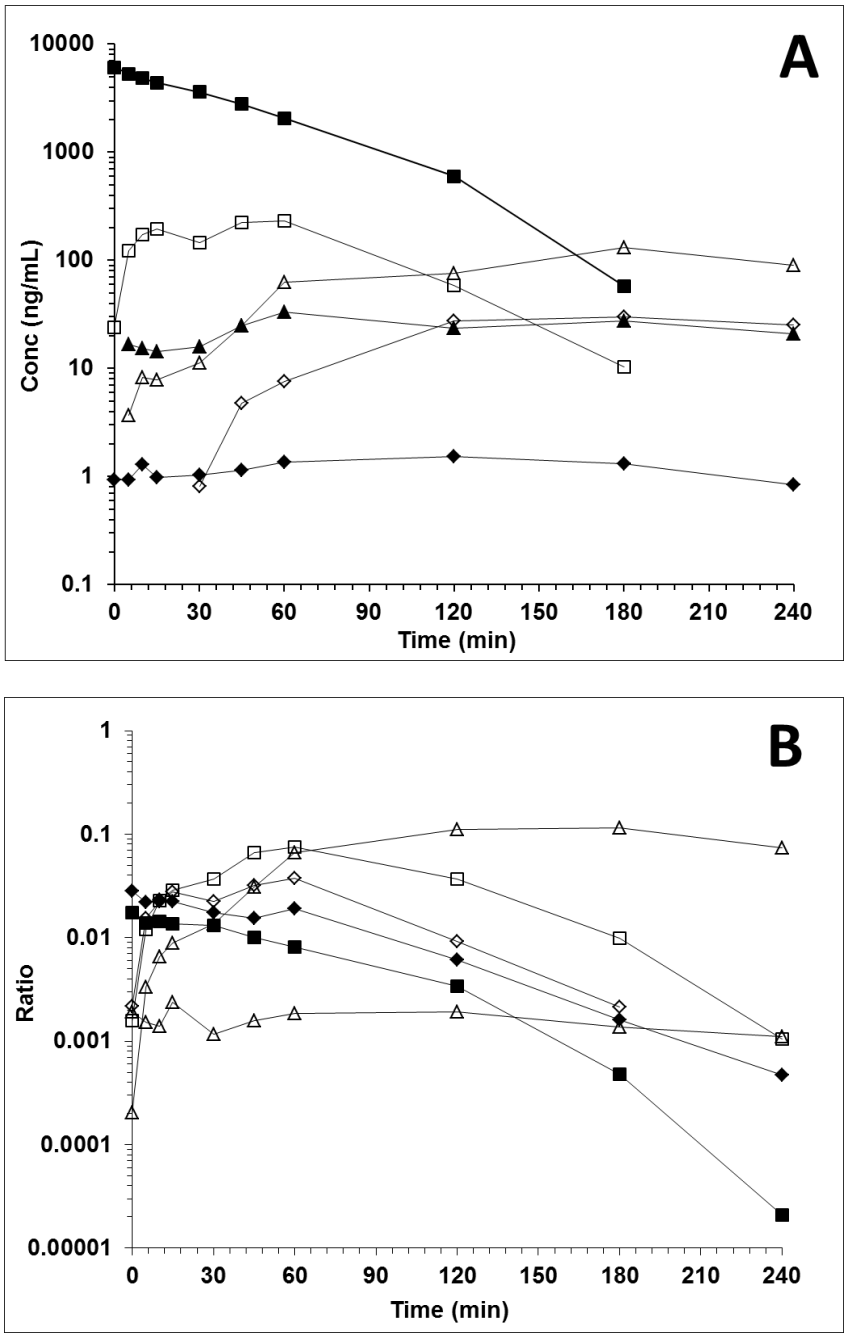

Figure 15. The disappearance of BEN in whole blood at 37° C from 0 to 240 minutes. A: BEN (■), BEN-Cl_2 (♦), BEN-$(OH)_2$ (▲), BA (□), BA-Cl_2 (◊) and BA-$(OH)_2$ (Δ). B: BEN-Cl (■), BEN-OH (♦), BEN-Cl-OH (▲), BA-Cl (□), BA-OH (◊) and BA-Cl-OH (Δ)

In addition, BEN-Cl_2, BA-Cl_2 and BEN-$(OH)_2$ were also incubated separately and their conversion to respective products was determined. When BEN-Cl_2 was placed into blood, BA-Cl_2 and BA-$(OH)_2$ were detected. The addition of either BA-Cl_2 or BEN-$(OH)_2$ to blood resulted in the detection of only BA-$(OH)_2$.

2.4.6 Incubation of BEN, BA, and products in human plasma

To test whether the decomposition of BEN and BA were related to the presence of red blood cells, we repeated the blood experiment in plasma. Incubated in plasma at 37 °C, BEN generated only BEN analogs (Figure 16) and BEN had an apparent half-life of 220 min. Incubation of BA only generated BA analogs (Figure 16 and Figure 17) and BA had an apparent half-life of 5 min. In both cases the levels of BEN-$(OH)_2$ and BA-$(OH)_2$ plateaued. This would indicate that these products are at the end of the metabolic pathway and that these compounds are stable. Plasma incubation of BEN-Cl_2 or BA-Cl_2 generated the respective Cl-OH and $(OH)_2$ analogs.

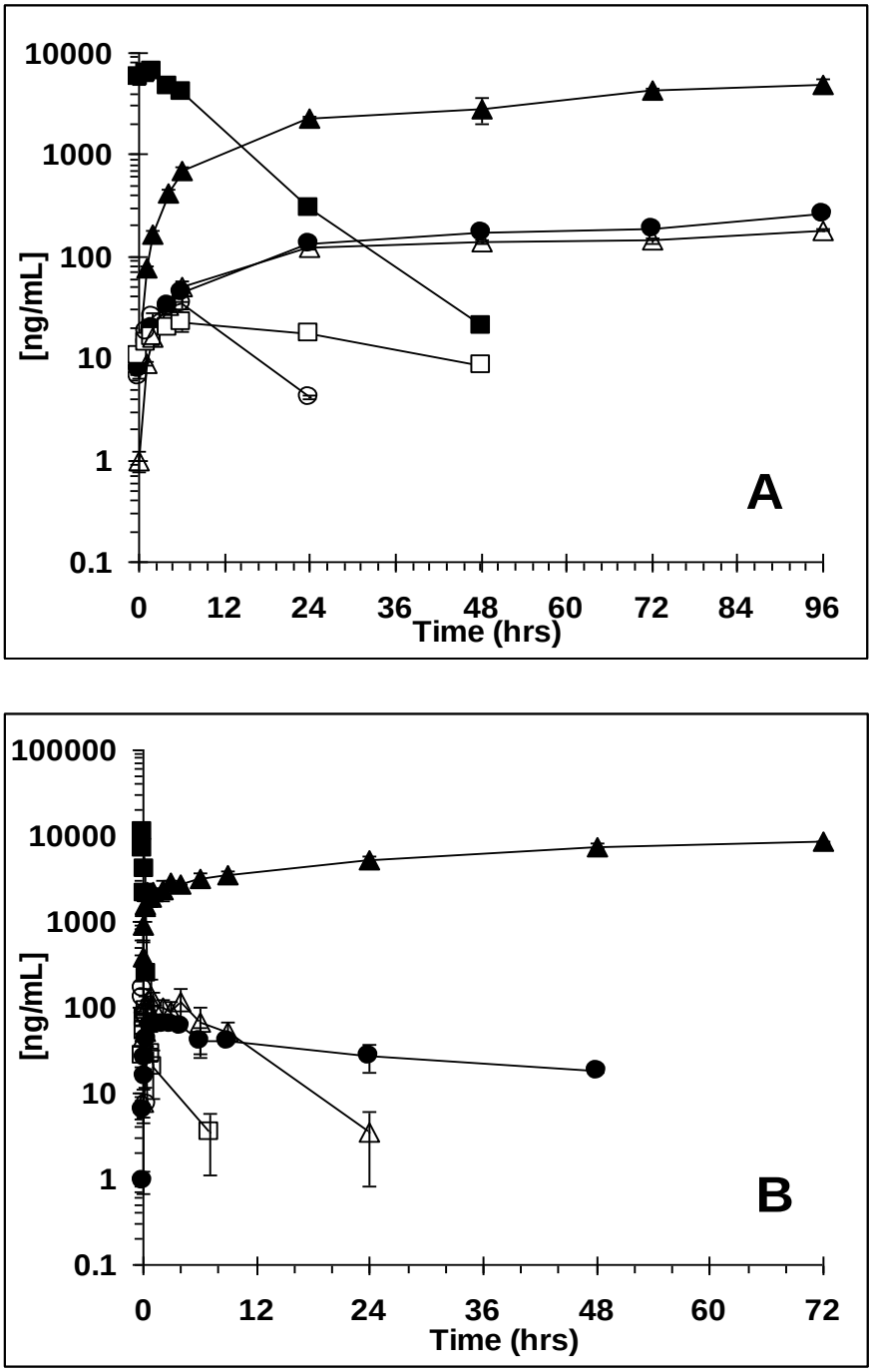

Figure 16. BEN 0-96hrs (A) and BA 0-72hrs (B) decomposition in plasma at 37 °C and formation of structural analogs. (A): BEN (■), BEN-Cl_2 (●), BEN-OH_2 (▲), BEN-Cl (□), BEN-Cl-OH (Δ)and BEN-OH (○). (B): BA (■), BA-Cl_2 (●), BA-OH_2 (▲), BA-Cl (□), BA-Cl-OH (Δ) and BA-OH (○). For the analytes in which no reference compound was available the ng/mL BEN equivalents were calculated by using the analyte to internal standard ratio back-calculated with the equation of the BEN standard curve.

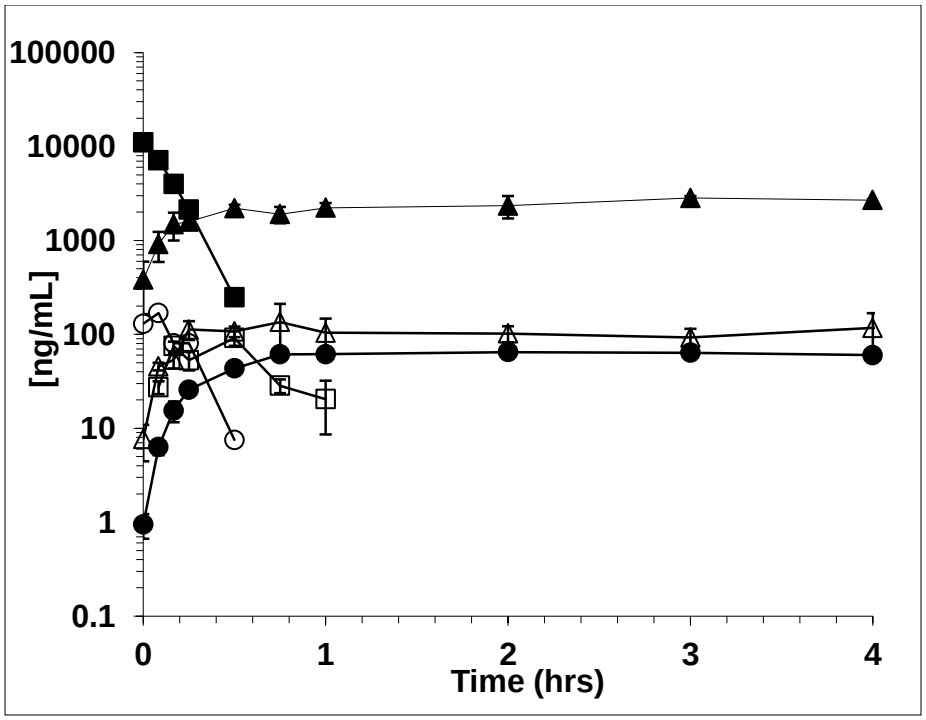

Figure 17. BA 0-4 hrs decomposition in plasma at 37 °C and formation of structural analogs. BA (■), BA-Cl_2 (●), BA-OH_2 (▲), BA-Cl (□), BA-Cl-OH (Δ) and BA-OH (○). For the analytes in which no reference compound was available the ng/mL BEN equivalents were calculated by using the analyte to internal standard ratio back-calculated with the equation of the BEN standard curve.

2.4.7 BA degradation in phosphate buffered saline

BA was added to human plasma, PBS, and 5% human albumin in PBS. The rate of BA disappearance was greatest in PBS with an apparent half-life of 4 min compared to 5 min in plasma and 8 min in PBS with albumin (Figure 18). Under the assumption that only unbound BA can degrade, the plasma protein binding of BA was determined to be 15% (3.7-26.7% 95% CI) when compared to degradation of BA in PBS, and the binding

of BA to 5% albumin was determined to be 49% (36.4-61.4% 95% CI). BEN is 74-85% protein bound in human plasma.[136]

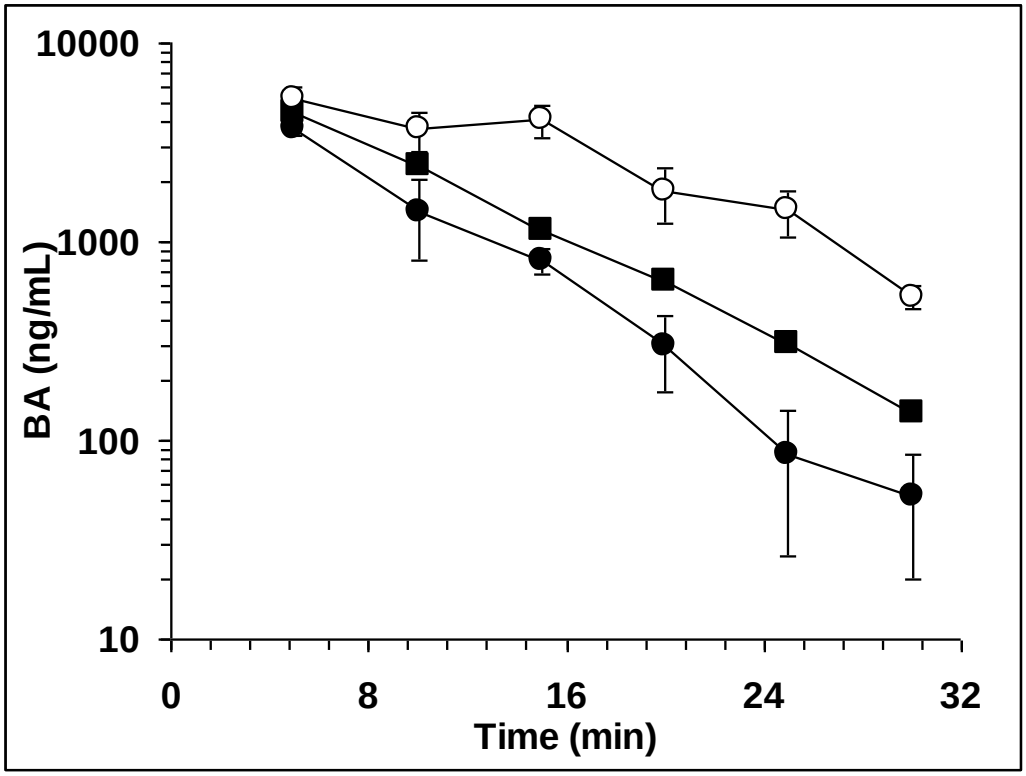

Figure 18. Degradation of BA in PBS (●), Plasma (■) and PBS/albumin (○).

2.4.8 Growth inhibitory potential of BEN and products

The growth inhibitory potential, as expressed by the IC_{50}, of BEN, BA, BEN-CL_2, BA-CL_2, BEN-$(OH)_2$ and BA-$(OH)_2$ was determined in human renal carcinoma cell lines. Although BEN was chemically stable, the IC_{50}'s of BEN in these cell lines were 1.5- to 500-fold lower than those of the other analytes tested (Table 3). The IC_{50}s for

BEN-$(OH)_2$ and BA-$(OH)_2$ could not be determined in the concentration range tested. The growth inhibitory potential for BEN in the cell lines was A498 > CAKI-1 > ACHN > 786-0 > SN12K1.

Table 3. Growth inhibition (IC50) for BEN and related analogs in human renal carcinoma cell lines. (SD)

Compound \ Cell	786-0	ACHN	SN12K1	CAKI-1	A498
BEN	0.267 (0.097)	0.263 (0.047)	0.790 (0.105)	0.202 (0.133)	0.0463 (0.0119)
BEN-Cl_2	6.88 (2.77)	6.13 (2.06)	10.4 (1.2)	1.30 (0.65)	0.0677 (0.0072)
BEN-$(OH)_2$	>10	>10	>10	>10	>10
BA	9.23 (5.53)	18.9 (8.9)	19.7 (5.6)	15.8 (8.1)	23.5 (9.6)
BA-Cl_2	4.74 (0.70)	5.72 (0.51)	9.35 (2.76)	6.60 (1.35)	6.57 (3.49)
BA-$(OH)_2$	>10	>10	>10	>10	>10

2.4.9 BEN metabolism in human renal carcinoma cells

BEN underwent either metabolism or chemical conversion to both BEN-$(OH)_2$ and BA-$(OH)_2$ in all cell lines. In contrast, BEN was converted to only BEN-$(OH)_2$ in control, cell-free medium (Figure 19). The rate of disappearance of BEN was greatest in A498 ($t_{1/2}$ = 32 min) cells followed by 786-0 ($t_{1/2}$ = 54 min), ACHN ($t_{1/2}$ = 56 min), CAKI-1 ($t_{1/2}$ = 60 min)and lastly SN12K1 cells ($t_{1/2}$ = 63 min).

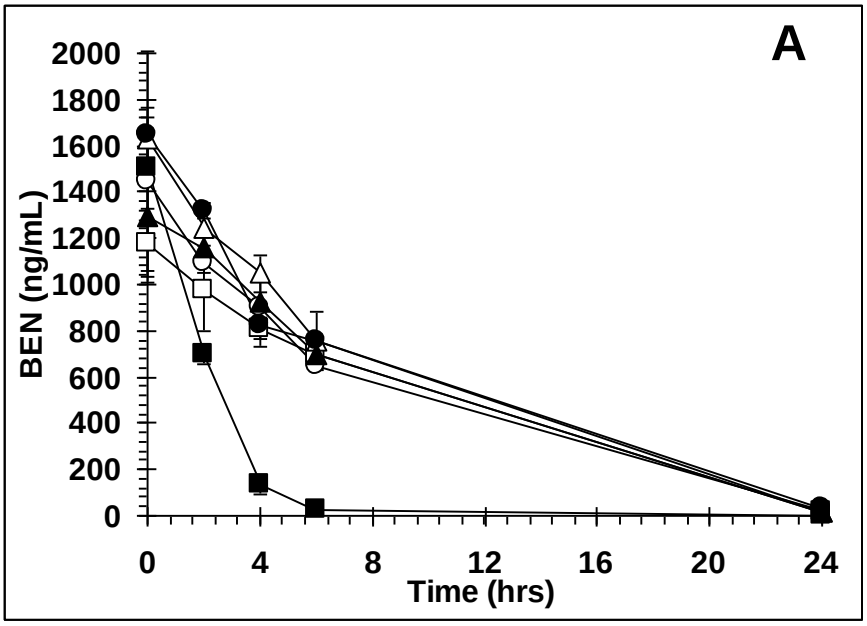
A
BEN (ng/mL)
2000
1800
1600
1400
1200
1000
800
600
400
200
0
0
4
8
12
16
20
24
Time (hrs)

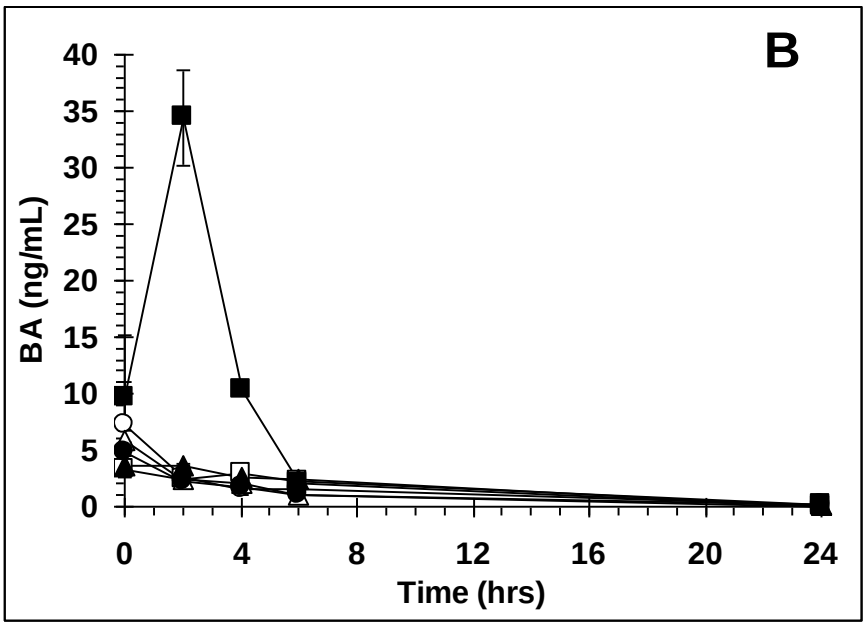
B
BA (ng/mL)
40
35
30
25
20
15
10
5
0
0
4
8
12
16
20
24
Time (hrs)

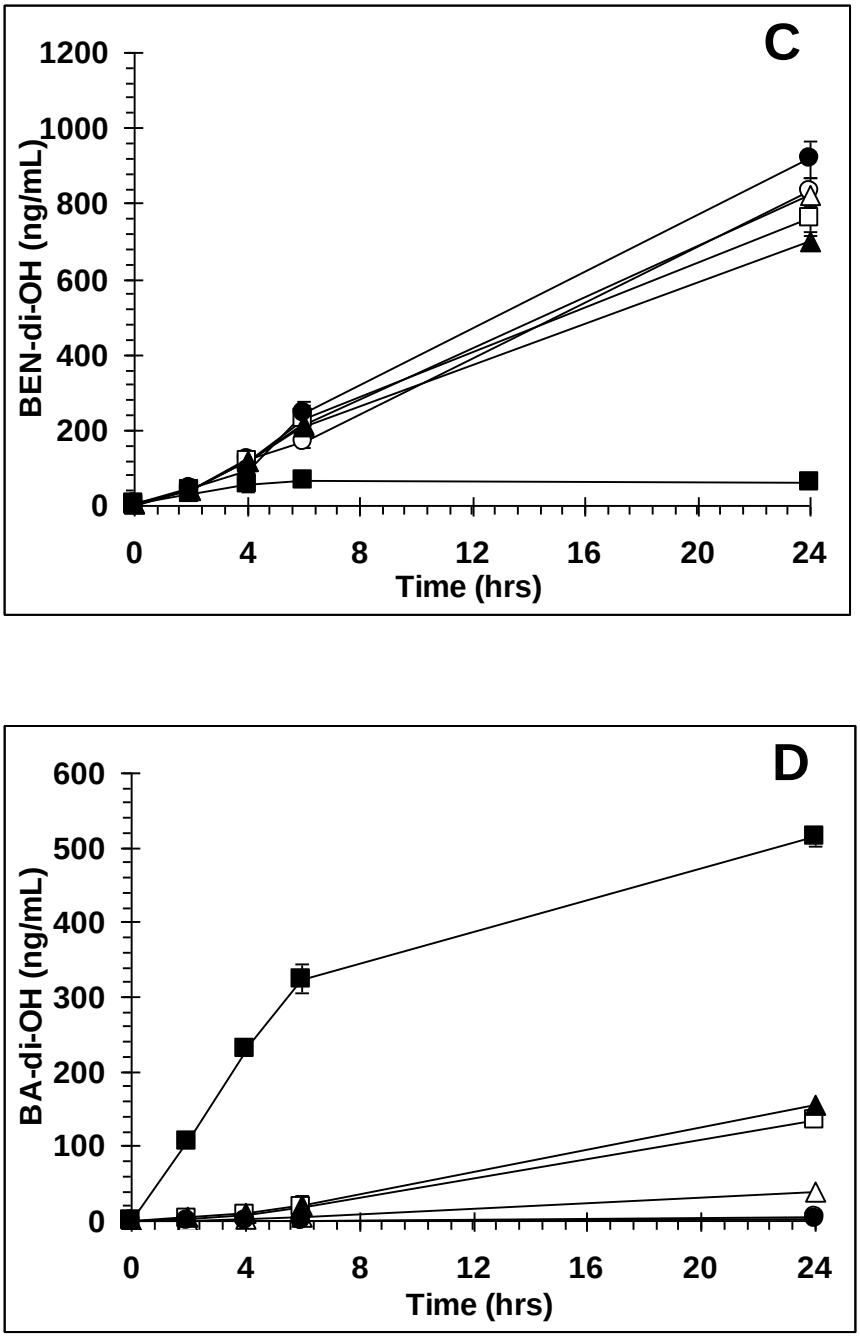

Figure 19. Metabolism of BEN (A) and formation of BA (B), BEN-$(OH)_2$ (C) and BA-$(OH)_2$ (D) in intact human renal carcinoma cells. SN12K1 (○), ACHN (□), CAKI-1 (Δ), 786-0 (▲), A498 (■), blank media (●)

2.4.10 Aldehyde dehydrogenase activity in cell lines

To explain the different fate of BEN incubated with different cell lines, we measured ALDH activity in human renal carcinoma A498 cells and SN12K1 cells, human lung tumor A549 cells and human colorectal HCT116 cells. These cell lines were chosen because the A498 cells generated the most BA-$(OH)_2$ and the SN12K1 cells generated the least amount of BA-$(OH)_2$ after incubation of BEN. As a positive and negative control we used the A459 and HCT116 cells which have been shown to have high and low levels of ALDH activity, respectively, in a screen of the NCI 60 cell lines for ALDH activity.[137] The A498 cell line had an aldehyde dehydrogenase activity 38 times greater than the SN12K1 cell line, 6.25 (±0.17) units/10^7 cells versus 0.163 (±0.102) units/10^7 cells, respectively. The A549 cells, used as a positive control, had an activity of 26.2 (±0.3) units/10^7 cells while HCT116 displayed no ALDH activity.

2.4.11 BEN products in plasma from a mouse dosed with BEN

We detected 12 different BA-derived products in plasma of a mouse dosed with BEN, 6 of which were glucuronides. Each of the BA products generated had a corresponding glucuronide. The non-glucuronide products were identical to the BA products generated in human blood and plasma.

2.5 DISCUSSION

BEN is an alkylating agent currently being investigated in phase I clinical trials, with structural similarities to busulfan and melphalan. BEN is reported to undergo hydrolysis in aqueous environment.[127] This led us to hypothesize that BEN likely undergoes hydrolysis in plasma and blood. The hydrolysis of BEN was expected to decrease the alkylating activity. In order to better understand the pharmacology of BEN and its products, we aimed to characterize the generation and growth inhibitory potential of BEN products.

First, we developed an assay that would allow us to quantitate BEN and its presumed products. The degradation of the analytes could be slowed by lowering temperature and pH. BEN and its analogs were found to be more stable than BA and its respective analogs.

In whole blood, but not in plasma, BEN was rapidly converted to its carboxylic acid analogue BA, suggesting conversion by an enzyme present in red blood cells. BA rapidly decomposed in plasma with a half-life of approximately 5 min. The rate of BA degradation in plasma was slightly slower than in PBS, which is not surprising since only free BA can react. However, the rate of degradation in plasma was greater than in PBS with human albumin at physiological concentrations. This may be due to the chemical environment of plasma. Plasma may have other components that enable BA to react faster than in PBS with albumin. Under the assumption that only free BA is subject to degradation, we can conclude that BA is likely approximately 15% protein bound, and that the decomposition of BA in plasma is most likely chemical in nature, not enzymatic.

In plasma, BEN and BA decomposed according to a parallel pathway to a number of hydroxylated and chlorinated analogs, as depicted in Figure 13. The relatively fast rate of production of BA products relative to the generation of BEN products is likely indicative of the relative reactivities of the acid analogs relative to the aldehyde analogs. We hypothesize that the unbound electron pair on the analine nitrogen is the initiator of an SN2 attack on the β-carbon, generating the reactive aziridinium intermediate. Mesomeric withdrawal of the analine unbound electron pair by the para-aldehyde moiety, or occupation of the electron pair by a proton under acidic conditions would be expected to decrease the generation of the aziridinium intermediate and thereby decrease the reactivity. (See **Figure 20**)

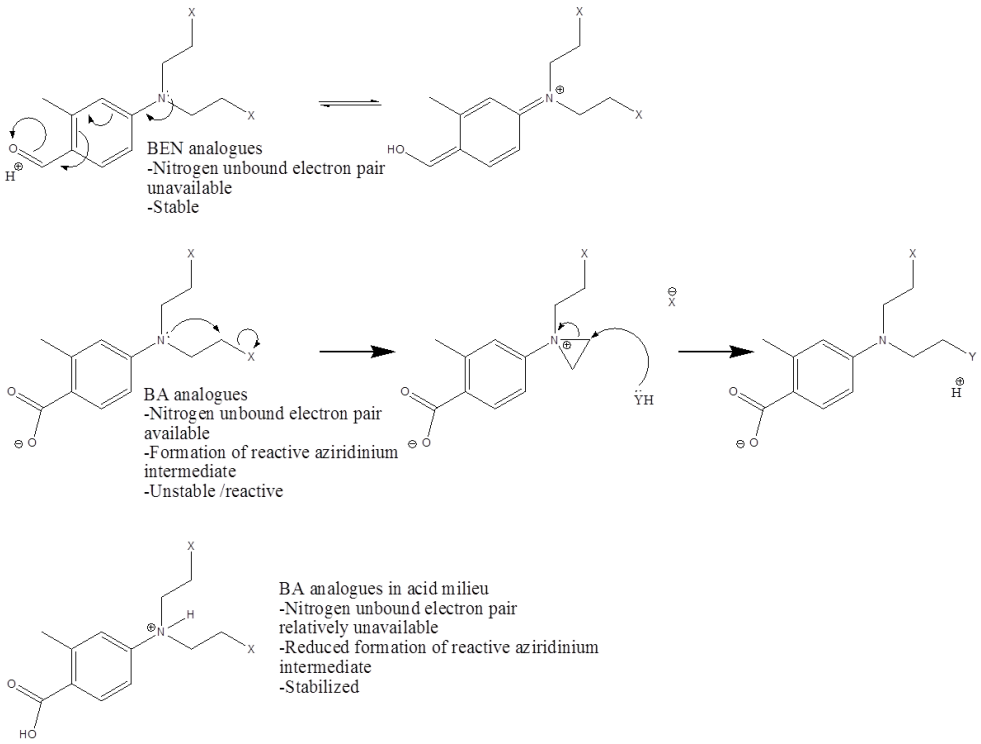

Figure 20. Hypothesis of the stability of BEN, BA and BA in the presence of acid.

The abundance of BA analogs and lack of BEN analogs after incubation of BEN in whole blood can be attributed to the relative rates of the competing pathways of BEN conversion. The conversion of BEN to BA is much more rapid than conversion of BEN to downstream aldehyde analogs. In addition, any aldehyde products formed may also be converted to their respective acid counterparts by the same enzymatic pathway that converts BEN to BA, as was shown for the conversion of BEN-$(OH)_2$ to BA-$(OH)_2$ in whole blood.

Intravenous administration of BEN to a mouse confirmed the presence of the BA related analytes and their glucuronides, but not BEN, 30 min after dosing. The detection of glucuronides of BA analogs without hydroxyethyl moieties suggests that glucuronidation takes place on the carboxylic acid functionality. A more complete assessment of the pharmacokinetics and metabolism of BEN in mice is currently being conducted.

Although ten of the 12 entities observed in plasma have the potential to alkylate DNA (all except the di-hydroxy metabolites), and BEN-Cl_2 has been shown to be cytotoxic in the NCI 60-cell line screen, the BEN products that are generated in plasma and blood had IC_{50} values that were several fold higher than those of BEN in a panel of human renal carcinoma cells. During incubation with human renal carcinoma cells, BEN undergoes chemical conversion to BEN-$(OH)_2$ or metabolism to BA and subsequent conversion to BA-$(OH)_2$ in all cell lines tested. A498 cells displayed the greatest metabolism of BEN to BA as shown by the amount of BA-$(OH)_2$ generated; in fact, no BEN-$(OH)_2$ could be detected. In contrast, SN12K1 cells generated very little BA-$(OH)_2$. The ratio of BEN disappearance for A498/SN12K1 was 35-fold. It is noteworthy that the

A498 cell line was the most sensitive to BEN demonstrated by the lowest IC_{50} value. To test whether ALDH may be responsible for the metabolic conversion of BEN to BA we measured the ALDH activity in A498 and SN12K1 cells. We found that A498 cells had ALDH activity ~40-fold greater than SN12K1 cells, paralleling the BA-$(OH)_2$ generating activity and conversely the metabolism of BEN to BA. These results are in line with previously reported ALDH activities.[137] These data support the notion that intracellular ALDH is responsible for the metabolism of BEN to BA in these cells, and that this intracellular conversion mediates its cytotoxic effects. ALDH may also be responsible for the observed metabolism of BEN to BA in whole blood as red blood cells contain ALDH.[138]

We hypothesize that the A498 cell line is able most efficiently to metabolize BEN to its more reactive metabolite BA by ALDH inside the cell, which then rapidly alkylates cellular constituents resulting in cell damage. The high IC_{50}s of BA added to medium suggest that BA reacts with other nucleophiles in the medium before it is able to reach its intracellular targets. BEN-Cl_2 and BA-Cl_2 had intermediary IC_{50}s. This suggests that BEN-Cl_2 gets into the cells and is locally converted to BA-Cl_2 which reacts with cellular targets. However, because BA-Cl_2 is not as reactive as BA, a fair amount likely diffuses out of the cell without exerting cytotoxic effects. Conversely, when BA-Cl_2 was added to the cell incubation, the relative stability of BA-Cl_2 allowed enough of it to diffuse into the cells to cause intracellular damage. Taken together, these data suggest that BEN is a pro-drug that requires intracellular activation to the highly reactive BA, which likely exerts rapid and localized damage via alkylation inside the cells.

In summary, we developed an analytical assay that will prove instrumental in defining the preclinical and clinical pharmacology of BEN in ongoing clinical trials. We have identified a number of products and metabolites of BEN and characterized their relative growth inhibitory properties. In addition, we have shown that ALDH may be responsible for the metabolism of BEN to BA, and that BEN is more active in cell lines that express high levels of ALDH. The potential importance of this finding lies in the reported overexpression of ALDH in stem cells of many tumor types making these stem cells potential targets for BEN therapy, existing polymorphisms in ALDH, and potential drug-drug interactions with inhibitors of ALDH such as disulfiram and metronidazole.[139-142] More complete *in vitro* and *in vivo* studies are underway to define BEN pharmacokinetics and metabolism, and the relative contribution of BEN and metabolites to plasma exposure of alkylating species.

3.0 CHARACTERIZATION OF THE METABOLISM OF BENZALDEHYDE DIMETHANE SULFONATE IN RED BLOOD CELLS

3.1 ABSTRACT

Benzaldehyde dimethane sulfonate (BEN, DMS612, NSC281612) is a bifunctional alkylating agent with activity against renal cell carcinoma, and is being evaluated clinically. We have previously characterized the degradation of BEN in plasma and blood. In plasma, BEN chemically degrades into five different analogs in which the dimethane sulfonate groups are replaced by either chlorine or hydroxyl groups. In whole blood, but not in plasma, BEN is rapidly converted to its carboxylic acid analogue BA, which then chemically converts to chlorine or hydroxyl intermediates similar to the degradation of BEN in plasma. The conversion of BEN to BA in whole blood, but not plasma, suggests that an enzyme in RBCs may be responsible for this conversion. BEN was also converted to BA in renal carcinoma cells. We have demonstrated a correlation between the generation of BA from BEN and the activity of with aldehyde dehydrogenase (ALDH) as determined by acetaldehyde metabolism, in renal carcinoma cell lines. To better understand the pharmacology of BEN we aimed to further characterize the conversion of BEN to BA in blood.

We evaluated the conversion of BEN to BA in six different lots of blood and calculated the average apparent V_{max} and apparent K_m to be 68 ng/mL•min^{-1}•[10% RBC]$^{-1}$ and 373 ng/mL, respectively. The conversion of BEN to BA in blood was not inhibited by carbon dioxide, nitrogen gas or menadione, an inhibitor of aldehyde oxidase. The conversion in blood was, however, inhibited by disulfiram, an inhibitor of ALDH. Furthermore, we performed studies with available purified ALDH isoforms ALDH1A1, ALDH3A1, ALDH2, and ALDH5A1. We found that BEN was converted to BA only by

ALDH1A1, which is reportedly present in the red blood cells. The work presented here contributes to a better understanding of the pharmacology of BEN.

3.2 INTRODUCTION

Approximately 13,000 people die from metastatic renal cell carcinoma (mRCC) in the United States every year.[1,143] Only 10-12% of patients achieve durable complete remission with high dose interleukin-2 therapy.[128] Agents targeting vascular endothelial growth factor and its receptor along with mTOR inhibitors have shown clinical activity.[94,129] However, responses to these agents are generally transient[130], and there is a need for new treatment options for mRCC patients.

Benzaldehyde dimethane sulfonate (BEN, DMS612, NSC281612) is one of a family of dimethane sulfonates that have demonstrated activity in the NCI 60 cell line screen. BEN is proposed to be a bifunctional alkylator with structural similarities to chlorambucil, busulfan and melphalan. However, unlike these compounds, BEN has specific activity against renal carcinoma cells (RCC) in the NCI 60 cell line screen.[124] BEN causes cell cycle arrest in the G2-M phases[124], and increases P53 levels, indicating DNA damage, in the renal carcinoma cell line 109, and in the breast cancer cell line MCF-7. In addition, BEN has demonstrated antitumor activity in mice with renal carcinoma xenografts, specifically against human A498 and RXF-393 implanted subcutaneously or orthotopically under the renal capsule [Personal communication, Dr. M. Hollingshead, unpublished data].[131,132] The significant *in vitro* and *in vivo* activity

against renal carcinoma has led to the ongoing evaluation of BEN in NCI-sponsored phase I clinical trials.

BEN, based on its structure, likely forms an aziridinium intermediate that is attacked by nucleophilic molecules such as DNA, proteins or water. Jumaa et al. reported hydrolysis of BEN in aqueous solution whereby the dimethane sulfonate groups are replaced by hydroxy groups.[127] In order to better understand the pharmacology of BEN we tested whether BEN would undergo hydrolysis in blood and plasma. In whole blood, but not in plasma, BEN was rapidly converted to its carboxylic acid analogue (BA).[144] Furthermore, BEN decomposed into at least eleven different products that were structural analogs of either BEN or BA. These compounds were identified by LC-MS/MS and their structures are depicted in Figure 13 (chapter 2). For both BEN and BA, we observed and structurally elucidated products in which one or both of the methane sulfonate leaving groups was replaced by either a chlorine (from plasma chloride ions) or hydroxyl (from plasma water) moiety, resulting in a total of 12 analytes, including the parent compound. To test whether the decomposition of BEN and BA were related to the presence of red blood cells, we repeated the experiment performed with blood using plasma. Incubated in plasma at 37 °C, BEN generated only BEN analogs and had an apparent half-life of 220 min. Incubation of BA only generated BA analogs, and BA had an apparent half-life of 5 min. Plasma incubation of BEN-Cl_2 or BA-Cl_2 generated the respective Cl-OH and $(OH)_2$ analogs. This led us to hypothesize that the conversion of BEN to BA in whole blood is an enzymatic process.[144]

BEN has shown activity against RCC lines. Because of this, we elucidated the metabolism of BEN in five different RCC lines. BEN underwent either metabolism or

chemical conversion in all cell lines to both BEN-$(OH)_2$ and BA-$(OH)_2$, however, at different rates and in blank control medium, only BEN-$(OH)_2$ was generated. We measured the aldehyde dehydrogenase (ALDH) activity of these 5 renal carcinoma cell lines and found that the ALDH activity correlated with the amount of BA-OH_2 generated.[144] This is further support for the idea that the conversion of BEN to BA is enzymatic and that ALDH is primarily responsible for this metabolic step.

Aldehydes are reactive electrophilic compounds that react with thiol and amino groups. Aldehydes are necessary for many physiologic and therapeutic processes, but aldehydes can also be cytotoxic, genotoxic and may be involved in carcinogenesis.[145] We hypothesized that BEN is metabolized into BA by an enzyme/s that is an aldehyde dehydrogenase and/or aldehyde oxidase (AO).

ALDHs are NAD(P)+ dependent enzymes that metabolize both aromatic and aliphatic aldehydes into carboxylic acids.[146] This process generally makes aldehydes less toxic and more readily excreted. There are nineteen different known human isoforms of ALDH. ALDHs are involved in many biological pathways and people that are deficient or have polymorphic isoforms of ALDH are susceptible to various metabolic diseases or have intolerance to alcohol.[145-147]

Aldehyde oxidase (AO) is a molybdoflavoenzyme that has broad specificity. Although the physiological function of this enzyme is unknown, it is known to oxidize a number of aldehydes and heterocyclic rings.[148] Some of the substrates of AO are retinaldehyde, 5-fluoro-2-pyrimidinone and methotrexate.

Disulfiram (Antabuse^{TM}) is an irreversible inhibitor of certain isoforms of ALDH and is prescribed to treat chronic alcoholism.[141,149] After ingestion, alcohol is converted to

acetaldehyde by alcohol dehydrogenase (ADH). Acetaldehyde is then metabolized to acetic acid by ALDH. Disulfiram causes the accumulation of acetaldehyde in the blood when alcohol is consumed, resulting in severe "hangover" side effects.[141]

Menadione is a synthetic form of vitamin K3 and is a specific inhibitor of AO. Menadione functions to aid in posttranslational modification of proteins, most importantly for blood clotting factors. In addition, menadione has been used as an anti-inflammatory agent and is a component of multivitamin products.[150] Currently, menadione is not used because of its associated toxicities, which include hemolytic anemia, neonatal brain damage, allergic reactions and hepatotoxicity.[151]

In the current chapter we describe the identification of the enzyme responsible for the conversion of BEN to BA, and further characterization of the reaction in biological fluids.

3.3 MATERIALS AND METHODS

3.3.1 Chemicals and reagents

4-[bis[2-[(methylsulfonyl)-oxy]ethyl]amino]-2-methyl-benzaldehyde (BEN, NSC 281612), 4-[bis[2-[(methylsulfonyl)-oxy]ethyl]amino]-2-methyl-benzoic acid (BA, NSC 733609), 4-[bis[2-chloro-ethyl]amino]-2-methyl-benzaldehyde (BEN-Cl_2), 4-[bis[2-chloro-ethyl]amino]-2-methyl-benzoic acid (BA-Cl_2), 4-[bis[2-[(methylsulfonyl)-oxy]ethyl]amino]-benzaldehyde (desmethyl-BEN), and 4-[bis[2-chloro-ethyl]amino]-benzaldehyde (desmethyl-BEN-Cl_2) were obtained from the National Cancer Institute (NCI, Bethesda, MD). 4-[bis[2-hydroxy-ethyl]amino]-2-methyl-benzaldehyde (BEN-$(OH)_2$) was generated by heating approximately 13.6 mg BEN in approximately 4 mL of 0.05 N aqueous NaOH for 48 h at 50 °C. The progression of the reaction was monitored by mass spectrometry. 4-[bis[2-hydroxy-ethyl]amino]-2-methyl-benzoic acid (BA-$(OH)_2$) was generated by heating approximately 13.2 mg BA in a solution of 0.03 N NaOH in 7 mL of acetonitrile/water (1:1, v/v) for 48 h at 50 ºC. The progression of the reaction was assessed by mass spectrometry and the conversion was 100% in both cases. The final solutions were neutralized with hydrochloric acid and acidified with formic acid for a final concentration of 1 mg/mL of the respective product. All solvents used for LC-MS/MS were high purity Burdick & Jackson and purchased from Fisher Scientific Co. (Fair Lawn, NJ). Formic acid was purchased from Sigma-Aldrich Chemical Co. (St. Louis, MO). Control human blood was obtained from the Central Blood Bank, Pittsburgh, PA and plasma was prepared by centrifugation of whole blood at 2000 x *g* at room temperature for 20 min. Nitrogen gas for the mass spectrometer was purified with a

Parker Balston Nitrogen Generator (Haverhill, MA). Nitrogen gas for the sample evaporation, and nitrogen gas and carbon monoxide gas was purchased from Valley National Gasses, Inc. (Pittsburgh, PA). Reduced nicotinamide adenine dinucleotide (NADH), reduced nicotinamide adenine dinucleotide phosphate (NADPH), and disulfiram used for metabolism studies were purchased from Sigma-Aldrich Chemical Co. (St. Louis, MO). Cellgro phosphate buffered saline. (PBS 1x) was purchased from Mediatech (Manassas, VA).

3.3.2 Analytical Equipment

We employed two LC-MS/MS assays. One to quantitate the metabolites generated in the blood metabolism experiments, and one to quantitate BEN and BA in the purified enzyme experiments. For the blood metabolism experiments we used a previously developed assay to quantitate the analytes in plasma (Assay1). The LC-MS/MS system consisted of an Agilent (Wilmington, DE, USA) 1200 SL thermostated autosampler, binary pump, thermal column compartment, and a ABI SCIEX (San Jose, CA, USA) 4000Q hybrid linear ion trap tandem mass spectrometer (ABI system). For the purified enzyme experiments we developed an assay to quantitate the analytes in PBS (Assay2). The LC-MS/MS system consisted of an Agilent (Wilmington, DE, USA) 1100 thermostated autosampler, binary pump, and a Waters (Milford, MA) Quattromicro desktop tandem mass spectrometer (QM system).

3.3.3 Assay 1

Assay 1 was the LC-MS/MS assay used for the experiments in chapter 2 and is detailed in that chapter. Briefly described, the liquid chromatography was performed with a gradient mobile phase consisting of A: acetonitrile/0.1% formic acid (v/v) and B: water/0.1% formic acid (v/v). The mobile phase was pumped at a flow rate of 0.2 mL/min and separation was achieved using a Phenomenex (Torrance, CA) Hydro Synergi-RP 4 micron 100 x 2mm column. The gradient mobile phase was as follows: at time zero, solvent A was 15% and was increased linearly to 40% in 20 min. The percentage of solvent A was increased linearly to 80% at 21 min and the flow rate was increased to 0.4 mL/min. This was maintained for two min at which time solvent A was decreased linearly to 15% at 24 min. This was maintained for six min. The total run time was 30 min. During the first two min and the last six min of the LC run the flow leaving the column was diverted to waste.

The parameters of the mass spectrometer were as follows; curtain gas 20, IS voltage 5500V, probe temperature 400 ºC, GS1 40, GS2 30, declustering potential 50V, and collision energy 40V. For MRM transitions, see table 1 chapter 2.

3.3.4 Assay 2

The liquid chromatography was performed with a gradient mobile phase consisting of A: acetonitrile/0.1% formic acid (v/v) and B: water/0.1% formic acid (v/v). The mobile phase was pumped at a flow rate of 0.3 mL/min and separation was achieved

using a Phenomenex (Torrance, CA) Hydro Synergi-RP 4 micron 100 x 2mm column. The gradient mobile phase was as follows: from time zero to until 4.5 min solvent A was maintained at 40% with a flow rate of 0.3 mL/min. At 4.6 min solvent A was increased linearly to 90% and the flow rate was increased to 0.5 mL/min. These conditions were maintained for 2.4 min at which time solvent A was decreased to 40%. The run time was 12 min. During the first two min and the last six min of the LC run the flow leaving the column was diverted to waste.

To develop the mass spectrometric assay, BEN, BA, and desmethyl-BEN were diluted to a concentration of 1 µg/mL in acetonitrile and each was continuously infused at a rate of 10 µL/min into the HPLC flow, which was an isocratic mobile phase of acetonitrile:water:formic acid (50:50:0.1, v/v/v) pumped at 0.3 mL/min. The tuning parameters of the mass spectrometer were adjusted to maximize the intensity of the $[M+H]^+$ ion of the analyte. After the largest $[M+H]^+$ ion was obtained, the mass spectrometer was operated in product mode and the collision voltage was adjusted so that the largest product ion was determined. The parameters for the mass spectrometer were as follows: Capillary voltage 4.0 kV, cone voltage 20 V, source temperature and desolvation temperature were 120 ˚C and 450 ˚C, respectively. Desolvation gas was 550 L/h and LM1, LM2, HM1 and HM2 were set to 12. The entrance, exit and collision voltages were 1, 23, and 6 respectively. The mass transitions for BEN, BA and desmethyl-BEN were 380>160, 396>300 and 366>270, respectively.

3.3.5 Standard curve for blood metabolism assays

Stock solutions of BEN, BEN-Cl_2, BA, BA-Cl_2, BEN-$(OH)_2$ and BA-$(OH)_2$ were prepared separately at concentrations of 1.0 mg/mL in acetonitrile containing 0.1% formic acid. A mixture was made containing all six analytes at a concentration of 0.1 mg/mL by adding 100 µL of each analyte to 400 µL of acetonitrile with 0.1% formic acid. All stock solutions were stored at -80 °C in the dark. On assay days, this solution was diluted with acetonitrile to obtain the lower calibration working solutions of 0.01, 0.001 and 0.0001 mg/mL. These calibration working solutions were diluted in plasma with 2 M H_2SO_4 (5%, v/v) to produce 200-µL aliquots of the following concentrations: 1, 3, 10, 30, 100, 300, 500, 750, and 1000 ng/mL. 10 µL of a mixture of desmethyl-BEN and desmethyl-BEN-Cl_2 (1 µg/mL of both in acetonitrile) were added as internal standards. The analyte-to-internal standard ratio (response) was calculated for each standard by dividing the area of the compound peak area by the area of the compound's respective internal standard peak. Standard curves of each compound were constructed by plotting the analyte-to-internal standard ratio versus the nominal concentration of each analyte in each sample. Standard curves were fit by linear regression with weighting by $1/y^2$, without forcing the line through the origin, followed by the back-calculation of the concentrations. The deviations of these back-calculated concentrations from the nominal concentrations, expressed as percentage of the nominal concentration, reflected the assay performance over the concentration range.

3.3.6 Standard curve for purified enzyme assays

The procedure for the preparation of standard curves in PBS was the same as the procedure for the preparation of the standard curves in plasma except for the following; PBS was used instead of plasma, and only BEN and BA where quantitated from 1 to 1000 ng/mL and desmethyl-BEN was used as the internal standard.

3.3.7 Sample processing

For all blood metabolism assays the aliquots taken were processed as described. At the specified time points, a 500 µL aliquot of blood was removed, and centrifuged at 12,000 x g for 2 min at 4 °C. 200 µL of the resultant plasma was removed and added to 10 µL 2M H_2SO_4. The sample was briefly vortexed and 10 µL of internal standard solution and 1 mL of acetonitrile were added. The samples were then vortexed on a vortex genie on a setting of high for one minute, and then were centrifuged at 12,000 x g for 5 min. The resultant supernatant was blown to dryness at room temperature under a stream of nitrogen. The samples were reconstituted with 100 µL of 20:80 acetonitrile/H_2O with 5% 2 M H_2SO_4 (v/v/v) and 10 µL was injected into the LC-MS/MS system.

3.3.8 Determination of the effect of RBC concentration on BEN metabolism

To determine the effect of increasing RBC concentrations on BEN metabolism and to determine an adequate amount of RBCs in further experiments, metabolism was performed with different amounts of RBCs. BEN was added separately to 10 mL of plasma, 0.1% RBCs, 1% RBCs, 10% RBCs and whole human blood to achieve a concentration of 10 µg/mL. The samples were incubated in a shaking water bath at 37 ºC. At 0, 5, 10, 15, 30, 45, 60, 120, 180, 240, 360 min, and 24 h, aliquots were taken and processed as described above.

3.3.9 Experiments with carbon monoxide and nitrogen gas

Carbon monoxide (CO) gas and nitrogen (N_2) gas were used to determine whether a heme group is involved in the metabolism of BEN. Either carbon monoxide (CO) or nitrogen gas was passed through a mixture of 10% RBCs in plasma at 37 ºC for 5 min in a shaking water bath. The reaction vessels were sealed with a septum. The gasses were continuously passed into the reaction vessel using a stainless steel needle 5 minutes prior and throughout the experiment. In addition, there was a second needle in the septum to allow the gasses to escape. BEN was added to obtain a concentration of 3 µg/mL and 200 µl aliquots were taken at 0, 60, 120 and 180 min and processed as described above.

3.3.10 Experiments with ALDH and AO inhibitor

Disulfiram and menadione were used to determine the effect of ALDH and aldehyde oxidase inhibitors on blood metabolism of BEN. 90 µL of 10 mM disulfiram in acetonitrile or 90 µl of 10 mM menadione in DMSO was added to 6 mL of 10% RBCs to obtain a concentration of 150 µM of these compounds.

Additional experiments were conducted with increasing concentrations of menadione of 750 µM and 3 mM. 90 µL of DMSO were added to separate tube as a solvent control. The resulting mixtures were incubated at 37 ºC for 10 min in a shaking water bath before BEN was added to obtain a concentration of 1 µg/mL. Five hundred µL aliquots were taken at 5, 15, 30, 45 and 60 min and processed as described above.

3.3.11 BEN in lysed blood

To determine the effect of hemolysis on the metabolism of BEN in blood we performed the metabolism of BEN with lysed RBCs. To lyse RBCs a mixture of 10% RBCs in plasma was freeze-thawed 3 times. 6 mL of both lysed and unlysed RBCs in plasma was incubated separately at 37 ºC on a shaking water bath before BEN in acetonitrile was added to obtain a concentration of 10 µg/mL. Aliquots were taken at 5, 60, 120, and 180 min and processed as described above.

We hypothesized the activity of the enzyme in RBCs could be affected by lysis through dilution of cofactors. To determine whether NADH or NADPH would restore the metabolism in lysed RBCs, we performed the metabolism in lysed RBC in the presence

of either NADH or NADPH. Either NADH or NADPH was added at a final concentration of 500 μM to 10% lysed RBCs in plasma and incubated at 37 ºC in a shaking water bath. Five hundred μL aliquots were taken at 5, 30, 60, 90 and 120 min and processed as described as above.

3.3.12 Determination of BEN blood partitioning

To determine the amount of BEN in blood compared to plasma we determined the blood to plasma partitioning ratio. Ten mL of blood containing 50% RBCs was placed into a 15 mL conical tube and placed on ice. Disulfiram was added to obtain a concentration of 1 mM. After 10 minutes BEN was added to obtain a final concentration of 1000 ng/mL. Five hundred μL aliquots of blood were taken at 5, 10, 15, 20 and 30 minutes and centrifuged at 12,000 x g for 2 minutes. Two hundred μL of the resulting plasma was pipetted into micro-centrifuge tubes that contained 10 μL of 2M H_2SO_4. The amount of BEN in the plasma samples was determined by LC-MS/MS as described above. The procedure was performed in parallel in 100% plasma to determine the total amount of BEN obtained in plasma without blood. Both experiments were performed in triplicate. The blood to plasma concentration partitioning was determined by dividing the concentration of BEN obtained in the 100% plasma experiment divided by the concentration of BEN in the plasma from the BEN added to 50% RBC experiment.

3.3.13 V_{max} and K_m determination

In order to determine the apparent V_{max} and K_m of human blood, different amounts of BEN in acetonitrile were added to 10% RBCs and the amount of BEN remaining was determined at various time points. BEN was added to RBCs that were pre-incubated at 37 ºC for five min to achieve a final concentration of 10,000, 5,000, 2,000, 1,000, 800, 600, 400 and 200 ng/mL. 500 µL aliquots were taken at 5, 15, 30, 45, 60, 75, 90, 105 and 120 min and processed as described above. These reactions displayed the saturation of the enzyme and allowed us to determine more optimal and fewer concentrations to use in future reactions for apparent V_{max} and K_m determination.

We determined the apparent V_{max} and K_m in six different lots of human blood. Plasma with 10% RBCs was pre-incubated at 37 ºC for five min followed by addition of BEN to achieve final concentrations of 5,000 and 400 ng/mL. 500 µL aliquots were taken at 5, 15, 30, 45, 60, 75, 90, 105 and 120 min and processed as described above (experiments were performed in triplicate). The resulting concentration versus time data was analyzed with a one compartmental model with saturable elimination using ADAPT5. In ADAPT we used the equations XP(1) = $-V_{max}/(K_m$ + X(1)/V400)*(X(1)/V400) and XP(2) = $-V_{max}/(K_m$ + X(2)/V5000)*(X(2)/V5000) to determine the K_m and V_{max} of each experiment.

To determine if time had an effect on enzyme activity we determined the apparent V_{max} and K_m of 7 day old blood compared to freshly obtained blood. Plasma with 10% RBCs was pre-incubated at 37 ºC for five min followed by addition of BEN in to achieve final concentrations of 5,000 and 400 ng/mL. Aliquots of 500 µL were taken at 5, 15, 30, 45, 60, 75, 90, 105 and 120 min and processed as described above.

3.3.14 Immunoprecipitation of RBCs

To determine if ALDH was responsible for the metabolism of BEN, we performed immunoprecipitation of ALDH1A1 enzyme and performed BEN metabolism in RBCs. One hundred µL of 50 % lysed RBCs in plasma were added to 900 µL of immunoprecipitation buffer which consisted of 5 mM EDTA, 0.02% sodium azide and 18 µL of 50x protease cocktail inhibitor (BD baculogold). The sample was briefly vortexed and centrifuged for 10 min at 12,000 x g at 4 ˚C. Either 5 µL of ALDH1A1 purified MaxPab rabbit polyclonal antibody (Abnova, Taipei, Taiwan) or IgG polyclonal rabbit control antibody (abcam, Cambridge, MA) was added. To a third control sample nothing was added. The samples were placed on a rotary agitator at 4 ˚C. After 24 h, 100 µL of protein A sepharose B conjugate was added to each tube and the sample was placed on a rotary agitator for 4 h at 4 ˚C. The sample was then centrifuged at 2,000 x g for 5 min and the resulting supernatant was used for BEN metabolism.

The samples were placed in a shaking heated water bath at 37 ˚C. After 10 min, BEN was added to each sample to achieve a concentration of 1000 ng/mL and NADH was added to achieve a concentration of 3 mM. Aliquots of 100 µL were taken at 0, 15, 30 and 60 min and added to microcentrifuge tubes that contained 5 µL 2 M H_2SO_4. 10 µL of 1 µg/mL internal standard and 500 µL of acetonitrile were added and the samples were briefly vortexed and centrifuged at 12,000 x g for 5 min. The resulting supernatant was transferred to 12 x 75 mm glass tubes and evaporated under a stream of nitrogen at 37 ˚C. The samples were reconstituted in 100 µL of 20:80 acetonitrile/H_2O with 5% 2 M H_2SO_4 (v/v/v) and 10 µL was injected into the LC-MS/MS system.

3.3.15 Western blot

To determine if RBCs had ALDH1A1 we performed Western blot analysis as previously described.[152] One hundred µL of 50 % lysed RBCs in plasma was added to 890 µL of cell lysate buffer containing 200 mM Tris–HCl, pH 7.4, 100 µM 4-(2-aminoethyl) benzenesulfonyl fluoride, 1 mM EGTA, and 1% Triton X-100. Protein concentration was determined using the BCA Protein Assay kit (Pierce, Invitrogen, Grand Island, NY, USA), and 10, 20, 40 and 80 µg protein were subjected to SDS–PAGE electrophoresis followed by electrotransfer to nitrocellulose membranes. Membranes were blocked with 5% nonfat milk in Tris-buffered saline and then probed with primary antibodies ALDH1A1 purified MaxPab rabbit polyclonal antibody (Abnova, Taipei, Taiwan), or GAPDH, followed by anti-rabbit secondary antibodies conjugated to horseradish peroxidase (Bio-Rad, Hercules, CA, USA). The enhanced chemiluminescence (ECL) Western blotting detection system (Amersham Biosciences, Piscataway, NJ, USA) was used to facilitate detection of protein bands.

3.3.16 Metabolism using purified ALDH

To determine whether BEN is a substrate for metabolism by different isoforms of ALDH we performed metabolism studies of BEN with purified human ALDH1A1, 2, 3A1, and 5A1 (PROSPEC, Israel) enzymes. In addition, we performed metabolism studies of BEN with these enzymes in the presence of their respective antibodies, if available, and disulfiram in an effort to inhibit metabolism.

Enzyme incubation mixtures contained 200 µM Tris-HCl buffer pH 7.4, 200 mM KCl, 4 mM DTT, 5 µg/mL purified enzyme and 1000 ng/mL BEN. After pre-incubation at 37 ˚C for 10 min, NAD or NADPH (depending on the cofactor that was required for each isozyme) was added to obtain a concentration of 1 mM. Aliquots of 100 µL were taken at 0, 10, 20, 30, 45, and 60 min. The aliquots were pipetted into a microcentrifuge tube that contained 5 µL of 2 M H_2SO_4. 10 µL of 1 µg/mL internal standard and 500 µL of acetonitrile were added and the samples were briefly vortexed and centrifuged at 12,000 x g for 5 min. The resulting supernatant was transferred to 12 x 75 mm glass tubes and evaporated under a stream of nitrogen at 37 ˚C. The samples were reconstituted in 100 µL of 20:80 acetonitrile/H_2O with 5% 2 M H_2SO_4 (v/v/v) and 10 µL was injected into the LC-MS/MS system.

3.3.17 Positive control using aldehyde dehydrogenase isoforms

To ensure that the ALDH enzymes were active we performed the positive controls as described by the manufactures instructions. The reaction mixtures contained 200 µM Tris-HCl buffer pH 7.4, 200 mM KCl, 4 mM DTT, 5 µg/mL purified enzyme and 5 mM NAD (for ALDH2 and ALDH5A1) and 5 mM NADP (for ALDH3A1). For ALDH2, acetaldehyde was added to obtain a final concentration of 2 mM and for ALDH5A1, succinic semialdehyde was added to obtain a final concentration of 2 mM. 4-nitro benzaldehyde was added at a concentration of 4 mM for the ALDH3A1 reaction. The tubes were vortexed and the sample was transferred into glass cuvettes and placed into a spectrophotometer along with a control sample that contained no enzyme. Absorbance at

340 nm was monitored for 5 min to measure the reduction of NAD or NADP to NADP or NADPH.

3.4 RESULTS

3.4.1 LC-MS/MS chromatography and curves.

Assay performance and chromatography has been described before in Chapter 2. A representative chromatogram of quantitatable analytes is displayed below.

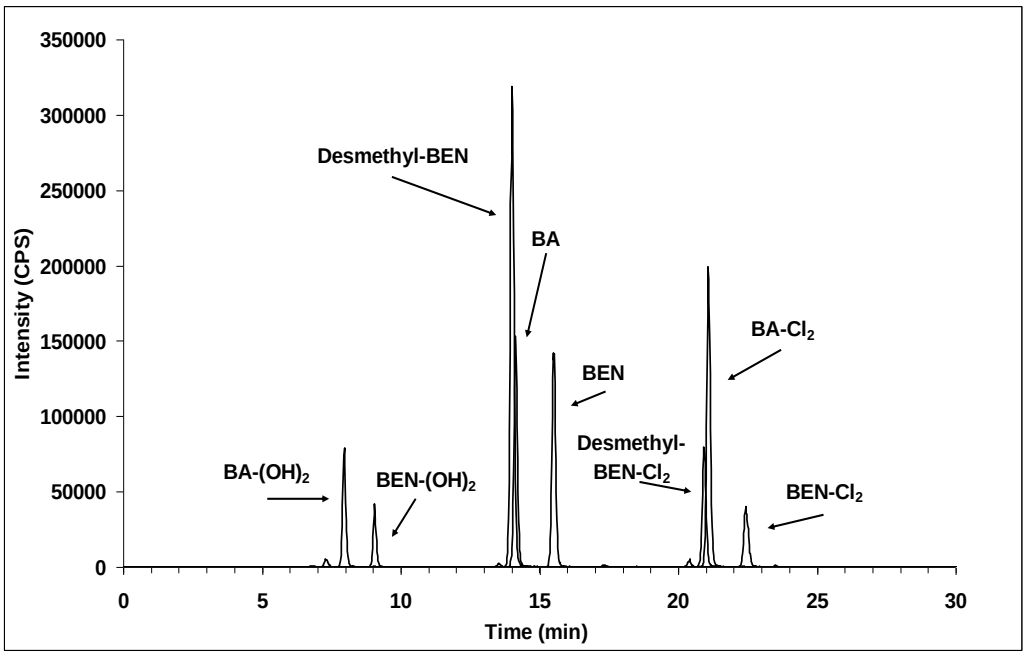

Figure 21. A representative chromatogram of BEN, BA, BEN-Cl_2, BEN-$(OH)_2$, BA-Cl_2, BA-$(OH)_2$ and desmethyl-BEN.

3.4.2 The effect of RBCs on BEN metabolism

The rate of disappearance of BEN increased as the percentage of RBCs was increased. After one hour the reaction that contained no RBCs had 99% of BEN remaining whereas the reaction with 10% RBCs had only 54% BEN remaining. After 6 hours the reaction with no RBCs had 59% remaining while the reaction with 10% RBCs had only 5% BEN remaining (Figure 22). Another measure of metabolism is the formation of BA-$(OH)_2$ or lack of metabolism is the formation of BEN-$(OH)_2$. The 10% RBC reaction produced the most BA-$(OH)_2$ and the least amount of BEN-$(OH)_2$ (Figure 23 and Figure 24).

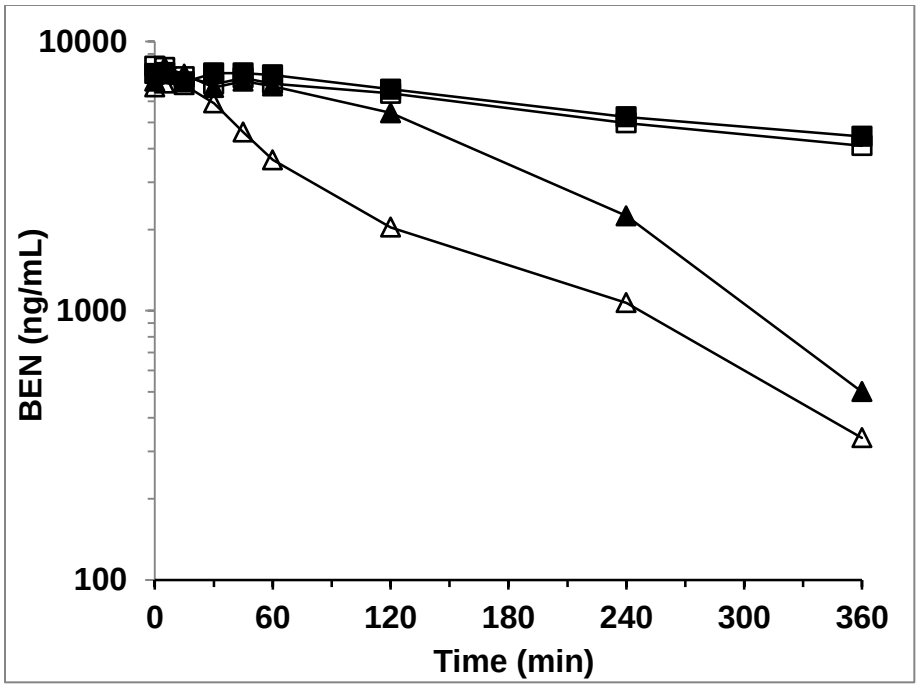

Figure 22. The disappearance of BEN with different percentages of RBCs. 0% RBCs (■), 0.1% RBCs (□), 1% RBCs (▲), and 10% RBCs (Δ).

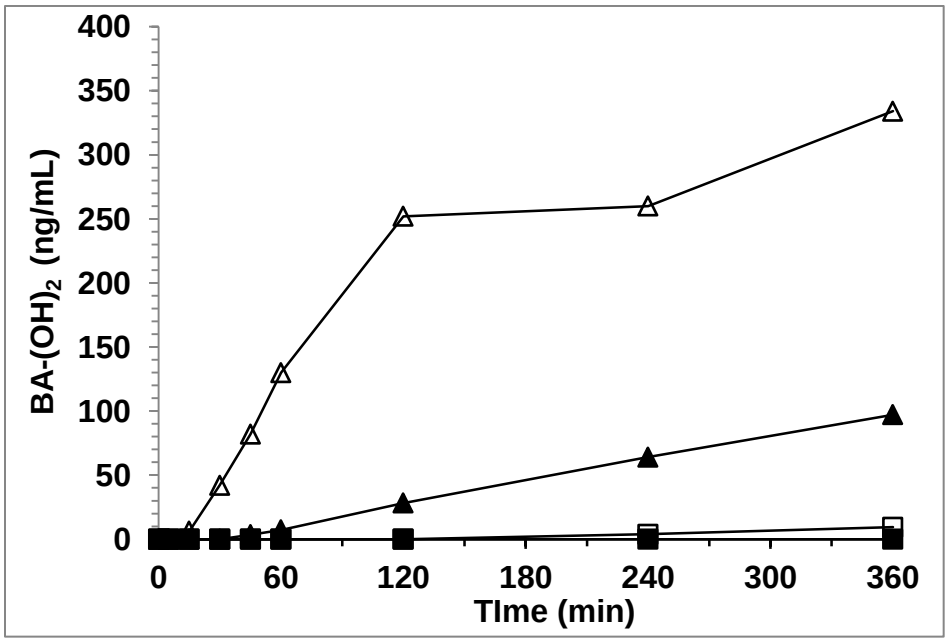

Figure 23. The production of BA-$(OH)_2$ when BEN is added to different concentrations of RBCs. 0% RBCs (■), 0.1% RBCs (□), 1% RBCs (▲), and 10% RBCs (Δ).

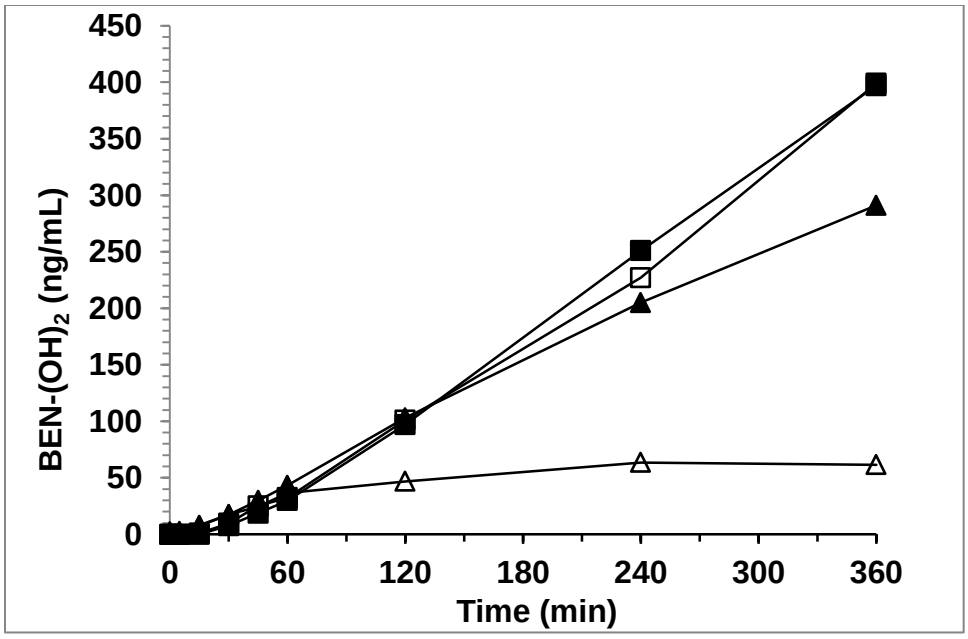

Figure 24. The production of BEN-$(OH)_2$ when BEN is added to different concentrations of RBCs. 0% RBCs (■), 0.1% RBCs (□), 1% RBCs (▲), and 10% RBCs (Δ).

3.4.3 Effects of carbon monoxide and nitrogen gas on BEN metabolism

We performed incubations of BEN in 10% RBCs in the presences of either carbon monoxide or nitrogen gas to determine if a heme group was involved in the metabolism of BEN. The metabolism of BEN was not appreciably inhibited by the presence of the gasses as the rate of disappearance of BEN appeared a little greater in the presence of the gasses. The half-life of BEN in the incubations up to 120 min was 56, 47 and 22 minutes for the control, CO gas and N_2 gas incubations, respectively

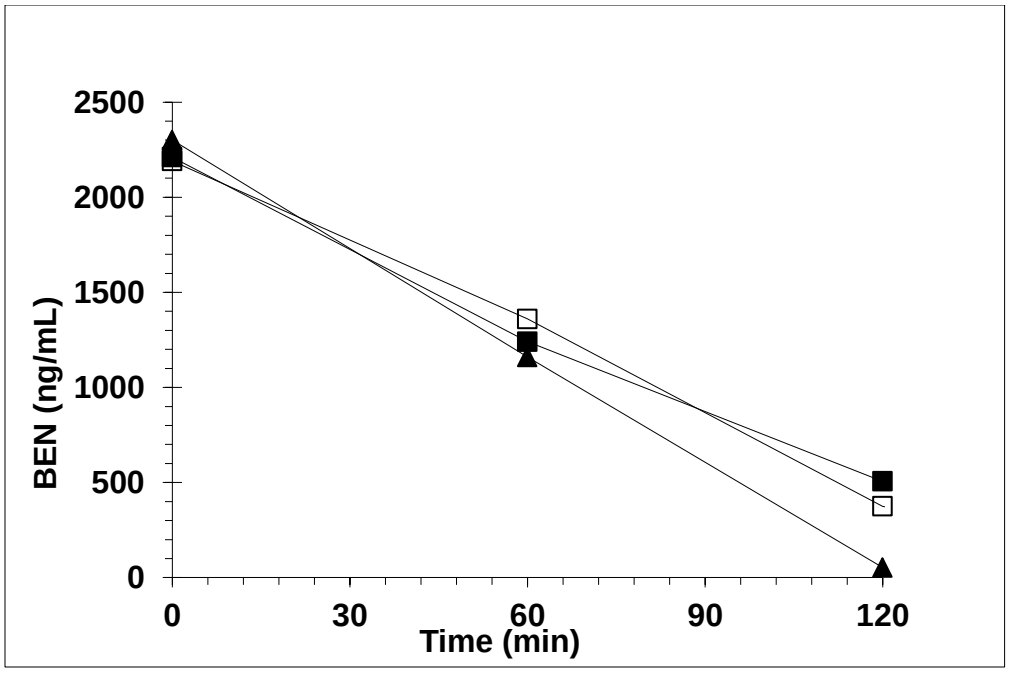

Figure 25. The disappearance of BEN in 10% RBCs: alone (■), in the presence of CO gas (□), and in the presence of nitrogen gas (▲).

3.4.4 Effects of disulfiram and menadione on BEN metabolism

To determine whether the metabolism of BEN in RBCs was due to ALDH or AO we performed incubations of BEN with RBCs in the presence of the ALDH inhibitor disulfiram or the AO inhibitor menadione. The incubation performed with the ALDH inhibitor disulfiram saw almost a complete inhibition of BEN metabolism, whereas the AO inhibitor menadione appeared to have only a partial inhibitory effect on metabolism of BEN. The amount of BEN remaining in the control, disulfiram and menadione sample was 0.5%, 92% and 18% respectively (Figure 26 and Figure 27).

Since menadione caused a partial inhibition of BEN metabolism, we performed additional experiments with increasing concentrations of menadione, in order to increase the inhibition of BEN. These experiments showed that DMSO alone (1.5% DMSO *v:v*) caused the same amount of inhibition of BEN in RBCs as 3 mM menadione (Figure 27).

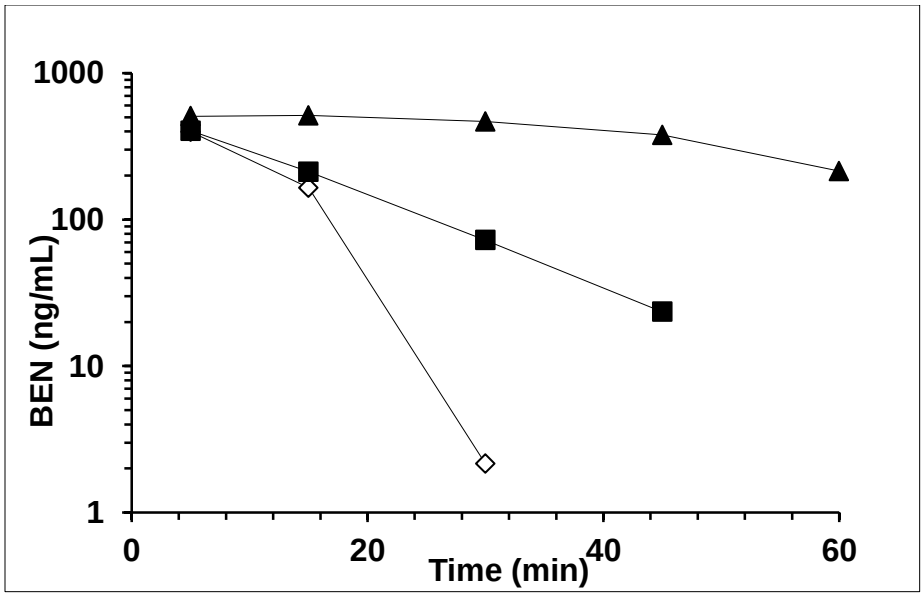

Figure 26. BEN added to 10% RBCs with and without inhibitors. BEN added to 10% RBCs (◊), BEN added to 10% RBCs in the presence of menadione (■), and BEN added to 10% RBCs in the presence of disulfiram (▲).

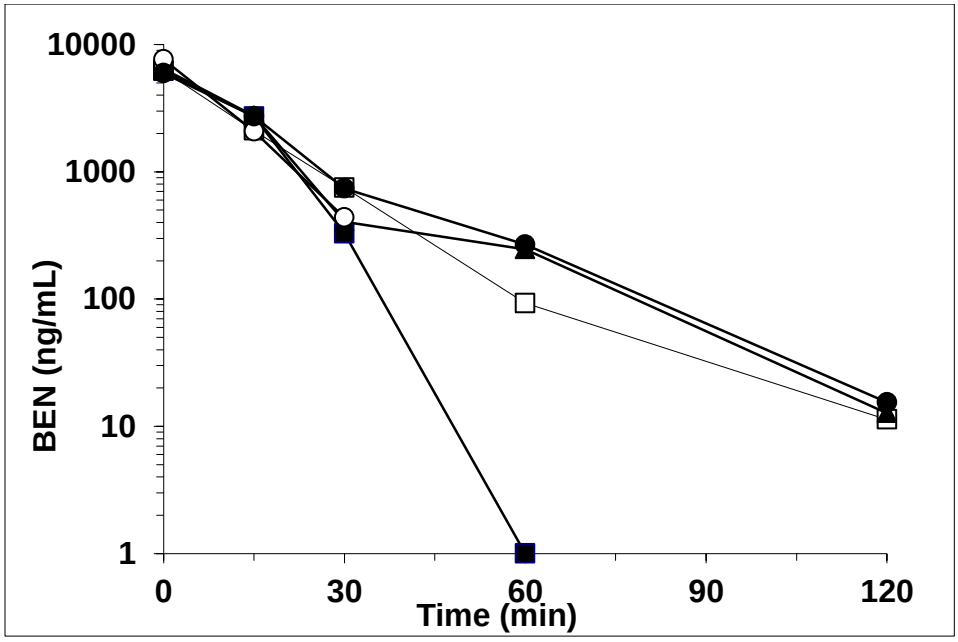

Figure 27. BEN added to 10% RBCs with and without different amounts of menadione. BEN alone(■), BEN + DMSO (□), BEN added after 1x menadione (▲), BEN added after 5x menadione (○), and BEN added after 20x menadione (●).

3.4.5 BEN in lysed blood

We performed experiments in lysed RBCs in order to determine whether a complete cell structure is required for the metabolism of BEN, or whether lysing the cells resulted in dilution of cofactors. RBCs that had been lysed before metabolism did not metabolize BEN (Figure 28). Adding NADH to the lysed RBCs incubation, however, restored the ability of lysed RBCs to metabolize BEN. Adding NADPH partially restored the ability of lysed RBCs to metabolize BEN. After 120 min the control non-lysed RBC reaction had 0.1% BEN remaining. Lysed RBCs with BEN alone showed 67% BEN remaining compared to 0.7% BEN remaining when NADH was added to lysed RBCs. Adding NADPH also led to metabolism of BEN. In this reaction there was 18% remaining after 120 min (Figure 29).

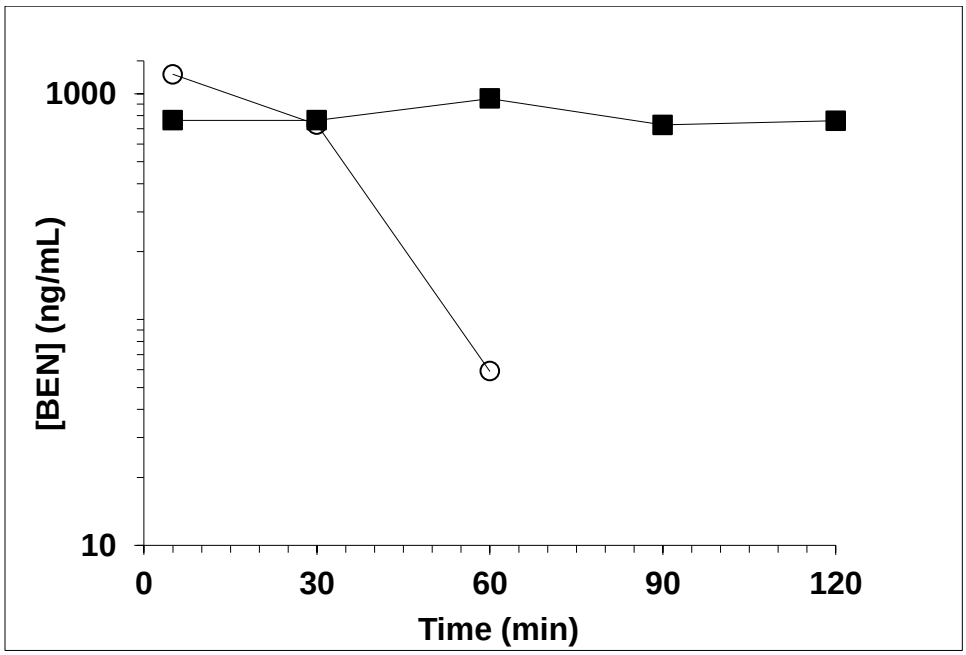

Figure 28. BEN added to 10% RBCs. 10% RBCs (○) and 10% lysed RBCs (■).

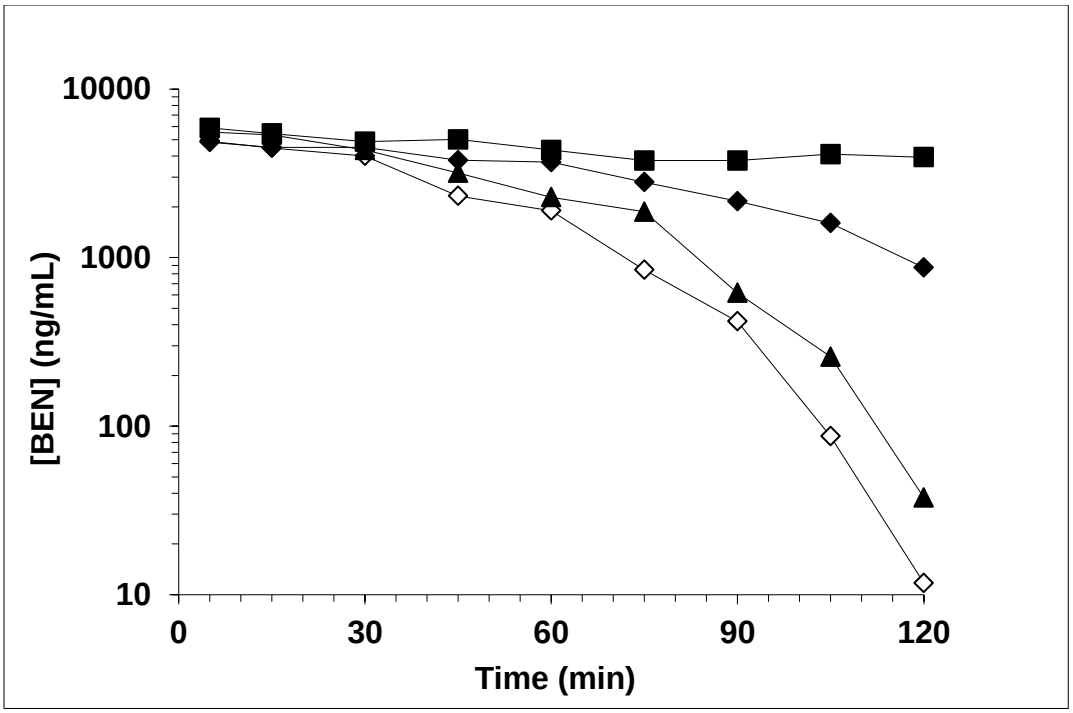

Figure 29. BEN added to lysed and non-lysed RBCs. 10% RBCs (◊), 10% lysed RBCs (■), 10% lysed RBCs + NADH (▲), and 10% lysed RBCs + NADPH (♦).

3.4.6 BEN blood to plasma concentration ratio

We determined the blood to plasma concentration ratio of BEN by measuring the amount of BEN added to blood that contained 50% RBCs to plasma alone as described in the methods section. The average partition ratio was found to be 1.25 ± 0.08. The amount of BEN detected in the blood remained nearly constant throughout the experiment, indicating that the equilibrium between RBCs and plasma was complete by 5 minutes and that BEN was not metabolized (Figure 30)

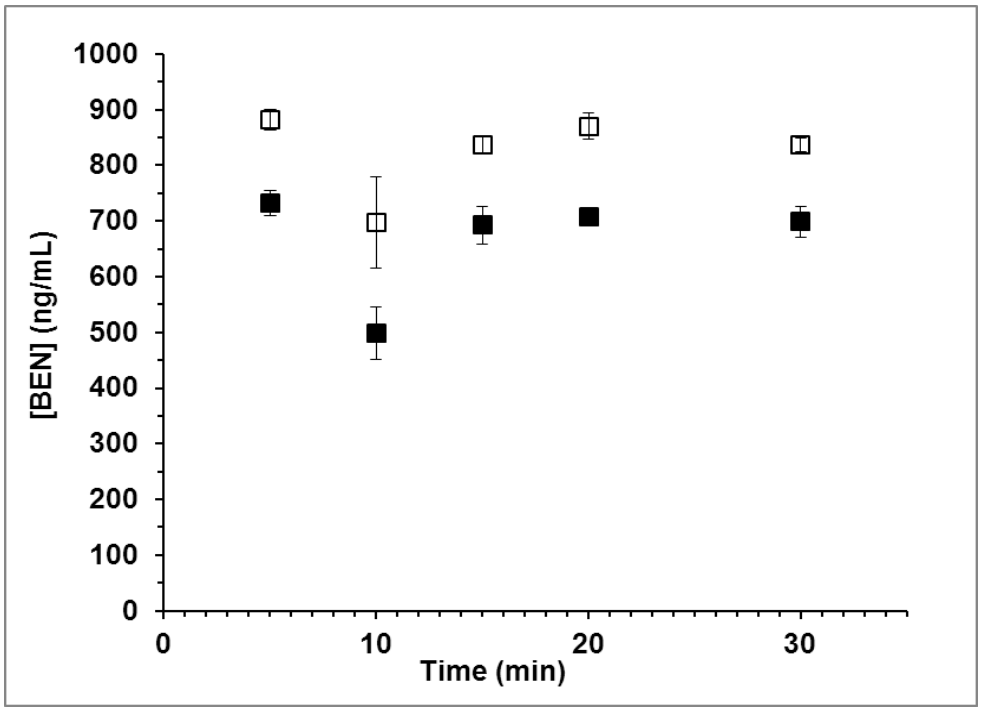

Figure 30. BEN blood to plasma partitioning. (■) BEN in the plasma portion of blood from blood that contained 50% RBCs and, (□) BEN in plasma.

3.4.7 Exploratory V_{max} and K_m determination

We performed metabolism of BEN at different concentrations in 10% RBCs to determine the concentration that would capture both the saturable and linear portion of the metabolism of BEN over time. We found that a starting concentration of 5000 ng/mL captured both the saturable and linear components of BEN metabolism (Figure 31). In addition, starting concentrations below 400 ng/mL appeared to mostly display linear metabolism.

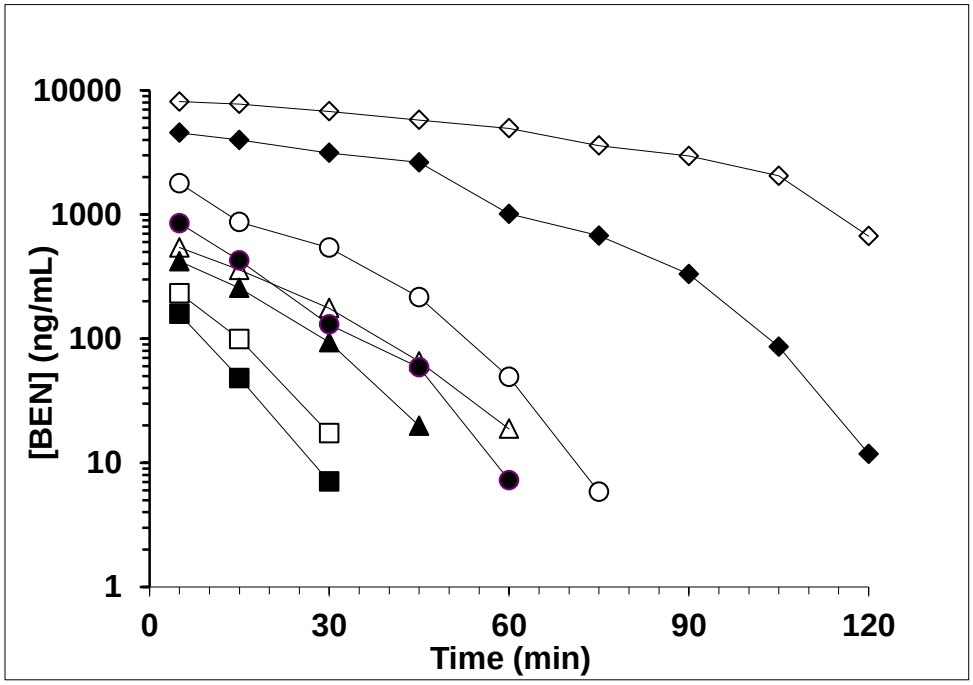

Figure 31. BEN metabolism with 10% RBCs. 200 ng/mL (■), 400 ng/mL (□), 600 ng/mL (▲), 800 ng/mL (Δ), 1000 ng/mL (●), 2000 ng/mL (○), 5000 ng/mL (♦), and 10000 ng/mL (◊).

3.4.8 V_{max} and K_m determination in 6 lots of blood

We tested six different lots of blood for the metabolism of BEN. Based on the exploratory data we choose to perform the metabolism of BEN using 5000 and 400 ng/mL to best capture the apparent V_{max} and K_m of BEN in blood. The apparent K_m ranged from 196.3 to 799.6 ng/mL and the apparent V_{max} ranged from 65.4 to 113.2

ng/mL^{-1}•min^{-1}•[10% RBC]$^{-1}$.(Table 4, Figure 32 and Figure 33). The average apparent V_{max} and K_m for the six lots of blood was 80.5 ng/mL•min^{-1}•[10% RBC]$^{-1}$ (SD 17.8, CV% 22.1) and 372.5 ng/mL (SD 152.1, CV% 40.8), respectively.

The fresh blood had an apparent V_{max} and K_m of 113.4 ng/mL^{-1}•min^{-1}•[10% RBC]$^{-1}$ (95% CI, 106.6 – 120.1) and 608.9 ng/mL (95% CI, 483.5 – 736.2 ng/mL) compared to 100.2 ng/mL-1•min^{-1}•[10% RBC]$^{-1}$ (95% CI, 95.17 – 105.2) and 699.6 ng/mL (95% CI, 594.5 – 804.7 ng/mL) for the seven day old blood that was stored at 4 ˚C for seven days.

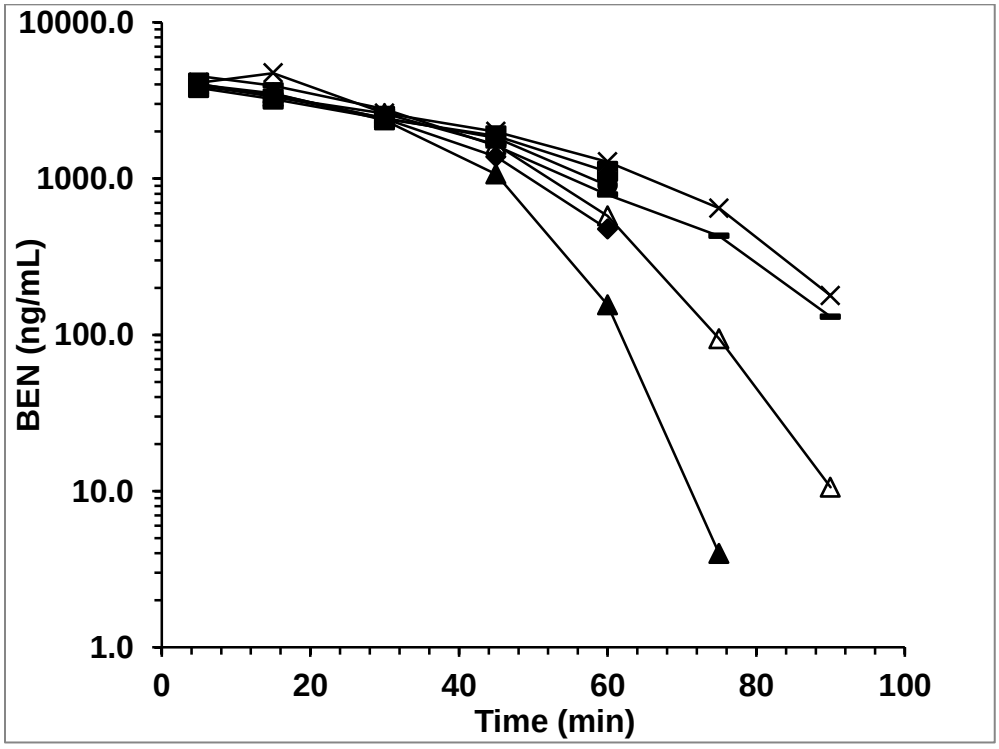

Figure 32. BEN (5000 ng/mL) in RBCs over time. Lot D (■), Lot E (♦), Lot F (●), Lot G (▲), Lot H (-), Lot I (x), and Lot G after stored at 4 C for one week (Δ).

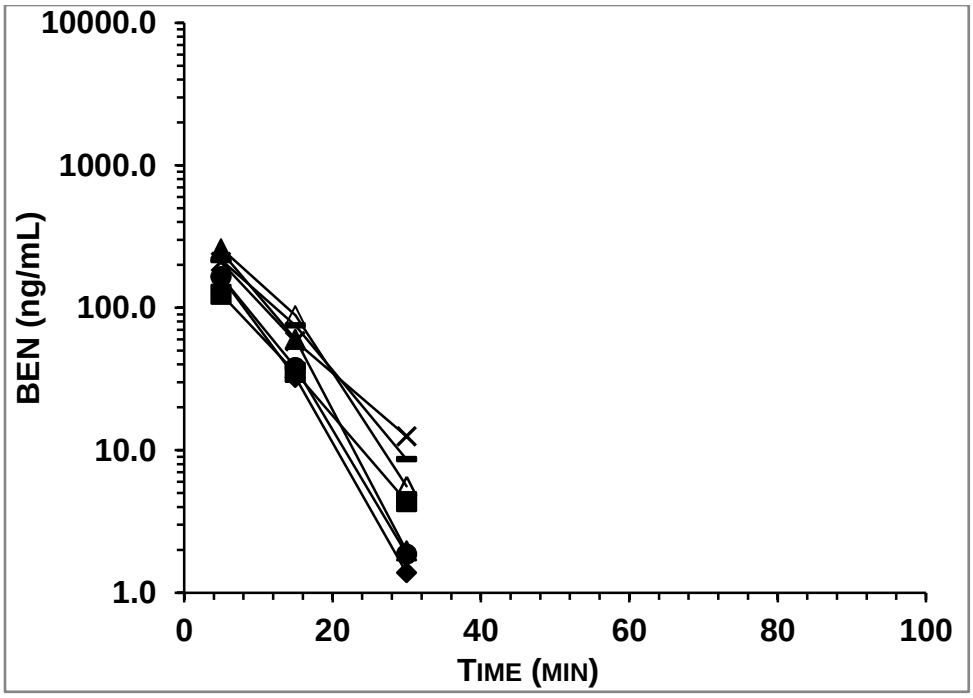

Figure 33. BEN (400 ng/mL) in RBCs over time. Lot D (■), Lot E (♦), Lot F (●), Lot G (▲), Lot H (-), Lot I (x), and Lot G after stored at 4 C for one week (Δ).

Table 4. K_m and V_{max} of BEN in six different lots of human blood

Lot 1 (D)		**SE (CV%)**	**Confidence interval (95%)**
Km	196.3	8.399	[161.7 , 230.9]
Vmax	65.44	4.288	[59.54 , 71.34]
V400	2.117	7.253	[1.795 , 2.440]
V5000	1.264	4.992	[1.132 , 1.397]
Cl	0.333	5.585	[0.2942 , 0.3725]
Lot 2 (E)		**SE (CV%)**	**Confidence interval (95%)**
Km	319.5	4.457	[289.6 , 349.4]
Vmax	87.42	1.125	[85.35 , 89.49]
V400	1.308	4.934	[1.172 , 1.443]
V5000	1.112	2.521	[1.053 , 1.170]
Cl	0.2736	3.643	[0.2527 , 0.2946]
Lot 3 (F)		**SE (CV%)**	**Confidence interval (95%)**
Km	256.2	5.414	[227.1 , 285.4]
Vmax	72.27	2.236	[68.88 , 75.67]
V400	1.373	4.85	[1.233 , 1.513]
V5000	1.186	3.158	[1.107 , 1.264]
Cl	0.282	3.978	[0.2585 , 0.3056]
Lot 4 (G)		**SE (CV%)**	**Confidence interval (95%)**
Km	609.8	10.04	[483.5 , 736.2]
Vmax	113.4	2.865	[106.6 , 120.1]
V400	0.9553	9.802	[0.7620 , 1.149]
V5000	0.8099	5.924	[0.7109 , 0.9090]
Cl	0.1859	7.653	[0.1565 , 0.2152]
Lot 5 (H)		**SE (CV%)**	**Confidence interval (95%)**
Km	481.8	7.136	[410.8 , 552.8]
Vmax	76.5	2.063	[73.24 , 79.76]
V400	1.05	6.87	[0.9008 , 1.198]
V5000	1.168	3.209	[1.091 , 1.245]
Cl	0.1588	5.253	[0.1416 , 0.1760]
Lot 6 (I)		**SE (CV%)**	**Confidence interval (95%)**
Km	371.2	7.729	[312.0 , 430.5]
Vmax	68.16	1.811	[65.61 , 70.71]
V400	1.405	8.624	[1.155 , 1.655]
V5000	1.063	4.026	[0.9745 , 1.151]
Cl	0.1836	6.142	[0.1603 , 0.2068]
Lot 4 (G) old		**SE (CV%)**	**Confidence interval (95%)**
Km	699.6	7.276	[594.5 , 804.7]
Vmax	100.2	2.416	[95.17 , 105.2]
V400	0.8615	6.687	[0.7426 , 0.9804]
V5000	0.9246	3.679	[0.8544 , 0.9948]
Cl	0.1432	5.145	[0.1280 , 0.1584]

3.4.9 Immunoprecipitation of RBCs

We performed immunoprecipitation of RBCs with antibodies for ALDH1A1. The purpose was to precipitate the ALDH1A1 enzyme, rendering it inactive and implicate it in the metabolism of BEN by RBCs. Despite our best efforts, however, the control RBC experiment with no antibodies added would not metabolize BEN after being subjected to the immunoprecipitation procedure. In an attempt to preserve metabolism of BEN with RBCs, we varied the amount of protease inhibitors and concentration of the different buffer used, without success.

3.4.10 Western blot

To determine whether RBCs have ALDH1A1 and to test whether the ALDH1A1 antibody used for the immunoprecipitation experiment would bind to the enzyme we performed a western blot assay. The western blot showed a band in the 55 kD region, which is the size of ALDH1A1 enzyme (55 kD). The intensity of the band increased with the addition of more protein (Figure 34).

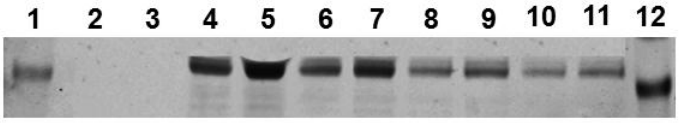

Figure 34. Western blot of ALDH1A1 from human RBCs. Lanes from left: lane 1 – ladder (49.9kDa), lanes 2 and 3 - blank, lanes 4 and 5 - 80 µg protein, 6 and 7 - 40 µg protein, 8 and 9 - 20 µg protein, lanes10 and 11 - 10 µg protein, and lane 12 ladder (49.9 kDa).

3.4.11 Metabolism using purified ALDH

To determine if ALDH is responsible for the metabolism of BEN we assessed the metabolism of BEN with the commercially available isoforms of ALDH. These included ALDH1A1, 2, 3A1 and 5A1. In addition, we studied the metabolism of BEN with ALDH1A1 in the presence of antibodies of 1A1 and disulfiram in order to inhibit the metabolism of BEN. ALDH1A1 was the only isoform that showed the ability to metabolize BEN. In three independent experiments the rate of disappearance of BEN was 0.172, 0.224 and 0.154 ng/min/µg of enzyme (Figure 35, Figure 37, and Figure 39). Also in these experiments, BA was generated as BEN concentrations decreased (Figure 36, Figure 38, and Figure 40). Disulfiram did not inhibit the reaction of ALDH1A1. This is likely due to the fact that disulfiram is inactivated by the dithiothreitol present in the reaction mixture, thereby preventing it from inhibiting ALDH. Furthermore, the addition

of 100x of the ALDH1A1 and IgG antibodies did not inhibit the metabolism of purified ALDH1A1 (Figure 41 and Figure 42).

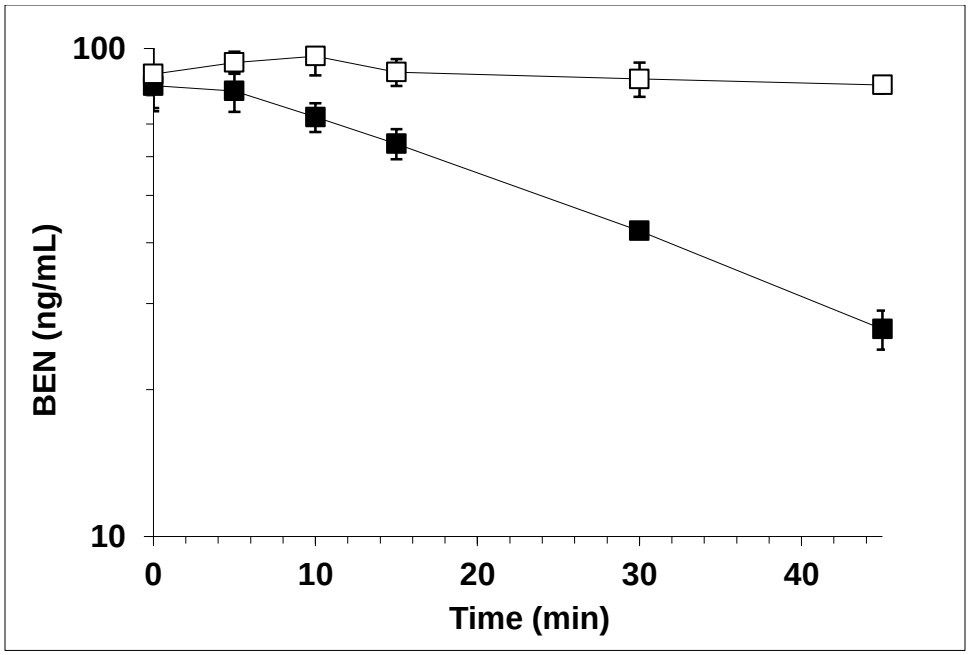

Figure 35. Metabolism of BEN by purified human ALDH1A. ALDH1A1 (■) and no enzyme (□). Each point is the average of three measurements.

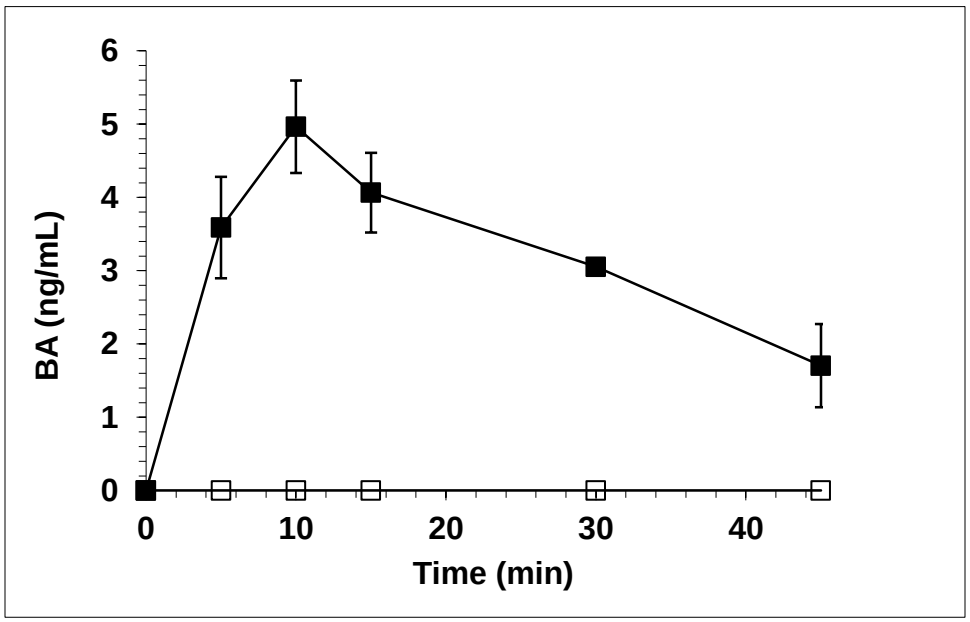

Figure 36. Generation of BA when BEN is added to purified human ALDH1A1. ALDH1A1 (■) and no enzyme (□). Each point is the average of three measurements.

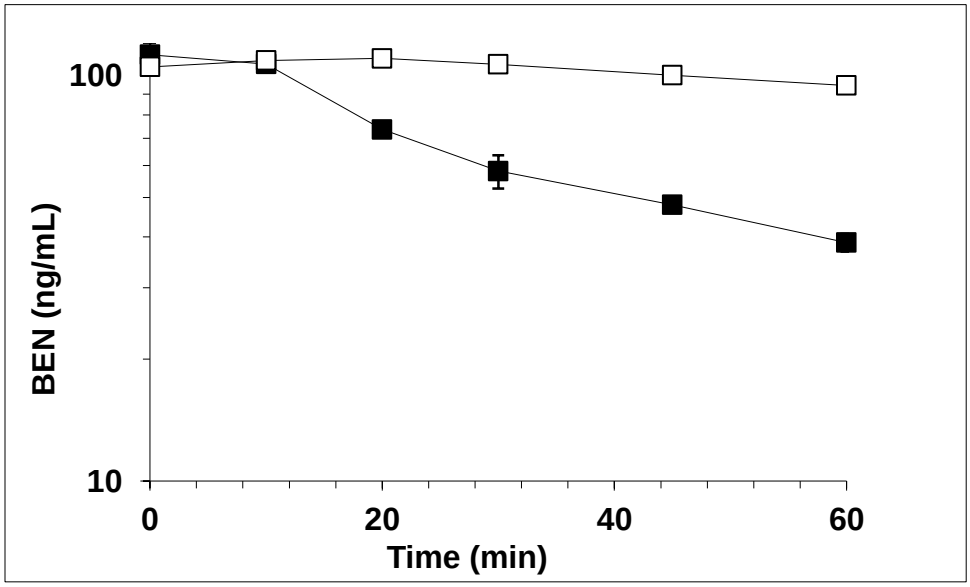

Figure 37. Metabolism of BEN by purified human ALDH1A. ALDH1A1 (■) and no enzyme (□). Each point is the average of three measurements.

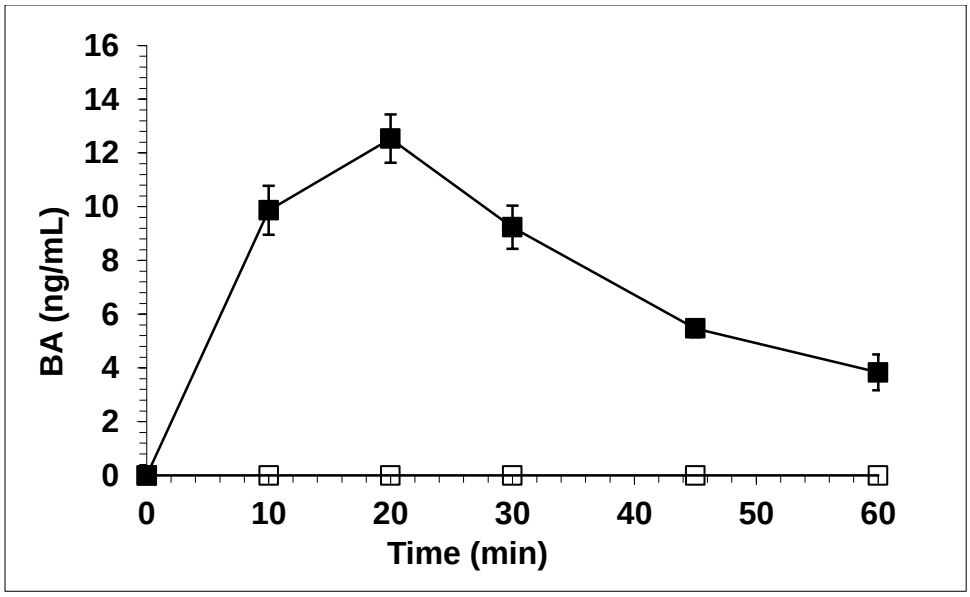

Figure 38. Generation of BA when BEN is added to purified human ALDH1A1. ALDH1A1 (■) and no enzyme (□). Each point is the average of three measurements.

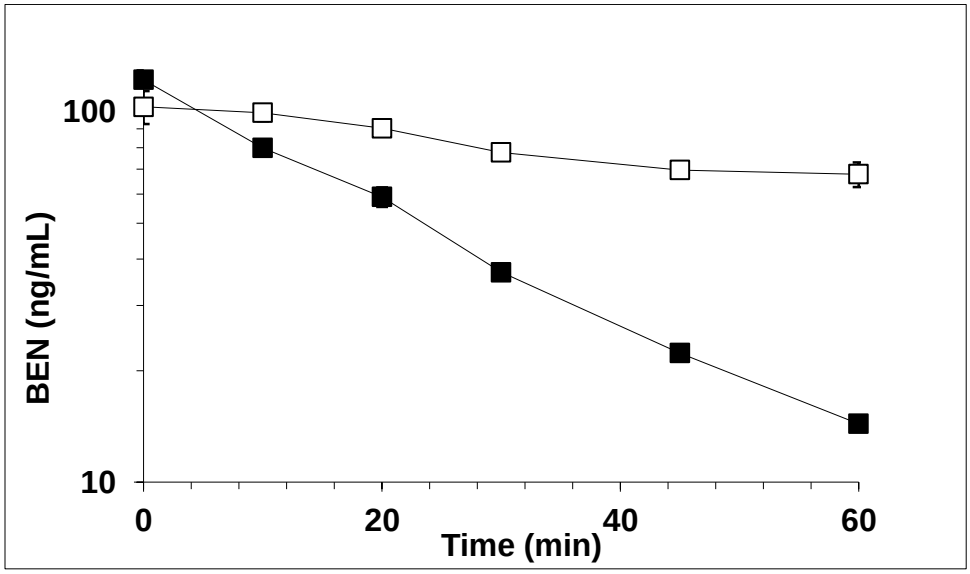

Figure 39. Metabolism of BEN by purified human ALDH1A. ALDH1A1 (■) and no enzyme (□).Each point is the average of three measurements.

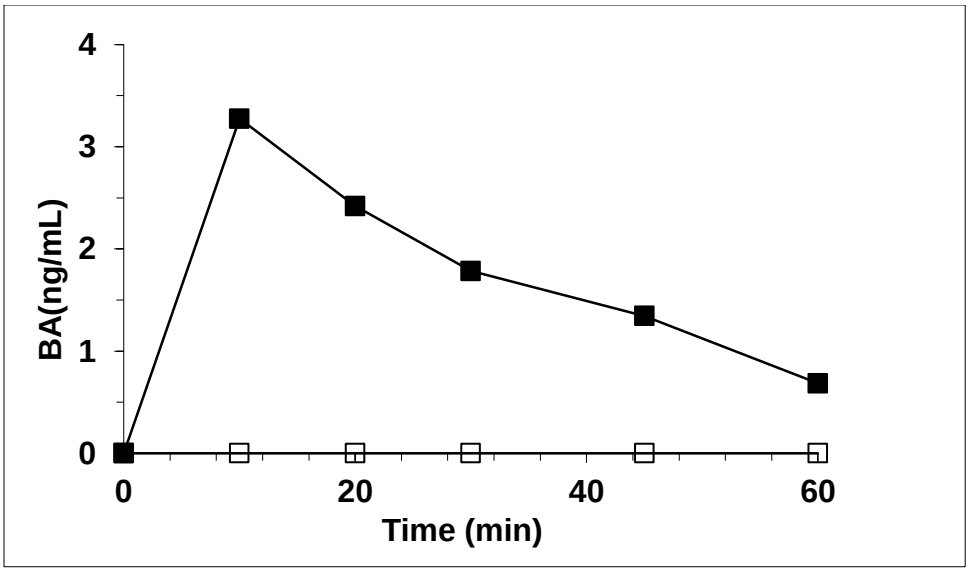

Figure 40. Generation of BA when BEN is added to purified human ALDH1A1. ALDH1A1 (■) and no enzyme (□).Each point is the average of three measurements.

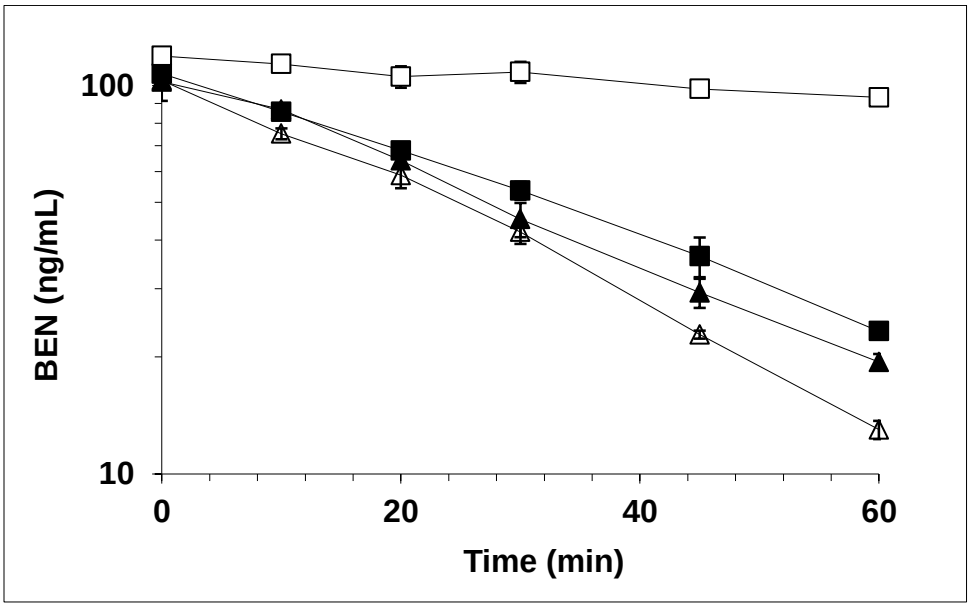

Figure 41. Metabolism of BEN by purified human ALDH1A. ALDH1A1 (■), no enzyme (□), ALDH1A1 with ALDH1A1 antibody (▲), and ALDH1A1 with IgG antibody (Δ). Each point is the average of three measurements.

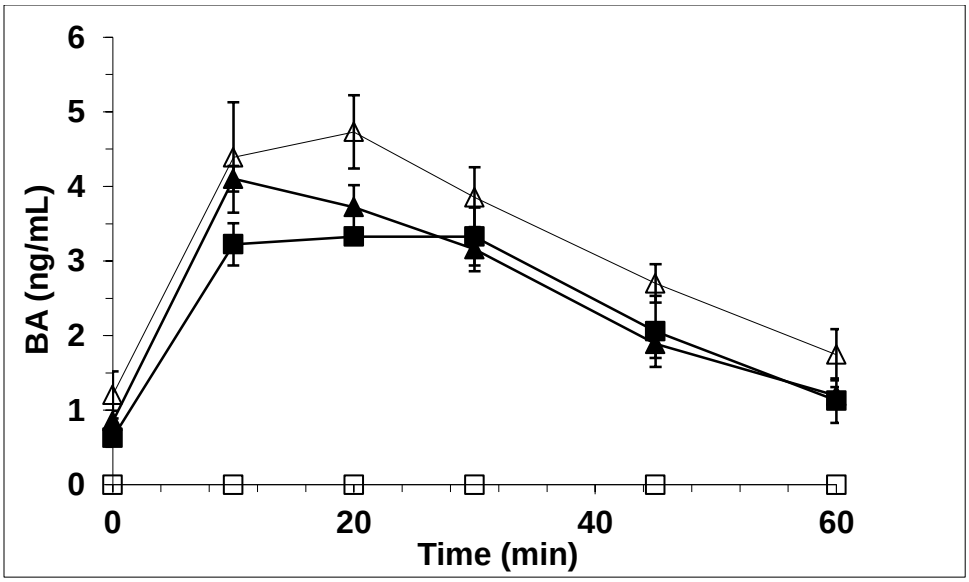

Figure 42. Generation of BA when BEN is added to purified human ALDH1A1. ALDH1A1 (■), no enzyme (□), ALDH1A1 with ALDH1A1 antibody (▲), and ALDH1A1 with IgG antibody (Δ). Each point is the average of three measurements.

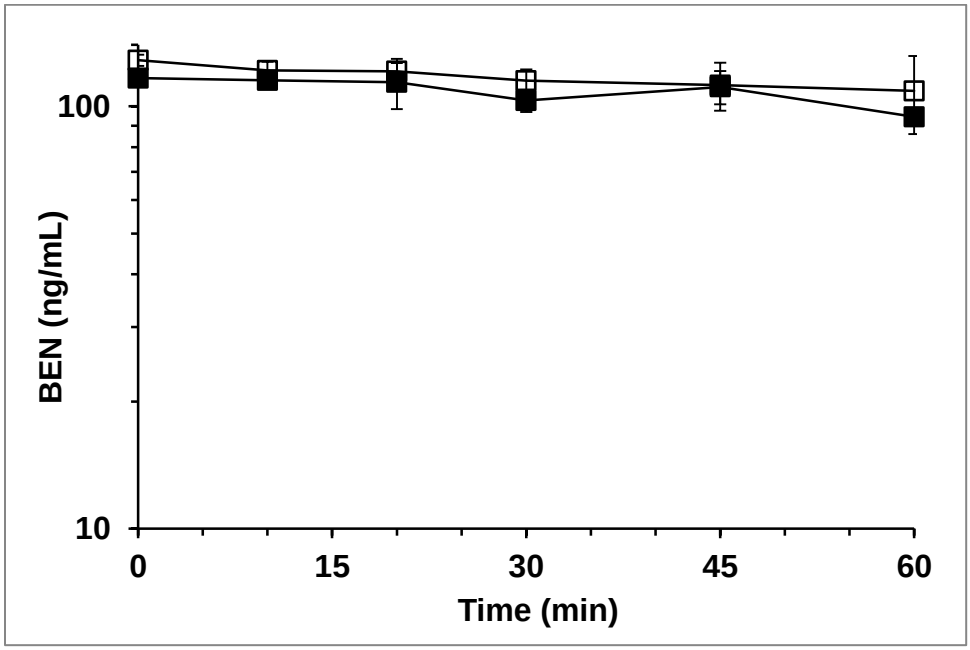

Figure 43. BEN metabolism with purified human ALDH2. ALDH2 (■) and no enzyme (□).Each point is the average of three measurements.

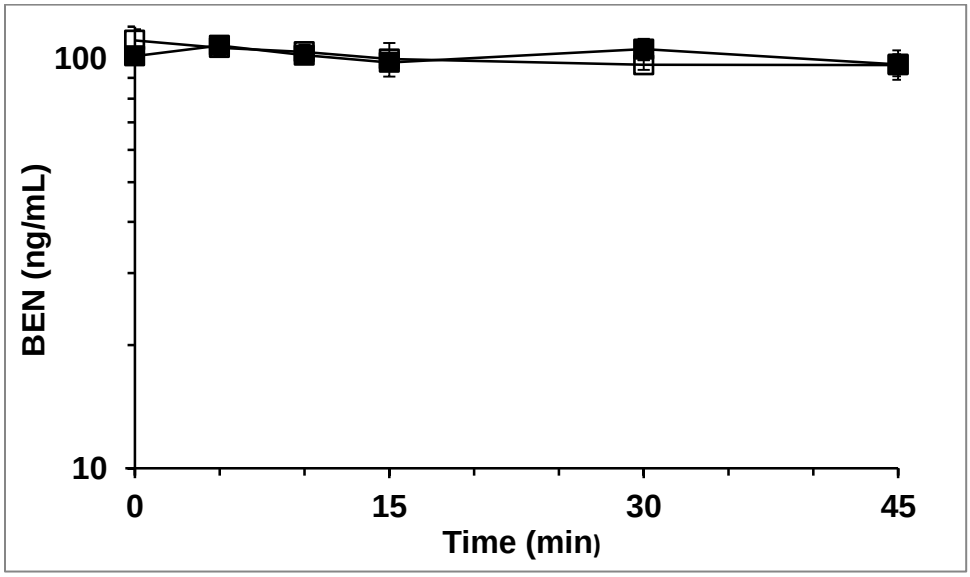

Figure 44. BEN metabolism with purified human ALDH3A1. ALDH3A1 (■) and no enzyme (□). Each point is the average of three measurements.

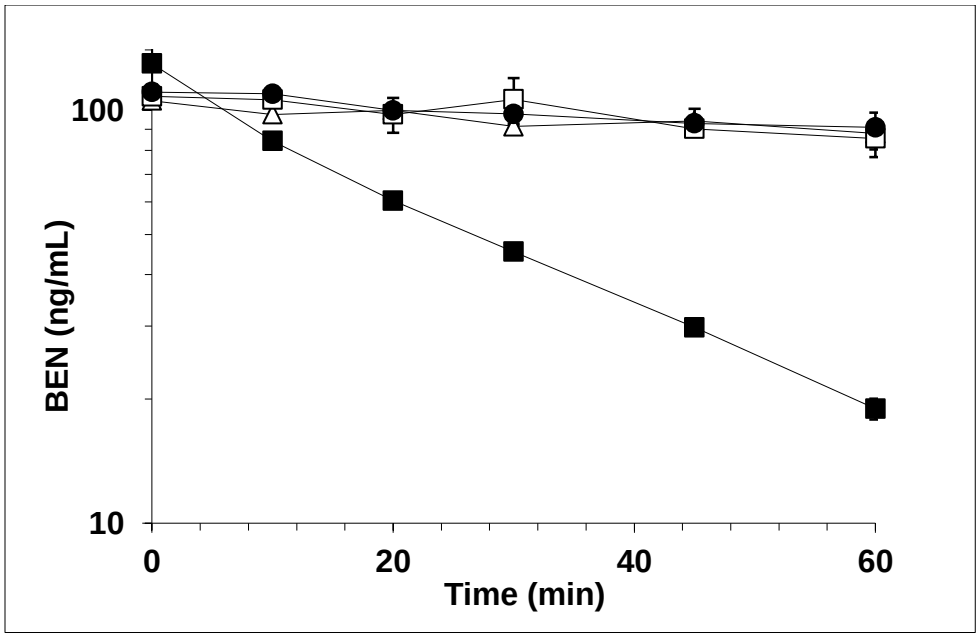

Figure 45. BEN metabolism with: purified ALDH1A1 (■), no enzyme (Δ), purified ALDH1A1 and no NAD (□), and purified ALDH5A1 (●).

3.4.12 Positive controls using purified ALDH isoforms on spectrophotometer

To ensure that the purified ALDH isoforms that were obtained were active, we performed metabolism of purified ALDH2, 3A1 and 5A1. In all cases, the purified enzymes showed activity, whereas the control samples, which contained enzyme but no substrate, did not show activity. (Figure 46, Figure 47, Figure 48).

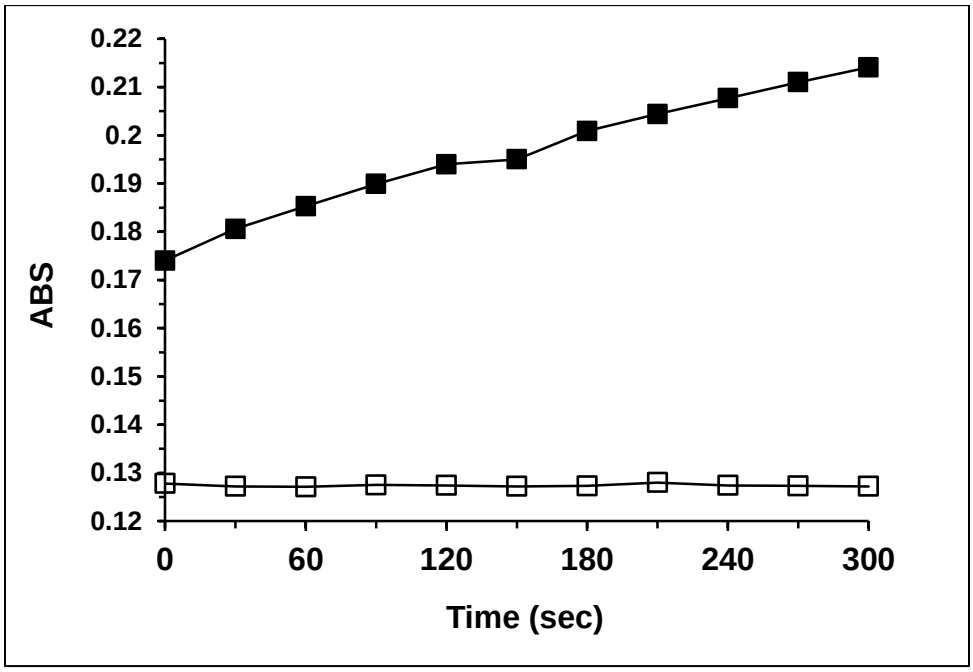

Figure 46. Measurement of the reduction of NAD to NADH by the activity of ALDH2. ALDH2 (■) and no enzyme (□).

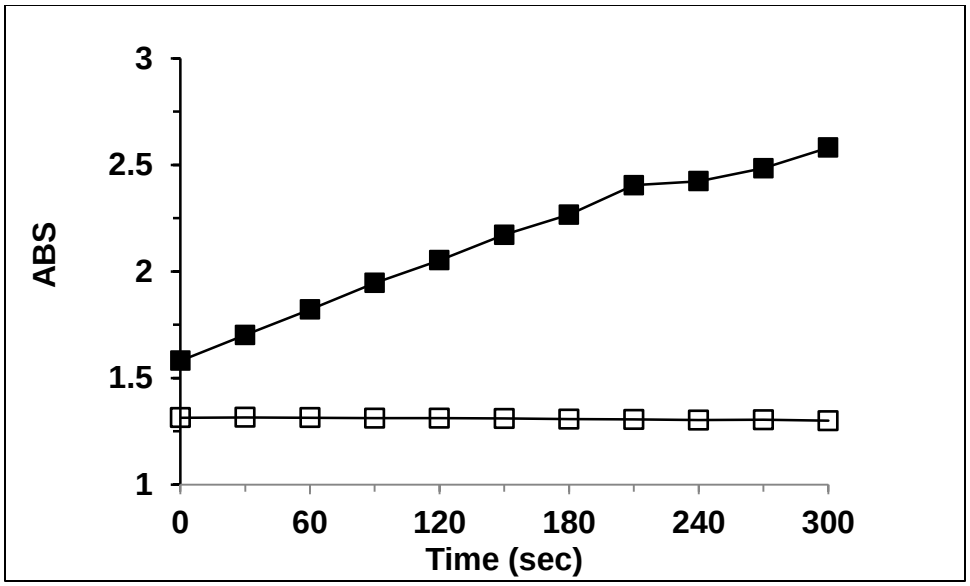

Figure 47. Measurement of the reduction of NAD to NADH by the activity of ALDH3A1. ALDH3A1 (■) and no enzyme (□).

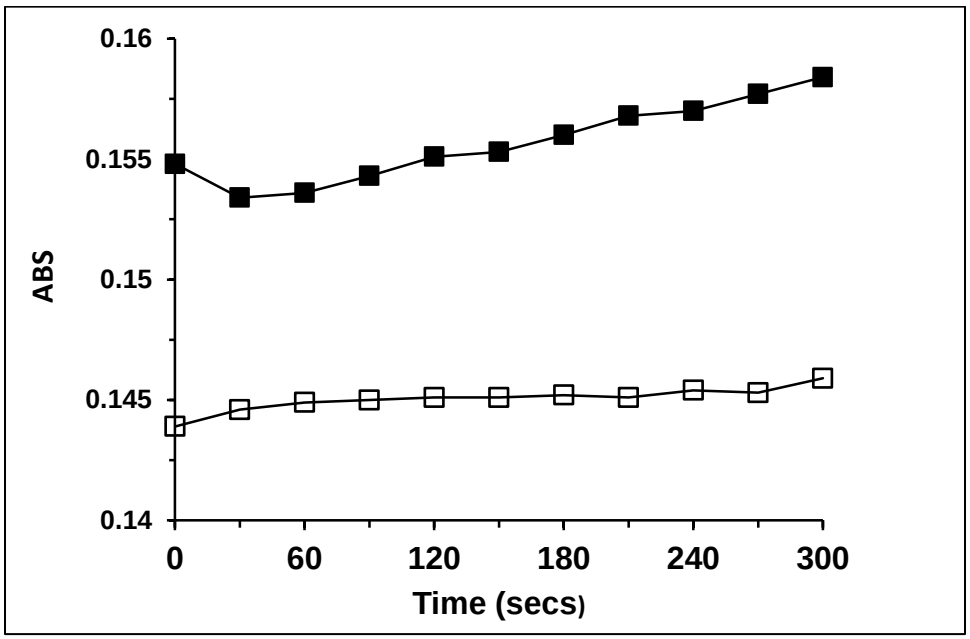

Figure 48. Measurement of the reduction of NAD to NADH by the activity of ALDH5A1. ALDH5A1 (■) and no enzyme (□).

3.5 DISCUSSION

BEN is an alkylating agent currently being investigated in phase I clinical trials. BEN has structural similarities to both busulfan and melphalan. As with related alkylators, we have previously shown that BEN undergoes hydrolysis in blood and plasma.[144] In whole blood, but not in plasma, BEN is rapidly converted to its carboxylic acid analogue BA, suggesting conversion by an enzyme present in red blood cells. In plasma, BEN and BA decompose according to a parallel pathway to a number of hydroxylated and chlorinated analogues, as depicted in Figure 13 chapter 2. The half-life of BA in plasma is very short ~5 min compared to BEN. We hypothesize that BA is more reactive than BEN because the unbound electron pair on the aniline nitrogen in BA is the initiator of an SN2 attack on the β-carbon, generating the reactive aziridinium intermediate. Mesomeric withdrawal of the aniline unbound electron pair by the para-aldehyde moiety on BEN would be expected to decrease the generation of the aziridinium intermediate and thereby decrease the reactivity.

We previously determined that some of the BEN and BA analogues displayed activity against renal carcinoma cells. In addition, we showed that the generation of BA from BEN in renal carcinoma cell lines correlates with ALDH activity and IC_{50} values. This led us to hypothesize that the enzyme responsible for the conversion in blood and renal carcinoma cells is ALDH. These data suggest that BEN is a pro-drug that requires intracellular activation to the highly reactive BA, which likely exerts rapid and localized damage via alkylation inside the cells.

In order to better understand the pharmacology of BEN, we aimed to characterize the enzyme responsible for the conversion of BEN to BA. This was done by evaluating

the metabolism of BEN in RBCs, determining the apparent V_{max} and K_m in blood, performing inhibition studies in RBCs and lastly by performing the metabolism of BEN by purified isoforms of ALDH.

We tested the effect that different concentrations of RBCs had on the rate of BEN metabolism. This was done to determine the suitable amount of RBCs for timed metabolism experiments. Also, we obtained units of blood for metabolism experiments from the central blood bank. Individuals differ in the percentage of RBCs in whole blood, or hematocrit. Generally, the hematocrit range for females is 37 to 47% and for men 42 to 52%.[153] The goal was to show an appreciable amount of BEN metabolism in a thirty minute incubation time and to have the same amount of RBCs in all reaction mixtures. We performed BEN metabolism with 0.1, 1 and 10% RBCs and determined that 10% RBC in plasma was adequate for future metabolism studies.

Our laboratory has previously performed BEN metabolism experiments with mouse liver microsomes. These experiments showed that BEN was not a substrate for CYP450s. Carbon monoxide binds tightly to heme groups in P450s rendering them ineffective for metabolism. We evaluated the metabolism of BEN in the presence of carbon monoxide gas and the metabolism was not slowed compared to control. ALDH and AO are the two major enzyme types that are responsible for the conversion of aldehydes to carboxylic acids. Disulfiram is an irreversible inhibitor of several ALDHs including ALDH1A1, the major isoform of ALDH in RBCs, and menadione is an inhibitor of AO. We evaluated the metabolism of BEN in RBCs in both the presence of disulfiram or menadione. Disulfiram almost completely inhibited BEN metabolism, while menadione inhibited the metabolism no more than the DMSO control.

We evaluated the metabolism of BEN in RBCs that were lysed to determine whether a complete red blood cell was needed for metabolism. Lysed RBCs did not metabolize BEN, which is most likely due to dilution of the necessary cofactors that occurs in the lysing process. Adding NADH to lysed RBCs restored the metabolism of BEN.

The apparent V_{max} and K_m of BEN were determined in 6 different lots of blood to evaluate biological central tendency and variability. BEN displayed saturable kinetics. We found that there was inter-subject variability between the lots of blood. The %CV for V_{max} and K_m were 22% and 41%, respectively, for the 6 lots of blood analyzed. This is not surprising as the inter-individual biological variability for the quantity of certain enzymes can be as much as 73 percent and the inter-individual activity of e.g. CYP3A4 can range from 200 to 300 percent.[154,155] In addition, there are two known polymorphism of ALDH1A1, ALDH1A1*2 and ALDH1A1*3.[156] These polymorphisms occur in 7% percent of the population and are responsible for reduced enzymatic activity.[157] Although there was variability, all lots of blood displayed K_m values above 16 ng/mL and 197 ng/mL which were the average C_{max} concentrations in mice that were either dosed with 20 mg/kg BEN alone or with 300 mg/kg ip of disulfiram before 20 mg/kg BEN in our recent study. A dose of 20 mg/kg in mouse is equivalent to 60 mg/m^2. The patients in the clinical study will start at a dose of 1.5 mg/m^2 which is 40 times less than the mice received. Thus we would expect linear kinetics of BEN in humans.

To determine if the ALDH1A1 enzyme was present and that the antibodies used recognized ALDH1A1 we performed a western blot assay using lysed RBCs. The

antibodies used did prove to be effective as ALDH1A1 was detected using the western blot assay.

To test whether ALDH1A1 is responsible for the metabolism of BEN in RBCs we performed immunoprecipitation experiments. The intent was to precipitate the ALDH1A1 enzyme from RBCs and perform metabolism experiments. The immunoprecipitation procedure proved to render the control RBCs ineffective for metabolism. We attempted to modify the immunoprecipitation procedure by changing the concentration of buffers used, with and without protease inhibitors and varying incubation times. These attempts proved to be fruitless as the positive control sample was never effective in metabolizing BEN.

We performed the metabolism of BEN with the purified ALDH enzymes that were commercially available. These included ALDH1A1, 3A1, 2 and 5A1. BEN was only a substrate for ALDH1A1. We also performed the metabolism of BEN with purified ALDH1A1 in the presence of 1A1 antibody, which was successful in binding the enzyme as evidenced by the western blot experiments. The ALDH1A1 antibody was not able to inhibit the reaction, which is possible if the antibody binds to an ALDH1A1 epitope without hindering ALDH1A1 metabolic activity. Also, adding disulfiram to the reaction mixture did not slow the metabolism. Dithiothreitol, which is a reducing agent that is required in the reaction mixture to reduce ALDH, also reduces disulfiram thereby rendering it ineffective as an inhibitor.

In conclusion, BEN has shown activity both *in vitro* and *in vivo* and is currently in phase I clinical trials. We hypothesize that BEN is actually a prodrug and that its main metabolite BA is more reactive and responsible for the alkylating activity. We have

previously demonstrated that the conversion of BEN to BA occurs in RBCs. In the current chapter we have demonstrated that ALDH1A1 likely is the enzyme that is responsible for this conversion. This could have implications as there are drugs that are known to inhibit ALDH1A1 such as disulfiram and metronidazole and also seven percent of the population has polymorphic ALDH1A1. Since patients that have polymorphic ALDH1A1 might not be able to metabolize BEN to BA in tissues, BEN may be less effective in these subjects Special consideration should be given when dosing patients in these circumstances. In addition, since BA is the more active species which is generated by ALDH1A1 metabolism, cancers that are known to over express this enzyme such as certain lung and ovarian tumors may be a target for BEN. It is noteworthy to mention that tumor stem cells have been found to over express ALDH1A1 and that BEN may be an ideal candidate for these cells as well.

4.0 EFFECTS OF THE ALDEHYDE DEHYDROGENASE INHIBITOR DISULFIRAM ON THE PLASMA PHARMACOKINETICS, METABOLISM, AND TOXICITY OF BENZALDEHYDE DIMETHANE SULFONATE (NSC281612, DMS612, BEN) IN MICE.

Parise RA, Beumer JH, Clausen DM, Rigatti LH, Ziegler JA, Gasparetto M, Smith CA, Eiseman JL. **Effects of the aldehyde dehydrogenase inhibitor disulfiram on the plasma pharmacokinetics, metabolism, and toxicity of benzaldehyde dimethane sulfonate (NSC281612, DMS612, BEN) in mice.** Cancer Chemother Pharmacol. 2013 Sep 24. [Epub ahead of print]

4.1 ABSTRACT

Benzaldehyde dimethane sulfonate (DMS612, NSC281612, BEN) is an alkylator with activity against renal cell carcinoma, currently in phase I trials. In whole blood, BEN is rapidly metabolized into its highly reactive carboxylic acid (BA), presumed to be the predominant alkylating species. We hypothesized that BEN is metabolized to BA by aldehyde dehydrogenase (ALDH) and aimed to increase BEN exposure in blood and tissues by inhibiting ALDH with disulfiram thereby shifting BA production from blood to tissues.

Female CD2F1 mice were dosed with 20 mg/kg BEN iv alone or 24 h after 300 mg/kg disulfiram ip. BEN, BA and metabolites were quantitated in plasma and urine, and organ toxicities were assessed.

BEN had a plasma t½ <5 min and produced at least 12 products. The metabolite half-lives were <136 min. Disulfiram increased BEN plasma exposure 368-fold, (AUC_{0-inf} from 0.11 to 40.5 mg•min/L), while plasma levels of BA remained similar. Urinary BEN excretion increased (1.0 to 1.5% of dose) while BA excretion was unchanged.

Hematocrit, white blood cells counts and % decrease in lymphocytes all decreased after BEN administration, while co-administration of disulfiram appeared to enhance these effects. Profound liver pathology was observed in mice treated with disulfiram and BEN.

BEN plasma concentrations increased after administration of disulfiram, suggesting that ALDH mediates the rapid metabolism of BEN *in vivo*, which may explain the increased toxicity seen with BEN after administration of disulfiram. Our results

suggest that the co-administration of BEN with drugs that inhibit ALDH or to patients that are ALDH deficient may cause liver damage.

4.2 INTRODUCTION

Approximately 13,000 people die from metastatic renal cell carcinoma (mRCC) in the United States every year.[1,143] Only a small minority of patients achieve durable complete remission with high dose interleukin-2 cytokine therapy.[94,128] Recently developed agents targeting the vascular endothelial growth factor or the mTOR pathway have shown clinical activity.[94,128,129] However, responses to these novel agents are generally not durable,[130] and there remains a need for new treatments of mRCC.

Benzaldehyde dimethane sulfonate (dimethane sulfonate, BEN, DMS612, NSC281612) has structural similarities to busulfan, melphalan and chlorambucil, and is presumed to be a bifunctional alkylating agent. COMPARE analysis suggested that the mechanism of action of BEN overlapped with that of chlorambucil.[124] However, unlike conventional bifunctional alkylating agents, BEN demonstrated specific activity against renal carcinoma cells in the NCI 60 cell line screen.[124] *In vitro,* BEN treatment resulted in S and G2/M cell cycle arrest.[124] BEN has demonstrated anti-tumor activity in mice with orthotopic renal cell carcinoma xenografts. Specifically, BEN showed significant activity against human 786-0 and ACHN renal cell tumors when administered to mice on a q4dx5 schedule.[131] Treatment of mice bearing orthotopically implanted, human RXF-393 renal carcinoma cell xenografts with BEN resulted in >70% cure rate whereas busulfan showed no activity.[131] In addition, treatment with BEN slowed the growth of A498 human renal

cell cancer xenografts.[131] It was hypothesized that BEN's activity against renal carcinoma cells may be due in part to the hydrophobic moiety in the molecule which allows BEN to pass through the cell membrane or due to its sequence specificity for DNA alkylation.[124] The fact that BEN has displayed significant *in vitro* and *in vivo* activity against renal carcinoma cells and tumor xenografts has led to the evaluation of BEN in an ongoing NCI-sponsored phase I clinical trial (clinicaltrials.gov NCT00923520).

We have shown that in plasma, BEN is chemically converted into 6 different BEN analogs. Further, our previous studies suggest that BEN is rapidly metabolized into its benzoic acid analogue (BA) by red blood cells, presumably through aldehyde dehydrogenase (ALDH) activity.[144] Preliminary studies in mice suggest that BEN is metabolized into at least 12 different BA products,[144] and has a very short plasma half-life.

ALDHs are NAD(P)+ dependent enzymes that metabolize both aromatic and aliphatic aldehydes into carboxylic acids.[146] Disulfiram (trade name Antabuse) is an irreversible inhibitor of ALDH and is prescribed to treat chronic alcoholism.

We showed that BA reacts faster with nucleophiles than BEN, and may therefore be an important effector of DNA alkylation.[144] The conversion of BEN to BA by RBCs is likely an activation step. However, the short half-life of BA may limit the ability of BA generated in RBCs to reach and alkylate tumor DNA. Therefore, a more prolonged and slower generation of BA from BEN, partly in tissues as opposed to primarily in RBCs, might increase the effects of BEN. The purpose of this study was to determine the pharmacokinetics and metabolism of BEN after iv administration in mice and to test our

hypothesis that inhibition of ALDH with disulfiram increases the exposure to BEN and thereby increases its effects in mice.

4.3 MATERIAL AND METHODS

4.3.1 Chemical and reagents

4-[bis[2-[(methylsulfonyl)-oxy]ethyl]amino]-2-methyl-benzaldehyde (NSC 281612, BEN), 4-[bis[2-[(methylsulfonyl)-oxy]ethyl]amino]-2-methyl-benzoic acid (BA), 4-[bis[2-chloro-ethyl]amino]-2-methyl-benzaldehyde (BEN-Cl_2), 4-[bis[2-chloro-ethyl]amino]-2-methyl-benzoic acid (BA-Cl_2), 4-[bis[2-[(methylsulfonyl)-oxy]ethyl]amino]-benzaldehyde (demethyl-BEN), and 4-[bis[2-chloro-ethyl]amino]-benzaldehyde (demethyl-BEN-Cl_2) were obtained from the Developmental Therapeutics Program, National Cancer Institute (NCI, Bethesda, MD). 4-[bis[2-hydroxy-ethyl]amino]-2-methyl-benzaldehyde (BEN-$(OH)_2$) and 4-[bis[2-hydroxy-ethyl]amino]-2-methyl-benzoic acid (BA-$(OH)_2$) were generated as previously described in chapter 2.

Tetraethylthiuram disulfide (disulfiram) and gum arabic were acquired from Sigma Chemical Co. (St. Louis, MO). PBS and saline were purchased from Fisher Scientific Co. (Fair Lawn, NJ). Hydroxypropyl-β-cyclodextran was obtained from The National Cancer Institute (NCI) Chemotherapeutics Repository (Bethesda, MD). All solvents used for LC-MS/MS were high purity Burdick & Jackson and purchased from

Fisher Scientific Co. Formic acid was purchased from Sigma Chemical Co. Nitrogen gas for the mass spectrometer was purified with a Parker Balston Nitrogen Generator (Haverhill, MA), and nitrogen gas for sample evaporation was purchased from Valley National Gases, Inc. (Pittsburgh, PA).

4.3.2 Animals

Specific-pathogen-free, adult CD2F1 female mice were purchased from Charles River Laboratory (Wilmington, MA). Mice were allowed to acclimate to the University of Pittsburgh Cancer Institute Animal Facility for ≥1 week before being used for study. Mice were maintained in micro-isolator cages in a separate room and handled in accordance with the Guide for the Care and Use of Laboratory Animals (National Research Council, 1996) and on a protocol approved by the Institutional Animal Care and Use Committee of the University of Pittsburgh. Ventilation and airflow were set to 12 changes per h. Room temperatures were regulated at 22±1 °C, and the rooms were kept on automatic 12-h light/dark cycles. Mice received Prolab ISOPRO RMH 3000 Irradiated Lab Diet (PMI Nutrition International, St. Louis, MO) and water ad libitum, except on the evening before dosing, when all food was removed. Mice were 6–8 weeks old and weighed approximately 20 g at the time of dosing. Sentinel animals were maintained in the room housing study mice and assayed at 3-month intervals for specific murine pathogens by mouse antibody profile testing (Charles River, Boston, MA). Sentinel animals remained free of specific pathogens, indicating that the study mice were pathogen free.

4.3.3 Pharmacokinetic Study design

Mice were dosed iv with 20 mg/kg BEN alone or 24 h after ip administration of 300 mg/kg disulfiram, as described before.[158] BEN was formulated in a 20% solution of hydroxypropyl-β-cyclodextran (HPβCD) in water and disulfiram was formulated as a suspension in 5% (w/v) gum arabic in PBS at a concentration of 30 mg/mL.

After administration of BEN, mice (three per time point) were euthanized with CO2 at multiple time points between 5 and 1440 min. Control animals received vehicle alone (0.01 mL/g fasted body weight) and were euthanized at 5 and 1440 min after dosing. Blood was collected by cardiac puncture in heparinized syringes and centrifuged for 4 min at 12,000×g at 4 °C to obtain plasma. A 200 µL aliquot of the resulting plasma was pipetted into a microcentrifuge tube containing 10 µL of 2 M H_2SO_4 and briefly vortexed to ensure stabilization of the analytes of interest. Plasma samples were stored at −70 °C until analysis.

4.3.4 Urinary excretion

Mice scheduled for euthanasia at 24 h after dosing were kept in metabolic cages. Urine was collected into tubes containing 2 M H_2SO_4 estimated to yield 5% acid by volume. At the end of the collection period, cages were washed with 15 mL of sterile water, and 2 M H_2SO_4 was added to all tubes in a ratio of 5 parts acid to 95 parts urine. Quantitation of analytes in urine and cage wash was accomplished by diluting an aliquot

of each sample (between 10 and 100-fold) with control plasma followed by quantitation relative to a plasma standard curve.

4.3.5 Bioanalysis

BEN, BEN-Cl_2, BA, BA-Cl_2, BEN-$(OH)_2$ and BA-$(OH)_2$ were quantitated by LC-MS/MS as previously described.[159] For intermediate metabolites (BEN-OH, BEN-Cl, BEN-Cl-OH, BA-OH, BA-Cl, and BA-Cl-OH), and glucuronide conjugates, for which there were no reference standards available, the resulting analyte peak area was divided by the internal standard and the resulting ratio was converted to BEN equivalents by back-calculation using the BEN response equation. This assay, developed in human plasma, was modified for mouse plasma. Control murine plasma (Lampire, Pipersville, PA) resulted in linear, accurate, and precise calibration curves for all analytes. However, when control Lampire plasma was used to quantitate quality control samples prepared in control study mouse plasma, the accuracy was inadequate. Further inspection of the data showed that this was due to a plasma source specific internal standard response, and that the assay displayed adequate performance when peak areas were not corrected by internal standard responses, suggesting a difference in matrix effect between commercially available control Lampire plasma and plasma obtained from our study mice. Consequently, all unknown plasma samples were assayed relative to a calibration curve prepared in control plasma obtained from untreated study mice to assure generation of accurate data. Sample dilution to within the linear range was also performed with control plasma from study mice.

4.3.6 Pharmacokinetic analysis

The maximum plasma concentration (C_{max}) and the time to reach C_{max} (T_{max}) were determined by visual inspection of the plasma concentration versus time data. Other pharmacokinetic parameters were calculated non-compartmentally using PK Solutions 2.0 (Summit Research Services, Montrose, CO http://www.summitPK.com). The area under the plasma concentration versus time curve (AUC) of all analytes was calculated with the log-linear trapezoidal rule. Renal clearance was calculated by dividing the absolute amount of analyte excreted in urine by the plasma AUC_{0-t} of the respective analyte.

4.3.7 Data analysis

Statistical analysis of AUC_{0-t} values consisted of the BEN alone to BEN with disulfiram pretreatment AUC ratio with the associated standard error (SE). After log-transformation, these ratios were subjected to a two-sided Students t-test, under the null hypothesis of log (AUC-ratio)=0. A value of $p<0.05$ was considered statistically significant, as described previously.[160] This approach is similar to that described by Bailer et al.[161] However, instead of using a z-test, we applied a more conservative t-test with 2 degrees of freedom (N=3 samples per time point).

4.3.8 Pathology Study

Mice, treated with a single dose of disulfiram alone at 300 mg/kg ip in gum arbic, BEN alone at either 20 mg/kg (the maximum tolerated dose) or 15 mg/kg iv, or mice treated with 300 mg/kg ip disulfiram 24 h prior to BEN at 20 and 15 mg/kg iv or the combination of vehicles (20% HPβCD or PBS (0.01 ml/g body weight)), were followed for 30 days after treatment. Mice were euthanized with CO_2 and bled by cardiac puncture one month after treatment. Complete gross necropsies were performed, livers were removed, weighed, and a portion of the medial lobe of each liver was placed in 10% phosphate buffered formalin, fixed, paraffin embedded, cut into 5 μm sections, processed and stained with hematoxylin and eosin.

4.3.9 Blood Counts

Blood was collected by orbital sinus bleed or by tail vein bleed from the treated mice for at least 14 days following treatment with disulfiram, BEN or the combination using a potassium EDTA coated microhematocrit tube and run on a Scil Vet abc Veterinary Hematology Analyzer (Scil Animal Care Company, Gurnee, IL, 60031) to count platelets, white blood cells and lymphocytes. Hematocrit as percentage was determined with a micro hematocrit centrifuge by measuring the packed red cell height, dividing by the total height, and multiplying by 100.

4.4 RESULTS

This study was conducted to determine if BEN is metabolized to BA by aldehyde dehydrogenase (ALDH) and if BEN exposure could be increased by inhibiting ALDH with disulfiram in blood and tissues thereby increasing BA production in tissues that express ALDH.

In order to measure the analytes generated when BEN is administered to mice we developed an LC-MS/MS assay. The assay for BEN and BA and analytes with known standards had a lower limit of detection of 1 ng/mL for all analytes and was accurate and precise from 10 to 1,000 ng/mL (Table 5) and the correlation coefficient (R^2) was > 0.97 for all analytes.

Table 5. Assay performance of BEN, BEN-Cl_2, BEN-$(OH)_2$, BA, BA-Cl_2 and BA-$(OH)_2$ from two duplicate standard curves.

BEN ng/mL	Mean	Precision (%)	Accuracy (%)	BA ng/mL	Mean	Precision (%)	Accuracy (%)
10	9.5	7.7	95.0	10	11.0	12.1	110.2
30	25.7	9.1	85.7	30	30.0	13.9	99.9
100	113.3	6.4	113.3	100	116.5	5.5	116.5
300	335.0	9.3	111.7	300	316.5	8.4	105.5
500	526.0	6.6	105.2	500	460.8	8.0	92.2
750	856.8	14.9	114.2	750	758.8	10.6	101.2
1000	985.8	3.3	98.6	1000	923.3	5.1	92.3
BEN-di-Cl ng/mL	**Mean**	**Precision (%)**	**Accuracy (%)**	**BA-di-Cl ng/mL**	**Mean**	**Precision (%)**	**Accuracy (%)**
10	10.7	9.3	106.8	10	9.9	8.4	97.7
30	25.4	9.5	84.6	30	33.1	11.0	97.0
100	113.5	16.8	113.5	100	124.0	2.1	119.3
300	340.8	15.6	113.6	300	336.8	1.5	106.2
500	510.3	5.8	102.1	500	471.8	5.4	96.8
750	795.0	8.0	106.0	750	719.0	6.6	106.1
1000	1035.3	8.4	103.5	1000	868.0	2.6	94.6
BEN-di-OH ng/mL	**Mean**	**Precision (%)**	**Accuracy (%)**	**BA-di-OH ng/mL**	**Mean**	**Precision (%)**	**Accuracy (%)**
10	10.6	9.1	106.1	10	9.8	15.0	98.8
30	27.3	14.7	90.8	30	29.1	8.8	110.2
100	119.8	26.1	119.8	100	119.3	1.4	124.0
300	332.3	17.1	110.8	300	318.5	9.5	112.3
500	518.8	7.6	103.8	500	484.0	8.0	94.4
750	872.5	24.3	116.3	750	796.0	8.5	95.9
1000	1047.0	11.5	104.7	1000	946.0	5.3	86.8

There were 12 different metabolites detected in both the mice to which BEN had been administered alone and those to which BEN had been administered after disulfiram pretreatment. The plasma concentration-*versus*-time profiles are shown in Figure 49, Figure 50, and Figure 51. Pharmacokinetic parameters associated with these profiles are displayed in Table 6 and Table 7.

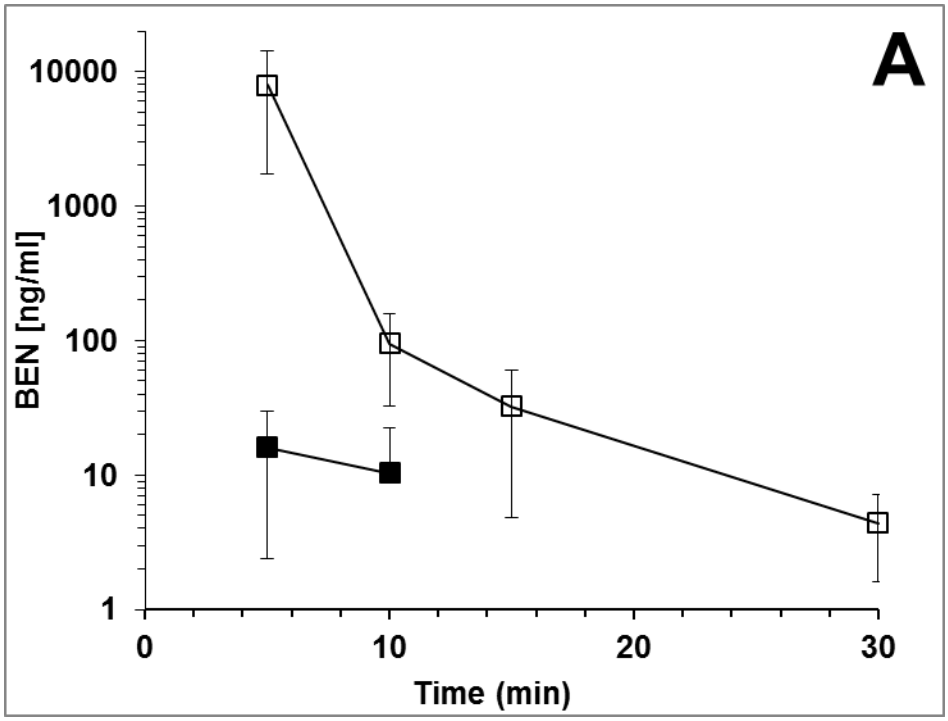
A
10000
1000
100
10
1
BEN [ng/ml]
0
10
20
30
Time (min)

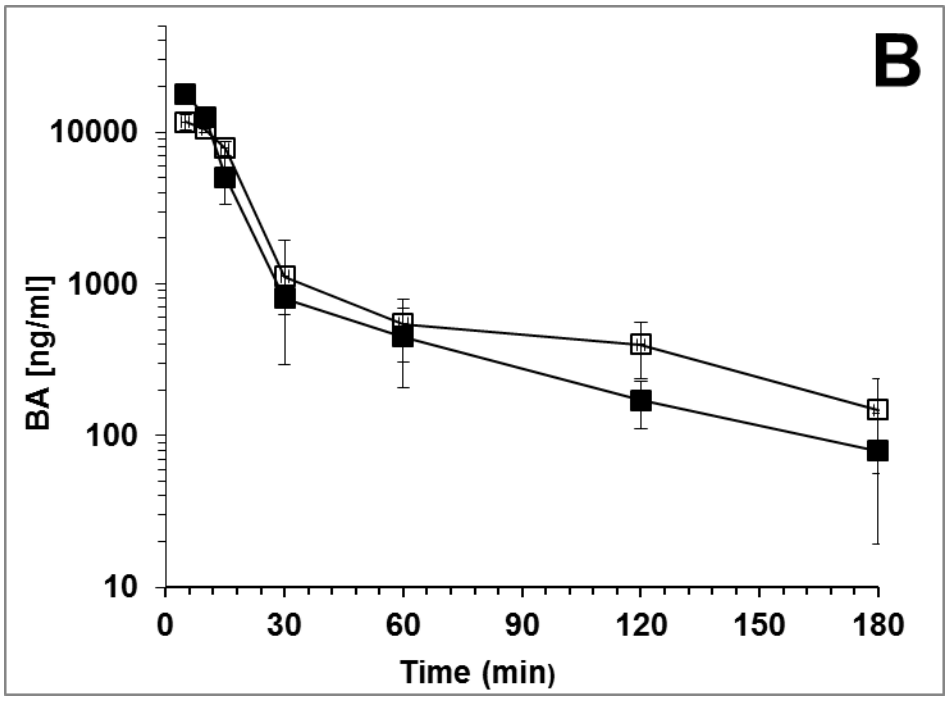
B
10000
1000
100
10
BA [ng/ml]
0
30
60
90
120
150
180
Time (min)

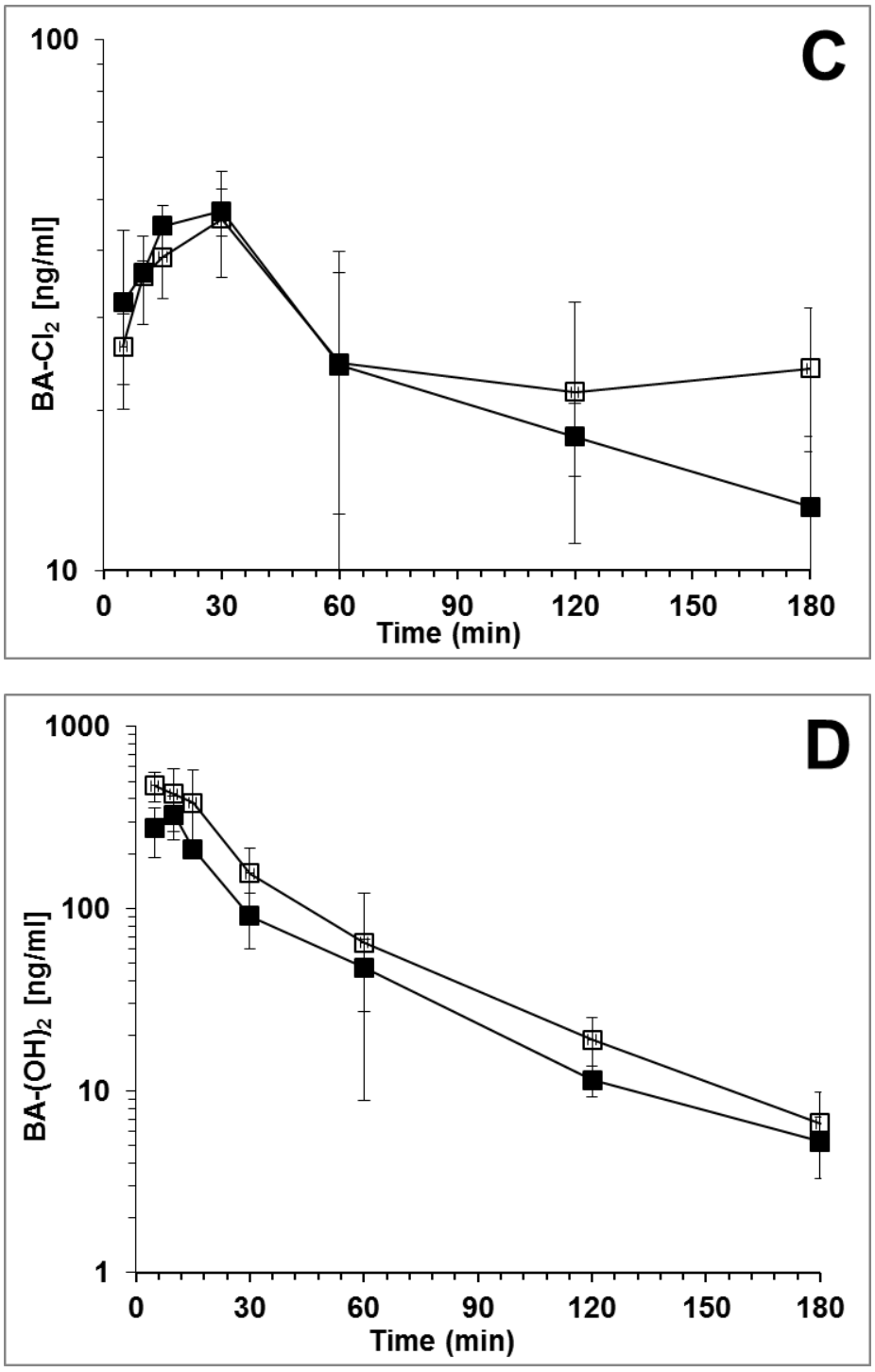

Figure 49. Concentration vs. time profile of BEN and quantitatable metabolites in mouse plasma. (A) BEN, (B) BA, (C) BA-Cl_2, and (D) BA-OH_2. (■) represents BEN administered alone and (□) represents BEN administered after disulfiram. Each point is the mean (±SD) of three mice.

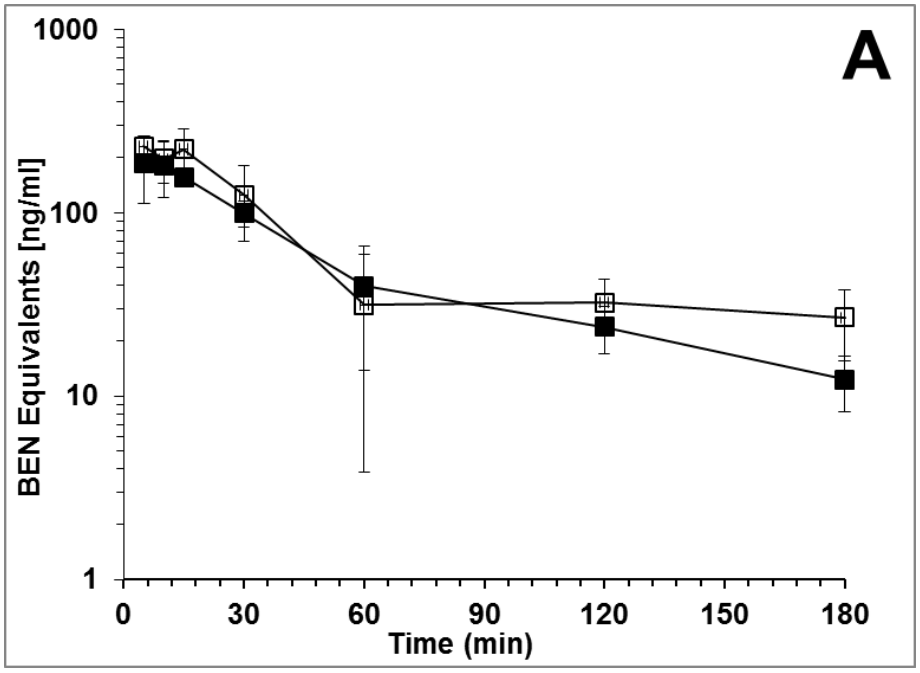
A
1000
100
10
1
BEN Equivalents [ng/ml]
0
30
60
90
120
150
180
Time (min)

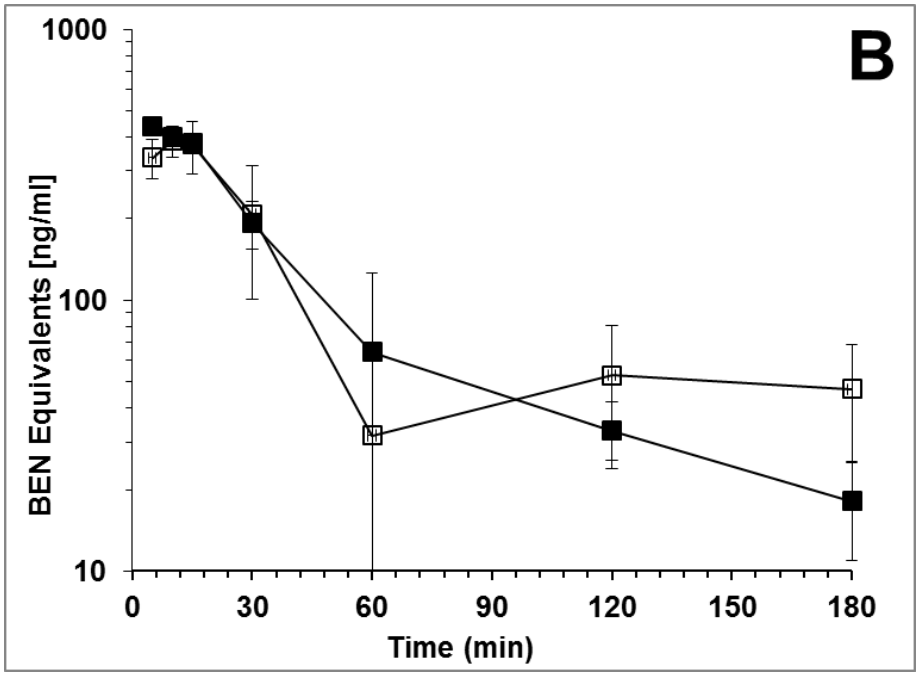
B
1000
100
10
BEN Equivalents [ng/ml]
0
30
60
90
120
150
180
Time (min)

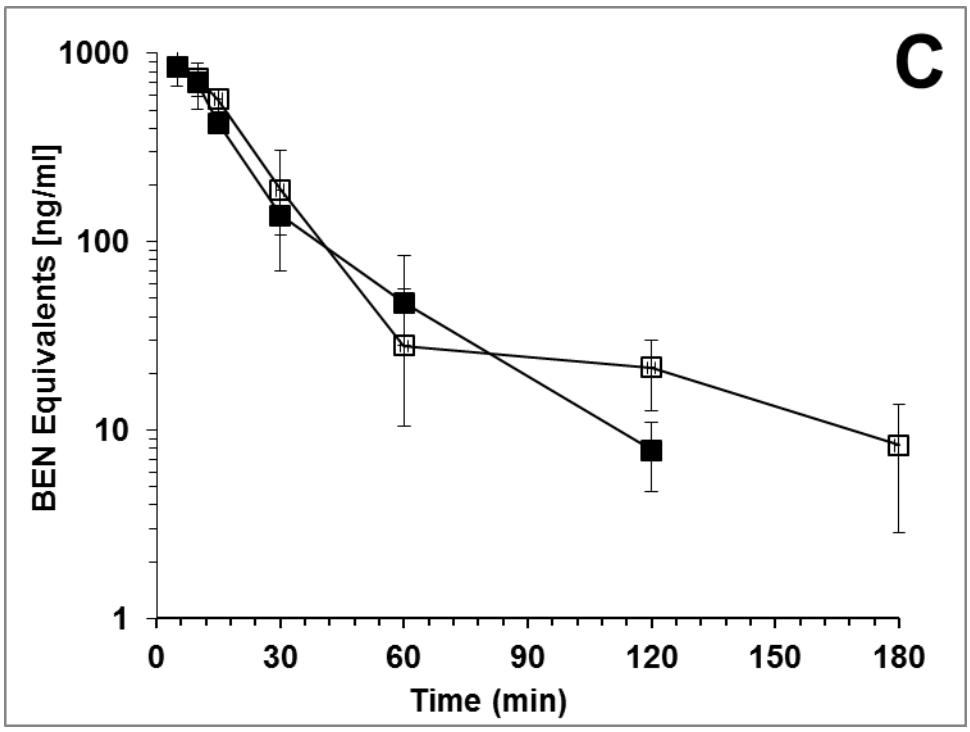

Figure 50. BEN equivalents vs. time profile of BEN metabolites. (A) BA-Cl-OH, (B) BA-Cl, and (C) BA-OH. (■) represents BEN administered alone and (□) represents BEN administered after disulfiram. Each point is the mean (±SD) of three mice.

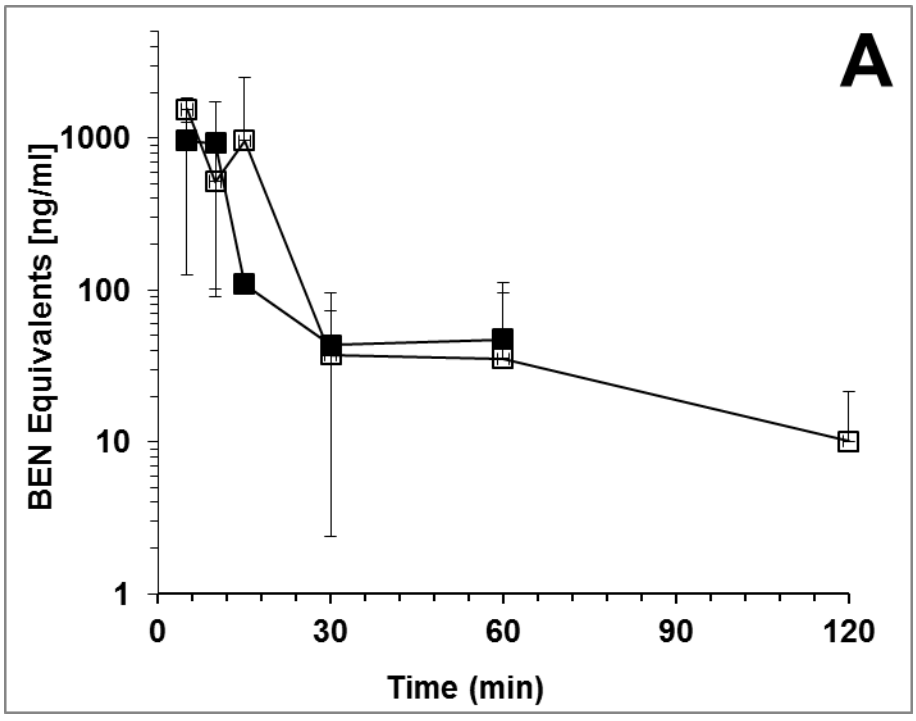

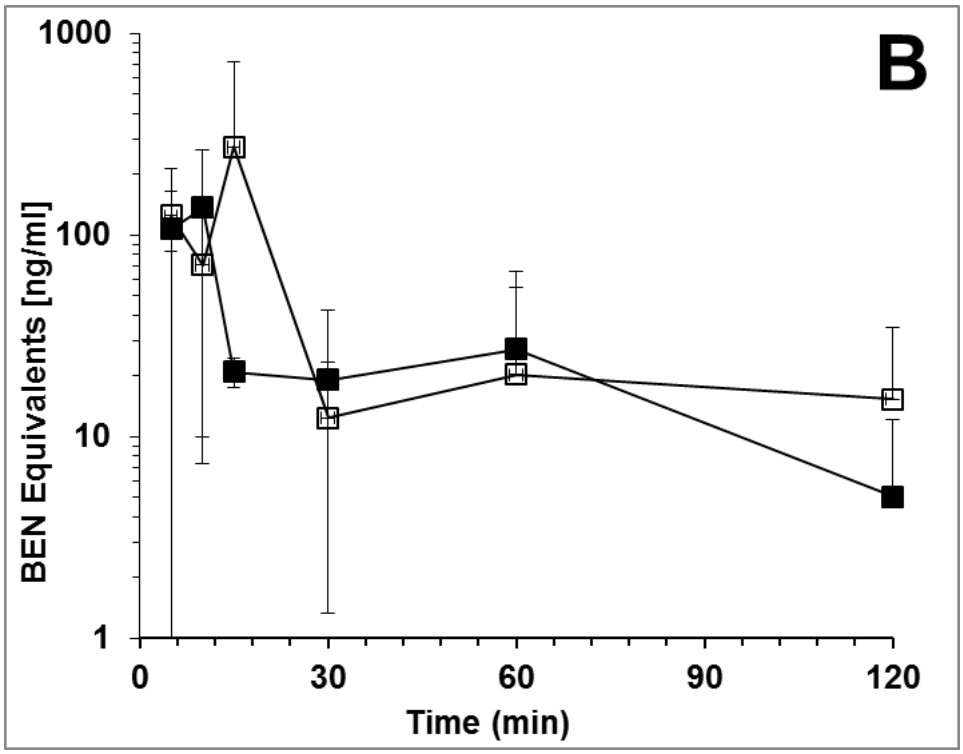
B
1000
100
10
1
BEN Equivalents [ng/ml]
0
30
60
90
120
Time (min)

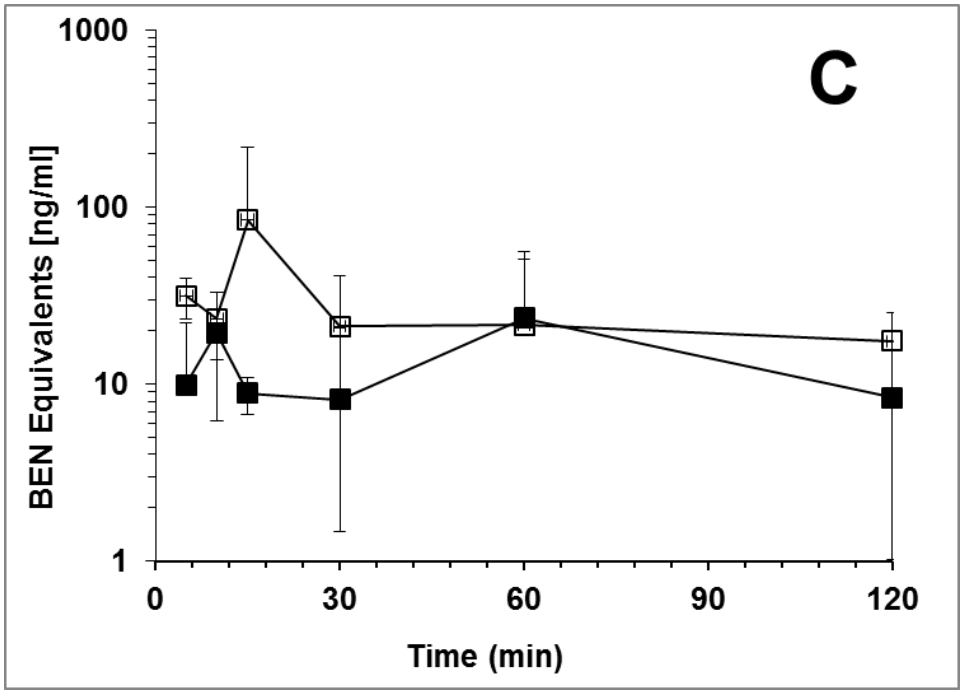
C
1000
100
10
1
BEN Equivalents [ng/ml]
0
30
60
90
120
Time (min)

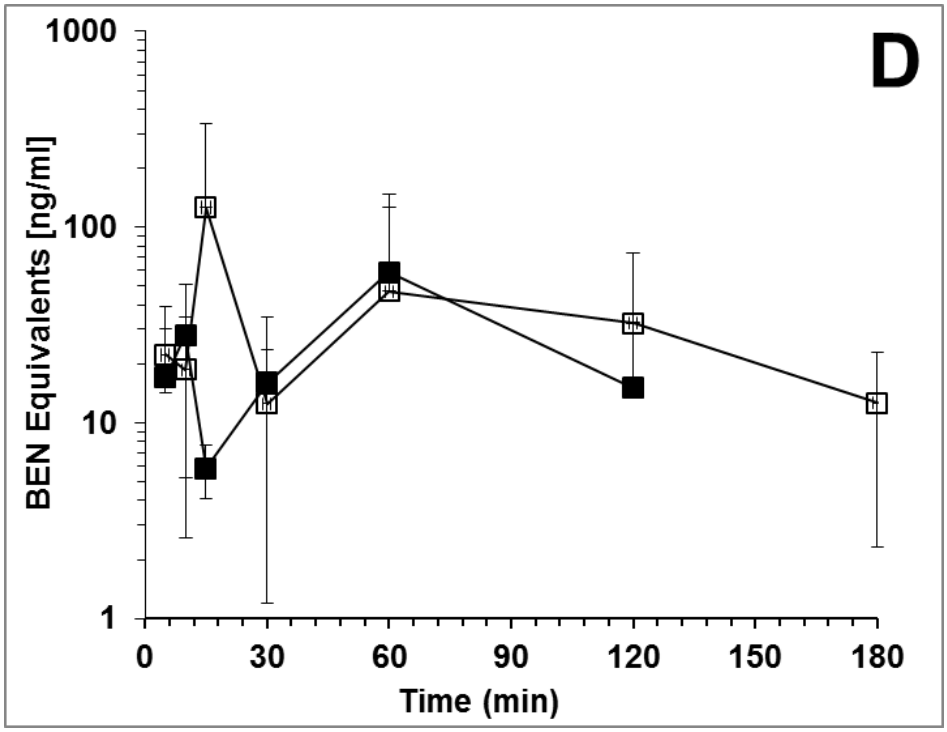
D
1000
100
10
1
BEN Equivalents [ng/ml]
0
30
60
90
120
150
180
Time (min)

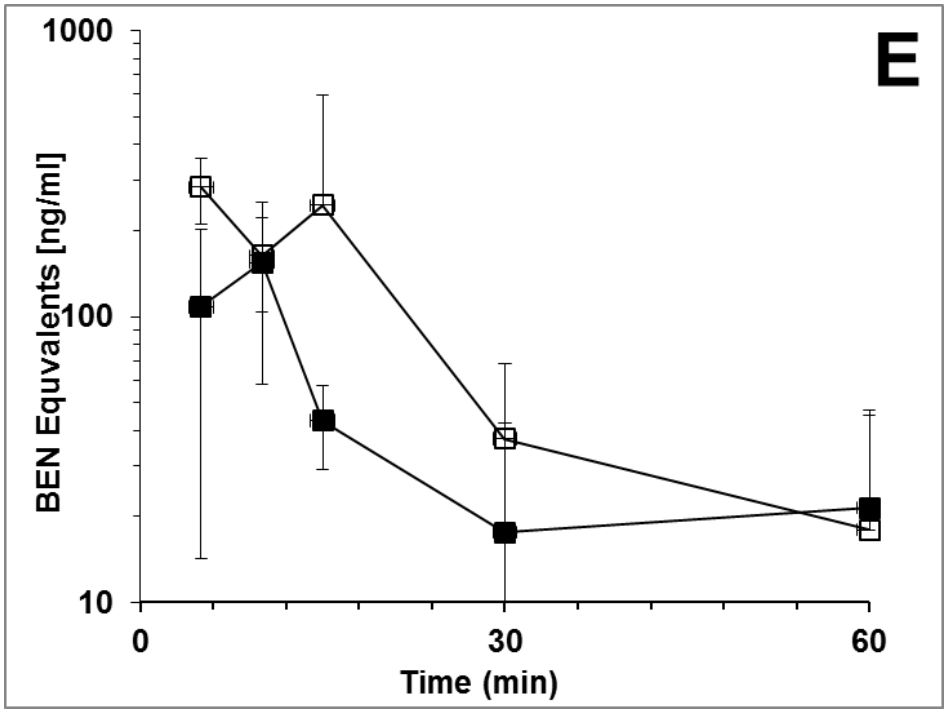
E
1000
100
10
BEN Equvalents [ng/ml]
0
30
60
Time (min)

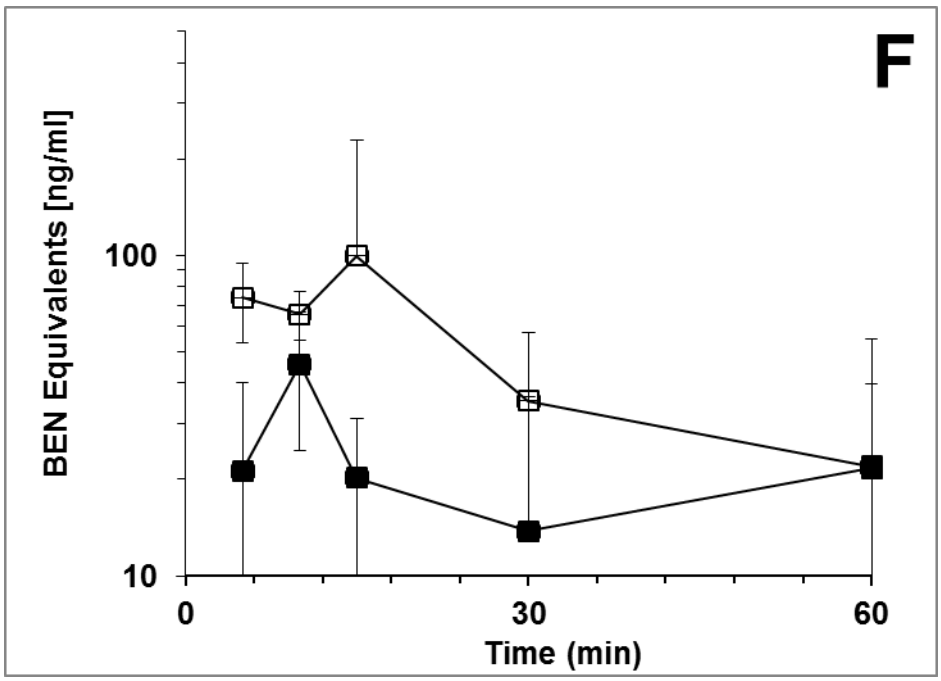

Figure 51. BEN equivalents vs. time profile of BA glucuronide metabolites. (A) BA-Gluc, (B) BA-Cl-Gluc, (C) BA-Cl-OH-Gluc, (D) BA-Cl_2-Gluc (E) BA-OH-Gluc and, (F) BA-(OH)2-Gluc. (■) represents BEN administered alone and (□) represents BEN administered after disulfiram. Each point is the mean (±SD) of three mice. The appearance of a second peak level is a possible indication of enterohepatic recycling.

Table 6. Non-compartmental plasma pharmacokinetic parameters of BEN and metabolites generated from the mouse PK experiments. Parameters followed by an asterisk (*) represent the experiment in which disulfiram was administered to the mice before BEN. In order to calculate statistical significance AUC_{0-t} values were compared at the same end time point in each study. AUC values followed by t denotes a $p<0.05$. ND: not determined, the parameter could not be defined due to fluctuation in the terminal phase concentrations. F is the fraction of BEN metabolized and F is not known.

Parameter	BEN	BA	BA-$(OH)_2$	BA-Cl_2	BA-Cl (BEN Eq)	BA-OH (BEN Eq)	BA-Cl-OH (BEN Eq)
C_{max} (ng/mL)	16	17967	327	48	440	847	185
C_{max} (ng/mL)*	197	11700	473	46	387	851	229
T_{max} (min)	5	5	10	30	5	5	5
T_{max} (min)*	5	5	10	30	10	5	5
Half-life (min)	1.5	55	29	136	69	19	63
Half-life (min)*	5.2	42	34	***	350	11	219
AUC_{0-t}(mg/L•min)	0.11*t*	254	9.66*t*	4.41	17.8	15.8	9.21
AUC_{0-t}(mg/L•min)*	40.5*t*	267	15.3*t*	4.86	18.1	18.3	11.3
AUC_{0-inf}(mg/L•min)	0.11	261	10.6	7.01	19.6	17.7	10.3
AUC_{0-inf}(mg/L•min)*	40.5	275	17.1	8.93	29.8	21.1	15.2
Vd/F (L/kg)	ND	ND	ND	ND	ND	ND	ND
Vd/F (L/kg)*	120	ND	ND	ND	ND	17	ND
Cl/F (mL/min/kg)	ND	ND	ND	ND	ND	ND	ND
Cl/F (mL/min/kg)*	0.18	ND	ND	ND	ND	ND	ND
% dose in urine (0-24 hr)	1	5.8	1.36	0.03	0.12	0.55	0.15
% dose in urine (0-24 hr)*	1.5	5.95	3.30	0.22	0.24	0.54	0.43
Cl_r mL/min	ND	0.22	1.25	0.05	0.06	0.32	0.17
Cl_r mL/min*	0.40	0.22	1.92	0.25	0.08	0.27	0.30

Table 7. BA glucuronide metabolites in mice from mouse PK experiments.

Parameter	BA-Gluc	BA-Cl_2-Gluc	BA-Cl-Gluc	BA-Cl-OH-Gluc	BA-OH-Gluc	BA-$(OH)_2$-Gluc
C_{max} (ng/mL)	961	59	137	24	155	46
C_{max} (ng/mL)*	1544	212	272	85	284	284
T_{max} (min)	5	60	10	30	10	10
T_{max} (min)*	15	15	15	15	15	15
Half-life (min)	ND	81	ND	ND	ND	ND
Half-life (min)*	378	30	ND	ND	28	44
AUC_{0-t}(mg/L•min)	12.2	6.06	2.26	0.77	2.47	1.17*t*
AUC_{0-t}(mg/L•min)*	21.3	8.88	4.28	1.92	5.81	2.81*t*
AUC_{0-inf}(mg/L•min)	13.8	3.61	3.40	2.27	ND	1.93
AUC_{0-inf}(mg/L•min)*	23.1	9.33	8.64	8.11	6.79	6.54
Vd/F (L/kg)	1765	ND	ND	ND	ND	ND
Vd/F (L/kg)*	269	ND	ND	ND	ND	ND
Cl/F (mL/min/kg)	ND	ND	ND	ND	ND	ND
Cl/F (mL/min/kg)*	0.49	ND	ND	ND	ND	ND
% dose in urine (0-24 hr)	0.99	0.06	0.17	0.09	0.25	0.21
% dose in urine (0-24 hr)*	1.48	0.30	0.32	0.29	0.35	0.52
Cl_r mL/min	0.72	0.15	0.50	0.42	1.20	1.26
Cl_r mL/min*	0.67	0.33	0.38	0.35	0.55	0.83

After iv administration of BEN to mice, BEN was rapidly metabolized resulting in a C_{max} of 16 ng/mL at 5 minutes (Figure 49A) (Table 6). While BEN became undetectable at 15 minutes after administration, BA was rapidly generated, had a plasma exposure 2300-fold greater than that of BEN, and an apparent half-life of 55 min (Figure 49B) (Table 6). In addition to BEN and BA, 11 other metabolites including 6 glucuronides of BA, where detected. The half-lives of the metabolites ranged from 19 min (BA-OH) to 136 min (BA-Cl_2) (Figure 50) (Table 6). All of the analytes detected in plasma were also detected in the urine of the mice collected between 0-6 and 6-24 h after dosing with BEN (Table 6 and Table 7).

Treatment of mice with disulfiram 24 h prior to BEN dosing increased exposure to BEN 368-fold. Interestingly, BA exposure was similar in both studies. The half-lives of the metabolites ranged from 28 min (BA-OH-Gluc) to 350 min (BA-Cl) (Figure 50 and Figure 51) (Table 6 and Table 7). Although the exposure of all of the analytes appeared to increase after pretreatment with disulfiram only BEN, BA-(OH)2 and BA-(OH)2-Gluc were found to be statistically different when comparing the AUC0-t between BEN administered alone and BEN administered after disulfiram (Table 6 and Table 7). All of the analytes detected in plasma were also detected in the urine.

The untreated mice and vehicle treated mice did not lose body weight. The mice treated with disulfiram, BEN or the combination, lost approximately 12% body weight by day 4 and regained body weight by day 12.

The hematocrits, white blood cells and percent lymphocytes decreased following treatment in mice receiving BEN alone and disulfiram before BEN (Table 8).

Table 8. Hematocrit (%), WBC and %Lymphocytes in mice treated with vehicle, BEN alone or disulfiram plus BEN. Each row represents the results of one mouse.

Treatment		Hematocrit (%)		WBC (x10^3 cells/µL)		%Lymphocyte	
Day -1	Day 0	Day -1	Nadir (day)	Day -1	Nadir (day)	Day -1	Nadir (day)
Vehicle	Vehicle	47.8	51.3 (6)	10.7	6.7 (4)	75.8	60.4 (1)
Vehicle	BEN 20 mg/kg	45.5	36.5 (4)	9.6	3.1 (4)	71.6	41.9 (8)
Disulfiram	BEN 20 mg/kg	50.0	39.5(4)	4.5	1.4 (4)	83.0	28.5 (8)
Disulfiram	BEN 20 mg/kg	43.8	37.0 (6)	6.4	0.4 (4)	72.6	35.5 (6)
Vehicle	BEN 15 mg/kg	48.0	39.5 (6)	5.9	2.7 (4)	81.4	48.1 (8)
Disulfiram	BEN 15 mg/kg	45.0	41.5 (6)	5.1	3.7 (8)	79.0	33.9 (6)
Disulfiram	BEN 15 mg/kg	53.0	40.0 (8)	5.8	3.1 (4)	75.2	29.5 (6)

The hematocrits reached the lowest level at day either day 4 or 6 when dosed with 20 mg/kg BEN or day 6 or 8 when dosed with 15 mg/kg BEN. The white blood cell count was the lowest on day 4 after dosing except for 1 mouse in which the low point was not seen until day eight. The percent lymphocyte was lowest on either day 6 or day 8 after dosing. All values returned to normal by day 14 after dosing. Pretreatment with disulfiram before BEN appeared to deepen the percentage lymphocytes nadir compared to treatment with BEN alone.

When mice were euthanized one month after single dose treatment with either disulfiram or BEN alone, mild hepatic lesions were present in the mice. These lesions included mild focal thickening of the connective tissue capsule and mild fibrosis within few of the portal areas. Hepatic pathology of mice treated with the disulfiram and BEN combination were profound and included a regional loss of overall hepatic vascular architecture with prominent swelling and clearing of hepatocyte cytoplasm, likely associated with areas of regenerative hyperplasia (Figure 52). The capsule was diffusely thickened by increased connective tissue, and scattered lymphoplasmacytic infiltrates were observed. Multiple chronic adhesions existed between the thickened hepatic capsule and the omentum. Portal areas were severely expanded by increased fibrous connective tissue, hyperplastic bile ducts, and lymphoplasmacytic infiltrates. Mild to moderate fibrosis also existed in centrilobular areas. Early bridging fibrosis spanned between portal areas and from portal to centrilobular areas (Figure 52).

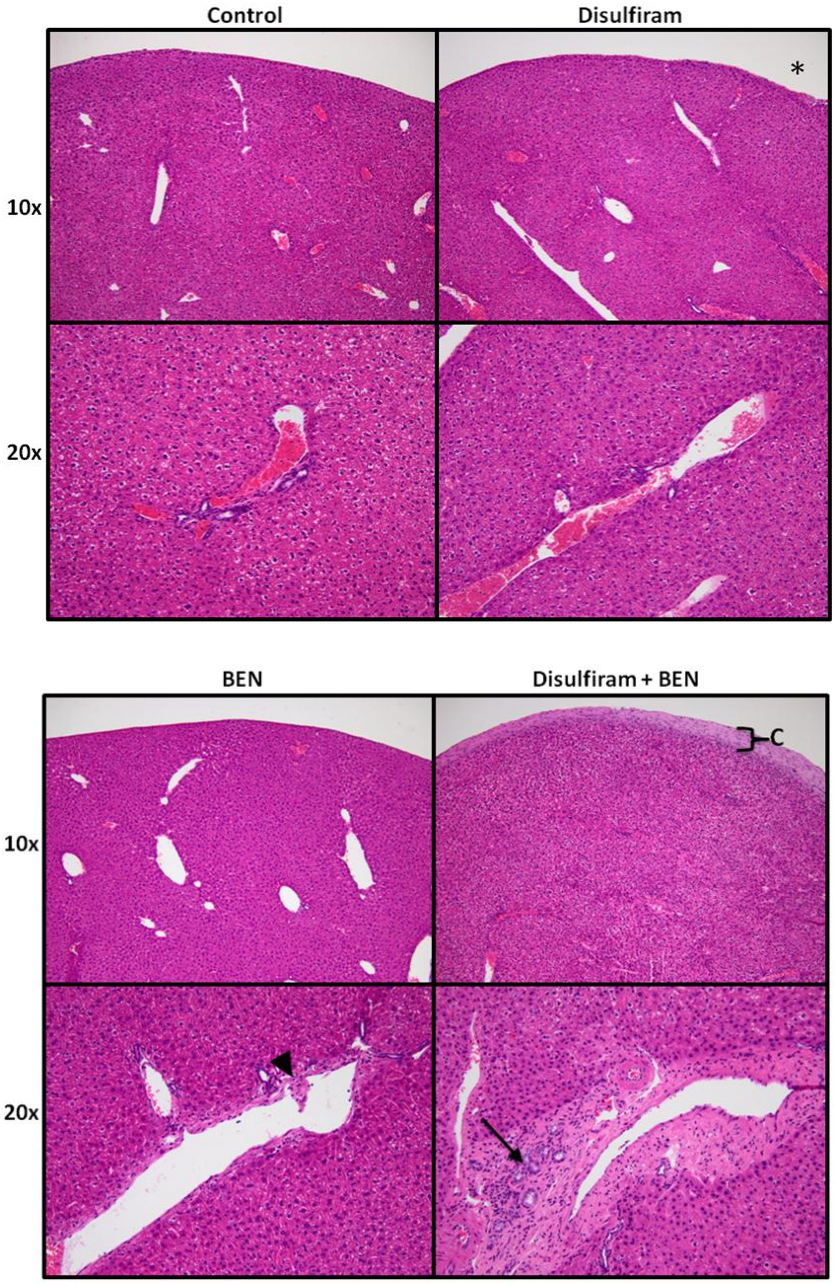

Figure 52. H&E stained liver sections from control, disulfiram-treated, BEN-treated, and disulfiram + BEN-treated mice. Only mild hepatic lesions are present in mice treated with either disulfiram or BEN alone including slight thickening of the capsule (asterix) and a mild increase in portal fibrous connective tissue (arrowhead). Severe lesions in animals treated with a disulfiram + BEN combination include swelling and clearing of hepatocytes with a loss of overall hepatic vascular architecture, extensive capsular thickening (C), and severe portal fibrosis with bile duct hyperplasia (arrow).

4.5 DISCUSSION

The present investigation was designed to characterize the pharmacokinetics and metabolism of BEN in mice, and to assess the effect of ALDH inhibition with disulfiram on BEN pharmacokinetics, metabolism, and pharmacodynamics in mice. Previous results suggested that BEN is metabolized *in vivo* and *in vitro* in blood into BA, presumably by the action of ALDH. We have demonstrated that BA reacts faster with nucleophiles than BEN, and may therefore be an important effector of DNA alkylation.[144] The conversion of BEN to BA by red blood cells (RBCs) is likely an activation step. However, the short *in vitro* half-life of BA (5 min),[144] may limit the ability of BA to reach and alkylate tumor DNA. Therefore, a more prolonged and slower generation of BA from BEN, partly in tissues as opposed to primarily in RBCs, might increase the effects of BEN administration. Disulfiram has been used previously in a mouse study for the purpose of inhibiting ALDH.[158] They found that a single 300 mg/kg dose of disulfiram administered ip caused the greatest inhibition of both RBC and liver ALDH activity at 24 h post dose in which the reductions of ALDH activity in RBC and liver were 81% and 27% compared to controls. Thus, we used the same dose of disulfiram 24 h prior to the dosing of BEN to ensure the greatest inhibition of ALDH in study mice.

After iv BEN administration to mice, the exposure to BEN was low and there were at least 12 metabolites generated, including 6 BA glucuronides. In contrast, the exposure to BA was relatively high and the half-life of BA was 55 min. The plasma half-life of BA in mice was much longer than the *in vitro* half-life of BA, (5 min).[144] The possibilities for the longer *in vivo* half-life of BA may be due to either BA being less reactive *in vivo* or more likely that there is continued production of BA from BEN in

tissues which reappears in plasma. Pretreatment with disulfiram increased BEN exposure 368-fold, suggesting that ALDH may be an enzyme responsible for metabolizing BEN into BA. Disulfiram is a non-specific inhibitor of multiple isoforms of ALDH and CYP P4502E1.[162-166] However, while disulfiram did increase BEN exposure, BA was still the predominant species and its exposure was not decreased by disulfiram. This could be due to a number of factors. First, while disulfiram has been shown to be an effective inhibitor of ALDH in RBCs, disulfiram was less effective in inhibiting ALDH in the liver.[158] This difference in inhibition may be explained because RBCs are not able to synthesize de novo ALDH, while the liver may synthesize ALDH in the 24 h between the disulfiram administration and BEN administration. Further, there are at least 19 different known isoforms of ALDH.[146] It is possible that in tissues BEN is metabolized to BA, in part, by an isoform of ALDH that is not inhibited by disulfiram. For instance ALDH1B1 is insensitive to inhibition by disulfiram.[167]

The 6 metabolites and their respective glucuronide conjugates that were observed after BEN administration were also observed when BEN was administered after disulfiram pretreatment. The plasma exposures of the glucuronides appeared to be higher after pretreatment with disulfiram, although the variability was too high to reach statistical significance (Table 7). This suggests that the inhibition of RBC ALDH increases BEN plasma exposure 368-fold driving greater BEN distribution into tissues where it is metabolized to BA. BA is then metabolized to downstream metabolites. In contrast, in the mice that were not pretreated with disulfiram, it is likely that the conversion of BEN to BA takes place in the RBCs to a greater extent. In this case, BA degrades to BA analogs in the blood and these compounds are less likely to enter tissues.

Most of the observed metabolites are likely relevant to BEN efficacy and/or toxicity because they still possess alkylating side arms.[144] Bifunctional alkylating agents have two side arms consisting of either a ethyl-methane sulfonate or ethyl-chloride that are active.[168] Monofunctional alkylators are much less potent than their bifunctional counterparts.[169] Of the non-glucuronide metabolites observed, BA-Cl_2 is bifunctional, and three other metabolites are monofunctional.

In addition, we observed six BA glucuronide metabolites, two of the glucuronides are bifunctional and three are monofunctional. It is unclear which glucuronyltransferases are responsible for the conjugation of these BA analogues, and this could have an impact on BEN safety and efficacy. All of the metabolites that were detected in the plasma were also detected in the urine. The percentage of the dose of BEN excreted unchanged in the urine was 50% increased after disulfiram pretreatment, although there was only one sample analyzed. Biliary or urinary excretion could lead to high local concentrations of cytotoxics and result in toxicities. Known examples include ifosfamide and acrolein,[170] and irinotecan and SN38(glucuronide).[171]

Toxicities associated with BEN treatment appear to be similar to those observed after treatment with other alkylating agents. After treatment with either busulfan or chlorambucil, bone marrow toxicity is observed and the nadir occurs sometime between day 4 and day 6 after a single treatment with these agents. The percentage decrease of all three measurements (hematocrit, WBC and %lymphocytes) was greater after pretreatment with disulfiram as compared to BEN alone. Again this could be due to the inhibition ALDH in blood by disulfiram allowing a greater concentration of BEN to reach the tissues, such as the bone marrow.

Although the pharmacokinetic study was conducted solely to determine the effect disulfiram has on the pharmacokinetic parameters of BEN, it was noted upon necropsy of the mice that the livers were abnormal. Further evaluation suggested that treating the mice with either disulfiram or BEN alone caused mild hepatic lesions, while mice that received the combination of disulfiram and BEN had severe and marked changes in the liver, as assessed 30 days after treatment. The cause of greater liver damage upon pretreatment with disulfiram may be due to the inhibition of blood ALDH, leading to an increase of BEN, and cellular metabolism of BEN to BA in the liver. This finding could have implications for the dosing of BEN in subjects: 1) on antabuse (disulfiram) therapy; 2) using other aldehyde dehydrogenase inhibitors, such as metronidazole;[142] or 3) with aldehyde dehydrogenase deficiencies.

In conclusion, BEN is rapidly metabolized to BA partly by an ALDH. BA is then converted into at least 11 metabolites of which 6 are glucuronides, and most of which are expected to have alkylating activity. The plasma half-life of BA in mice was much longer than the *in vitro* half-life of BA, (5 min). This suggest that BEN may enter tissues where it is converted to BA by ALDH. Inhibition of ALDH with a single ip dose of disulfiram before the administration of BEN slowed the metabolic degradation of BEN, however, BA was still the major plasma metabolite. The blood chemistry data and liver pathology suggests pretreatment with disulfiram and its inhibition of ALDH in RBCs and/or liver may cause more BEN to enter tissues. More local metabolism of BEN to BA, a more reactive compound, could lead to more tissue localized damage. This could be relevant to patients who are on antabuse therapy, have polymorphic ALDH1A1, or on a drug that

inhibits ALDH as these conditions could result in severe liver damage and/or exacerbation of BEN toxicities.

5.0 THE HUMAN PHARMACOKINETICS OF BEN (NSC281612, DMS612, BEN) AS PART OF A FIRST-IN-HUMAN PHASE I CLINICAL TRIAL.

5.1 ABSTRACT

Benzaldehyde dimethane sulfonate (DMS612, NSC281612, BEN) is an alkylator with activity against renal cell carcinoma, currently in phase I clinical trials. In whole blood, BEN is rapidly metabolized into its highly reactive carboxylic acid (BA), presumed to be the predominant alkylating species. We have previously demonstrated that ALDH1A1 is the predominant enzyme responsible for the conversion of BEN to BA in red blood cells. BEN dosed 20 mg/kg to mice had a plasma t½ <5 min and produced at least 12 products. The metabolite half-lives were <136 min. In the current study we determined the pharmacokinetics of BEN administered to patients that had solid tumors as part of a phase I clinical trial that was conducted to determine the maximum tolerated dose (MTD) for future trials.

BEN was administered to 33 patients with advanced solid tumors as an iv bolus dose ranging from 1.5 to 12 mg/m^2. The maximum tolerated dose was determined to be 9.0 mg/m^2, and there were two partial responses. The dose limiting toxicities observed at 12.0 mg/m^2 were grade 3 thrombocytopenia and grade 4 neutropenia. Pharmacokinetics of BEN and metabolites were calculated non-compartmentally. BEN was detected in only 2 patients at the earliest time point, and the half-life could not be determined in any of the patients. The $AUC_{0\text{-}t}$ and C_{max} of two of the metabolites BA and BA-$(OH)_2$ increased with dose. The C_{max} adjusted for dose increased with dose for BA while the BA-$(OH)_2$ C_{max} adjusted for dose was constant with dose. Apparent clearance (Cl/F) of BA decreased with dose while the Cl/F of BA-$(OH)_2$ was unchanged with dose.

5.2 INTRODUCTION

Approximately 13,000 people die from metastatic renal cell carcinoma (mRCC) in the United States every year.[1,143] Only a small minority of patients achieve durable complete remission with high dose interleukin-2 cytokine therapy.[128] Recently developed agents targeting the vascular endothelial growth factor or the mTOR pathway have shown clinical activity.[128,129,172] However, responses to these novel agents are generally not durable,[130] and there remains a need for new treatments of mRCC.

Benzaldehyde dimethane sulfonate (dimethane sulfonate, BEN, DMS612, NSC281612) has structural similarities to busulfan, melphalan and chlorambucil (Figure 53), and is presumed to be a bifunctional alkylating agent. COMPARE analysis suggested that the mechanism of action of BEN overlapped with that of chlorambucil.[124] However, unlike conventional bifunctional alkylating agents, BEN demonstrated specific activity against renal carcinoma cells in the NCI 60 cell line screen.[124] *In vitro*, BEN treatment resulted in S and G2/M cell cycle arrest.[124] BEN has demonstrated anti-tumor activity in mice with orthotopic renal cell carcinoma xenografts. Specifically, BEN showed significant activity against human 786-0 and ACHN renal cell tumors when administered to mice on a q4dx5 schedule.[131] BEN treatment of mice bearing orthotopically implanted, human RXF-393 renal carcinoma cell xenografts resulted in >70% cure rate whereas busulfan showed no activity.[131,132] In addition, treatment with BEN slowed the growth of A498 human renal cell cancer xenografts.[131] It was hypothesized that BEN's activity against renal carcinoma cells may be due in part to the hydrophobic moiety in the molecule which allows BEN to pass through the cell membrane or due to its sequence specificity for DNA alkylation.[124] The fact that BEN has displayed significant *in vitro*

and *in vivo* activity against renal carcinoma cells and tumor xenografts has led to the evaluation of BEN in an ongoing NCI-sponsored phase I clinical trial (clinicaltrials.gov NCT00923520).

We have shown that in plasma, BEN is chemically converted into 6 different BEN analogs (chapter 2). Further, our previous studies demonstrate that BEN is rapidly metabolized into its benzoic acid analogue (BA) by red blood cells, catalyzed by aldehyde dehydrogenase 1A1 (ALDH1A1) (chapter3). We showed that BA reacts faster with nucleophiles than BEN, and may therefore be an important effector of DNA alkylation,[144] and the conversion of BEN to BA by RBCs is likely an activation step. The *in vivo* metabolic pathway of BEN is shown in Figure 54.

We previously performed a pharmacokinetic study in mice dosed 20 mg/kg iv.[173] BEN was rapidly metabolized and became undetectable at 15 minutes after administration, BA was rapidly generated, had a plasma exposure 2300-fold greater than that of BEN, and an apparent half-life of 55 min. In addition to BEN and BA, 11 other metabolites including 6 glucuronides of BA analogues, were detected. The half-lives of the metabolites ranged from 19 min (BA-OH) to 136 min ($BA\text{-}Cl_2$). All of the analytes detected in plasma were also detected in the urine of the mice collected between 0-6 and 6- 24 h after dosing with BEN.

Preclinical *in vivo* toxicology studies in rats and beagle dogs determined that dose-limiting toxicities were mainly hematologic (leukopenia, thrombocytopenia, and reduced reticulocyte counts) and gastrointestinal (diarrhea and nausea/vomiting). The rat was the most sensitive preclinical species at 15 mg/m^2. With a safety factor of 10, this resulted in a proposed starting dose in humans of 1.5 mg/m^2.[174] The aim of the current

study was to determine the MTD, the dose limiting toxicities and the pharmacokinetics of BEN administered to humans by 10-min infusion on days 1, 8, and 15 of a 28-day cycle.

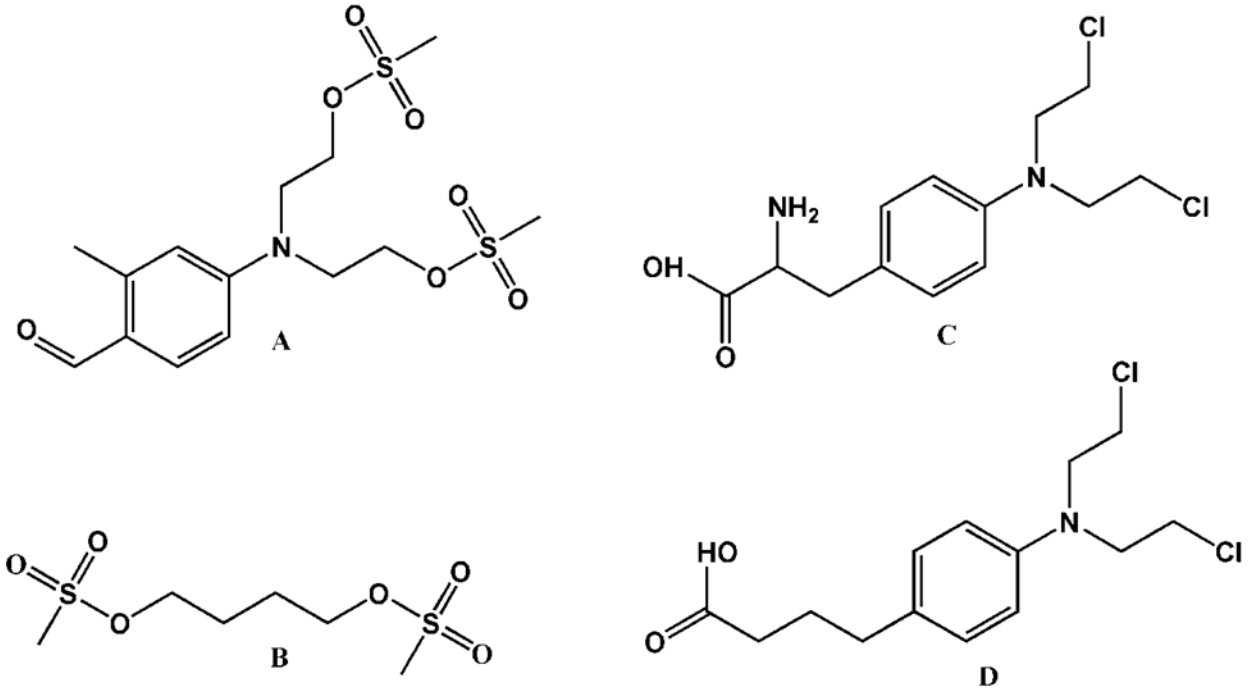

Figure 53. Chemical structures of BEN (A), busulfan (B), melphalan (C) and chlorambucil (D).

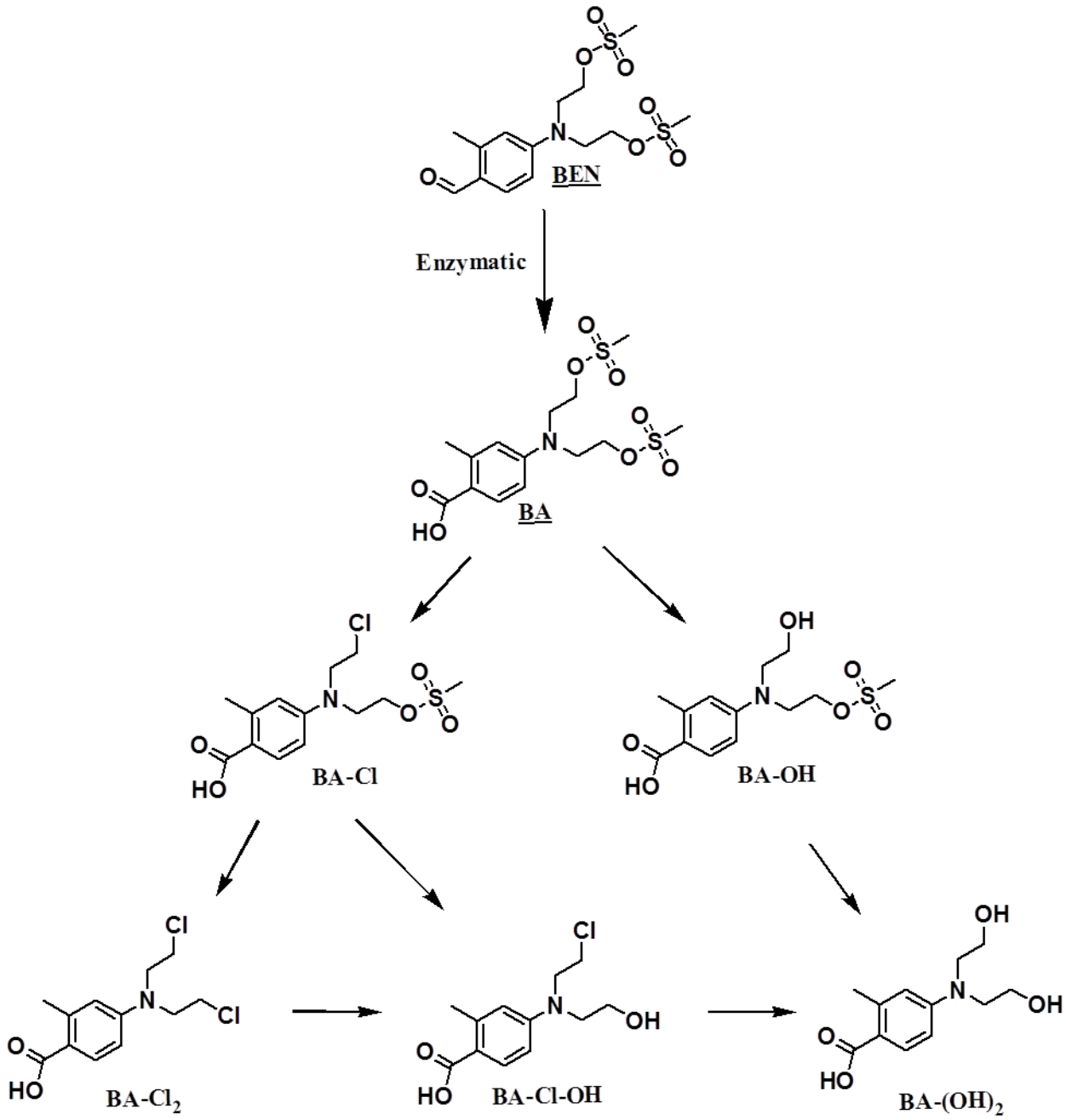

Figure 54. Proposed metabolic scheme for BEN in murine plasma. After iv injection to mice BEN is rapidly converted to BA. The methane sulfonate groups on BA are replaced with either chlorides or hydroxyl groups. Each analyte generated is also glucuronidated.

5.3 PATIENTS AND METHODS

5.3.1 Study Design

This multicenter study (ClinicalTrials.gov Identifier: NCT00923520) was conducted at the NCI Clinical Center (Bethesda, MD), University of Pittsburgh Cancer Institute, and Penn State Hershey Cancer Center, in accordance with the Declaration of Helsinki, and this study was approved by the institutional review boards at the respective institutions. All patients read and signed consent prior to enrollment in the protocol.

5.3.2 Patient Selection

Eligible patients were ≥18 years of age with advanced solid tumors or lymphoma for which effective therapy did not exist or was no longer effective. There was no limit on prior chemotherapy treatment, although prior radiation to more than 25% of bone marrow was prohibited. Patients had to be ≥4 weeks from prior chemotherapy, monoclonal antibody therapy or experimental therapy, ≥2 weeks from prior sorafenib, sunitinib, or temsirolimus treatment, ≥6 weeks from prior mitomycin C or nitrosoureas, and ≥8 weeks from prior UCN01. Adequate renal, hepatic, marrow function, and functional status was required, as was Eastern Cooperative Oncology Group performance status 0-2 and life expectancy ≥3 months. Toxicities from prior treatment had to have resolved to ≤grade 1. Inhibitors and inducers of CYP3A4 were prohibited. Patients with

uncontrolled medical illness including myocardial infarction within the past 6 months were excluded.

5.3.3 Study Treatment and Safety Evaluation

BEN was supplied by the Division of Cancer Treatment and Diagnosis of the NCI in sterile, single-use vials containing a lyophilized powder/cake of 10 mg DMS612 and 1000 mg hydroxypropyl-beta-cyclodextrin for reconstitution in 9.3 mL water for injection. After dilution in 0.9% sodium chloride or 5% dextrose, DMS612 was administered intravenously by central or peripheral catheter over 10 minutes on days 1, 8, and 15 of a 28-day cycle. There was no set limit on the number of cycles of study treatment administered. A standard 3+3 design was used for dose escalation. The starting dose was 1.5 mg/m^2 and the dose was escalated to 3, 5, 7, 9 and 12 mg/$m^{2.}$ In absence of toxicity observed at level 6, pharmacokinetic data would be analyzed before any further dose escalation and continuation of the study.

5.3.4 Safety Assessments

Adverse events were assessed using Common Terminology Criteria for Adverse Events version 4.0. Vital signs and laboratory safety assessments were performed prior to each study treatment, and history and physical exam were performed at the start of each cycle. DLT was defined as febrile neutropenia or grade 4 neutropenia without fever for

>5 days; grade 4 thrombocytopenia or anemia; grade 3 non-hematologic toxicity except for nausea, vomiting, diarrhea or electrolyte abnormality corrected within 48 hours, or elevated creatinine corrected within 24 hours. The MTD was defined as the highest dose at which ≤1 out of 6 patients experienced a DLT.

5.3.5 Response Evaluation

Response and progression was evaluated every 2 cycles (8 weeks) using the international criteria published by the Response Evaluation Criteria in Solid Tumors Committee (RECIST 1.0) [6].

5.3.6 Pharmacokinetic Study Design

Blood samples were collected in 4 mL heparinized green top tubes. Originally, blood was collected prior to infusion and at 2, 5, 15, 30, 45, 60, 120, 180, 240, 360, 480, and 1440 min after the end of infusion. After pharmacokinetic analysis of several patients revealed that BEN was rapidly metabolized, the protocol was amended. A blood draw at 5 min into infusion was added and the 180 min draw was deleted. The obtained blood was immediately placed on ice and centrifuged for 10 min at 2,000×g at 4 °C to obtain plasma. A 1 mL aliquot of the resulting plasma was pipetted into a microcentrifuge tube containing 50 µL of 2 M H_2SO_4 and briefly vortexed to ensure stabilization of the analytes of interest. Plasma samples were stored at −70 °C until analysis.

5.3.7 Bioanalysis

BEN, BEN-Cl_2, BA, BA-Cl_2, BEN-$(OH)_2$ and BA-$(OH)_2$ were quantitated by LC-MS/MS as previously described (Parise et al., 2012, Chapter 2). For intermediate metabolites (BEN-OH, BEN-Cl, BEN-Cl-OH, BA-OH, BA-Cl, and BA-Cl-OH), and glucuronide conjugates, for which there were no reference standards available, the resulting analyte peak area was divided by the internal standard and the resulting ratio was converted to BEN equivalents by back-calculation using the BEN response equation.

5.3.8 Pharmacokinetic analysis

The maximum plasma concentration (C_{max}) and the time to reach C_{max} (T_{max}) were determined by visual inspection of the plasma concentration versus time data. Other pharmacokinetic parameters were calculated non-compartmentally using PK Solutions 2.0 (Summit Research Services, Montrose, CO http://www.summitPK.com). The area under the plasma concentration versus time curve (AUC) of all analytes was calculated with the log-linear trapezoidal rule.

Statistical analysis to determine the relationship of dose to C_{max} and AUC was determined linear regression by first performing log transformation of the data and then linear regression using SPSS as described.[175]

5.4 RESULTS

This study was conducted to determine the pharmacokinetics of BEN administered to humans. Thirty-one subjects with advanced solid tumors were enrolled in this phase I study. Subjects with a range of solid tumors were enrolled, including 4 with renal cell carcinoma (RCC) and 11 with colorectal carcinoma (CRC). The median number of prior chemotherapy regimens was 4 (range 0-13). Subjects were treated at six dose levels: 1.5 mg/m^2 (n=3), 3.0 mg/m^2 (n=3), 5.0 mg/m^2 (n=6), 7.0 mg/m^2 (n=3), 9.0 mg/m^2 (n=12), and 12.0 mg/m^2 (n=3).

Myelosuppression with thrombocytopenia and neutropenia was the principal dose-limiting toxicity. Two of 3 subjects treated at the 12 mg/m^2 dose level experienced dose limiting toxicity (DLT) with grade 4 neutropenia and prolonged grade 3 thrombocytopenia, respectively. At the lower dose level of 9 mg/m^2 only 1 of 12 subjects experienced a DLT, therefore, the MTD was determined to be 9 mg/m^2.

One subject with RCC and one subject with cervical cancer had a confirmed partial response. Both patients were treated at the MTD of 9 mg/m^2 (dose level 4). Stable disease was observed in 2 additional patients. Neither the responses nor the toxicities observed appeared to correlate with the plasma pharmacokinetics or metabolism of BEN as the pharmacokinetic parameters in these patients were not different than the rest of the cohort (Figure 66).

BEN was only detected in two patients at the earliest time point, and the half-life could not be determined in any of the patients. BA was detected in all patients except for two. In addition to BEN and BA, 11 other metabolites including 6 glucuronides of BA,

were detected. A representative concentration versus time profile for the analytes in a patient is shown in Figure 55.

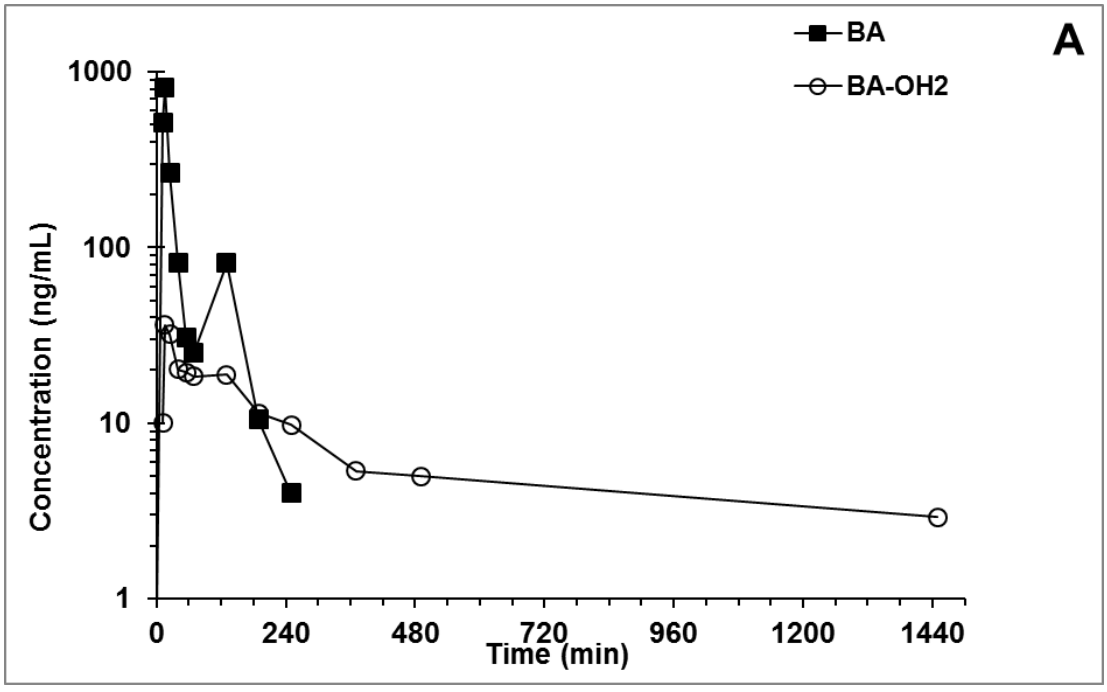

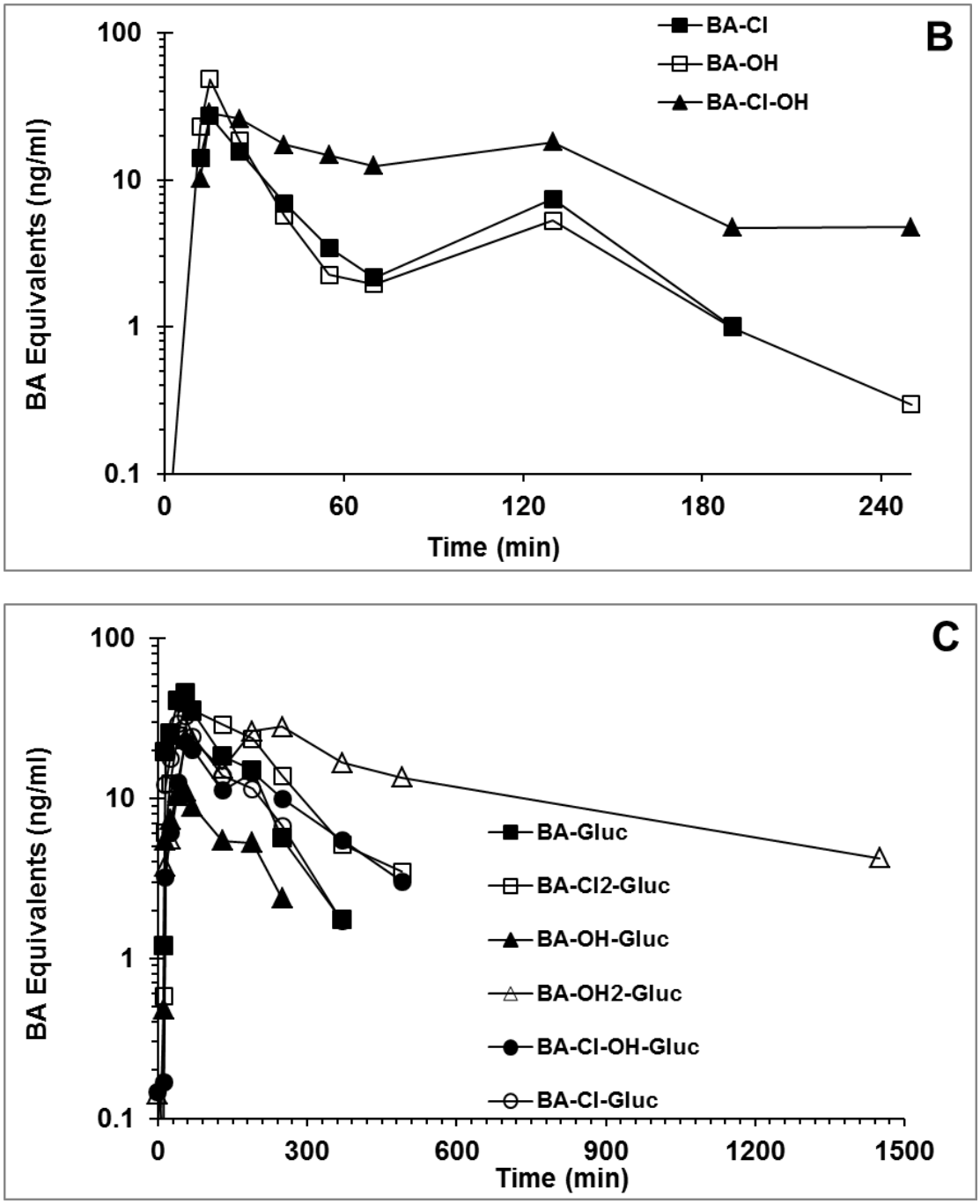

Figure 55. Plasma concentration or BA equivalents (ng/ml) versus time for a patient that received 5.0 mg/ml BEN. A) BA (■) and BA-OH_2 (○). B) BA-Cl (■), BA-OH (□), and BA-Cl-OH (▲). C) BA-Gluc (■), BA-Cl_2-Gluc (□), BA-OH-Gluc (▲), BA-$(OH)_2$-Gluc (Δ), BA-Cl-OH-Gluc (●), and BA-Cl-Gluc (○). Note the second peak in the glucuronide metabolites. This could be an indication of enterohepatic recycling.

The half-life of all analytes was variable amongst dose levels (Table 9). The major metabolite, BA, had a half-life of 7.5 minutes when patients were dosed at 1.5 mg/m^2 and 770 minutes at the 9.0 mg/m^2 dose level. The AUC and C_{max} of the metabolites appeared to increase with dose except in a few cases (Figure 56 to Figure 66). The PK parameters for the metabolites are listed in Table 1.

The AUC_{0-t} and C_{max} of BA increased more than proportionally with dose, 2.03 (95% CI, 1.47 – 2.58) and 1.87 (95% CI, 1.37 – 2.31) respectively (Figure 56). The AUC_{0-t} and C_{max} of BA-$(OH)_2$ (the end metabolite) increased proportionally with dose, 2.08 (95% CI, 0.97 – 3.18) and 1.13 (95%CI, 0.51 – 1.75) respectively (Figure 57). Apparent clearance (Cl/F) of BA decreased with dose while the Cl/F of BA-OH_2 was unchanged with dose. The half-lives of the metabolites ranged from 7.5 min (BA) to 2634 min (BA-Cl-OH) (Table 9).

There were four patients that had RCC on the clinical trial. The pharmacokinetic parameters of these patient were not different from the other patients being administered BEN. Also, there were 3 patients that were dosed at 2 different dose levels. Two of these patients were first administered 1.5 mg/m^2 and then 3.0 mg/m^2 of BEN. The third patient was administered 3.0 and then 5.0 mg/m^2 of BEN. There was a large variation of C_{max} of BEN in the plasma in these patients. Upon dose escalation, the C_{max} doubled in one patient, decreased by one half in another patient and increased by ten times in the third patient.

Table 9. The C_{max}, T_{max}, AUC_{0-t}, Cl/F and half-life of BEN and its metabolites, mean (SD).

BA					
Dose (mg/m^2)	C_{max} (ng/mL)	T_{max} (min)	AUC (ug/mL*min)	Cl/F (L/min)	Half-life (min)
1.5 (N=4)	99.1 (54.8)	12 (0)	2010 (1953)	1.59 (1.44)	7.5 (2.8)
3 (N=5)	183.0 (193.1)	12.6 (1.3)	2827 (2600)	1.77 (1.24)	33.3 (29.1)
5 (N=6)	470.6 (460.1)	13 (1.5	12857 (9469.2)	0.72 (0.60)	69.6 (66.0)
7 (N=2)	771.5 (61.5)	42.5 (38.9)	28735 (11309)	0.26 (0.10)	26.6 (23.3)
9 (N=11)	2430 (1725)	15.9 (17.4)	73585 (78888)	0.30 (0.33)	770.6 (1708.4)
12 (N=2)	3742 (4126)	5 (NA)	50106 (52547)	0.53 (0.56)	20.0 (NA)

$BA-(OH)_2$				
Dose (mg/m^2)	C_{max} (ng/mL)	T_{max} (min)	AUC (ug/mL*min)	Half-life (min)
1.5 (N=1)	12.5 (NA)	12 (NA)	213.4 (NA)	44.5 (NA)
3 (N=1)	14.5 (NA)	12 (NA)	204.0 (NA)	10.4 (NA)
5 (N=7)	31.3 (9.9)	13.7 (1.6)	1669 (139)	48.8 (29.9)
7 (N=2)	58.9 (NA)	12 (NA)	18878 (NA)	1700 (NA)
9 (N=12)	102.2 (153.2)	21.2 (19.1)	13061 (22340)	126.9 (124.2)
12 (N=2)	124.7 (NA)	15.0 (NA)	7083 (NA)	155.8 (NA)

$BA-Cl_2$				
Dose (mg/m^2)	C_{max} (ng/mL)	T_{max} (min)	AUC (ug/mL*min)	Half-life (min)
9 (N=1)	43.3	25	1998	25.2

BA-Cl				
Dose (mg/m^2)	C_{max} (ng/mL)	T_{max} (min)	AUC (ug/mL*min)	Half-life (min)
1.5 (N=4)	12.8 (15.0)	12.0 (0)	220.7 (176.6)	24.9 (13.4)
3 (N=5)	5.9 (4.7)	13.2 (1.6)	128.5 (65.0)	30.1 (0.9)
5 (N=6)	15.6 (14.3)	14.7 (4.8)	551.8 (651.2)	454.7 (953.8)
7 (N=2)	20.0 (NA)	42.5 (NA)	933.2 (NA)	17.3 (NA)
9 (N=11)	72.2 (72.4)	16.5 (16.2)	3292 (4482)	233.1 (371.1)
12 (N=2)	70.9 (NA)	8.5 (NA)	1719 (NA)	7.7 (NA)

BA-Cl-OH				
Dose (mg/m^2)	C_{max} (ng/mL)	T_{max} (min)	AUC (ug/mL*min)	Half-life (min)
1.5 (N=4)	4.1 (3.2)	12 (0)	180.1 (181.2)	46.4 (19.5)
3 (N=4)	3.5 (2.0)	13.5 (1.7)	156.5 (45.1)	234.8 (206.1)
5 (N=7)	19.6 (9.6)	18.4 (6.3)	1528 (1119)	222.0 (345.5)
7 (N=2)	27.4 (NA)	15 (NA)	5269 (NA)	308.8 (NA)
9 (N=12)	57.5 (40.8)	25.6 (19.0)	4739 (4770)	2634 (6402)
12 (N=2)	277.8 (NA)	15 (NA)	4534 (NA)	52.6 (NA)

BA-OH				
Dose (mg/m^2)	C_{max} (ng/mL)	T_{max} (min)	AUC (ug/mL*min)	Half-life (min)
1.5 (N=3)	5.6 (4.1)	12 (0)	119.7 (123.6)	41.3 (NA)
3 (N=5)	6.9 (1.3)	12.6 (1.3)	116.4 (136.7)	27.8 (25.2)
5 (N=6)	26.0 (19.5)	13.5 (1.6)	778.5 (500.3)	65.0 (49.0)
7 (N=2)	38.3 (NA)	13.5 (NA)	961.5 (NA)	21.0 (NA)
9 (N=12)	109.0 (84.8)	14.7 (16.1)	3106 (2812)	61.4 (48.4)
12 (N=2)	182 (NA)	8.5 (NA)	2387 (2812)	16.9 (NA)

BA-Gluc				
Dose (mg/m^2)	C_{max} (ng/mL)	T_{max} (min)	AUC (ug/mL*min)	Half-life (min)
1.5 (N=4)	17.3 (16.6)	36.3 (14.4)	1547 (2107)	120.9 (144.9)
3 (N=5)	17.1 (12.1)	24.0 (10.3)	1075 (586)	166.2 (180.8)
5 (N=6)	35.8 (26.7)	31.7 (20.9)	3474 (3561)	519.4 (947.9)
7 (N=2)	71.9 (NA)	35	6359 (NA)	38.2 (NA)
9 (N=11)	75.4 (65.0)	33.6 (11.4)	6545 (5239)	194.8 (223.7)
12 (N=2)	136.1 (NA)	20 (NA)	10612 (NA)	93.6 (NA)

BA-$(OH)_2$-Gluc				
Dose (mg/m^2)	C_{max} (ng/mL)	T_{max} (min)	AUC (ug/mL*min)	Half-life (min)
1.5 (N=4)	7.5 (9.9)	88.8 (48.0)	3470 (5397)	418.9 (389.6)
3 (N=5)	3.3 (1.3)	100.0 (59.1)	1601 (1016)	319.9 (517.8)
5 (N=7)	17.0 (8.5)	164.3 (185.1)	9767 (7667)	594.5 (201.5)
7 (N=2)	30.9 (NA)	190.0 (NA)	14121 (NA)	575.8 (NA)
9 (N=12)	34.2 (25.6)	236.3 (396.2)	13724 (12851)	513.4 (835.1)
12 (N=2)	65.2 (NA)	190.0 (NA)	23697 (NA)	2381.1 (NA)

BA-Cl_2-Gluc				
Dose (mg/m^2)	C_{max} (ng/mL)	T_{max} (min)	AUC (ug/mL*min)	Half-life (min)
1.5 (N=4)	4.1 (4.1)	36.3 (14.4)	586.7 (749.6)	83.2 (49.7)
3 (N=5)	3.0 (1.4)	38.4 (25.1)	267.6 (359.1)	125.7 (89.7)
5 (N=7)	19.7 (17.4)	50.7 (16.7)	2725 (3446)	189.2 (74.3)
7 (N=2)	32.1 (NA)	92.5 (NA)	6478 (NA)	361.6 (NA)
9 (N=12)	30.9 (30.7)	43.8 (18.2)	4215 (4058)	283.3 (502.3)
12 (N=2)	97.2 (NA)	47.5 (NA)	14244 (NA)	189.6 (NA)

BA-Cl-Gluc				
Dose (mg/m^2)	C_{max} (ng/mL)	T_{max} (min)	AUC (ug/mL*min)	Half-life (min)
1.5 (N=4)	6.5 (5.7)	26.3 (10.3)	603.0 (880.2)	84.8 (48.6)
3 (N=5)	3.6 (1.7)	23.0 (4.5)	313.1 (161.4)	90.0 (39.6)
5 (N=7)	18.6 (17.1)	32.9 (19.3)	1930 (2158)	152.9 (126.9)
7 (N=2)	34.2 (NA)	35.0 (NA)	4069 (NA)	781.0 (NA)
9 (N=10)	31.4 (22.4)	28.0 (11.1)	3002 (2431)	162.5 (3.7)
12 (N=1)	89.2 (NA)	12.0 (NA)	10140 (NA)	121.7 (NA)

BA-Cl-OH-Gluc				
Dose (mg/m^2)	C_{max} (ng/mL)	T_{max} (min)	AUC (ug/mL*min)	Half-life (min)
1.5 (N=4)	3.1 (3.0)	36.3 (22.5)	767 (1228)	105.8 (65.5)
3 (N=4)	1.9 (0.9)	47.5 (15.0)	402.0 (362.8)	137.1 (69.1)
5 (N=7)	13.7 (9.8)	57.1 (13.5)	2727 (2204)	272.7 (100.8)
7 (N=2)	19.6 (NA)	92.5 (NA)	4463 (NA)	693.4 (NA)
9 (N=10)	24.4 (15.1)	92.5 (101.3)	4981 (5311)	422.9 (474.6)
12 (N=2)	49.6 (NA)	70 (NA)	9990 (NA)	49.6 (NA)

BA-OH-Gluc				
Dose (mg/m^2)	C_{max} (ng/mL)	T_{max} (min)	AUC (ug/mL*min)	Half-life (min)
1.5 (N=4)	3.5 (2.5)	26.3 (10.3)	331.6 (447.1)	311.6 (281.9)
3 (N=5)	2.8 (2.1)	32 (15.7)	210.3 (134.0)	114.4 (90.8)
5 (N=7)	9.1 (6.1)	36.4 (19.7)	995.6 (817.5)	115.0 (66.3)
7 (N=2)	16.2 (NA)	35.0 (NA)	2236 (NA)	395.0 (NA)
9 (N=8)	15.7 (11.9)	23.8 (10.9)	1599 (875)	221.6 (414.6)
12 (N=2)	26 (NA)	18.5 (NA)	27912 (NA)	193.8 (NA)

5.5 DISCUSSION

This study aimed to characterize the safety, tolerability, pharmacokinetics and metabolism of BEN in patients with solid tumors. Previous results suggested that BEN is metabolized *in vivo* and *in vitro* in blood into BA by ALDH. We have demonstrated that BA reacts faster with nucleophiles than BEN, and may therefore be an important effector of DNA alkylation.[159]

The maximum tolerated dose of BEN was 9 mg/m^2 when administered on days 1, 8, and 15 of a 28-day schedule. Three patients experienced dose-limiting toxicities of neutropenia and thrombocytopenia which is consistent with the proposed mechanism of BEN as an alkylating agent. In addition, many patients exhibited prolonged but reversible myelosuppression. Tumor responses were seen in one subject with mRCC and in one subject with advanced cervical carcinoma following BEN administration. Neither the responses nor the toxicities observed could be correlated to the plasma pharmacokinetics (ie. AUC, C_{max} or $T_{1/2}$) or metabolism of BEN.

BEN was rapidly metabolized in all patients and was only detected in 2 patients. This was similar to our previous observations in mice showed rapid metabolism of BEN to BA even though the dose of BEN administered to mice was 8 times higher than that given to patients in this trial. All of the BEN metabolites and glucuronides that were detected in mice were also observed in patients, which further support the translation of previous preclinical findings relating to BEN pharmacology. There was a large inter-patient variability in the concentration and AUC of BA and downstream metabolites. This may be due in part to sample handling and processing as BA has a half-life of 5 minutes in blood at room temperature. BA was present in all but two patients; however,

these two patients did have downstream BA metabolites. The BA plasma half-life was several-fold longer than the 5 min *in vitro* plasma half-life of this very reactive compound, suggesting continued metabolic generation of BA from BEN in tissues, followed by re-distribution into the plasma compartment. This finding is indirect proof of the ability of BEN to reach tissues with subsequent intracellular activation to BA.[159]

The AUC and C_{max} of the metabolites increased linearly with dose. The dose adjusted C_{max} remained constant for all analytes with an increase in dose except for BA in which the dose adjusted C_{max} increased with dose. This may be due in part to e.g. a saturated efflux transporter that causes more BEN to remain in the cells at higher concentrations which is then converted to BA.

BEN is a lipophilic pro-drug of BA. Intracellularly generated, BA is a much more reactive analog and the likely alkylator of cellular targets. We previously showed that ALDH may be responsible for the intracellular metabolism of BEN to BA, and that BEN is more active in cell lines that express high levels of ALDH.[159] Therefore, BEN appears to be able to target cells that over express ALDH. The potential importance lies in the reported overexpression of ALDH in stem cells of many tumor types making these stem cells potential targets for BEN therapy. The prolonged myelosuppression observed with BEN is suggestive of toxicity to bone marrow stem cells. Hematopoietic stem cells express high levels of aldehyde dehydrogenase,[176] potentially facilitating the rapid conversion of BEN to BA, with ensuing intracellular alkylation and cytotoxicity.

This trial produced a response rate of 2/16 in a heavily pre-treated population. One of the responses was from a patient had RCC. There were a total of 4 patients enrolled in the trial that suffer from RCC. The responses that were observed were at the 9

mg/m^2 dose level in which a total of 12 patients were treated. All of which suggests that further investigation of anti-tumor activity is warranted. While a predictable pattern of reversible myelosuppression was observed, toxicities such as alopecia and peripheral neuropathy were not, and gastrointestinal toxicity was relatively modest. In addition, an alternative schedule of drug administration on day 1 and 2 on an every 21-day schedule is being currently investigated in a phase I cohort of patients with advanced solid tumors. We hypothesize that a prolonged (20-day) interval of this modified schedule would allow for greater hematopoietic recovery, and would potentially be associated with reduced myelosuppression at clinically effective doses.

In conclusion, the maximum tolerated dose of BEN on a weekly times 3 every 4 weeks schedule was 9.0 mg/m^2. There were 3 subjects that experienced dose limited toxicities and two subjects exhibited partial responses. Neither the toxicities nor the responses correlated with the plasma pharmacokinetics of BEN. BEN was very rapidly metabolized to BA, and the same metabolites that were detected in mice were also detected in humans.

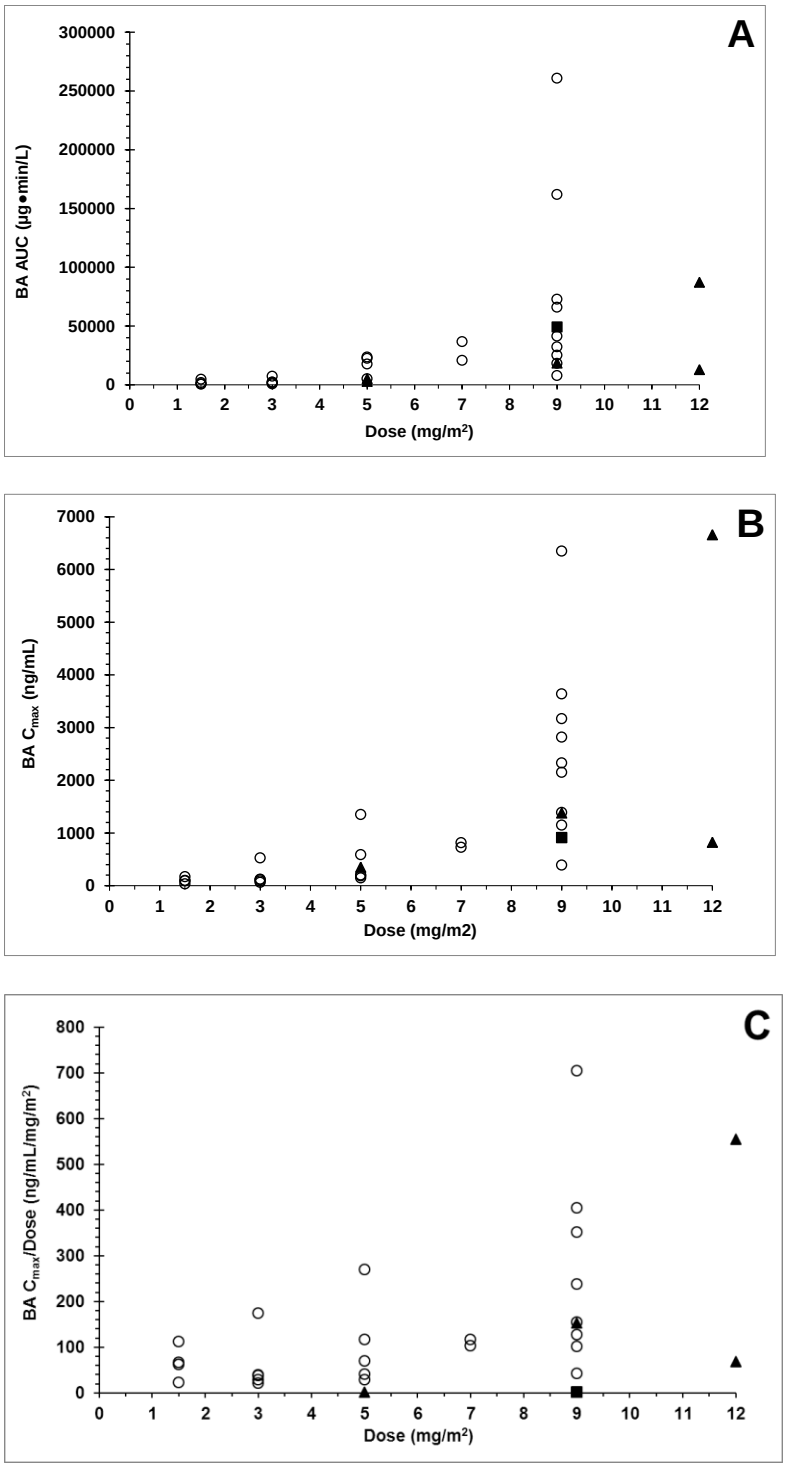

Figure 56. A) AUC vs dose B) Cmax vs dose and C) Cmax/dose vs dose for BA. (▲toxicity ■ partial response).

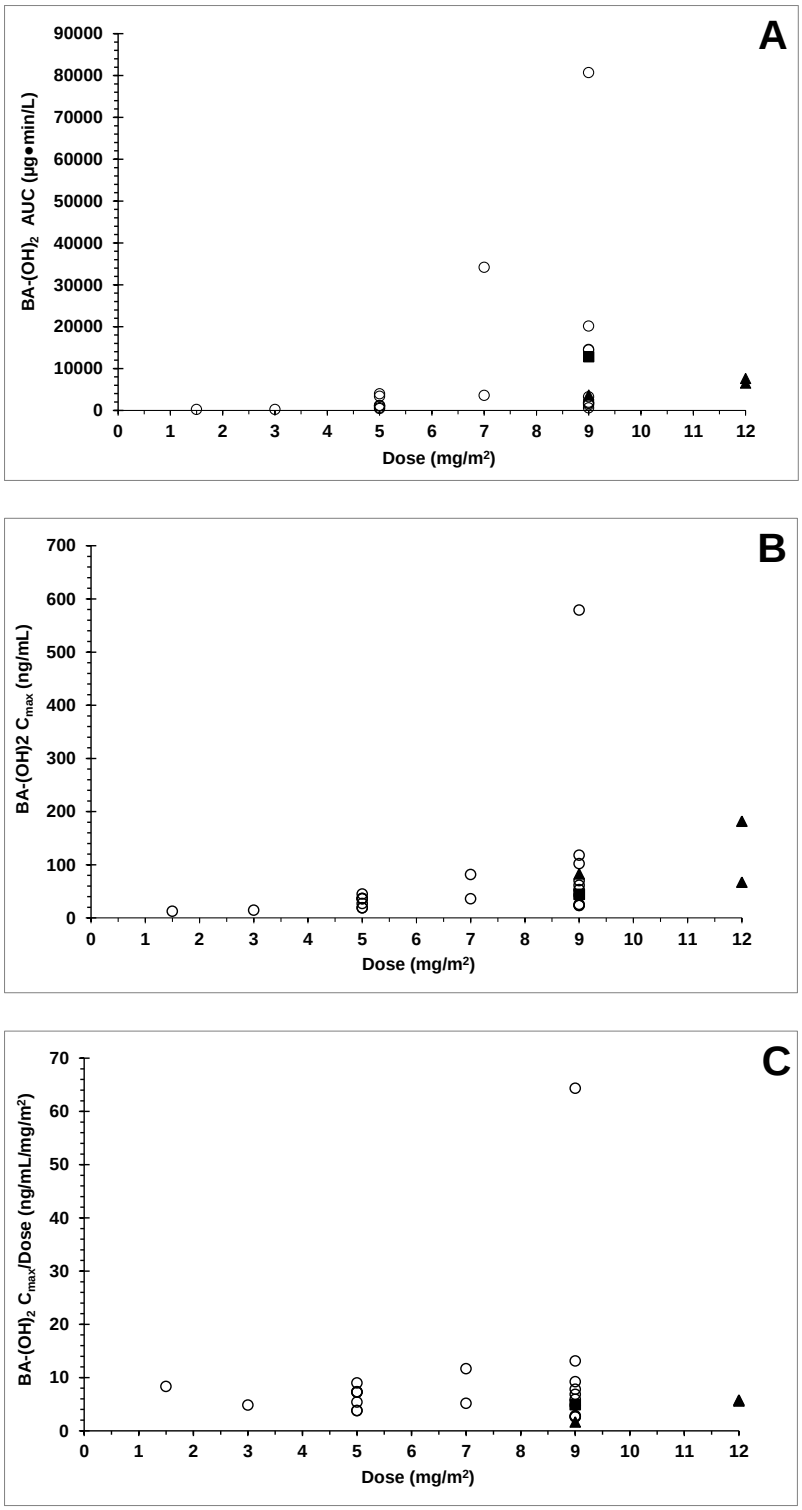

Figure 57. A) AUC vs dose B) Cmax vs dose and C) Cmax/dose vs dose for BA-$(OH)_2$. (▲toxicity ■ partial response).

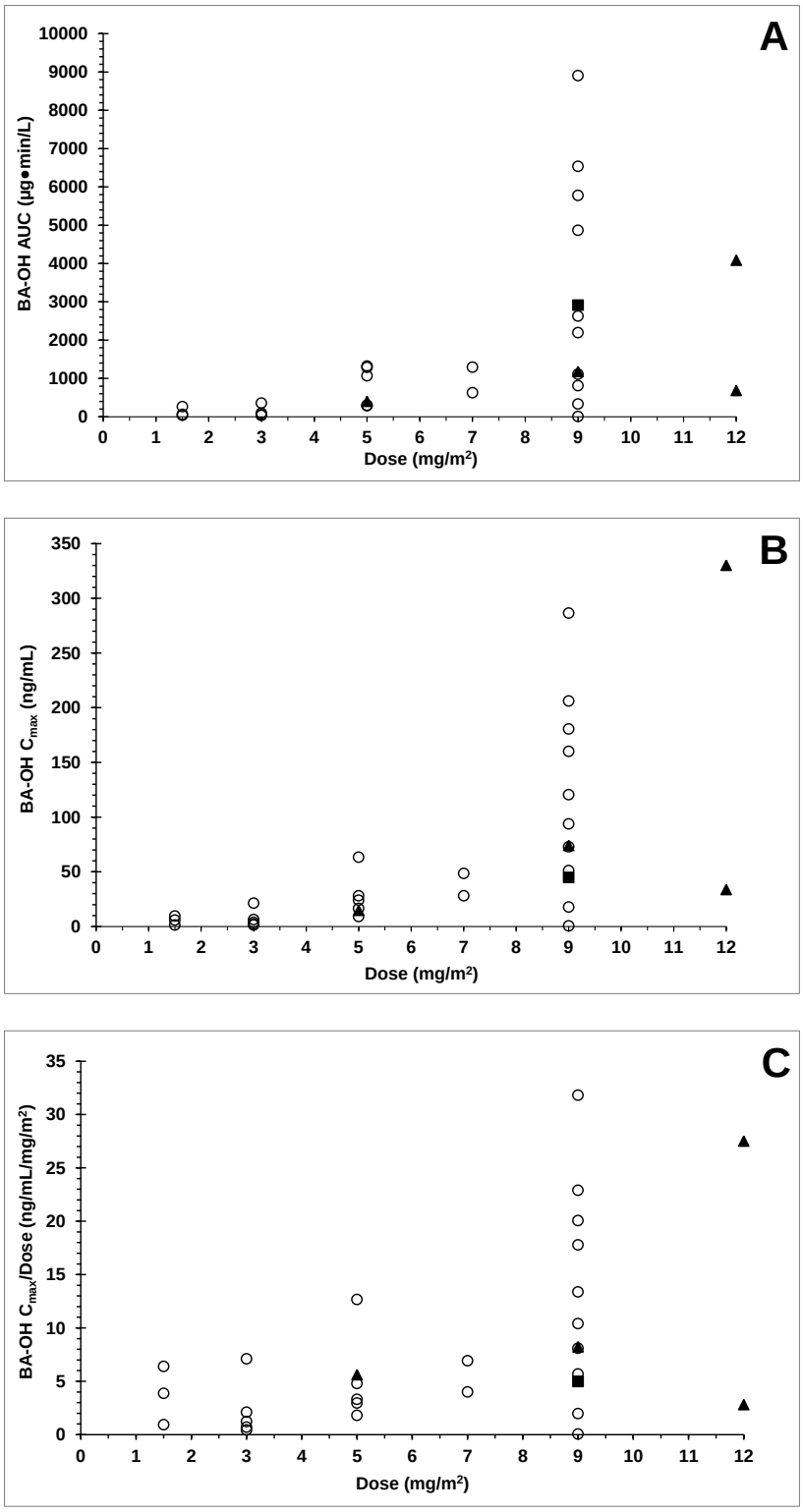

Figure 58. A) AUC vs dose B) Cmax vs dose and C) Cmax/dose vs dose for BA-OH. (▲toxicity ■ partial response).

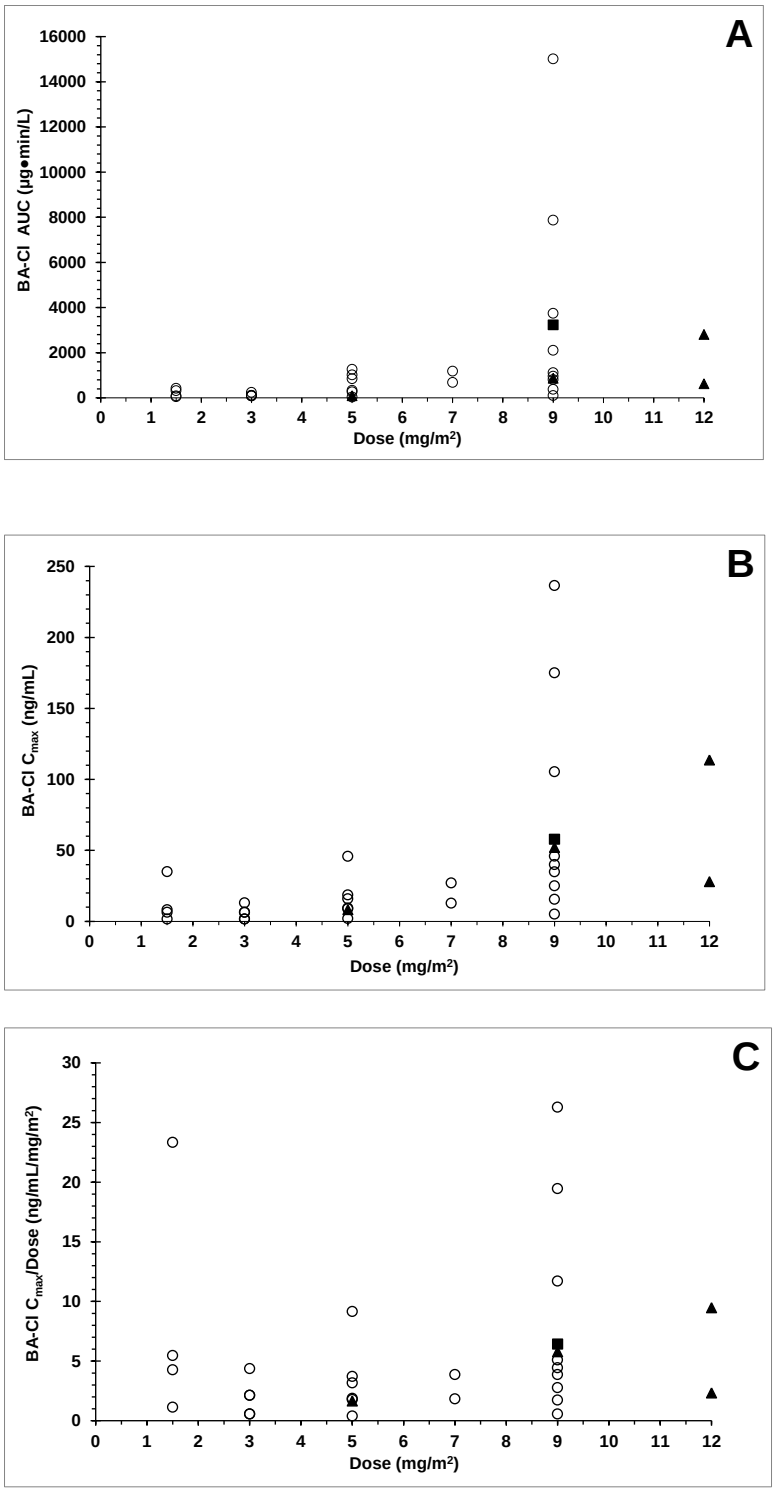

Figure 59. A) AUC vs dose B) Cmax vs dose and C) Cmax/dose vs dose for BA-Cl. (▲toxicity ■ partial response).

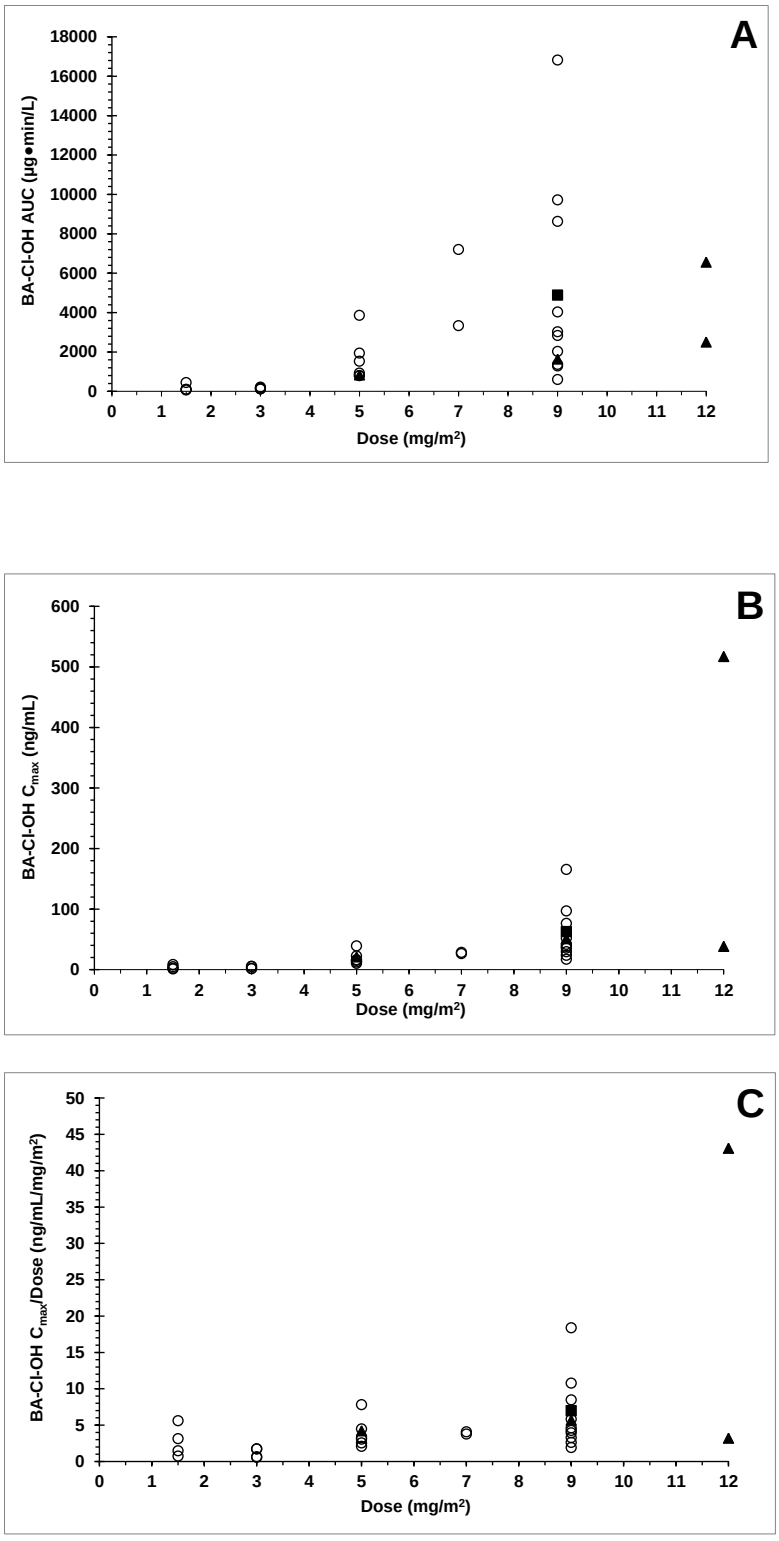

Figure 60. A) AUC vs dose B) Cmax vs dose and C) Cmax/dose vs dose for BA-Cl-OH. (▲toxicity ■ partial response).

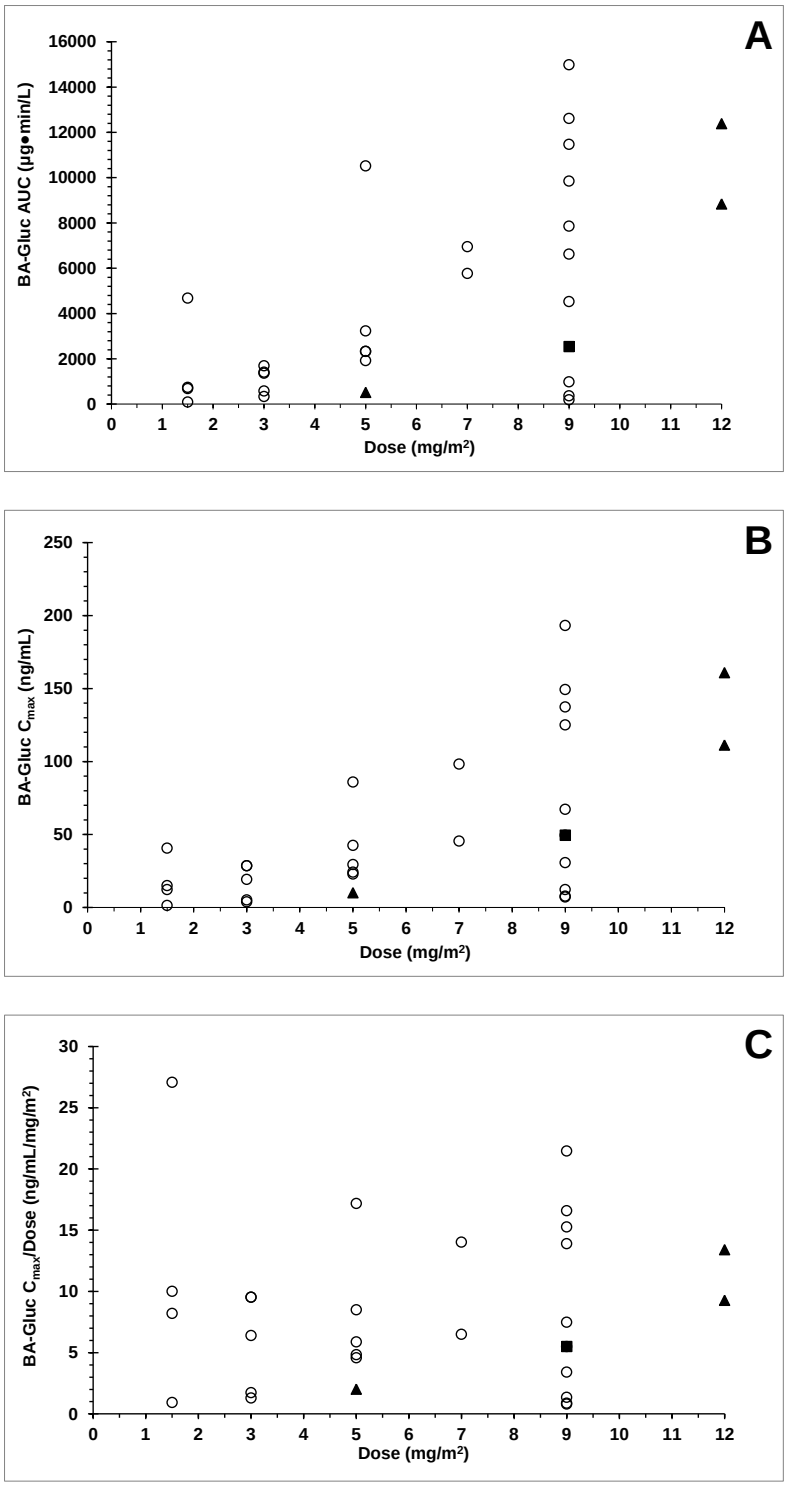

Figure 61. A) AUC vs dose B) Cmax vs dose and C) Cmax/dose vs dose for BA-Gluc. (▲toxicity ■ partial response).

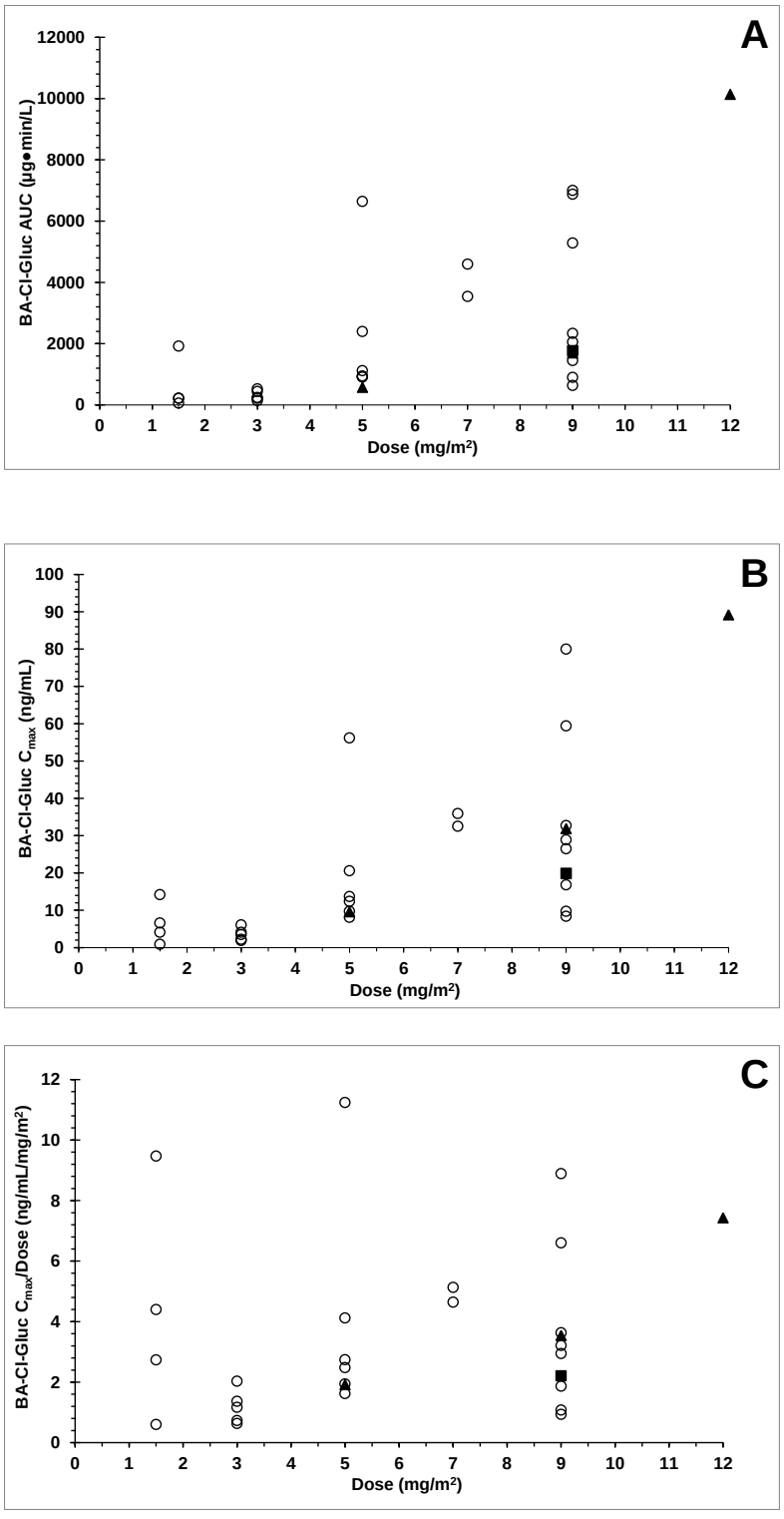

Figure 62. A) AUC vs dose B) Cmax vs dose and C) Cmax/dose vs dose for BA-Cl-Gluc. (▲toxicity ■ partial response).

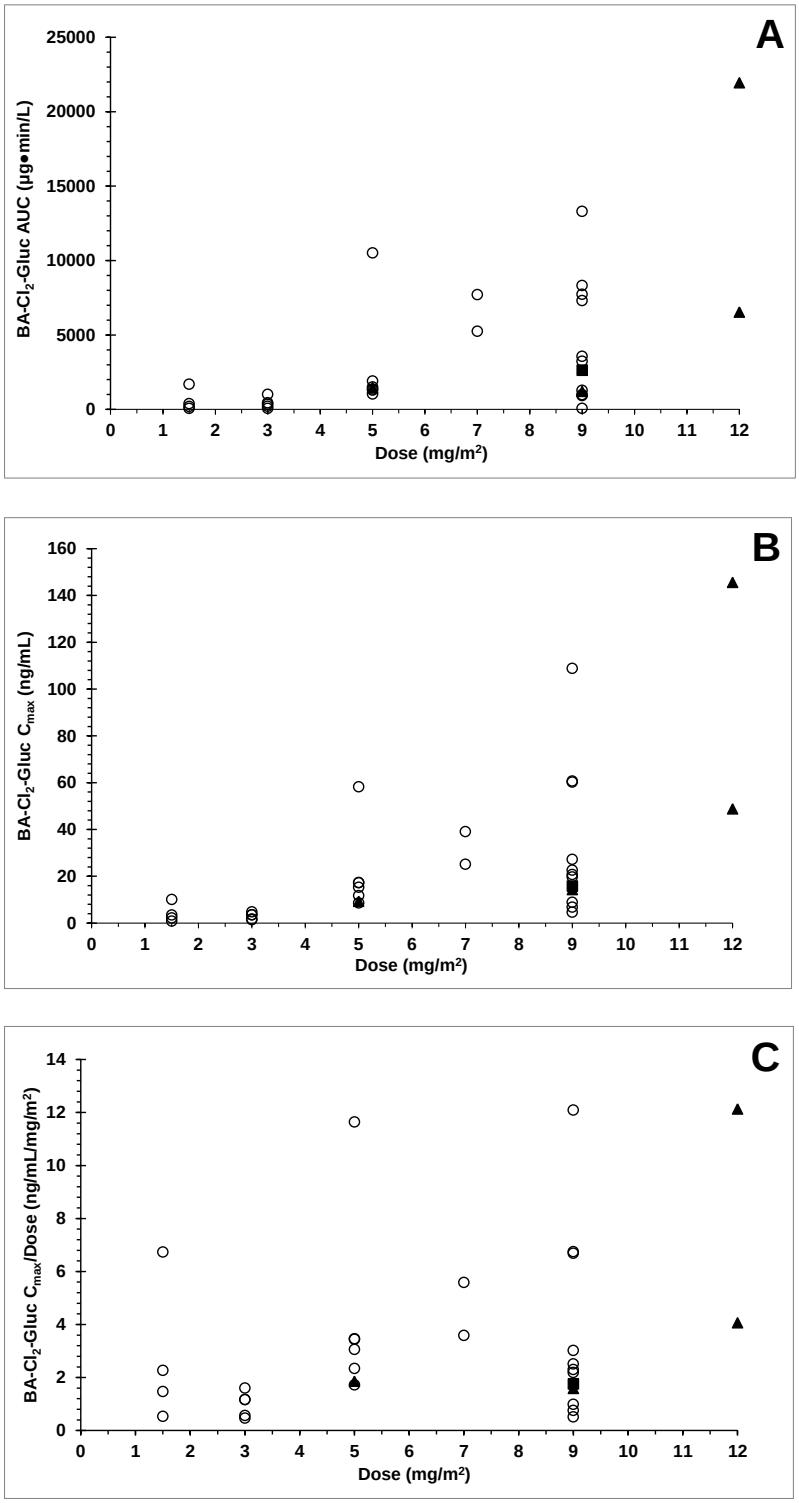

Figure 63. A) AUC vs dose B) Cmax vs dose and C) Cmax/dose vs dose for BA-Cl_2-Gluc. (▲toxicity ■ partial response).

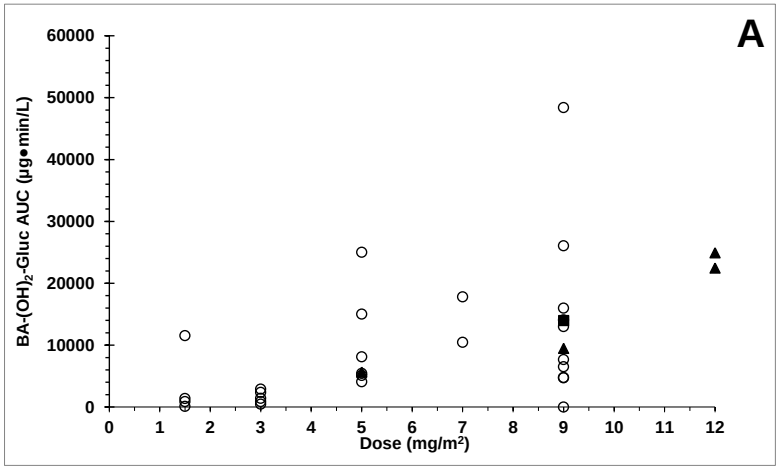

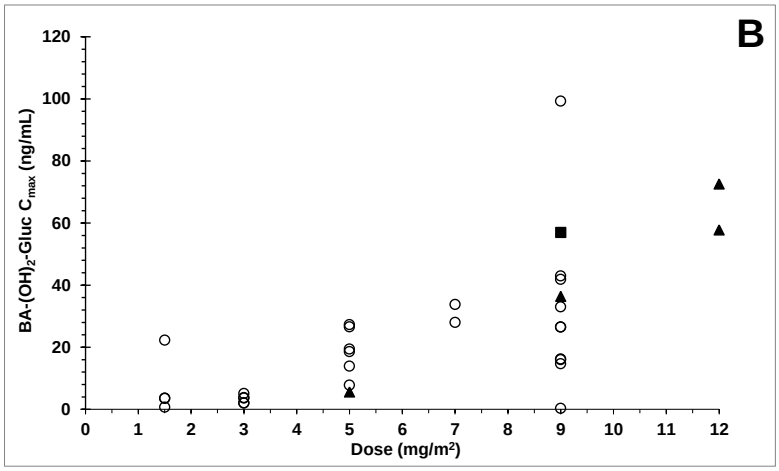

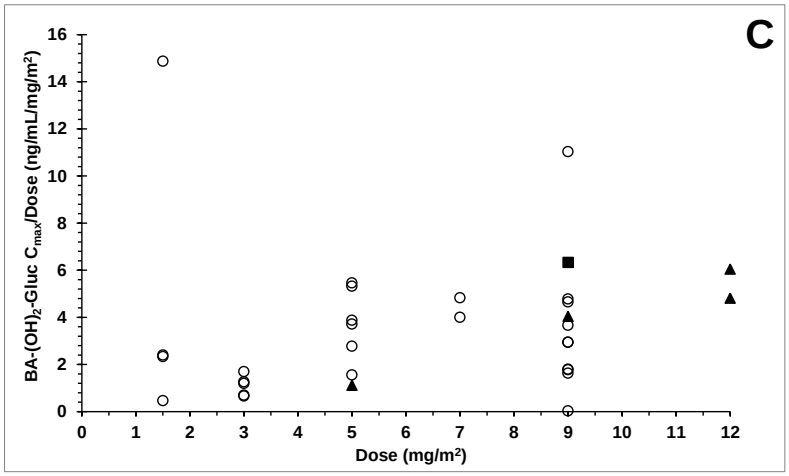

Figure 64. A) AUC vs dose B) Cmax vs dose and C) Cmax/dose vs dose for BA-$(OH)_2$-Gluc. (▲toxicity ■ partial response).

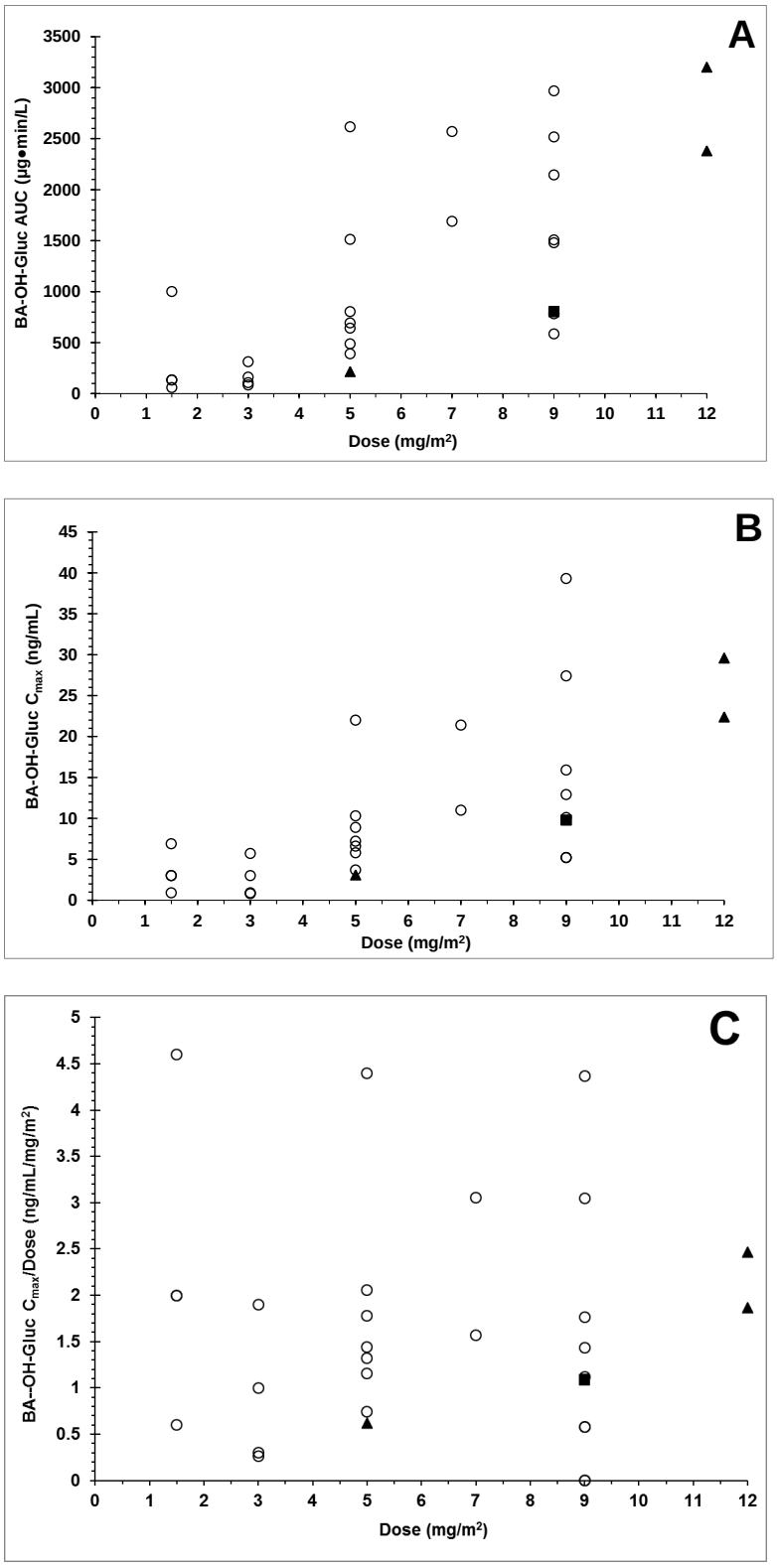

Figure 65. A) AUC vs dose B) Cmax vs dose and C) Cmax/dose vs dose for BA-OH-Gluc. (▲toxicity ■ partial response).

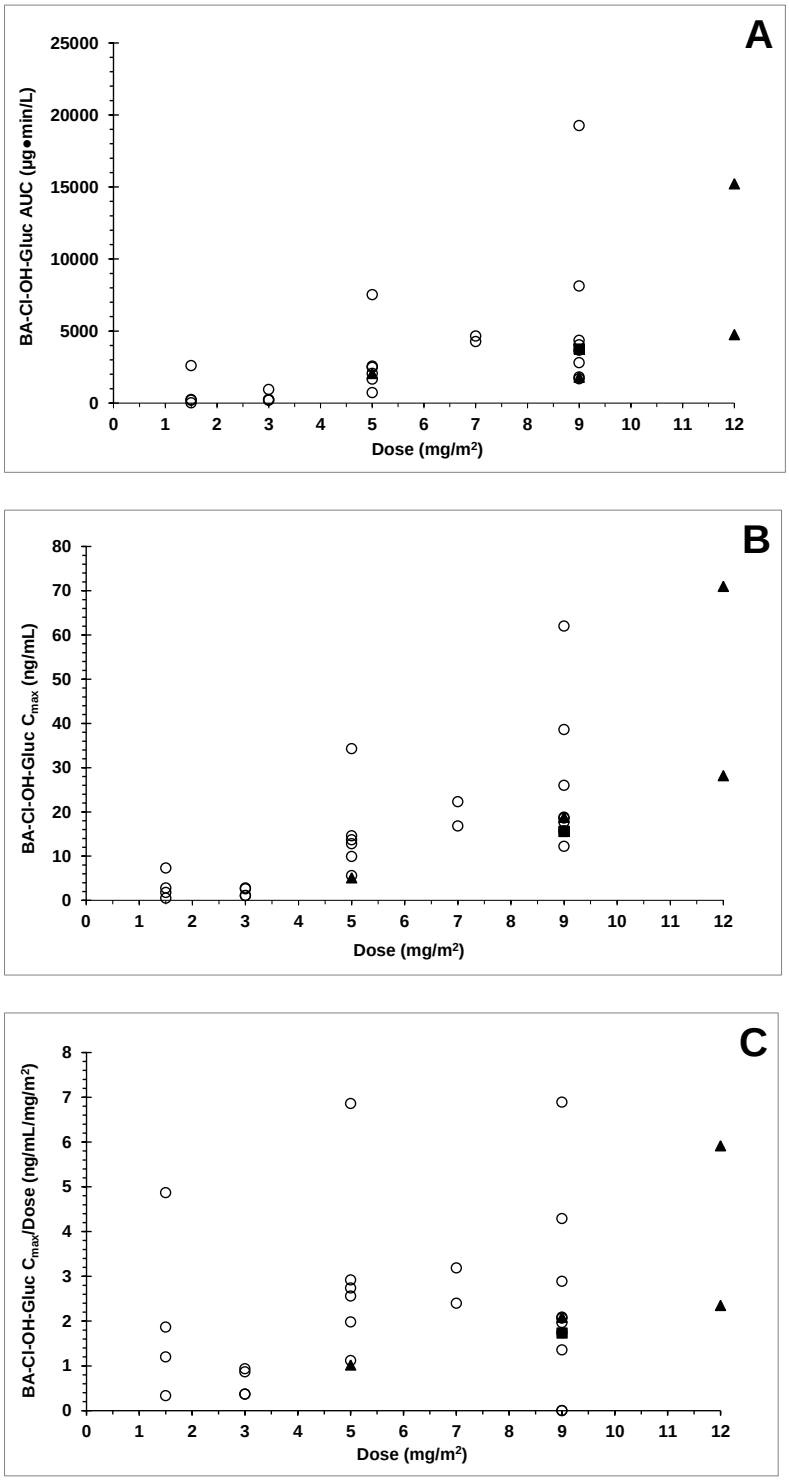

Figure 66. A) AUC vs dose B) Cmax vs dose and C) Cmax/dose vs dose for BA-Cl-OH-Gluc. (▲toxicity ■ partial response).

6.0 MAJOR FINDINGS, LIMITATIONS, AND FUTURE DIRECTION

6.1 CONCLUSIONS

The work in this dissertation was conducted to gain a better understanding of the preclinical and clinical pharmacology of benzaldehyde dimethane sulfonate (BEN), an alkylating agent that was shown to have activity against renal carcinoma cell lines and was to be administered to patients in a phase I clinical trial.

Limited basic metabolism and pharmacokinetic data was available to successfully implement the clinical studies. We first studied the characteristics of BEN in various biological matrices including plasma and blood (Chapter 2 and 3). We then conducted studies in renal carcinoma cells to evaluate its effect and mice to determine the metabolism and pharmacokinetics in animals (Chapters 2 and 4). Lastly, we assessed the pharmacokinetics of BEN administered to people as part of a first in humans clinical trial (Chapter 5).

In whole blood, but not in plasma, BEN was rapidly converted to its carboxylic acid analogue BA, suggesting conversion by an enzyme present in red blood cells. BA rapidly decomposed in plasma with a half-life of approximately 5 min. In plasma, BEN and BA decomposed according to a parallel pathway to a number of hydroxylated and chlorinated analogs. The relatively fast rate of production of BA products relative to the

generation of BEN products is likely indicative of the relative reactivities of the acid analogs relative to the aldehyde analogs. We hypothesize that the unbound electron pair on the aniline nitrogen is the initiator of an SN2 attack on the β-carbon, generating the reactive aziridinium intermediate. Mesomeric withdrawal of the aniline unbound electron pair by the para-aldehyde moiety, or occupation of the electron pair by a proton under acidic conditions would be expected to decrease the generation of the aziridinium intermediate and thereby decrease the reactivity. The abundance of BA analogs and lack of BEN analogs after incubation of BEN in whole blood can be attributed to the relative rates of the competing pathways of BEN conversion. The conversion of BEN to BA is much more rapid than conversion of BEN to downstream aldehyde analogs. In addition, any aldehyde products formed may also be converted to their respective acid counterparts by the same enzymatic pathway that converts BEN to BA, as was shown for the conversion of BEN-$(OH)_2$ to BA-$(OH)_2$ in whole blood. During incubation with human renal carcinoma cells, BEN undergoes chemical conversion to BEN-$(OH)_2$ or metabolism to BA and subsequent conversion to BA-$(OH)_2$ in all cell lines tested. A498 cells displayed the greatest metabolism of BEN to BA as shown by the amount of BA-$(OH)_2$ generated; in fact, no BEN-$(OH)_2$ could be detected. In contrast, SN12K1 cells generated very little BA-$(OH)_2$. The ratio of BEN disappearance for A498/SN12K1 was 35-fold. It is noteworthy that the A498 cell line was the most sensitive to BEN demonstrated by the lowest IC_{50} value. To test whether ALDH may be responsible for the metabolic conversion of BEN to BA we measured the ALDH activity in A498 and SN12K1 cells. We found that A498 cells had ALDH activity approximately 40-fold greater than SN12K1 cells, paralleling the BA-$(OH)_2$ generating activity and conversely the

metabolism of BEN to BA. These results are in line with previously reported ALDH activities.[137] These data support the notion that intracellular ALDH is responsible for the metabolism of BEN to BA in these cells, and that this intracellular conversion mediates its cytotoxic effects. ALDH may also be responsible for the observed metabolism of BEN to BA in whole blood as red blood cells contain ALDH.

We hypothesize that the A498 cell line is able to most efficiently metabolize BEN to its more reactive metabolite BA by ALDH inside the cell, which then rapidly alkylates cellular constituents resulting in cell damage. The high IC_{50}s of BA added to medium suggest that BA reacts with other nucleophiles in the medium before it is able to reach its intracellular targets. BEN-Cl_2 and BA-Cl_2 had intermediary IC_{50}s. This suggests that BEN-Cl_2 gets into the cells and is locally converted to BA-Cl_2 which reacts with cellular targets. However, because BA-Cl_2 is not as reactive as BA, a fair amount likely diffuses out of the cell without exerting cytotoxic effects. Conversely, when BA-Cl_2 was added to the cell incubation, the relative stability of BA-Cl_2 allowed enough of it to diffuse into the cells to cause intracellular damage. Taken together, these data suggest that BEN is a pro-drug that requires intracellular activation to the highly reactive BA, which likely exerts rapid and localized damage via alkylation inside the cells.

The second part of our work focused on the determination of the enzyme responsible for the metabolic conversion of BEN to BA. Also we performed K_m and V_{max} experiments to better understand the metabolism of BEN.

We performed the metabolism of BEN with the purified enzymes that were commercially available. These included ALDH1A1, 3A1, 2 and 5A1. Of the ALDH isoforms we tested BEN was only a substrate for ALDH1A1. Although we found that

ALDH1A1 was the only enzyme that metabolized BEN there may be other ALDH isoforms that also metablize BEN as there are 19 known isoforms of ALDH. Most of these ALDHs are not commercially available and the substrates for these isoforms have yet to be determined.

The apparent V_{max} and K_m of BEN were determined in 6 different lots of blood to evaluate biological central tendency and variability. BEN displayed saturable kinetics in all of the lots of blood we tested. In addition, we found that there was inter-subject variability between the lots of blood. However, the k_m values displayed are higher than the expected peak concentrations of BEN in humans. Therefore we expect linear pharmacokinetics in humans.

The third part of this work focused on determining the pharmacokinetic parameters of BEN in mice and to determine whether the administration of the ALDH inhibitor disulfiram could change the exposure of BEN. After iv BEN administration to mice, the exposure to BEN was low and there were at least 12 metabolites generated, including 6 BA glucuronides.

The plasma half-life of BA in mice was much longer than the *in vitro* half-life of BA, (5 min). The longer *in vivo* half-life of BA suggests that although BEN is metabolized in RBCs, BEN also enters into tissues where it is also metabolized to BA. The BA that is produced in the tissues then re-enters the blood where it degrades into downstream BA products as demonstrated in the *in vitro* experiments. Pretreatment with disulfiram increased BEN exposure 368-fold, giving further evidence that ALDH may be an enzyme responsible for metabolizing BEN into BA.

The last part of this dissertation was to determine the plasma pharmacokinetics of BEN administered to humans as part of a phase I clinical trial. The maximum tolerated dose of BEN was 9 mg/m^2 when administered on days 1, 8, and 15 of a 28-day schedule. Three patients experienced dose-limiting toxicities of neutropenia and thrombocytopenia which is consistent with the proposed mechanism of BEN as an alkylating agent. In addition, many patients exhibited prolonged (14 days) but reversible myelosuppression. Tumor responses were seen in one subject with mRCC and in one subject with advanced cervical carcinoma following BEN administration. Neither the responses nor the toxicities witnessed could be correlated to the pharmacokinetics or metabolism of BEN. BEN was rapidly metabolized in all patients and was only detected in 2 patients. This was similar to our previous mouse study which resulted in the rapid metabolism of BEN to BA even though the dose of BEN administered to mice was 8 times higher than that given to patients in this trial. All of the BEN metabolites and glucuronides that were detected in mice were also observed in patients. In addition, a decrease in the white blood cell count and the percent lymphocytes in mice administered BEN showed that BEN is toxic to the bone marrow. This was also demonstrated in humans as many patients exhibited neutropenia and thrombocytopenia, which further support the translation of previous preclinical findings relating to BEN pharmacology. There was a large inter-patient variability in the concentration and AUC of BA and downstream metabolites. BA was present in all but two patients; however, these two patients did have downstream BA metabolites. The BA plasma half-life was several-fold longer than the 5 min *in vitro* plasma half-life of this very reactive compound, suggesting continued metabolic generation of BA from BEN in tissues, followed by re-distribution into the plasma

compartment. This finding is indirect proof of the ability of BEN to reach tissues with subsequent intracellular activation to BA.[173]

The AUC and C_{max} of the metabolites increased linearly with dose. This is expected with linear kinetics. The dose adjusted C_{max} remained constant for all analytes with an increase in dose except for BA in which the dose adjusted C_{max} increased with dose. This may be due in part to e.g. a saturated efflux transporter that causes more BEN to remain in the cells at higher concentrations which is then converted to BA. BEN is a lipophilic pro-drug of BA. Intracellularly generated, BA is a much more reactive analog and the likely alkylator of cellular targets. We previously showed that ALDH may be responsible for the intracellular metabolism of BEN to BA, and that BEN is more active in cell lines that express high levels of ALDH. Therefore, BEN appears to be able to target cells that over express ALDH. The potential importance lies in the reported overexpression of ALDH in stem cells of many tumor types making these stem cells potential targets for BEN therapy. The prolonged myelosuppression observed with BEN is suggestive of toxicity to bone marrow stem cells. Hematopoietic stem cells express high levels of aldehyde dehydrogenase, potentially facilitating the rapid conversion of BEN to BA, with ensuing intracellular alkylation and cytotoxicity.

6.2 FUTURE DIRECTION

1). Although multiple clinical trials with various agents for the treatment of RCC have been performed the outcome has been poor. More research needs to be conducted to elucidate why RCC is so resistant to current therapies.

2). Benzaldehyde dimethane sulfonate has proven to be more active *in vitro* and *in vivo* against RCC than other alkylating agents. One reason may be because certain RCC cells have high levels of ALDH activity, however, it may also be due in part to the structure of BEN. Specifically, the hydrophobic moiety on the molecule is better able to enter into the cell. Transporter experiments testing this theory should be conducted.

3). We hypothesize that BEN acts as a prodrug and that BA actually causes the cytotoxicity to RCC cells. Future experiments should be performed that more precisely measures the levels of BEN and BA in tissues. These experiments could include mass spectrometric determination of DNA alkylation by BEN and BA or ^{14}C-labeled BEN studies.

4). We have shown that BEN has greater activity in RCC cell lines that have higher levels of ALDH. Experiments to determine the effects of BEN on other cell lines that have high levels of ALDH such as certain lung cancer cell lines and tumor stem cells may prove to be beneficial. In addition, patients for BEN treatment could be selected based on the ALDH levels in their tumor. Studies can then relate ALDH expression levels and clinical outcome.

5). A large inter individual variability was displayed in the pharmacokinetic parameters of BEN and its metabolites in the clinical trial. Part of this variability may be due to the metabolism of BEN and degradation of BA during sample collection. In future trials, there should be more emphasis on sample collection to ensure that both BEN and BA are stabilized. First, the addition of disulfiram to the blood collection vials should be considered. This would ensure that the metabolism of BEN to BA would be inhibited. In addition, experiments that limit the degradation of BA into BA degradation products should be considered. One example of this would be to immediately centrifuge the collected blood at 4 ºC as soon as the blood is drawn from the patient. Another method would be to add acetonitrile that contained sulfuric acid directly to the blood sample immediately after sample collection

6). In the current human clinical trial of BEN, many patient experienced neutropenia and thrombocytopenia. The dosing schema in any future clinical trials should consider a longer wash out period between dosing.

7). In the current clinical trial 16 different analytes where measured. These included BEN, BA, their analogs and the glucuronides of the BA products. Since most of the analytes are not active or not detected the LC-MS/MS method should be modified to measure fewer analytes. An assay to quantitate BEN, BA, BA-$(OH)_2$ and BA-$(OH)_2$-glucuronide should be adequate to characterize the pharmacokinetics of any future clinical trial of BEN administered to patients.

8). The current clinical trial of BEN prevents enrolled patients from taking drugs that are substrates for CYP3A4. Since BEN is not a substrate for CYP3A4, future trials should remove this exclusion criterium.

9). The pharmacokinetics, metabolism and resulting toxicity of BEN administered to mice was similar to that of BEN administered in humans. This is an indication that CD2F1 mice are a good model for any future experiments of BEN in an animal study.

9). This trial produced a response rate of 2/16 in a heavily pre-treated population. One of the responses was from a patient had RCC. There were a total of 4 patients enrolled in the trial that suffer from RCC. The responses that were observed were at the 9 mg/m^2 dose level in which a total of 12 patients were treated. All of which suggests that further investigation of anti-tumor activity is warranted. The recommended phase II dose should be at least 9.0 mg/m2 as the response witnessed in the phase I trial was at this dose level.

7.0 BIBLIOGRAPHY

1. Cohen HT, McGovern FJ. Renal-cell carcinoma. NEnglJMed 2005;353:2477-90.
2. Siegel R, Naishadham D, Jemal A. Cancer statistics, 2012. CA Cancer J Clin 2012;62:10-29.
3. Cho E, Adami HO, Lindblad P. Epidemiology of renal cell cancer. Hematol Oncol Clin North Am 2011;25:651-65.
4. Pantuck AJ, Zisman A, Belldegrun AS. The changing natural history of renal cell carcinoma. JUrol 2001;166:1611-23.
5. Jayson M, Sanders H. Increased incidence of serendipitously discovered renal cell carcinoma. Urology 1998;51:203-5.
6. Cooperberg MR, Mallin K, Ritchey J, Villalta JD, Carroll PR, Kane CJ. Decreasing size at diagnosis of stage 1 renal cell carcinoma: analysis from the National Cancer Data Base, 1993 to 2004. JUrol 2008;179:2131-5.
7. Hollingsworth JM, Miller DC, Daignault S, Hollenbeck BK. Rising incidence of small renal masses: a need to reassess treatment effect. JNatlCancer Inst 2006;98:1331-4.
8. Siegel R, Ward E, Brawley O, Jemal A. Cancer statistics, 2011: the impact of eliminating socioeconomic and racial disparities on premature cancer deaths. CA Cancer JClin 2011;61:212-36.
9. Siemer S, Hack M, Lehmann J, Becker F, Stockle M. Outcome of renal tumors in young adults. JUrol 2006;175:1240-3.
10. Thompson RH, Ordonez MA, Iasonos A, et al. Renal cell carcinoma in young and old patients--is there a difference? JUrol 2008;180:1262-6.
11. Cook A, Lorenzo AJ, Salle JL, et al. Pediatric renal cell carcinoma: single institution 25-year case series and initial experience with partial nephrectomy. JUrol 2006;175:1456-60.
12. Hunt JD, van der Hel OL, McMillan GP, Boffetta P, Brennan P. Renal cell carcinoma in relation to cigarette smoking: meta-analysis of 24 studies. IntJCancer 2005;114:101-8.
13. Sorensen HT, Norgard B, Friis S, Laurberg S, Olsen JH, Kronberg O. [Non-steroidal anti-inflammatory agents and prevention of colorectal cancer and other types of cancer]. UgeskrLaeger 2003;165:1260-1.
14. Mandel JS, McLaughlin JK, Schlehofer B, et al. International renal-cell cancer study. IV. Occupation. IntJCancer 1995;61:601-5.
15. Tsivian M, Moreira DM, Caso JR, Mouraviev V, Polascik TJ. Cigarette smoking is associated with advanced renal cell carcinoma. JClinOncol 2011;29:2027-31.
16. Cho E, Curhan G, Hankinson SE, et al. Prospective evaluation of analgesic use and risk of renal cell cancer. ArchInternMed 2011;171:1487-93.

17. Gago-Dominguez M, Yuan JM, Castelao JE, Ross RK, Yu MC. Regular use of analgesics is a risk factor for renal cell carcinoma. BrJCancer 1999;81:542-8.
18. Brauch H, Weirich G, Hornauer MA, Storkel S, Wohl T, Bruning T. Trichloroethylene exposure and specific somatic mutations in patients with renal cell carcinoma. JNatlCancer Inst 1999;91:854-61.
19. Kolonel LN. Association of cadmium with renal cancer. Cancer 1976;37:1782-7.
20. Maclure M. Asbestos and renal adenocarcinoma: a case-control study. EnvironRes 1987;42:353-61.
21. Chow WH, Gridley G, Fraumeni JF, Jr., Jarvholm B. Obesity, hypertension, and the risk of kidney cancer in men. NEnglJMed 2000;343:1305-11.
22. Flaherty KT, Fuchs CS, Colditz GA, et al. A prospective study of body mass index, hypertension, and smoking and the risk of renal cell carcinoma (United States). Cancer Causes Control 2005;16:1099-106.
23. Grantham JJ. Acquired cystic kidney disease. Kidney Int 1991;40:143-52.
24. Weikert S, Boeing H, Pischon T, et al. Blood pressure and risk of renal cell carcinoma in the European prospective investigation into cancer and nutrition. AmJEpidemiol 2008;167:438-46.
25. Zucchetto A, Dal Maso L, Tavani A, et al. History of treated hypertension and diabetes mellitus and risk of renal cell cancer. AnnOncol 2007;18:596-600.
26. Choi MY, Jee SH, Sull JW, Nam CM. The effect of hypertension on the risk for kidney cancer in Korean men. Kidney Int 2005;67:647-52.
27. Lindblad P, Chow WH, Chan J, et al. The role of diabetes mellitus in the aetiology of renal cell cancer. Diabetologia 1999;42:107-12.
28. Wideroff L, Gridley G, Mellemkjaer L, et al. Cancer incidence in a population-based cohort of patients hospitalized with diabetes mellitus in Denmark. JNatlCancer Inst 1997;89:1360-5.
29. Pischon T, Lahmann PH, Boeing H, et al. Body size and risk of renal cell carcinoma in the European Prospective Investigation into Cancer and Nutrition (EPIC). IntJCancer 2006;118:728-38.
30. Setiawan VW, Stram DO, Nomura AM, Kolonel LN, Henderson BE. Risk factors for renal cell cancer: the multiethnic cohort. AmJEpidemiol 2007;166:932-40.
31. Brennan JF, Stilmant MM, Babayan RK, Siroky MB. Acquired renal cystic disease: implications for the urologist. BrJUrol 1991;67:342-8.
32. Hurst FP, Jindal RM, Fletcher JJ, et al. Incidence, predictors and associated outcomes of renal cell carcinoma in long-term dialysis patients. Urology 2011;77:1271-6.
33. Zbar B, Tory K, Merino M, et al. Hereditary papillary renal cell carcinoma. JUrol 1994;151:561-6.
34. Maher ER, Kaelin WG, Jr. von Hippel-Lindau disease. Medicine (Baltimore) 1997;76:381-91.
35. Zbar B, Glenn G, Merino M, et al. Familial renal carcinoma: clinical evaluation, clinical subtypes and risk of renal carcinoma development. JUrol 2007;177:461-5.
36. Gordon SC, Moonka D, Brown KA, et al. Risk for renal cell carcinoma in chronic hepatitis C infection. Cancer EpidemiolBiomarkers Prev 2010;19:1066-73.
37. Li L, Kaelin WG, Jr. New insights into the biology of renal cell carcinoma. Hematol Oncol Clin North Am 2011;25:667-86.

38. Presti JC, Jr., Rao PH, Chen Q, et al. Histopathological, cytogenetic, and molecular characterization of renal cortical tumors. Cancer Res 1991;51:1544-52.
39. Delahunt B, Eble JN. Papillary renal cell carcinoma: a clinicopathologic and immunohistochemical study of 105 tumors. ModPathol 1997;10:537-44.
40. Yang XJ, Tan MH, Kim HL, et al. A molecular classification of papillary renal cell carcinoma. Cancer Res 2005;65:5628-37.
41. Pignot G, Elie C, Conquy S, et al. Survival analysis of 130 patients with papillary renal cell carcinoma: prognostic utility of type 1 and type 2 subclassification. Urology 2007;69:230-5.
42. Waldert M, Haitel A, Marberger M, et al. Comparison of type I and II papillary renal cell carcinoma (RCC) and clear cell RCC. BJUInt 2008;102:1381-4.
43. Klatte T, Pantuck AJ, Said JW, et al. Cytogenetic and molecular tumor profiling for type 1 and type 2 papillary renal cell carcinoma. ClinCancer Res 2009;15:1162-9.
44. Thoenes W, Storkel S, Rumpelt HJ, Moll R, Baum HP, Werner S. Chromophobe cell renal carcinoma and its variants--a report on 32 cases. JPathol 1988;155:277-87.
45. Storkel S, Steart PV, Drenckhahn D, Thoenes W. The human chromophobe cell renal carcinoma: its probable relation to intercalated cells of the collecting duct. Virchows ArchB Cell PatholInclMolPathol 1989;56:237-45.
46. Ortmann M, Vierbuchen M, Fischer R. Sialylated glycoconjugates in chromophobe cell renal carcinoma compared with other renal cell tumors. Indication of its development from the collecting duct epithelium. Virchows ArchB Cell PatholInclMolPathol 1991;61:123-32.
47. Akhtar M, Kardar H, Linjawi T, McClintock J, Ali MA. Chromophobe cell carcinoma of the kidney. A clinicopathologic study of 21 cases. AmJSurgPathol 1995;19:1245-56.
48. Speicher MR, Schoell B, du MS, et al. Specific loss of chromosomes 1, 2, 6, 10, 13, 17, and 21 in chromophobe renal cell carcinomas revealed by comparative genomic hybridization. AmJPathol 1994;145:356-64.
49. Klatte T, Han KR, Said JW, et al. Pathobiology and prognosis of chromophobe renal cell carcinoma. UrolOncol 2008;26:604-9.
50. Zerban H, Nogueira E, Riedasch G, Bannasch P. Renal oncocytoma: origin from the collecting duct. Virchows ArchB Cell PatholInclMolPathol 1987;52:375-87.
51. Lieber MM. Renal oncocytoma: prognosis and treatment. EurUrol 1990;18 Suppl 2:17-21.
52. Dechet CB, Bostwick DG, Blute ML, Bryant SC, Zincke H. Renal oncocytoma: multifocality, bilateralism, metachronous tumor development and coexistent renal cell carcinoma. J Urol 1999;162:40-2.
53. Hwang JJ, Uchio EM, Linehan WM, Walther MM. Hereditary kidney cancer. UrolClinNorth Am 2003;30:831-42.
54. Courtney KD, Choueiri TK. Optimizing recent advances in metastatic renal cell carcinoma. CurrOncolRep 2009;11:218-26.
55. Lonser RR, Glenn GM, Walther M, et al. von Hippel-Lindau disease. Lancet 2003;361:2059-67.
56. Latif F, Tory K, Gnarra J, et al. Identification of the von Hippel-Lindau disease tumor suppressor gene. Science 1993;260:1317-20.

57. Kim WY, Kaelin WG. Role of VHL gene mutation in human cancer. JClinOncol 2004;22:4991-5004.
58. Vickers MM, Heng DY. Prognostic and predictive biomarkers in renal cell carcinoma. Target Oncol 2010;5:85-94.
59. Devita V. Cancer Principles & Practice of Oncology. In. 9th ed: Lippincott Williams & Wilkins; 2011.
60. Tang PA, Vickers MM, Heng DY. Clinical and molecular prognostic factors in renal cell carcinoma: what we know so far. Hematol Oncol Clin North Am 2011;25:871-91.
61. Schmidt L, Duh FM, Chen F, et al. Germline and somatic mutations in the tyrosine kinase domain of the MET proto-oncogene in papillary renal carcinomas. NatGenet 1997;16:68-73.
62. Schmidt L, Junker K, Weirich G, et al. Two North American families with hereditary papillary renal carcinoma and identical novel mutations in the MET proto-oncogene. Cancer Res 1998;58:1719-22.
63. Alam NA, Bevan S, Churchman M, et al. Localization of a gene (MCUL1) for multiple cutaneous leiomyomata and uterine fibroids to chromosome 1q42.3-q43. AmJHumGenet 2001;68:1264-9.
64. Pollard P, Wortham N, Barclay E, et al. Evidence of increased microvessel density and activation of the hypoxia pathway in tumours from the hereditary leiomyomatosis and renal cell cancer syndrome. JPathol 2005;205:41-9.
65. Ooi A, Wong JC, Petillo D, et al. An antioxidant response phenotype shared between hereditary and sporadic type 2 papillary renal cell carcinoma. Cancer Cell 2011;20:511-23.
66. Menko FH, van Steensel MA, Giraud S, et al. Birt-Hogg-Dube syndrome: diagnosis and management. Lancet Oncol 2009;10:1199-206.
67. Nickerson ML, Warren MB, Toro JR, et al. Mutations in a novel gene lead to kidney tumors, lung wall defects, and benign tumors of the hair follicle in patients with the Birt-Hogg-Dube syndrome. Cancer Cell 2002;2:157-64.
68. Baba M, Hong SB, Sharma N, et al. Folliculin encoded by the BHD gene interacts with a binding protein, FNIP1, and AMPK, and is involved in AMPK and mTOR signaling. ProcNatlAcadSciUSA 2006;103:15552-7.
69. Baba M, Furihata M, Hong SB, et al. Kidney-targeted Birt-Hogg-Dube gene inactivation in a mouse model: Erk1/2 and Akt-mTOR activation, cell hyperproliferation, and polycystic kidneys. JNatlCancer Inst 2008;100:140-54.
70. Kuhbock J. Survey of chemotherapy of metastatic renal cancer. Semin Surg Oncol 1988;4:87-90.
71. Yagoda A, Abi-Rached B, Petrylak D. Chemotherapy for advanced renal-cell carcinoma: 1983-1993. SeminOncol 1995;22:42-60.
72. Lilleby W, Fossa SD. Chemotherapy in metastatic renal cell cancer. World J Urol 2005;23:175-9.
73. Klapper JA, Downey SG, Smith FO, et al. High-dose interleukin-2 for the treatment of metastatic renal cell carcinoma : a retrospective analysis of response and survival in patients treated in the surgery branch at the National Cancer Institute between 1986 and 2006. Cancer 2008;113:293-301.

74. Rosenblatt J, McDermott DF. Immunotherapy for renal cell carcinoma. Hematol Oncol Clin North Am 2011;25:793-812.
75. Albiges L, Salem M, Rini B, Escudier B. Vascular endothelial growth factor-targeted therapies in advanced renal cell carcinoma. Hematol Oncol Clin North Am 2011;25:813-33.
76. Abraham M, Lazareth I, Bonardel G, et al. [Kikuchi disease and lupus: case report, literature review and FDG PET/CT interest]. J Mal Vasc 2011;36:274-9.
77. Voss MH, Molina AM, Motzer RJ. mTOR inhibitors in advanced renal cell carcinoma. Hematol Oncol Clin North Am 2011;25:835-52.
78. Motzer RJ, Hutson TE, Tomczak P, et al. Sunitinib versus interferon alfa in metastatic renal-cell carcinoma. NEnglJMed 2007;356:115-24.
79. Motzer RJ, Hutson TE, Tomczak P, et al. Overall survival and updated results for sunitinib compared with interferon alfa in patients with metastatic renal cell carcinoma. JClinOncol 2009;27:3584-90.
80. Escudier B, Eisen T, Stadler WM, et al. Sorafenib in advanced clear-cell renal-cell carcinoma. NEnglJMed 2007;356:125-34.
81. Escudier B, Eisen T, Stadler WM, et al. Sorafenib for treatment of renal cell carcinoma: Final efficacy and safety results of the phase III treatment approaches in renal cancer global evaluation trial. JClinOncol 2009;27:3312-8.
82. Eisen T, Oudard S, Szczylik C, et al. Sorafenib for older patients with renal cell carcinoma: subset analysis from a randomized trial. JNatlCancer Inst 2008;100:1454-63.
83. Sternberg CN, Davis ID, Mardiak J, et al. Pazopanib in locally advanced or metastatic renal cell carcinoma: results of a randomized phase III trial. JClinOncol 2010;28:1061-8.
84. Carew JS, Kelly KR, Nawrocki ST. Mechanisms of mTOR inhibitor resistance in cancer therapy. Targeted oncology 2011;6:17-27.
85. Khokhar NZ, Altman JK, Platanias LC. Emerging roles for mammalian target of rapamycin inhibitors in the treatment of solid tumors and hematological malignancies. Current opinion in oncology 2011;23:578-86.
86. van Brussel JP, Mickisch GH. Circumvention of multidrug resistance in genitourinary tumors. IntJUrol 1998;5:1-15.
87. Gamelin E, Mertins SD, Regis JT, et al. Intrinsic drug resistance in primary and metastatic renal cell carcinoma. JUrol 1999;162:217-24.
88. Kong CZ, Zeng Y, Wu XX, Li JQ, Zhu YY, Chen Y. Increased expression of lung resistance-related protein in lower grade urothelial carcinoma of the renal pelvis and ureter. International journal of urology : official journal of the Japanese Urological Association 2004;11:721-7.
89. Walsh N, Larkin A, Kennedy S, et al. Expression of multidrug resistance markers ABCB1 (MDR-1/P-gp) and ABCC1 (MRP-1) in renal cell carcinoma. BMC urology 2009;9:6.
90. Chen ZS, Tiwari AK. Multidrug resistance proteins (MRPs/ABCCs) in cancer chemotherapy and genetic diseases. The FEBS journal 2011;278:3226-45.
91. Mossink MH, van Zon A, Scheper RJ, Sonneveld P, Wiemer EA. Vaults: a ribonucleoprotein particle involved in drug resistance? Oncogene 2003;22:7458-67.

92. Shibayama Y, Nakano K, Maeda H, et al. Multidrug resistance protein 2 implicates anticancer drug-resistance to sorafenib. Biological & pharmaceutical bulletin 2011;34:433-5.
93. Hodorova I, Rybarova S, Solar P, et al. Multidrug resistance proteins in renal cell carcinoma. Folia biologica 2008;54:187-92.
94. Rini BI, Atkins MB. Resistance to targeted therapy in renal-cell carcinoma. Lancet Oncol 2009;10:992-1000.
95. Lee W, Kim RB. Transporters and renal drug elimination. Annual review of pharmacology and toxicology 2004;44:137-66.
96. Hofmockel G, Bassukas ID, Wittmann A, Dammrich J. Is the expression of multidrug resistance gene product a prognostic indicator for the clinical outcome of patients with renal cancer? British journal of urology 1997;80:11-7.
97. Kanamaru H, Kakehi Y, Yoshida O, Nakanishi S, Pastan I, Gottesman MM. MDR1 RNA levels in human renal cell carcinomas: correlation with grade and prediction of reversal of doxorubicin resistance by quinidine in tumor explants. Journal of the National Cancer Institute 1989;81:844-9.
98. Rochlitz CF, Lobeck H, Peter S, et al. Multiple drug resistance gene expression in human renal cell cancer is associated with the histologic subtype. Cancer 1992;69:2993-8.
99. Tobe SW, Noble-Topham SE, Andrulis IL, Hartwick RW, Skorecki KL, Warner E. Expression of the multiple drug resistance gene in human renal cell carcinoma depends on tumor histology, grade, and stage. Clinical cancer research : an official journal of the American Association for Cancer Research 1995;1:1611-5.
100. Townsend DM, Tew KD. The role of glutathione-S-transferase in anti-cancer drug resistance. Oncogene 2003;22:7369-75.
101. Sau A, Pellizzari Tregno F, Valentino F, Federici G, Caccuri AM. Glutathione transferases and development of new principles to overcome drug resistance. Archives of biochemistry and biophysics 2010;500:116-22.
102. Chuang ST, Chu P, Sugimura J, et al. Overexpression of glutathione s-transferase alpha in clear cell renal cell carcinoma. American journal of clinical pathology 2005;123:421-9.
103. Simic T, Mimic-Oka J, Ille K, Dragicevic D, Savic-Radojevic A. Glutathione S-transferase isoenzyme profile in non-tumor and tumor human kidney tissue. World journal of urology 2003;20:385-91.
104. Di Ilio C, Aceto A, Bucciarelli T, et al. Glutathione transferase isoenzymes in normal and neoplastic human kidney tissue. Carcinogenesis 1991;12:1471-5.
105. Klone A, Weidner U, Hussnatter R, et al. Decreased expression of the glutathione S-transferases alpha and pi genes in human renal cell carcinoma. Carcinogenesis 1990;11:2179-83.
106. Clairmont A, Ebert T, Weber H, et al. Lowered amounts of the tissue-specific transcription factor LFB1 (HNF1) correlate with decreased levels of glutathione S-transferase alpha messenger RNA in human renal cell carcinoma. Cancer research 1994;54:1319-23.
107. Rodilla V, Benzie AA, Veitch JM, Murray GI, Rowe JD, Hawksworth GM. Glutathione S-transferases in human renal cortex and neoplastic tissue: enzymatic

activity, isoenzyme profile and immunohistochemical localization. Xenobiotica; the fate of foreign compounds in biological systems 1998;28:443-56.
108. Howie AF, Forrester LM, Glancey MJ, et al. Glutathione S-transferase and glutathione peroxidase expression in normal and tumour human tissues. Carcinogenesis 1990;11:451-8.
109. Gajewska J, Szczypka M, Pych K, Borowka A, Laskowska-Klita T. Glutathione S-transferase isoenzymes and glutathione in renal cell carcinoma and kidney tissue. Neoplasma 1995;42:167-72.
110. Oudard S, Levalois C, Andrieu JM, et al. Expression of genes involved in chemoresistance, proliferation and apoptosis in clinical samples of renal cell carcinoma and correlation with clinical outcome. Anticancer research 2002;22:121-8.
111. Dekel Y, Frede T, Kugel V, Neumann G, Rassweiler J, Koren R. Human DNA topoisomerase II-alpha expression in laparoscopically treated renal cell carcinoma. Oncology reports 2005;14:271-4.
112. Heck MM, Earnshaw WC. Topoisomerase II: A specific marker for cell proliferation. The Journal of cell biology 1986;103:2569-81.
113. Nitiss JL, Liu YX, Harbury P, Jannatipour M, Wasserman R, Wang JC. Amsacrine and etoposide hypersensitivity of yeast cells overexpressing DNA topoisomerase II. Cancer research 1992;52:4467-72.
114. Davies SM, Robson CN, Davies SL, Hickson ID. Nuclear topoisomerase II levels correlate with the sensitivity of mammalian cells to intercalating agents and epipodophyllotoxins. The Journal of biological chemistry 1988;263:17724-9.
115. Scheltema JM, Romijn JC, van Steenbrugge GJ, Beck WT, Schroder FH, Mickisch GH. Decreased levels of topoisomerase II alpha in human renal cell carcinoma lines resistant to etoposide. Journal of cancer research and clinical oncology 1997;123:546-54.
116. Monnin KA, Bronstein IB, Gaffney DK, Holden JA. Elevations of DNA topoisomerase I in transitional cell carcinoma of the urinary bladder: correlation with DNA topoisomerase II-alpha and p53 expression. Human pathology 1999;30:384-91.
117. Schor-Bardach R, Alsop DC, Pedrosa I, et al. Does arterial spin-labeling MR imaging-measured tumor perfusion correlate with renal cell cancer response to antiangiogenic therapy in a mouse model? Radiology 2009;251:731-42.
118. Rini BI. New strategies in kidney cancer: therapeutic advances through understanding the molecular basis of response and resistance. ClinCancer Res 2010;16:1348-54.
119. Childs R, Chernoff A, Contentin N, et al. Regression of metastatic renal-cell carcinoma after nonmyeloablative allogeneic peripheral-blood stem-cell transplantation. The New England journal of medicine 2000;343:750-8.
120. Rini BI, Zimmerman T, Stadler WM, Gajewski TF, Vogelzang NJ. Allogeneic stem-cell transplantation of renal cell cancer after nonmyeloablative chemotherapy: feasibility, engraftment, and clinical results. Journal of clinical oncology : official journal of the American Society of Clinical Oncology 2002;20:2017-24.
121. Galligioni E, Quaia M, Merlo A, et al. Adjuvant immunotherapy treatment of renal carcinoma patients with autologous tumor cells and bacillus Calmette-Guerin: five-year results of a prospective randomized study. Cancer 1996;77:2560-6.

122. Brookman-May S, Burger M, Wieland WF, Rossler W, May M, Denzinger S. Vaccination therapy in renal cell carcinoma: current position and future options in metastatic and localized disease. Expert review of vaccines 2011;10:837-52.
123. Mertins SD, Myers TG, Hollingshead M, et al. Screening for and identification of novel agents directed at renal cell carcinoma. ClinCancer Res 2001;7:620-33.
124. Mertins SD, Myers TG, Holbeck SL, et al. In vitro evaluation of dimethane sulfonate analogues with potential alkylating activity and selective renal cell carcinoma cytotoxicity. MolCancer Ther 2004;3:849-60.
125. Shoemaker RH. The NCI60 human tumour cell line anticancer drug screen. Nature reviews Cancer 2006;6:813-23.
126. Wallqvist A, Rabow AA, Shoemaker RH, Sausville EA, Covell DG. Linking the growth inhibition response from the National Cancer Institute's anticancer screen to gene expression levels and other molecular target data. Bioinformatics 2003;19:2212-24.
127. Jumaa M, Chimilio L, Chinnaswamy S, Silchenko S, Stella VJ. Degradation of NSC-281612 (4-[bis[2-[(methylsulfonyl)oxy]ethyl]amino]-2-methyl-benzaldehyde), an experimental antineoplastic agent: effects of pH, solvent composition, (SBE)7m-beta-CD, and HP-beta-CD on stability. J Pharm Sci 2004;93:532-9.
128. Facchini G, Perri F, Caraglia M, et al. New treatment approaches in renal cell carcinoma. Anticancer Drugs 2009;20:893-900.
129. Rini BI. Metastatic renal cell carcinoma: many treatment options, one patient. JClinOncol 2009;27:3225-34.
130. Reeves DJ, Liu CY. Treatment of metastatic renal cell carcinoma. Cancer ChemotherPharmacol 2009;64:11-25.
131. Mertins S. Treating Renal Cancer Using a 4-[Bis[2-[(methylsulfonyl)oxy]ethyl]amino]-2-methyl-benzaldehyde. In. United States: Patent Application Publication; 2011.
132. Carter J. In vivo efficacy of an aldehyde degradation product of dimethane sulfonate (NSC 281612) in an orthotopic RXF-393 human renal tumor model. In: Proceedings of the American Association of Cancer Research; 2005; 2005. p. 322-3.
133. Wang X, Schumitzky A, D'Argenio DZ. Nonlinear Random Effects Mixture Models: Maximum Likelihood Estimation via the EM Algorithm. Computational statistics & data analysis 2007;51:6614-23.
134. Ehrsson H, Lonroth U, Wallin I, Ehrnebo M, Nilsson SO. Degradation of chlorambucil in aqueous solution--influences of human albumin binding. J Pharm Pharmacol 1981;33:313-5.
135. Beumer JH, Eiseman JL, Gilbert JA, et al. Plasma pharmacokinetics and oral bioavailability of the 3,4,5,6-tetrahydrouridine (THU) prodrug, triacetyl-THU (taTHU), in mice. Cancer chemotherapy and pharmacology 2011;67:421-30.
136. Covey JM. Preclinical pharmacokinetics and metabolism of benzaldehyde dimethane sulfonate (BEN) (NSC 281612). In: Proceedings of the American Association of Cancer Research; 2005; 2005. p. 321-2.
137. Sreerama L, Sladek NE. Class 1 and class 3 aldehyde dehydrogenase levels in the human tumor cell lines currently used by the National Cancer Institute to screen for potentially useful antitumor agents. Adv Exp Med Biol 1997;414:81-94.
138. Wierzchowski J, Wroczynski P, Laszuk K, Interewicz E. Fluorimetric detection of aldehyde dehydrogenase activity in human blood, saliva, and organ biopsies and kinetic

differentiation between class I and class III isozymes. Analytical biochemistry 1997;245:69-78.
139. Ma I, Allan AL. The role of human aldehyde dehydrogenase in normal and cancer stem cells. Stem Cell Rev 2011;7:292-306.
140. Ekhart C, Doodeman VD, Rodenhuis S, Smits PH, Beijnen JH, Huitema AD. Influence of polymorphisms of drug metabolizing enzymes (CYP2B6, CYP2C9, CYP2C19, CYP3A4, CYP3A5, GSTA1, GSTP1, ALDH1A1 and ALDH3A1) on the pharmacokinetics of cyclophosphamide and 4-hydroxycyclophosphamide. Pharmacogenet Genomics 2008;18:515-23.
141. Petersen EN. The pharmacology and toxicology of disulfiram and its metabolites. Acta Psychiatr Scand Suppl 1992;369:7-13.
142. Karamanakos PN, Pappas P, Boumba VA, et al. Pharmaceutical agents known to produce disulfiram-like reaction: effects on hepatic ethanol metabolism and brain monoamines. Int J Toxicol 2007;26:423-32.
143. Jemal A, Siegel R, Xu J, Ward E. Cancer statistics, 2010. CA Cancer JClin 2010;60:277-300.
144. Parise RA, Anyang BN, Eiseman JL, Egorin MJ, Covey JM, Beumer JH. Formation of active products of benzaldehyde dimethane sulfonate (NSC 281612, DMS612) in human blood and plasma and their activity against renal cell carcinoma lines. Cancer chemotherapy and pharmacology 2013;71:73-83.
145. Vasiliou V, Pappa A. Polymorphisms of human aldehyde dehydrogenases. Consequences for drug metabolism and disease. Pharmacology 2000;61:192-8.
146. Marchitti SA, Brocker C, Stagos D, Vasiliou V. Non-P450 aldehyde oxidizing enzymes: the aldehyde dehydrogenase superfamily. ExpertOpinDrug Metab Toxicol 2008;4:697-720.
147. Vasiliou V, Bairoch A, Tipton KF, Nebert DW. Eukaryotic aldehyde dehydrogenase (ALDH) genes: human polymorphisms, and recommended nomenclature based on divergent evolution and chromosomal mapping. Pharmacogenetics 1999;9:421-34.
148. Guo J, Clausen DM, Beumer JH, et al. In vitro cytotoxicity, pharmacokinetics, tissue distribution, and metabolism of small-molecule protein kinase D inhibitors, kb-NB142-70 and kb-NB165-09, in mice bearing human cancer xenografts. Cancer chemotherapy and pharmacology 2013;71:331-44.
149. Kiesel BF, Parise RA, Tjornelund J, et al. LC-MS/MS assay for the quantitation of the HDAC inhibitor belinostat and five major metabolites in human plasma. Journal of pharmaceutical and biomedical analysis 2013;81-82:89-98.
150. Sebastian-Gambaro MA, Gonzalez-de-la-Presa B, Fuentes-Arderiu X. An improvement on the criterion of the state of the art to estimate the maximal allowable imprecision. European journal of clinical chemistry and clinical biochemistry : journal of the Forum of European Clinical Chemistry Societies 1996;34:445-6.
151. Oh SJ, Han HK, Kang KW, Lee YJ, Lee MY. Menadione serves as a substrate for P-glycoprotein: implication in chemosensitizing activity. Archives of pharmacal research 2013;36:509-16.
152. Lavalle CR, Bravo-Altamirano K, Giridhar KV, et al. Novel protein kinase D inhibitors cause potent arrest in prostate cancer cell growth and motility. BMC chemical biology 2010;10:5.

153. Kameneva MV, Garrett KO, Watach MJ, Borovetz HS. Red blood cell aging and risk of cardiovascular diseases. Clinical hemorheology and microcirculation 1998;18:67-74.
154. Sebastian-Gambaro MA, Liron-Hernandez FJ, Fuentes-Arderiu X. Intra- and inter-individual biological variability data bank. European journal of clinical chemistry and clinical biochemistry : journal of the Forum of European Clinical Chemistry Societies 1997;35:845-52.
155. Chen M, Nafziger AN, Bertino JS, Jr. Drug-metabolizing enzyme inhibition by ketoconazole does not reduce interindividual variability of CYP3A activity as measured by oral midazolam. Drug metabolism and disposition: the biological fate of chemicals 2006;34:2079-82.
156. Liu J, Zhou Z, Hodgkinson CA, et al. Haplotype-based study of the association of alcohol-metabolizing genes with alcohol dependence in four independent populations. Alcoholism, clinical and experimental research 2011;35:304-16.
157. Spence JP, Liang T, Eriksson CJ, et al. Evaluation of aldehyde dehydrogenase 1 promoter polymorphisms identified in human populations. Alcoholism, clinical and experimental research 2003;27:1389-94.
158. Tottmar O, Hellstrom E. Aldehyde dehydrogenase in blood: a sensitive assay and inhibition by disulfiram. PharmacolBiochemBehav 1983;18 Suppl 1:103-7.
159. Parise RA, Anyang BN, Eiseman JL, Egorin MJ, Covey JM, Beumer JH. Formation of active products of benzaldehyde dimethane sulfonate (NSC 281612, DMS612) in human blood and plasma and their activity against renal cell carcinoma lines. Cancer chemotherapy and pharmacology 2012.
160. Beumer JH, Franke NE, Tolboom R, et al. Disposition and toxicity of trabectedin (ET-743) in wild-type and mdr1 gene (P-gp) knock-out mice. Investigational new drugs 2010;28:145-55.
161. Bailer AJ. Testing for the equality of area under the curves when using destructive measurement techniques. Journal of pharmacokinetics and biopharmaceutics 1988;16:303-9.
162. Pratt-Hyatt M, Lin HL, Hollenberg PF. Mechanism-based inactivation of human CYP2E1 by diethyldithocarbamate. Drug metabolism and disposition: the biological fate of chemicals 2010;38:2286-92.
163. Moreb JS, Ucar D, Han S, et al. The enzymatic activity of human aldehyde dehydrogenases 1A2 and 2 (ALDH1A2 and ALDH2) is detected by Aldefluor, inhibited by diethylaminobenzaldehyde and has significant effects on cell proliferation and drug resistance. Chem Biol Interact 2012;195:52-60.
164. Chippendale TW, Hu B, El Haj AJ, Smith D. A study of enzymatic activity in cell cultures via the analysis of volatile biomarkers. Analyst 2012.
165. Kong D, Kotraiah V. Modulation of aldehyde dehydrogenase activity affects (+/-)-4-hydroxy-2E-nonenal (HNE) toxicity and HNE-protein adduct levels in PC12 cells. J Mol Neurosci 2012;47:595-603.
166. Kotraiah V, Pallares D, Toema D, Kong D, Beausoleil E. Identification of aldehyde dehydrogenase 1A1 modulators using virtual screening. J Enzyme Inhib Med Chem 2012.
167. Stagos D, Chen Y, Brocker C, et al. Aldehyde dehydrogenase 1B1: molecular cloning and characterization of a novel mitochondrial acetaldehyde-metabolizing

enzyme. Drug metabolism and disposition: the biological fate of chemicals 2010;38:1679-87.
168. Povirk LF, Shuker DE. DNA damage and mutagenesis induced by nitrogen mustards. MutatRes 1994;318:205-26.
169. Hall AG, Tilby MJ. Mechanisms of action of, and modes of resistance to, alkylating agents used in the treatment of haematological malignancies. Blood Rev 1992;6:163-73.
170. Ciarimboli G, Holle SK, Vollenbrocker B, et al. New Clues for Nephrotoxicity Induced by Ifosfamide: Preferential Renal Uptake via the Human Organic Cation Transporter 2. MolPharm 2010.
171. Schulz C, Boeck S, Heinemann V, Stemmler HJ. UGT1A1 genotyping: a predictor of irinotecan-associated side effects and drug efficacy? Anticancer Drugs 2009;20:867-79.
172. Rini BI, Wilding G, Hudes G, et al. Phase II study of axitinib in sorafenib-refractory metastatic renal cell carcinoma. JClinOncol 2009;27:4462-8.
173. Parise RA, Beumer JH, Clausen DM, et al. Effects of the aldehyde dehydrogenase inhibitor disulfiram on the plasma pharmacokinetics, metabolism, and toxicity of benzaldehyde dimethane sulfonate (NSC281612, DMS612, BEN) in mice. Cancer chemotherapy and pharmacology 2013.
174. Reigner BG, Blesch KS. Estimating the starting dose for entry into humans: principles and practice. European journal of clinical pharmacology 2002;57:835-45.
175. Smith BP, Vandenhende FR, DeSante KA, et al. Confidence interval criteria for assessment of dose proportionality. Pharmaceutical research 2000;17:1278-83.
176. Kastan MB, Schlaffer E, Russo JE, Colvin OM, Civin CI, Hilton J. Direct demonstration of elevated aldehyde dehydrogenase in human hematopoietic progenitor cells. Blood 1990;75:1947-50.